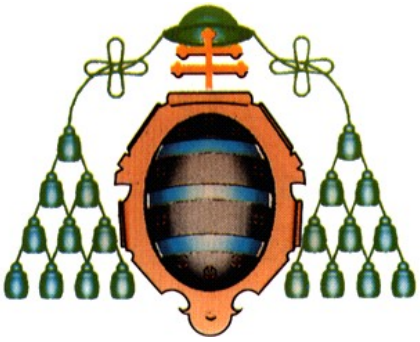

UNIVERSIDAD DE OVIEDO

Programa de Doctorado de Ciencia y Tecnología de Materiales

SÍNTESIS DE XEROGELES DE CARBONO INDUCIDA POR MICROONDAS PARA SU USO COMO ELECTRODOS EN SUPERCONDENSADORES

TESIS DOCTORAL

ESTHER GÓMEZ CALVO

ABRIL 2013

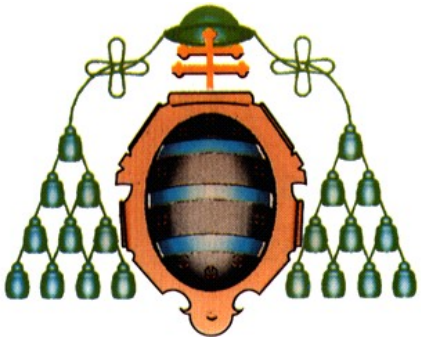

UNIVERSIDAD DE OVIEDO

Programa de Doctorado de Ciencia y Tecnología de Materiales

SÍNTESIS DE XEROGELES DE CARBONO INDUCIDA POR MICROONDAS PARA SU USO COMO ELECTRODOS EN SUPERCONDENSADORES

TESIS DOCTORAL

DIRECTORES

ANA ARENILLAS DE LA PUENTE

J. ÁNGEL MENÉNDEZ DÍAZ

RESUMEN DEL CONTENIDO DE TESIS DOCTORAL

1.- Título de la Tesis	
Español: Síntesis de xerogeles de carbono inducida por microondas para su uso como electrodos en supercondensadores	Inglés: Microwave-induced synthesis of carbon xerogels for their application as electrodes in supercapacitors

2.- Autor	
Nombre: Esther Gómez Calvo	
Programa de Doctorado: Ciencia y Tecnología de Materiales	
Órgano responsable: Departamento de Ciencia de los Materiales e Ingeniería Metalúrgica	

RESUMEN (en español)

Las investigaciones sobre los supercondensadores se centran, fundamentalmente, en la búsqueda de nuevos materiales de electrodo y utilización de diferentes electrolitos y configuraciones, con el objeto de incrementar el voltaje de trabajo y mejorar, con ello, los valores de energía y potencia específica. La tesis doctoral se ha dividido en dos partes, una de ellas enfocada hacia la síntesis y caracterización de xerogeles de carbono y otra en la que se evalúa la capacidad de almacenamiento energética de xerogeles de carbono sintetizados en el laboratorio, utilizados como material de electrodo en supercondensadores de diversa tipología.

Con respecto a la fabricación de los materiales, se ha desarrollado un método basado en la tecnología microondas que permite obtener xerogeles de carbono con propiedades análogas a los sintetizados convencionalmente, pero de una manera mucho más rápida y sencilla. La radicación microondas también ha sido utilizada durante los procesos de activación, lo que ha permitido desarrollar notablemente su microporosidad empleando tiempos de operación muy cortos. Los xerogeles de carbono así activados han presentado áreas superficiales > 2000 $m^2 g^{-1}$ y cierto contenido en mesoporos, características idóneas para la aplicación propuesta en este trabajo. Tanto el proceso de síntesis como el post-tratamiento ponen de relieve la versatilidad de los xerogeles de carbono puesto que sus propiedades texturales y químicas han sido diseñadas a partir de la modificación de alguna variable de operación.

En la segunda parte del trabajo se ha determinado la capacidad de almacenamiento de energía de diferentes xerogeles de carbono. Varias han sido las estrategias desarrolladas con el propósito de incrementar la cantidad de energía almacenada por el supercondensador: empleo de electrodos de diferente porosidad; adición de compuestos conductores; preparación de celdas asimétricas y, finalmente; uso de electrolitos de diversa naturaleza. Algunas de estas estrategias han resultado francamente eficaces. Por ejemplo, el uso de electrodos desiguales o líquidos iónicos como electrolitos, han permitido que el supercondensador funcione correctamente aplicando un voltaje de trabajo ~ 1.6 V, en el primer caso, y > a 2.0 V en el segundo, lo que repercute positivamente sobre su densidad de energía. Los xerogeles de carbono han dado lugar a elevados valores de capacidad (~200 F g^{-1}) y, además, con una excelente ciclabilidad.

RESUMEN (en Inglés)

Supercapacitors research is mainly focused on the search of new electrode materials and the use of different electrolytes and configurations, in order to increase the potential window and, therefore, improve the values of energy and power density. The thesis has been divided in two different sections, one focused on the synthesis and characterization of carbon xerogels and the second designated to the evaluation of energy storage capacitance of these carbon xerogels synthesized, used as electrodes in supercapacitors of different type.

This work present a novel method for the synthesis of carbon xerogels based on microwave heating. By means of this synthesis method, carbon xerogels with analogous properties to those conventionally obtained have been produced in a quicker, easier and more efficient way. Microwave radiation has been also used during activation processes, allowing the development of its microporosity with much shorter operating times. The activated carbon xerogels obtained have displayed values of surface area around 2000 m^2 g^{-1} and a high mesopore content, textural characteristics highly suitable for the application proposed in this work. Both the synthesis procedure and the post-treatment highlight the versatility of carbon xerogels since their textural and chemical properties has been tailored by modifying some operating variable.

In the second section, the energy storage capacitance of several carbon xerogels has been determined. Various strategies have been carried out in order to increase the amount of energy stored such as: the use of electrodes of different porosity; the addition of high-conductivity materials; the preparation of asymmetric cells and, finally; the use of electrolytes of different nature. Some of these strategies have turned out to be highly successful. For example, the use of unequal electrodes or ionic liquids as electrolytes produces supercapacitors than are able to operate effectively within a voltage window of 1.6 V, in the first case, and > 2.0 V in the second, which has a positive effect on its energy density. Carbon xerogels have presented high specific capacitance values (~ 200 F g-1) and, in addition, with a very long cycle life.

SR. DIRECTOR DE DEPARTAMENTO DE CIENCIA DE LOS MATERIALES E INGENIERÍA METALURGICA

A mis padres

Índice

Página

Agradecimientos

Deseo expresar mi más sincero agradecimiento a los Dres. Ana Arenillas de la Puente y J. Ángel Menéndez Díaz por el asesoramiento brindado durante el desarrollo de esta Tesis Doctoral, por su dedicación, sus sugerencias e ideas pero, sobretodo, por la confianza depositada en mí en todo momento.

Al Consejo Superior de Investigaciones Científicas (CSIC), por autorizar la realización de este trabajo en el Instituto Nacional del Carbón (INCAR). En especial, a los directores del centro durante mis años de doctorando, los Dres. Carlos Gutiérrez Blanco y Juan Manuel Díez Tascón.

A los Dres. Conchi Ovín Ania y José B. Parra por la ayuda ofrecida al inicio de este trabajo tanto en el campo de la electroquímica como de la caracterización textural. Al Dr. François Béguin del *Equipe Matériaux carbonés, Energie et Environnement* (CRMD, Orléans) y los Dres. Pietro Staiti y Francesco Lufrano pertenecientes al *Istituto di Tecnologie Avanzate per l'Energia "Nicola Giordano"*(ITAE, Messina), por darme la oportunidad de realizar con ellos estancias predoctorales, por su excelente acogida y ayuda en la realización del trabajo allí desarrollado. Especialmente, estoy muy agradecida a la Dra. Encarnación Raymundo Piñero (CRMD, Orléans) por haberme ayudado y apoyado desde mi llegada a Orléans, por hacerme sentir como una más dentro del grupo *hispanos en Orléans* y por las comidas y risas de los viernes, lo que ha hecho que recuerde mi paso por Orléans con un especial cariño.

No me quiero olvidar de la Dra. Leire Zubizarreta por haberme ayudado y enseñado todo durante mis comienzos en el laboratorio, por su compañerismo y simpatía. Aunque fueron pocos los meses que compartimos en MCAT, eres una de las personas del Instituto que con más cariño recuerdo.

A mis compañeros del INCAR, tanto los que ya no están como los que acaban de llegar, por nuestras conversaciones de sobremesa ajenas al mundo de la investigación, por las confidencias y las risas, que ayudaron a hacer las jornadas más amenas, por su apoyo en momentos difíciles, en definitiva, gracias por los buenos momentos compartidos tanto dentro como fuera del INCAR. Muy especialmente, me gustaría dar las gracias a María, Esteban, Jose, Marina y Sara por estar siempre dispuestos a ayudarme,

por vuestros ánimos y cariño pero, sobretodo, por permitirme formar parte de vuestra vida y habernos convertido en verdaderos amigos.

A mis amigas. Muy especialmente a Gracy, por sentirse orgullosa de mí con cada triunfo conseguido, por darme su apoyo y ánimo en los momentos difíciles, por las risas, confidencias y cotilleos. En resumen, gracias por ser mi mejor amiga desde niñas.

Me gustaría agradecer de corazón a mis padres y mi hermano su constante apoyo, paciencia y comprensión. Nunca tendré la oportunidad de devolveros todos vuestros esfuerzos y empeño para que tuviera una buena formación académica...*lo habéis conseguido*! Pero, sin duda, lo que más me gustaría agradecer es que soy la persona que soy gracias a vosotros, porque me habéis educado y guiado por un camino en el que el cariño y el amor han estado siempre presentes. Gracias por todo, os quiero. A Sergio, por estar a mi lado en cada momento, por tu paciencia y tus ánimos, que me han ayudado a no derrumbarme en las épocas más estresantes. Gracias por valorarme, escucharme, hacerme reír, en definitiva...gracias por ser mi pareja. A Leo, porque aunque aún eres muy pequeñín para entender lo que hace tu *tita Esther*, simplemente quiero darte las gracias por haber nacido y traer tanta felicidad a toda la familia.

Resumen

La presente memoria se ha dividido en dos partes bien diferenciadas. En la primera parte se presenta una nueva tecnología que permite obtener xerogeles de carbono con propiedades diseñadas a medida, mientras que en la segunda se evalúan dichos xerogeles como material activo en supercondensadores.

Con respecto a la fabricación de los materiales de electrodo, en este trabajo se ha desarrollado un novedoso método basado en el calentamiento con microondas que permite obtener xerogeles de carbono con propiedades análogas a los sintetizados mediante rutas convencionales, pero de una manera mucho más rápida y eficiente. La radiación microondas también ha sido utilizada como fuente de calor en procesos de activación, lo que ha permitido desarrollar notablemente la microporosidad de los xerogeles empleando tiempos de operación muy cortos. Los xerogeles de carbono así activados presentan áreas superficiales superiores a 2000 m^2 g^{-1} y cierto contenido en mesoporos, características idóneas para la aplicación estudiada en este trabajo.

En la segunda parte del trabajo se ha evaluado la capacidad de almacenamiento de energía de algunos xerogeles de carbono sintetizados en el laboratorio. Varias han sido las estrategias llevadas a cabo con el propósito de incrementar la cantidad de energía almacenada por el supercondensador, como son: empleo de materiales de electrodo de diferente porosidad; adición de compuestos conductores; preparación de celdas asimétricas (xerogel de carbono como electrodo negativo y MnO_2 como electrodo positivo) y, finalmente; uso de electrolitos de diversa naturaleza (disoluciones acuosas de distinto pH y líquidos iónicos próticos formados por diferentes aniones/cationes). Así, por ejemplo, el empleo de electrodos desiguales o líquidos iónicos como electrolitos, hace que el supercondensador pueda funcionar correctamente al aplicar un voltaje de trabajo próximo a 1.6 V, en el primer caso, y superior a 2.0 V en el segundo, lo que tiene una repercusión positiva sobre su densidad de energía. La optimización de las propiedades de los xerogeles de carbono empleados como material de electrodo ha permitido alcanzar valores de capacidad específica elevados (~ 200 F g^{-1}), pero además, dicha cantidad de energía se ha mantenido durante un número importante de ciclos de carga-descarga.

Abstract

The present memory has been divided into two different sections, the first devoted to the production, by means of microwave technology, of carbon xerogels with tuneable properties, while the second is focused on the evaluation of these laboratory-synthesized carbon xerogels as active materials in supercapacitors.

This work presents a novel method for the synthesis of carbon xerogels based on microwave heating. By means of this synthesis method, carbon xerogels with analogous properties to those obtained by conventional routes have been produced in a quicker and more efficient way. Microwave radiation has been also used as heating source in activation processes allowing the development of xerogels microporosity with much shorter operating times. The activated carbon xerogels obtained have displayed surface areas above 2000 m^2 g^{-1} and certain presence of mesopores, textural properties highly suitable for the application proposed in this work.

In the second section, the energy storage capacitance of several in-lab synthesized carbon xerogels has been evaluated. Various strategies have been carried out in order to improve the energy stored by the supercapacitor, such as: the use of electrode materials with different pore texture; the addition of high-conductivity materials; the preparation of asymmetric cells (a carbon xerogel as negative electrode and MnO_2 as the positive electrode) and, finally; the use of diverse electrolytes (aqueous solutions with different pH values and protic ionic liquids composed of different cations/anions). Thus, the use of unequal electrodes or ionic liquids as electrolyte produces supercapacitors that are able to operate effectively within a voltage window of 1.6 V, in the first case, and higher than 2.0 V in the second, which has a positive effect on their energy density. The properties optimization of carbon xerogel electrodes results in high values of specific capacitance (~ 200 F g^{-1}) and, in addition, they are able to maintain such energy stored during a large number of charge-discharge cycles.

Lista de Figuras y Tablas

FIGURAS

Página

TABLAS

Lista de Símbolos y Abreviaturas

A	Área de contacto electrodo-electrolito (m^2)
AILs	Aprotic Ionic Liquids
BDDT	Brunauer-Deming-Deming-Teller
BET	Brunauer-Emmet-Teller
C	Capacidad de la celda electroquímica
C_a	Capacidad del ánodo
C_c	Capacidad del cátodo
CVD	Chemical Vapor Deposition
d	Espesor de la doble capa eléctrica (m)
d_{poro}	Tamaño de poro (nm)
D	Relación de dilución (disolvente total/relación molar de reactivos) utilizada en la síntesis de los xerogeles de carbono
DFT	Density Functional Theory
DR	Dubinin-Raduskevich
E	Energía específica (Wh kg^{-1})
EDL	Electric Double Layer
EDLC	Electric Double-Layer Capacitor
EIS	Electrochemical Impedance Spectroscopy
ESR	Equivalent Series Resistance
F	Formaldehído
HE	Horno Eléctrico

I	Intensidad de corriente (A)
IEA	International Energy Agency
IR	Caída ohmica
IUPAC	International Union of Pure Applied Chemistry
KERS	Kinetic Energy Recovery System
MWNT	Multi Walled Carbon Nanotubes
MW	Microondas
p	Presión
p/p°	Presión relativa
pH_{PZC}	pH del punto de carga cero
P	Potencia específica (W kg^{-1})
PID	Proporcional Integral Derivativo
PILs	Protic Ionic Liquids
PSD	Pore Size Distribution
PTFE	Politetrafluoroetileno (teflón)
Q	Carga almacenada por el supercondensador (culombios)
r	Radio de poro (nm)
R	Resorcinol
R/F	Relación molar resorcinol/formaldehído utilizada en la síntesis de los xerogeles de carbono
s	Velocidad de barrido (mV s^{-1})
SAI	Sistemas de Alimentación Ininterrumpida
S_{BET}	Área superficial equivalente en la ecuación BET (m^2 g^{-1})
SEM	Scaning Electron Microscope
SWNT	Single Walled Carbon Nanotubes
t	Tiempo
t_g	Punto de gelación
T	Temperatura

TEM	Transmission Electron Microscope
TPD	Temperatura Programmed Desorption
V	Diferencia de potencial (voltios)
V_{DUB}	Volumen total de microporos accesibles al adsorbato en la ecuación DR aplicada a las isotermas de N_2 a 196 ºC (V_{DUB-N2}) y CO_2 a 0 ºC ($V_{DUB-CO2}$), ($cm^3\ g^{-1}$)
V_{meso}	Volumen de mesoporos ($cm^3\ g^{-1}$)
V_p	Volumen total de poros presentes en la muestra ($cm^3\ g^{-1}$)
Z	Impedancia
Z'	Parte real de la impedancia
Z''	Valor de la impedancia en la parte imaginaria
Δt_c	Tiempo destinado a la carga del supercondensador
Δt_d	Tiempo que tarda en descargarse el supercondensador
ΔV_d	Ventana de potencial correspondiente a la descarga del condensador electroquímico
ε	Constante dieléctrica del electrolito ($F\ m^{-1}$)
ε_0	Constante dieléctrica del vacío ($8.85 \cdot 10^{-12}\ F\ m^{-1}$)
σ	Tensión superficial
θ	Ángulo de contacto sólido-líquido
ω	Frecuencia angular

1. Introducción

1.1. Necesidad de los sistemas de almacenamiento de energía

El elevado consumo de energía eléctrica a nivel mundial, unido a que la mayor parte de la demanda energética se cubre mediante combustibles fósiles, supone un verdadero problema ya que dichas fuentes de energía dan lugar a diversos problemas medioambientales (acumulación de gases de efecto invernadero, contaminación del aire o perforación de la capa de ozono, por ejemplo) pero, además, constituyen un recurso finito. La Figura 1.1 muestra el aumento sufrido por el consumo energético mundial en los últimos 40 años, así como el tipo de recurso empleado para cubrir dicha demanda energética. Según datos de la Agencia Internacional de la Energía *(International Energy Agency, IEA)*, en el año 2010, más del 70 % de la energía primaria fue obtenida a partir de combustibles fósiles: petróleo, carbón y gas natural [IEA, 2012]. A día de hoy, las reservas mundiales de combustibles fósiles siguen siendo abundantes, además de ser considerados como la fuente de energía primaria más barata y accesible. Sin embargo, es necesario reducir paulatinamente su utilización como fuente de energía ya que, como se ha mencionado en líneas superiores, su explotación masiva supone una amenaza para el medioambiente.

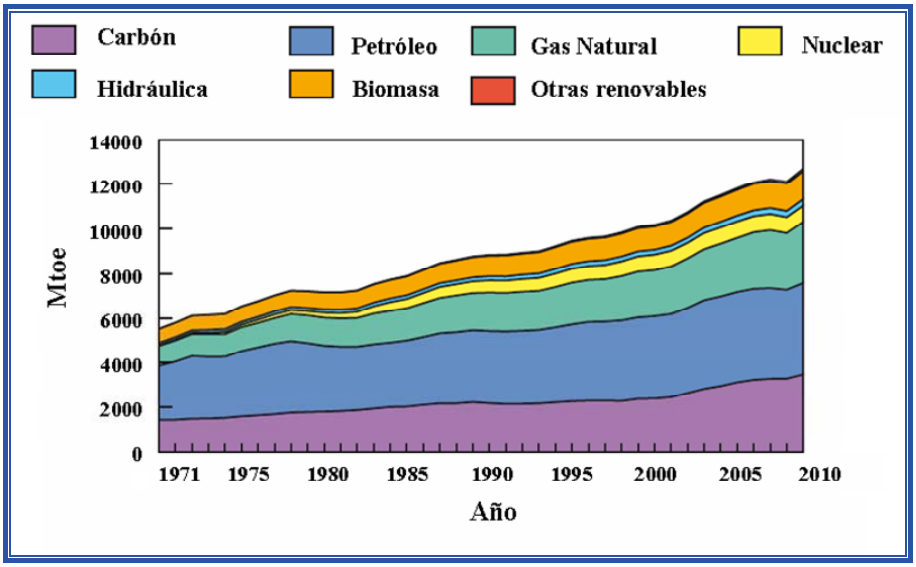

Figura 1.1. Evolución de la demanda de energía primaria mundial. (Fuente: IEA, 2012).

Una alternativa para solucionar los problemas ambientales derivados del excesivo consumo de combustibles fósiles pasa por desarrollar nuevos sistemas de generación y acumulación de energía que sean altamente eficientes, seguros y compatibles con el medioambiente. En este sentido, la explotación de fuentes de energía de carácter renovable (hidráulica, solar, eólica, biomasa, etc.) ha suscitado un creciente interés en las últimas décadas ya que puede contribuir a resolver y mejorar los problemas ambientales anteriormente citados y, además, a reducir la dependencia de las importaciones energéticas y aumentar la seguridad del suministro. Pese a las innumerables ventajas asociadas a las energías renovables, su naturaleza aleatoria, discontinua y, en la mayoría de casos, dependiente de factores climáticos, hace que sea totalmente necesario disponer de sistemas de almacenamiento de energía que permitan obtener su máximo rendimiento y ofrecer continuidad en el suministro eléctrico [BAÑOS, 2011; HALL, 2008; KALDELLIS, 2007].

1.2. SISTEMAS DE ALMACENAMIENTO DE ENERGÍA

En un dispositivo de acumulación de energía es importante tanto la cantidad de energía eléctrica que es capaz de almacenar como la potencia máxima suministrada, magnitudes que se expresan generalmente en forma de energía (Wh kg^{-1}) y potencia específica (W kg^{-1}). Además de estas características, tanto la autonomía que ofrecen los sistemas de almacenamiento de energía como los costes de fabricación y mantenimiento asociados son factores a tener muy en cuenta.

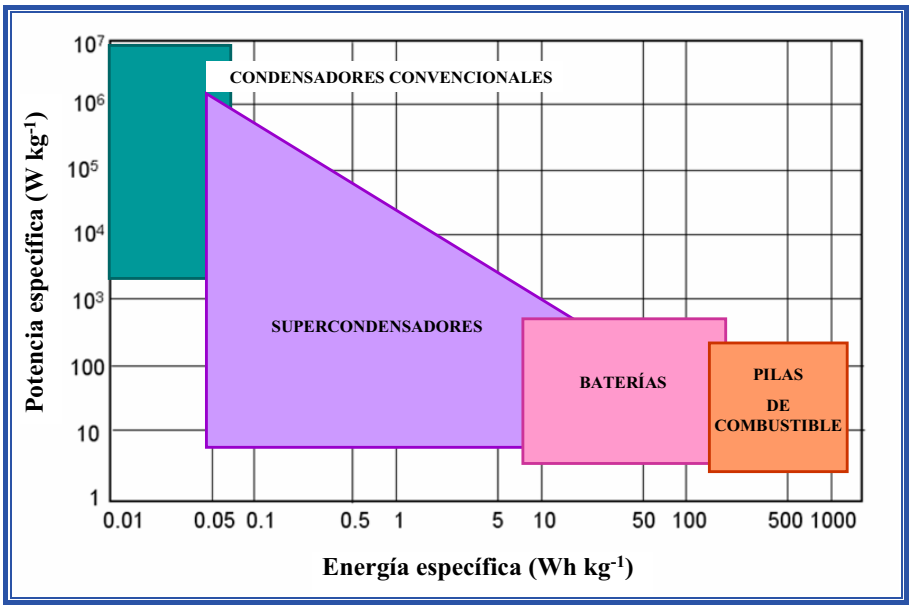

Figura 1.2. Diagrama de Ragone para distintos dispositivos de generación y almacenamiento de energía. Adaptado de la referencia [WINTER, 2004].

Entre los diversos dispositivos utilizados para almacenar el excedente de energía eléctrica producida a partir de recursos renovables se encuentran las baterías, pilas de combustible, condensadores convencionales y supercondensadores, también conocidos como condensadores electroquímicos

(véase Figura 1.2). A continuación, se explica brevemente el funcionamiento y las principales características de cada uno de ellos.

❖ *Baterías*: Son dispositivos de almacenamiento energético ampliamente conocidos y utilizados en diversos tipos de aplicaciones (vehículos eléctricos, equipos industriales tales como carretillas elevadoras, herramientas militares, dispositivos portátiles como teléfonos móviles, mp4, notebook, etc.). Su funcionamiento se basa en la conversión de energía química en energía eléctrica a partir de reacciones reversibles que tienen lugar entre el ánodo y cátodo. Los reactivos se almacenan en el interior de la batería por lo que una vez que éstos son consumidos, la batería también se agota. Las baterías ofrecen elevada densidad de energía y modulabilidad. Sin embargo, su asignatura pendiente está asociada con la baja densidad de potencia suministrada y con la pérdida de capacidad producida al cabo de unos pocos miles de ciclos de carga-descarga, lo que implica que deban ser reemplazadas por unas nuevas [GUTMANN, 2009]. Existen diferentes tipos de baterías: Pb-ácido, NaS, Ni-Cd, ión-Li, etc., siendo éstas últimas las que mayores ventajas presentan en cuanto a densidades de energía, voltaje, eficiencia en el almacenamiento y rendimiento en la descarga [KURZWEIL, 2009; TARASCÓN, 2001]. No obstante, en la actualidad se están llevando a cabo proyectos de investigación cuyo objetivo es lograr el máximo aprovechamiento de estos dispositivos y superar alguna de sus debilidades como son su limitada potencia específica y los problemas ambientales derivados del uso de metales pesados que presentan una elevada toxicidad.

❖ *Pilas de combustible*: En realidad, las pilas de combustible no son exactamente sistemas de almacenamiento energético sino más bien, dispositivos de generación de energía. En ellos, la corriente eléctrica se obtiene a partir de reacciones redox entre O_2 y H_2, que tienen lugar en presencia de un catalizador (principio de funcionamiento inverso al de la electrolisis del H_2O). Existen diferentes compuestos que se pueden utilizar como combustible (hidrógeno H_2, metano CH_4, metanol CH_3OH, etanol CH_3-CH_2OH, etc.) que junto con una especie oxidante (oxígeno O_2 ó aire) intervienen en reacciones electroquímicas dando lugar a energía eléctrica, agua y calor [SATTLER, 2000]. Al contrario que las baterías, una pila de combustible no se agota ni necesita ser reemplazada, ya que funciona mientras exista una alimentación continua de los reactivos. Parte de sus catalizadores son escasos y caros, motivo por el cual las pilas de combustible llevan asociados elevados costes de operación y fabricación. Estos dispositivos de generación de energía se clasifican en función de la naturaleza del electrolito utilizado (ácido fosfórico, hidróxido potásico, membrana polimérica, componente cerámico, etc.) que, a su vez, es el que determina la temperatura de operación de la celda, combustible empleado y tipo de aplicación [EDWARDS, 2008]. La densidad de energía obtenida a partir de las pilas de combustible es superior a la de las baterías (mientras que la potencia específica es bastante similar), lo que significa que, una vez que se reduzcan los costes de fabricación, las pilas de combustible podrán tener cabida en aplicaciones actualmente destinadas a las baterías.

❖ *Condensadores electrolíticos o convencionales*: Un condensador es un dispositivo que almacena energía en el interior de campos electrostáticos cuando se produce una separación de cargas. En su expresión más simple, un condensador está formado por dos placas metálicas, separadas mediante un material no conductor de la electricidad (vacío o cualquier otro dieléctrico), unidas a un circuito externo. Cuando se aplica una diferencia de potencial entre las dos placas metálicas se produce un flujo de electrones, de manera que una lámina es deficiente en electrones y la otra tiene un exceso. Existen diferentes tipos de materiales que se pueden utilizar como dieléctrico (papel, material cerámico, poliestireno, polipropileno, nylon, etc.) y el tipo de material empleado es clave en la determinación de las características del condensador, ya que puede definir la tensión máxima de funcionamiento y la capacidad total del dispositivo [NISHINO, 1996]. Los condensadores pueden utilizarse como sistemas alternativos o complementarios a las baterías y pilas de combustible puesto que proporcionan una densidad de potencia superior y son capaces de acumular la energía eléctrica durante un número muy elevado de ciclos de carga-descarga. No obstante, su principal debilidad está relacionada con la limitada densidad de energía que ofrecen.

❖ *Condensadores electroquímicos o supercondensadores*: Los condensadores electroquímicos son dispositivos que almacenan la energía directamente en campos eléctricos. Cuando los electrodos y el electrolito se ponen en contacto, se establece una diferencia de potencial entre ambos y ello da lugar a la separación de cargas de distinto signo en la interfase electrodo-electrolito. La cantidad de carga acumulada depende de la diferencia de potencial aplicada entre los dos electrodos y de las características de la celda electroquímica (material de electrodo, tipo de electrolito, etc.) [CONWAY, 1999]. En realidad, los fenómenos fisicoquímicos que rigen el funcionamiento de un supercondensador son los mismos que en un condensador convencional. Sin embargo, el efecto combinado de electrodos de elevada área superficial y pequeña separación entre ellos ha permitido que los supercondensadores sean capaces de almacenar más cantidad de energía que los condensadores convencionales, a costa de proporcionar una potencia específica inferior (véase Figura 1.2). Aún así, la densidad de potencia suministrada es superior a la ofrecida por las baterías y pilas de combustible. Los supercondensadores son capaces de generar corrientes eléctricas muy intensas durante décimas o centésimas de segundo, lo que implica que la mayoría de aplicaciones en las que se utilizan sean aquellas que requieren un aporte moderado de energía en momentos puntuales.

1.3. SUPERCONDENSADORES

Las principales ventajas e inconvenientes acerca del uso de los condensadores electroquímicos se muestran en la Tabla 1.1 [NOMOTO, 2001; OBREJA, 2008], propiedades que son las que determinan su rango de aplicabilidad. Por ejemplo, como consecuencia de su alta velocidad de respuesta (del orden de pocos segundos), los supercondensadores son especialmente apropiados para responder ante necesidades de punta de potencia o ante interrupciones de suministro de poca duración. Además, su

elevada ciclabilidad los hace también atractivos para dispositivos electrónicos portátiles, ya que alarga su vida útil con respecto a otros sistemas de almacenamiento energético.

Pese a sus excelentes prestaciones, el principal inconveniente está relacionado con su limitada capacidad de almacenamiento de carga. Por este motivo, las investigaciones están orientadas, a día de hoy, hacia la búsqueda de nuevas alternativas que permitan incrementar la densidad de energía (empleo de electrodos de elevada superficie activa, mayor tensión de trabajo conseguida mediante celdas asimétricas o supercondensadores basados en electrolitos cuyo potencial de descomposición es superior al del H_2O, etc.).

Tabla 1.1 – Principales características de los supercondensadores

PUNTOS FUERTES	PUNTOS DÉBILES
✓ Proporcionan la energía de manera muy rápida (del orden de unos pocos segundos) ✓ Elevada ciclabilidad (~ 10^6 ciclos de carga-descarga) ✓ Pueden operar en condiciones extremas de temperatura ✓ Componentes menos tóxicos que otros dispositivos de almacenamiento energético ✓ Escaso mantenimiento	✖ Limitada densidad de energía ✖ Costes de fabricación

1.3.1. Mecanismos de almacenamiento de energía

Los condensadores electroquímicos se pueden clasificar en dos categorías atendiendo al mecanismo de almacenamiento de carga: condensadores electroquímicos de doble capa (EDLCs) y condensadores electroquímicos basados en procesos pseudocapacitivos (pseudocondensadores). A continuación se presenta una breve descripción de ambos mecanismos de almacenamiento de energía eléctrica.

❖ *Mecanismo de doble capa eléctrica (EDL):* Su funcionamiento se basa en la formación de una doble capa eléctrica producida al aplicar una diferencia de potencial al sistema. Cuando el electrodo se pone en contacto con el electrolito, se establece una diferencia de potencial que hace que uno de los electrodos se cargue positivamente y el otro negativamente. Esto provoca una difusión de iones desde el seno de la disolución utilizada como electrolito hacia la superficie del electrodo con carga opuesta, dando lugar a la interfase electrodo-electrolito. La formación de la doble capa eléctrica implica únicamente un reordenamiento de los cationes y aniones del electrolito, proceso que ocurre en un

tiempo próximo a 10^{-8} segundos, tiempo inferior al necesario para que se produzcan muchas reacciones redox (10^{-2}-10^{-4} segundos) [WINTER, 2004], lo que repercute en una mayor velocidad de respuesta del dispositivo. De acuerdo con este mecanismo de almacenamiento de carga, los electrodos empleados en este tipo de sistemas electroquímicos deben poseer una elevada área superficial, una distribución de tamaños de poro adecuada para permitir la adsorción y fácil difusión de los iones de electrolito y una notable conductividad eléctrica [LOTA, 2008].

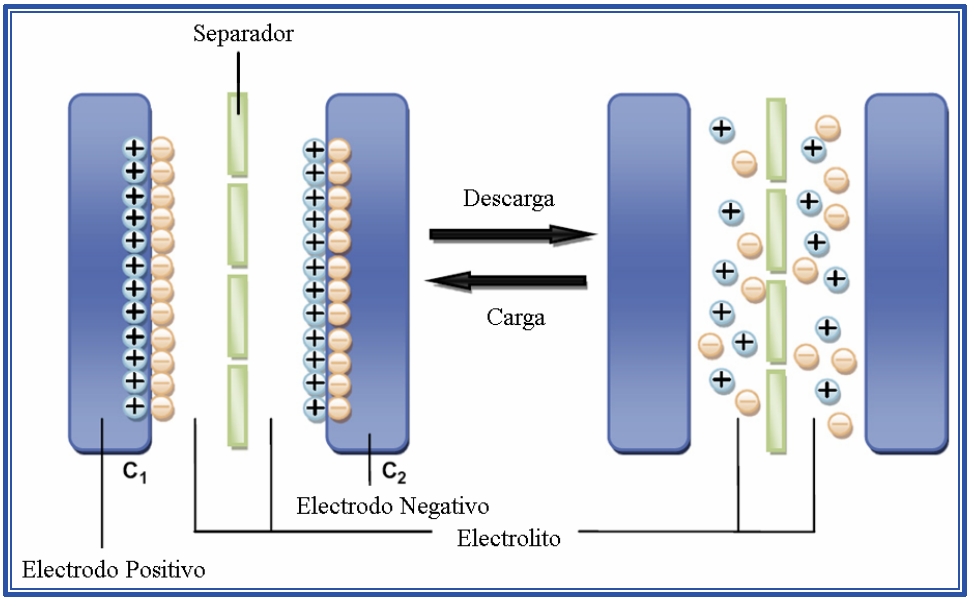

Figura 1.3. Esquema básico de un condensador electroquímico de doble capa (EDLC) durante los estados de carga y descarga. Adaptado de la referencia [LI, 2013].

Como se muestra en la Figura 1.3, un condensador electroquímico de doble capa (*EDLC, Electric Double-Layer Capacitor*) está constituido por dos electrodos impregnados de un electrolito que puede ser un medio acuoso, orgánico u otro tipo de electrolito más novedoso basado en polímeros conductores o líquidos iónicos [ARBIZZANY, 2008; WEI, 2009; YU 2012]. Entre los dos electrodos se coloca un separador (material inerte poroso) cuyo objetivo es aislar los electrodos para evitar que se produzca un cortocircuito en el sistema y permitir el flujo de iones de electrolito a su través. Cada electrodo, además, está en contacto con un colector de corriente.

❖ *Mecanismo de pseudocapacidad:* La pseudocapacidad surge como consecuencia de la aparición de reacciones faradaicas que tienen lugar entre el electrodo y el electrolito. Existen tres mecanismos que dan lugar a fenómenos pseudocapacitivos: adsorción de iones, reacciones redox e intercalación-desintercalación [WINTER, 2004]. La densidad de energía desarrollada por estos dispositivos es superior a la generada por un supercondensador cuyo almacenamiento de carga tiene un origen puramente electrostático. Sin embargo, su vida útil es inferior puesto que se produce una pérdida en la densidad de energía ofrecida a medida que el supercondensador se carga y se descarga. El estudio de materiales que contribuyen a aumentar la energía almacenada en un supercondensador

debido a reacciones faradaicas se basa generalmente en óxidos de metales de transición tales como RuO_2 [KIM, 2006; LIU, 2008; PANIĆ, 2010; PICO, 2009], MnO_2 [STAITI, 2009; YE, 2013], CoO_x [LIN, 1998], NiO_x [WU, 2006], entre otros, y polímeros conductores como polianilina [MI, 2008], polipirrol [FAN, 2006] y derivados de politiofeno [LAFORGUE, 1999]. Entre los óxidos más prometedores se encuentra el MnO_2, que es menos tóxico y más económico que el RuO_2, óxido que da lugar a los mejores valores de capacidad específica (750 F g^{-1} , [ZHENG, 1995]).

1.3.2. Materiales de electrodo

❖ *Óxidos de metales de transición:* Son los materiales de electrodo que ofrecen una mayor capacidad de almacenamiento energético, lo que junto con su baja resistencia, repercute en elevados valores de energía y potencia específica. Como se ha mencionado en la sección anterior, el óxido de rutenio (RuO_2) es uno de los metales de transición más atractivos para su aplicación en el campo del almacenamiento de energía. Los supercondensadores basados en RuO_2 presentan una elevada capacidad específica, excelente ciclabilidad, alta conductividad y buena reversibilidad electroquímica [KIM, 2006; ZHENG, 1995]. Sin embargo, debido a la falta de disponibilidad y al elevado coste del metal noble (Ru), la producción comercial de estos supercondensadores no es muy rentable, convirtiéndolos en dispositivos viables, únicamente, para el sector militar y aeroespacial. Otros óxidos metálicos alternativos al RuO_2 son NiO_x, CoO_x, MnO_2, Fe_3O_4, IrO_2, V_2O_5, etc. [LOKHANDE, 2011; STAITI, 2009; WU, 2003; WU, 2006; YE, 2013], los cuales pueden utilizarse como único material de electrodo o bien, en combinación con el Ru formando óxidos binarios, siendo ambas estrategias muy interesantes desde un punto de vista económico y medioambiental. Además de estas dos alternativas, una manera de aprovechar las sobresalientes propiedades pseudocapacitivas de los óxidos metálicos pero reduciendo el impacto ambiental y los costes de fabricación consiste en mezclar un óxido metálico con otro tipo de material (materiales de carbono porosos o polímeros conductores, por ejemplo), bien sea formando un composite o utilizando el material por separado en cada electrodo [KHOMENKO, 2006; LIN, 1998; PANIĆ, 2010; STAITI, 2007; YE, 2013; ZHU, 2012; SHOYEBMOHAMAD, 2013]. Precisamente, la fabricación de supercondensadores basados en un material carbonoso poroso (xerogel de carbono) y un óxido metálico (MnO_2) ha sido una de las estrategias llevadas a cabo en el presente trabajo (véase *Publicación V*).

❖ *Polímeros conductores:* Son materiales de electrodo muy prometedores debido a las siguientes características: (i) fácil preparación en medio acuoso, (ii) alta conductividad en su estado cargado y (iii) elevada capacidad de almacenamiento energético [RAMYA, 2013]. El problema de este tipo de materiales de electrodo radica en su inestabilidad y, por consiguiente, escasa ciclabilidad, ya que durante los procesos de carga-descarga se producen cambios volumétricos (hinchamientos y contracciones) que provocan la degradación de los electrodos. Por este motivo, muchas investigaciones van dirigidas hacia el estudio de electrodos compuestos por materiales capaces de

ofrecer elevados valores de energía almacenada y posibilidad de suministrar dicha energía durante un número de ciclos elevado, características que se pueden conseguir mediante la combinación de materiales de carbono porosos (carbones activos, nanotubos, nanofibras, geles de carbono, etc.) y polímeros conductores (polipirroles, politiofenos, polianilinas) [AN 2010; JUREWICZ, 2001; RAMYA, 2013; SALINAS-TORRES, 2013; ZHANG, 2009]. En estos casos, las propiedades electroquímicas del sistema se ven mejoradas ya que, por un lado, se aprovecha la elevada pseudocapacidad y conductividad eléctrica de los polímeros y, por otro, las buenas propiedades mecánicas, estructurales y capacitivas del material carbonoso.

- *Materiales de carbono:* Son los compuestos más extensamente estudiados y utilizados como material de electrodo para EDLCs debido a una combinación de propiedades físico-químicas: elevada área superficial específica, buenas propiedades conductoras, alta estabilidad térmica, disponibilidad, fácil procesabilidad y coste de fabricación relativamente bajo [ALONSO, 2006; BURKE, 2000; FRACKOWIAK, 2007; KÖTZ, 2000]. En este tipo de supercondensadores, el almacenamiento de energía se produce por la formación de la doble capa eléctrica. Por este motivo, materiales de electrodo con elevadas áreas superficiales favorecen capacidades de carga elevadas. Los carbones activos son los materiales de carbono que han tenido mayor implantación tecnológica en el campo de los EDLCs. Sin embargo, en los últimos tiempos, otros materiales como nanotubos, nanofibras, aerogeles y xerogeles de carbono, entre otros, han empezado a reivindicarse como excelentes candidatos para el almacenamiento de energía en supercondensadores [CALVO, 2010; FANG, 2006; HALAMA, 2010; OBREJA, 2008; RASINES, 2012; SALIGER, 1998; XU, 2007; ZAPATA-BENABHITE, 2013].

El gran potencial de los carbones activos, es decir, su elevada área superficial, puede suponer, en ciertas ocasiones, una complicación en el proceso de almacenamiento de carga. Teóricamente, cuanto mayor es el área superficial del material de electrodo, mayor capacidad de almacenamiento de energía. Sin embargo, la situación en la práctica es más complicada ya que no todo el área S_{BET} es electroquímicamente accesible cuando se pone en contacto con los iones de electrolito [FRACKOWIAK, 2007]. Algunos autores sugieren que la microporosidad estrecha, es decir, aquella con un diámetro inferior a 0.7 nm, no siempre lleva asociada una elevada capacidad de carga, puesto que poros de tamaño tan pequeño pueden suponer un obstáculo para que tenga lugar una rápida difusión y adsorción de los iones de electrolito [LARGEOT, 2008; SALITRA, 2000; FRACKOWIAK, 2007]. De forma general se acepta que la microporosidad (< 2 nm) es la que más contribuye a la capacidad de almacenamiento de carga, ya que la adsorción de iones tiene lugar fundamentalmente en los microporos. No obstante, una porosidad constituida por micro y mesoporos (diámetro de poro comprendido entre 2-50 nm) es preferible puesto que los mesoporos facilitan el movimiento de los iones de electrolito, dando lugar a un dispositivo electroquímico con mejores prestaciones, especialmente en aplicaciones que requieren elevada potencia y gran rapidez de carga y descarga [FERNÁNDEZ, 2009; FRACKOWIAK, 2007].

En lo que respecta a la mesoporosidad, no existe un tamaño mínimo que propicie la difusión de los iones (puesto que los aniones y cationes solvatados tienen un tamaño inferior al de los mesoporos), pero sí se podría indicar un tamaño de mesoporo máximo (~ 15 nm), ya que mesoporos de gran tamaño contribuyen a reducir la capacidad volumétrica del sistema [ESCRIBANO, 1998; FRACKOWIAK, 2007; QU, 1998].

Con los microporos no ocurre lo mismo. Ya se ha comentado que algunos autores consideran que los ultramicroporos no son útiles para la formación de la doble capa eléctrica. Sin embargo, no es posible definir un diámetro de microporo óptimo puesto que dependerá del tamaño de los cationes y aniones del electrolito empleado. Supercondensadores basados en electrolitos orgánicos y líquidos iónicos precisarán electrodos compuestos por microporos más anchos que cuando se utilizan disoluciones acuosas como electrolito. Por ejemplo, R. Mysyk y col. [MYSYK, 2009] publicaron un trabajo sobre la importancia de la distribución de tamaños de microporo en la acumulación de carga mediante la formación de la doble capa eléctrica. Los autores evaluaron el comportamiento electroquímico de varios carbones activos frente a electrolitos acuosos (H_2SO_4 y KOH) y un electrolito orgánico ($TEABF_4$). De acuerdo con los resultados de capacidad volumétrica, los autores sugieren que en medios acuosos, la eficiencia de los poros para formar la EDL aumenta cuando los poros tienen un tamaño próximo a 0.7 nm, mientras que el tamaño debe ser ligeramente superior para el caso del electrolito orgánico (~ 0.8-0.9 nm), resultados similares a los obtenidos por otros investigadores [CHMIOLA, 2006; GUO, 2012]. B. Xu y col. [XU, 2013], presentaron recientemente un estudio en el que se ensalza la importancia de los ultramicroporos en los procesos de almacenamiento de energía. Como material de electrodo se emplea un carbón poroso formado por ultramicroporos cuyo distribución de tamaños de poro se centra en 0.55 nm (ultramicroporos comprendidos entre 0.4 y 0.7 nm). En este caso, los autores plantean un diámetro de poro de 0.55 nm, como el tamaño ideal para que se produzca el almacenamiento de carga en un medio acuoso (KOH), mientras que dicho tamaño es insuficiente en el caso del electrolito orgánico $TEABF_4$/PC, ya que da lugar a valores de capacidad específica muy pobres. Las dimensiones del catión Et_4N^+ solvatado y sin solvatar son 1.30 y 0.68 nm, respectivamente, tamaños muy superiores al de los poros presentes en el material de electrodo, por lo que la difusión de los iones para formar la doble capa eléctrica se ve muy impedida. Todos estos trabajos ponen de manifiesto la importancia de adaptar el tamaño de los poros del material de electrodo a las dimensiones de los iones de la solución utilizada como electrolito.

Es evidente que los materiales de carbono almacenan energía, fundamentalmente, gracias al mecanismo de la doble capa eléctrica. Sin embargo, también puede haber cierta contribución pseudocapacitiva como consecuencia de reacciones redox que sufren especies electroactivas presentes en la superficie del material de electrodo. Los heteroátomos más comúnmente encontrados en materiales de carbono empleados como electrodos en supercondensadores son oxígeno (-COOH, =CO,

-OH...), nitrógeno (estructuras tipo piridina, pirrol, N cuaternario, N-óxido, etc.), fósforo, boro, especies metálicas (Mo, W, Mn, Fe), etc. [HULICOVA-JURCAKOVA, 2009; INAGAKI, 2010; LOZANO-CASTELLÓ, 2003; SEPEHRI, 2009; ZAPATA-BENABITHE, 2012; ZAPATA-BENABITHE, 2013]. La presencia de estas especies no sólo contribuye a un aumento de la capacidad global del sistema debido a la pseudocapacidad originada sino que, además, mejora la mojabilidad de los electrodos facilitándose el transporte de iones. La contribución a la capacidad de grupos superficiales oxigenados ha sido ampliamente investigada por diferentes autores [BLEDA-MARTÍNEZ, 2005; CENTENO, 2009; HSIEH, 2002; INAGAKI, 2010 LOZANO-CASTELLÓ, 2003; RUIZ, 2013; ZAPATA-BENABHITE, 2012]. La mayoría de ellos coincide en que no todos los grupos oxigenados tienen un efecto positivo sobre el comportamiento electroquímico del supercondensador. Es más, muchos autores han afirmado que los grupos oxigenados superficiales que desorben como CO (por ejemplo, funcionalidades oxigenadas tipo carbonilo o quinona) contribuyen a mejorar las propiedades electroquímicas del supercondensador mientras que aquellos que evolucionan dando lugar a CO_2 (grupos oxigenados de carácter ácido) pueden tener un efecto negativo.

1.3.3. EDLCs basados en materiales carbonosos

La capacidad de un condensador de doble capa eléctrica viene determinada por la ecuación 1.1:

$$C = \frac{Q}{V} \qquad [1.1]$$

donde Q es la carga que es capaz de almacenar el sistema electroquímico (culombios) y V la diferencia de potencial aplicada (voltios). Además de esta ecuación, por analogía con un condensador de placas paralelas, la capacidad también viene determinada por la siguiente expresión:

$$C = \frac{A\varepsilon\varepsilon_0}{d} \qquad [1.2]$$

donde A representa el área de contacto entre el electrodo y electrolito (m^2), d es el espesor de la doble capa eléctrica (longitud que está influenciada por la concentración del electrolito y el tamaño de sus iones, siendo generalmente del orden de $5\text{-}10\cdot10^{-10}$ m para disoluciones concentradas), ε es la permitividad o constante dieléctrica del electrolito (F m^{-1}) y ε_0 corresponde con la permitividad del vacío ($8.85\cdot10^{-12}$ F m^{-1}).

Además de la capacidad, el comportamiento de un supercondensador también viene caracterizado por la máxima cantidad de energía que es capaz de almacenar y la máxima potencia suministrada, magnitudes que se determinan a partir de las siguientes ecuaciones:

$$E = \frac{CV^2}{2} \qquad [1.3]$$

$$P = \frac{V^2}{4R} \qquad [1.4]$$

donde R designa la resistencia en serie equivalente (ESR) del dispositivo electroquímico, que viene determinada por la resistencia intrínseca de los electrodos, resistencia de contacto entre los electrodos y colectores de corriente y resistencia iónica del electrolito (dificultad de los iones para acceder a los poros del electrodo y para difundir por el material separador) [LI, 2013].

Como se ha indicado en líneas superiores, la capacidad de un supercondensador depende esencialmente del material de electrodo, el cuál debe presentar una elevada superficie activa y una distribución de tamaños de poro determinada. No obstante, de acuerdo con las expresiones 1.3 y 1.4, tanto la densidad de energía como la densidad de potencia aumentan cuanto mayor es el voltaje de trabajo, parámetro que viene restringido por la ventana de estabilidad del electrolito. En el caso de electrolitos acuosos el voltaje de una celda simétrica está limitado a ~ 1 V, puesto que por encima de ese valor tiene lugar la descomposición electrolítica del agua (1.23 V). Sin embargo, es posible incrementar el voltaje de trabajo y, por consiguiente, la energía y potencia específica de un supercondensador mediante el uso de electrolitos de naturaleza orgánica, los cuales permiten trabajar en el rango de 2.0-2.5 V y líquidos iónicos, en cuyo caso es posible utilizar un voltaje de trabajo de 2.5-3.5 V [BURKE, 2000; LI, 2013]. El empleo de estos dos tipos de electrolito no implica necesariamente una mejoría en la potencia suministrada por el supercondensador puesto que, de acuerdo con la ecuación 1.4, la potencia específica es inversamente proporcional a la resistencia en serie equivalente de la celda (ESR), parámetro que está notablemente influenciado por la conductividad iónica del electrolito (por ejemplo, disoluciones de H_2SO_4 y KOH presentan valores de conductividad iónica de 730 y 540 mS cm^{-1}, respectivamente, mientras que ese valor no supera los 60 mS cm^{-1} para una mezcla de $TEABF_4$/acetonitrilo) [GALINSKI, 2006]. Por este motivo, hay que alcanzar un compromiso entre voltaje de trabajo y conductividad iónica del electrolito. En este sentido, se están llevando a cabo diferentes estrategias como son: (i) fabricación de supercondensadores asimétricos basados en electrolitos acuosos (electrodo negativo constituido por un material de carbono y un óxido metálico actuando como electrodo positivo [HONG, 2002; KHOMENKO, 2006]), lo que permite ampliar el voltaje de trabajo de la celda sin que ello suponga el empleo de electrolitos muy resistivos; (ii) empleo de electrolitos basados en líquidos iónicos, que incrementan la capacidad de almacenamiento de energía de los supercondensadores puesto que les permite cargarse a voltajes más altos [ARBIZZANY, 2008; BALDUCCI, 2004; KUMAR, 2010]. Más información acerca de este tipo de electrolitos aparece recogida en el Capítulo 5 de la presente memoria, puesto que uno de los trabajos que ha dado lugar a esta Tesis Doctoral versa sobre el empleo de líquidos iónicos próticos de diversa naturaleza como electrolitos de supercondensadores basados en xerogeles de carbono (*Publicación IX*).

En concordancia con lo expuesto anteriormente, la investigación que ha dado lugar a esta Tesis Doctoral se ha centrado, fundamentalmente, en dos puntos: (i) síntesis de materiales de electrodo altamente porosos que garanticen una elevada capacidad de almacenamiento energético y (ii) preparación de supercondensadores compuestos por diversos electrolitos y diferente configuración para poder así incrementar el voltaje de trabajo de la celda y suprimir una de las limitaciones de los supercondensadores en comparación con otros dispositivos de almacenamiento energético, su limitada densidad de energía.

1.3.4. Aplicaciones

Por todo lo mencionado hasta el momento sobre los supercondensadores, su principal campo de aplicación se centra en aquellas aplicaciones que requieren potencias elevadas durante periodos breves ($10^{-2} \leq t \leq 10^{2}$ segundos) o aquellas en las que lo verdaderamente importante es un ciclo de vida largo, como es el caso de algunos dispositivos electrónicos portátiles. Es necesario señalar que en muchas de estas aplicaciones, los supercondensadores no se utilizan como único dispositivo de almacenamiento de energía sino como sistemas complementarios a las baterías o pilas de combustible [KÖTZ, 2000]. Actualmente, el campo de aplicación de los supercondensadores se puede dividir en tres sectores:

- *Sector del transporte:* Una aplicación muy interesante de los condensadores electroquímicos es su utilización en vehículos eléctricos (automóviles, autobuses, furgonetas, ferrocarril, tranvía, etc.). En este caso, los supercondensadores se encargan de suministrar las puntas de potencia necesarias en pendientes o adelantamientos y recuperar la energía generada durante el frenado, mientras que otro dispositivo de almacenamiento de energía (batería o pila de combustible) es el que proporciona la energía que necesita el vehículo en condiciones de circulación normal. Ejemplos: París (2009), se ha lanzado una flota de autobuses híbridos (construidos por la empresa Alemana *Maschinenfabrik Augsburg-Nürnberg*), propulsados por un motor diesel y un sistema de supercondensadores. En este caso la energía necesaria para el arranque de los autobuses es suministrada por los supercondensadores mientras que el motor diesel se pone en funcionamiento una vez que los autobuses están ya en marcha. Otro ejemplo es el sistema KERS (*Kinetic Energy Recovery System*) implantado en algunas escuderías de Fórmula 1. Este sistema se utiliza para capturar la energía generada en la frenada y liberarla en otros puntos del circuito durante unos segundos. Inicialmente, el sistema KERS estaba formado por baterías de Ion-Litio, sin embargo, escuderías como Red Bull han empezado a utilizar un sistema de almacenamiento de energía híbrido empleando supercondensadores para el almacenamiento de energía a corto plazo y rápidas descargas de energía y baterías de Ion-Li para la acumulación de mayor duración. Otros medios de transporte presentes en el mercado que utilizan sistemas basados en supercondensadores son: *Honda FCX Clarity*, *BMW X3 Hybrid*, *Mazda 6*, tranvías *Mitrac Energy Bombardier* presentes en Heidelberg (Alemania), tranvías fabricados por la factoría *CAF* que actualmente están en fase de prueba en las ciudades de Sevilla y Zaragoza, etc.

❖ *Apoyo energético:* Consiste en emplear los supercondensadores como apoyo a la red eléctrica para compensar fluctuaciones de corta duración. En el caso de producirse un problema en la red de distribución de energía eléctrica, la fuente primaria dejará de funcionar y es el supercondensador el que se encargará de generar pulsos de potencia hasta que se restablezca el funcionamiento normal, momento en el que el supercondensador se recargará de nuevo con el objetivo de estar disponible frente a otro fallo en el suministro eléctrico. También se ha planteado el uso de supercondensadores para nivelar el suministro eléctrico aportado por fuentes intermitentes de energía, como la solar y la eólica. Por ejemplo, en el caso de la energía solar, durante el día la carga eléctrica es suministrada por celdas fotovoltaicas que convierten la energía solar en electricidad mientras que, a lo largo de la noche, puede ser el supercondensador el encargado de ofrecer la potencia necesaria. En la actualidad ya existen algunos dispositivos basados en esta tecnología: linternas solares, señales de tráfico, etc.

❖ *Industria electrónica:* Los supercondensadores aún no pueden competir totalmente con las características de las baterías, ya que no alcanzan los valores de densidad de energía que éstas ofrecen. En cambio, pueden alargar el tiempo de vida, lo que es realmente importante en el caso de dispositivos electrónicos. En este tipo de aparatos, los supercondensadores suelen actuar como fuente principal de almacenamiento de energía. Algunos de los dispositivos electrónicos que emplean condensadores electroquímicos son: cámaras fotográficas, teléfonos móviles, atornilladores eléctricos, juguetes, etc.

Figura 1.4. Ejemplo de diversas presentaciones de supercondensadores comerciales.

1.4. XEROGELES DE CARBONO

Los geles de carbono son unos materiales nanoporosos, formados mayoritariamente por carbono (C > 90 %), que se obtienen mediante reacciones de policondensación entre bencenos hidroxilados (**resorcinol**, fenol, catecol, etc.) y aldehídos (**formaldehído**, furfural, etc.), en un disolvente determinado (**agua**, metanol o acetona, entre otros), seguidas de una etapa de secado y posterior carbonización [MORENO-CASTILLA, 2005].

Entre sus principales características se pueden encontrar su elevada área superficial, baja resistencia eléctrica, diseño de sus propiedades porosas y estructurales en función de las condiciones de síntesis y procesado, diversas morfologías (polvo, monolitos, esferas, etc.), entre otras [AL-MUHTASEB, 2003; MAHATA, 2008; MORALES-TORRES, 2012; SCHMIT, 2001; ZAPATA-BENABHITE, 2012; ZUBIZARRETA, 2008A]. Por este motivo, los geles de carbono, y más concretamente los xerogeles de carbono (materiales sintetizados en el presente trabajo) se han postulado como una alternativa muy prometedora para el almacenamiento de energía en condensadores de doble capa eléctrica. Sin duda, entre todas sus propiedades, el punto fuerte para la aplicación investigada en esta Tesis Doctoral pasa por el control de sus características porosas puesto que, como se ha comentado en la sección anterior, un requisito imprescindible de los electrodos para EDLCs es poseer una elevada área superficial junto con una distribución de tamaños de poro adecuada.

Existen diferentes variables que determinan la porosidad de los geles de carbono (monómeros, disolvente, pH inicial, catalizador, tiempo y temperatura de polimerización, mecanismo de calentamiento, condiciones de secado, carbonización y activación, etc.), aunque no todas ellas tienen repercusión sobre el mismo rango de porosidad [FAIRÉN-JIMÉNEZ, 2006; GALLEGOS-SUÁREZ, 2012; HORIKAWA, 2004; JOB, 2004; LIN, 2000; MAHATA, 2008; MORALES-TORRES, 2012; XU, 2012; ZAPATA-BENABITHE, 2012; ZUBIZARRETA, 2008A; ZUBIZARRETA, 2008B]. Por ejemplo, variables como pH inicial, disolvente o mecanismo de calentamiento tienen una notable influencia sobre la meso-macroporosidad de estos materiales, mientras que la microporosidad, en cambio, se controla gracias a procesos de carbonización y activación.

El principal punto débil de los geles de carbono se asocia con su largo y tedioso proceso de fabricación, repercutiendo en un precio superior al de carbones activos comerciales obtenidos a partir del tratamiento de diferentes clases de residuos. La obtención de xerogeles de carbono mediante rutas convencionales pasa por un primer calentamiento, a una temperatura no superior a 100 ºC, durante aproximadamente 72 h (tiempo en el que se producen las reacciones de polimerización entre el resorcinol y formaldehído, monómeros utilizados en este trabajo), seguido de otra etapa de calentamiento a ~ 150 ºC durante 24 h que permite la completa evaporación del disolvente [PEKALA, 1989; JOB, 2004], proceso excesivamente largo para implantarlo a escala industrial y obtener un producto final competitivo y económicamente rentable.

Como se puede comprobar a partir de las publicaciones científicas recogidas en la presente memoria, la fabricación de xerogeles de carbono se puede simplificar enormemente gracias a la tecnología microondas. El proceso de síntesis asistido con microondas se ha desarrollado desde su origen en el grupo de investigación *Microondas y Carbones para Aplicaciones Tecnológicas* [ARENILLAS, 2009] y actualmente dicha tecnología está siendo explotada por la spin-off *Xerolutions S.L.* La radiación microondas aplicada a las etapas de gelación, curado y secado ha permitido obtener xerogeles

resorcinol-formaldehído en un tiempo no superior a 5 horas, con propiedades muy similares a sus homólogos obtenidos a partir de rutas convencionales (xerogeles de carbono micro-mesoporosos o micro-macroporosos, dependiendo de las condiciones de síntesis). Como se muestra en la *Publicación III* adjuntada en el Capítulo 4, el calentamiento con microondas también se puede aplicar durante la etapa de activación, lo que es un punto a favor de esta tecnología ya que permite obtener xerogeles de carbono altamente porosos mediante una dispositivo simple, barato y fácilmente escalable.

Más información acerca de la síntesis y propiedades de los xerogeles de carbono, procesos de activación, post-tratamientos (oxidación, dopaje, etc.), aplicaciones, etc., se puede encontrar en el capítulo del libro "Nanomaterials", *Designing Nanostructured Carbon Xerogels* adjuntado a continuación como *Publicación I.*

Publicación I

DESIGNING NANOSTRUCTURED CARBON XEROGELS

Nanomaterials

(Edited by Mohammed Muzibur Rahman)

9 (187-234)

Año: 2011

9

Designing Nanostructured Carbon Xerogels

Esther G. Calvo, J. Ángel Menéndez and Ana Arenillas
Instituto Nacional del Carbón (CSIC), Oviedo, Spain

1. Introduction

Until the discovery of carbon gels in 1890, inorganic gels had dominated sol-gel literature. Traditional inorganic gels based upon hydrolysis-condensation reactions of metal alkoxides are well known as a result of their high specific surface areas and their unique morphological and structural properties (De Sousa et al., 2001). Some of the precursors used for the preparation of such inorganic gels are aluminates, titanates and borates but the most frequently employed alkoxides are alkoxysilanes, leading to the extensively investigated silica gels (Mauritz, 1998; Zareba-Grodz et al., 2004). The reaction mechanism of silica gels is based on the hydrolysis of alkoxysilanes to yield silicic acid moities, $Si(OH)_4$, which spontaneously condensate to generate, after a sequence of specific stages, the final silica gel consisting of siloxane groups (Si-O-Si) within its framework and silanol groups (Si-OH) on its surface (Salazar-Hernández et al., 2009). Some of the attractive features of silica gels are: the tailored textural and structural properties, abundance and low cost, high sorption capacity, very high thermal shock resistance, insolubility in most solvents and lower index of refraction compared to other inorganic gels. It is for these reasons that they are used in a wide range of industrial applications including catalysis, chromatography, drug delivery and ion exchange (Qu et al., 2008; Teng et al., 2010).

It was the great interest aroused by inorganic gels, especially in the case of silica gels, in different fields of application together with the advantages associated with sol-gel methods, i.e. low temperature processing, the high homogeneity of final products and the possibility of controlling their surface properties (Houmard et al., 2009), that persuaded Pekala and co-workers to go an step further and apply this sol-gel methodology to the synthesis of organic gels (Pekala, 1989). The first organic gel was obtained by sol-gel polymerization of resorcinol and formaldehyde under alkaline conditions and supercritical drying. This produced a material called organic aerogel, consisting of interconnected colloidal particles approximately 10 nm in diameter. Properties such as low density, highly porous material and high versatility of the sol-gel process turned the carbon gel into a prominent member of the "carbon family".

Basically, an organic gel is a solid nanostructure comprised of nano-sized pores and interlinked primary particles obtained by means of polymerization reactions between hydroxylated benzenes and aldehydes, and then subjected to a drying process. The most commonly used monomers are resorcinol and formaldehyde (Al-Mutasheb & Ritter, 2003; Czzakel et al., 2005; Job et al., 2004; Tian et al., 2011a; Zhang et al., 2007; Zhu et al., 2007; Zubizarreta et al., 2008a) but, there are other potential combinations such as phenol/formaldehyde (Mukai et al., 2005a; Scherdel & Reichenauer, 2009; Teng & Wang,

2000), phenol/furfural (Dingcai & Ruowen, 2006; Long et al., 2008a; Pekala et al., 1995), phenol/melamine/formaldehyde (Long et al., 2008b), cresol/formaldehyde (Li et al., 2001; Zhu et al., 2006), etc. As shown in Figure 1, the formation of organic gels involves the following stages: (i) formation of a three-dimensional polymer in a solvent, known as gelation step, (ii) curing period where the crosslinking of previously formed polymer clusters (particles) takes place and, finally, (iii) drying step, that can be performed under subcritical, supercritical or freezing conditions, resulting in xerogels, aerogels and cryogels, respectively (Al-Mutasheb & Ritter, 2003; Czzakel et al., 2005; Job et al., 2004; Zubizarreta et al., 2008a). The last step needed to produce carbon gels is carbonization, with the purpose of removing any remaining oxygen and hydrogen groups, yielding a thermally stable nanostructure mainly composed of carbon. This carbonization is usually performed at high temperatures (approximately 600-1000 °C) under an inert atmosphere, such as N_2, He or Ar (Al-Mutasheb & Ritter, 2003; Calvo et al., 2011a; Lin & Ritter, 2000; Job et al., 2004). However, as will be discussed in Section 2.2 of this chapter, it is possible to use other reactive gases in order to modify the chemical composition of carbon gels (Kang et al., 2009).

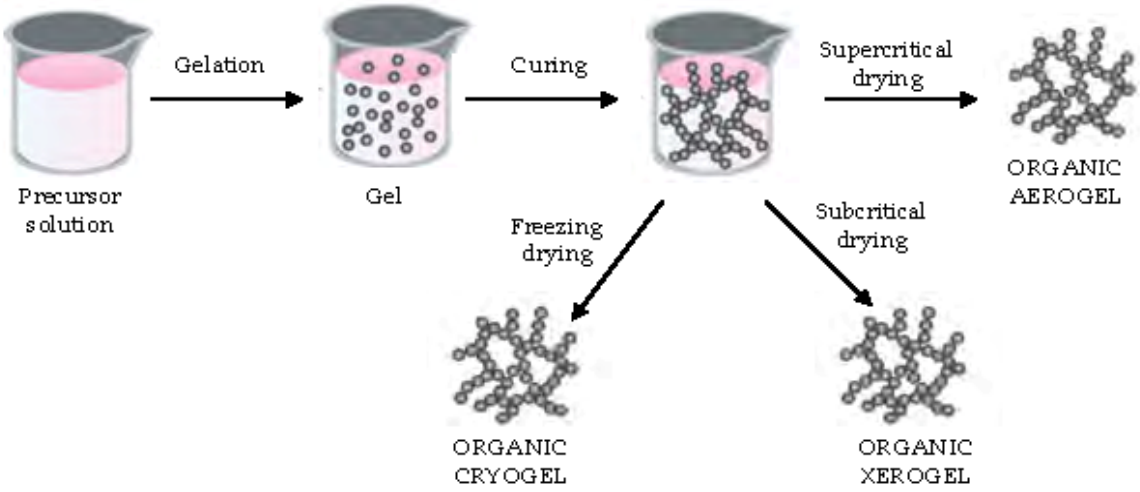

Fig. 1. Schematic representation of the steps involved in the synthesis of organic gels.

All the synthesis steps, referred to in the preceding paragraph, interfere in the development of the porosity of carbon gels. This gives an idea not only of the versatility of this type of carbonaceous materials but also of their complexity, since most of variables involved in the synthesis procedure are not independent, i.e. each one influences not only in certain properties of the gel but may also modify the effect of other variables (Job et al., 2006; Quin & Guo, 2001). The most important parameters that affect the properties of carbon gels are the pH of the precursor solution and the nature and concentration of the reactants, since variations in these parameters cause significant changes in the final porous properties of the carbon gel, making it possible to go from a totally non-porous material to a very highly porous carbon gel by only modifying one of these parameters. However, there are also other variables to consider such as temperature and time of gelation and curing stages, the nature of the solvent and addition of surfactants during the drying step, as these also have an important influence on the development of different properties of carbon gels (Al-Mutasheb & Ritter, 2003; Job et al., 2007a; Kraiwattanawong et al., 2011; Matos et al., 2006; Tian et al., 2011b). In so far as the carbonization step is concerned, there are several parameters that

have a notable impact on the final characteristics of carbon gels, these include the carbonization temperature and time or the nature and flow rate of the carrier gas (Al-Mutasheb & Ritter, 2003; Lin & Ritter, 2000; Tamon et al., 1998).

The increasing popularity of carbon gels is largely due to their unique and controllable physicochemical properties such as their specific surface areas ranging from about 500 to 1200 m^2 g^{-1}, high pore volumes, low density, excellent electrical conductivity, high purity and the possibility of synthesizing them in the form of monoliths, powders, microspheres or thin films, with high packing densities (some of these shapes are shown in Figure 2) (Al-Mutasheb & Ritter, 2003; Juárez-Pérez et al., 2010; Mahata et al., 2008). The combination of these properties makes carbon gels the perfect candidates for diverse applications such as supercapacitors, fuel cells, desalination systems, catalyst supports, liquid and gas-phase adsorbents, etc. (Calvo et al., 2008; Frackowiak & Béguin, 2001; Moreno-Castilla et al., 2005; Zheivot et al., 2010; Zubizarreta et al., 2010). However, despite the large number of advantages associated with carbon gels, there are still some applications where it is preferable to use activated carbons as a result of their low production costs. The method of synthesis of carbon gels is the main hindrance to their implantation at industrial scale because with conventional methods, where gelation, curing and drying stages are performed in conventional furnaces, several days are required to produce the final materials. Of the three stages involved in the synthesis of organic gels, drying is the most expensive. This is due to, except in the case of subcritical drying, under supercritical and freezing conditions, it is necessary to perform solvent exchanges, which requires several days, and in the most extreme conditions of drying entails a substantial increase in production costs (Liu et al., 2006; Tamon et al., 2000; Zhang et al., 2007). Consequently, the research in this field is being addressed to the development of faster and cheaper methods of synthesizing carbon gels in order to make them more attractive and competitive than the activated carbons used until now (Calvo et al., 2008, 2011; Conceição et al., 2009; Tonamon et al., 2006; Zubizarreta et al., 2008b). Some of these works are based on the use of different types of electromagnetic radiation as a heating source for one or several stages of the synthesis process. As will be explained in more detail in Section 2.4, microwave and ultrasonic radiation are the most widely investigated of the new synthesis techniques, being the results very promising not only because they meet the target of lower production times and costs but also they produce carbon gels with properties similar to those obtained using more established methods (Calvo et al., 2008, 2011; Zubizarreta et al., 2008b).

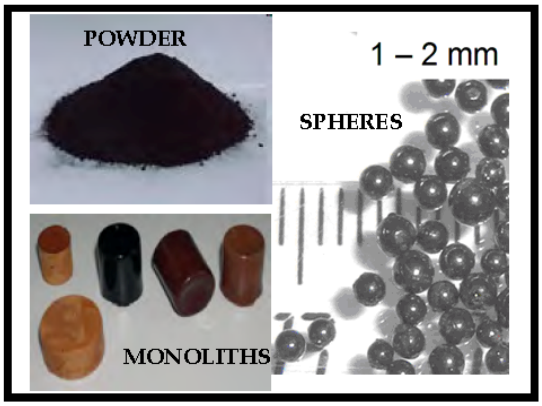

Fig. 2. Carbon xerogels presented in different shapes.

To increase the porosity of carbon gels or to enrich their chemical structure, carbon gels can be subjected to various activation, oxidation and doping processes. Activation processes can be performed during or after the carbonization step and the properties of the final carbonaceous material will be greatly influenced by the sequence used. The purpose of activation is to increase the surface area and pore volume created during the synthesis of organic gels and to promote pore widening, especially in the case of narrow pores (Contreras et al., 2010; Silva et al., 2009; Zubizarreta et al., 2008c). In Section 2.2, the different types of activation processes and the corresponding properties of carbonaceous materials produced are reviewed in more detail but, by way of introduction it may be said that there are two types of activation processes, chemical and physical activation, both with their respective advantages and disadvantages, and each of them generating carbon gels with specific textural and structural characteristics (Contreras et al., 2010). The surface areas of most carbon gels vary between 600-700 $m^2 g^{-1}$, but after an activation process, this value may increase to 2000-3000 $m^2 g^{-1}$. In other words, the porosity may be tripled which is a great advantage in applications that require highly porous materials such as supercapacitors, hydrogen storage or catalysis.

There are several published works that deal with ways to modify the chemical nature of carbon gels by means of doping or oxidizing processes in order to widen their range of applications (Gryzb et al., 2010, Job et al., 2007b; Lee et al., 2011; Sepheri et al., 2009; Silva et al., 2009; Zubizarreta et al., 2010). The porous texture of carbon gels is a crucial property in most of the fields of application. However, it is not the only one that determines the performance as the surface chemistry is also a key factor. Thus, several studies focus on the incorporation of oxygen functional groups by means of different oxidation processes (Mahata et al., 2008; Silva et al., 2009), the incorporation of nitrogen groups by using nitrogen-containing monomers or post-synthesis treatments (Gorgulho et al., 2009; Kang et al., 2009; Long et al., 2008b; Pérez-Cadenas, 2009) and the modification of carbon gels with the incorporation of metal species into the carbon framework (Bekyarova & Kaneko, 2000; Chandra et al., 2011; Cotet et al., 2006; Job et al., 2007b; Liu et al., 2006; Tian et al., 2010). In the synthesis process of carbon gels based on sol-gel methodology, these above-mentioned treatments can be performed using different reagents and conditions, making it necessary to optimize the operating conditions to meet the requirements of each individual case. In Section 2.3, different types of oxidative treatments and doping processes will be discussed in the light of the characteristics of the carbon gels produced. There are a lot of variables suitable to be adjusted in order to tailor the properties of the final carbon gel. All these tailored characteristics of the designed material (i.e. porous, chemical, mechanical characteristics) are described in Section 3 and directly connected to both the operating conditions of the synthesis of the materials and the suitability of the further application. Due to the great versatility of these kind of materials there area a wide range of applications in very different fields like adsorption (in gas and liquid media), catalysis, energy storage, etc. A review of these possible application fields are presented in the Section 4 of this chapter.

2. Synthesis of nanostructured carbon xerogels

Carbon gels are polymeric nanostructured carbon materials that can be synthesized by different procedures, all of them based on a hydrolysis-condensation reaction between hydroxybenzenes and aldehydes. There are several precursors that can be used to develop carbon gels including phenol, resorcinol or cresol in the case of hydroxybenzenes whereas as aldehyde it is possible to use formaldehyde, furfural, etc. (Czzakel et al., 2005; Dingcai &

Rouwen, 2006; Long et al., 2008a, 2008b; Pekala et al., 1995; Scherdel & Reichenauer, 2009). Amongst all the possible variations, probably the most commonly synthesized carbon gels are those based on resorcinol and formaldehyde, although in order to reduce the cost of the materials involved in the synthesis process, some less expensive precursors, such as phenol (Mukai et al., 2005a; Scherdel & Reichenauer, 2009; Teng & Wang, 2000) or cellulose (Gryzb et al., 2010), have attracted interest in recent years. Another important parameter for the preparation of carbon gels is the reaction media because there are several available solvents such as deionised water (Job et al., 2004; Pekala, 1989; Zhu et al., 2007), acetone (Berthon et al., 2001) or methanol (Zubizarreta et al., 2008a). It goes without saying that the least expensive reaction media is water, although other solvents are preferred in certain conditions in order to obtain specific final properties. Once the reagents involved in the sol-gel process have been selected, the recipe for producing carbon gels is the following. First, hydroxybenzene, aldehyde, solvent and catalyst are mixed in suitable molar ratios and then the solution is heated in order to obtain a stable crosslinked gel, which is saturated with solvent and it must next be dried. As will be seen throughout this section, there are several drying methods resulting in materials with different properties (Czzakel et al., 2005; Job et al., 2005). The last essential step for obtaining carbon gels is thermal stabilization, i.e. treatment at high temperature under inert atmosphere, yielding a thermally and chemically stable carbon gel.

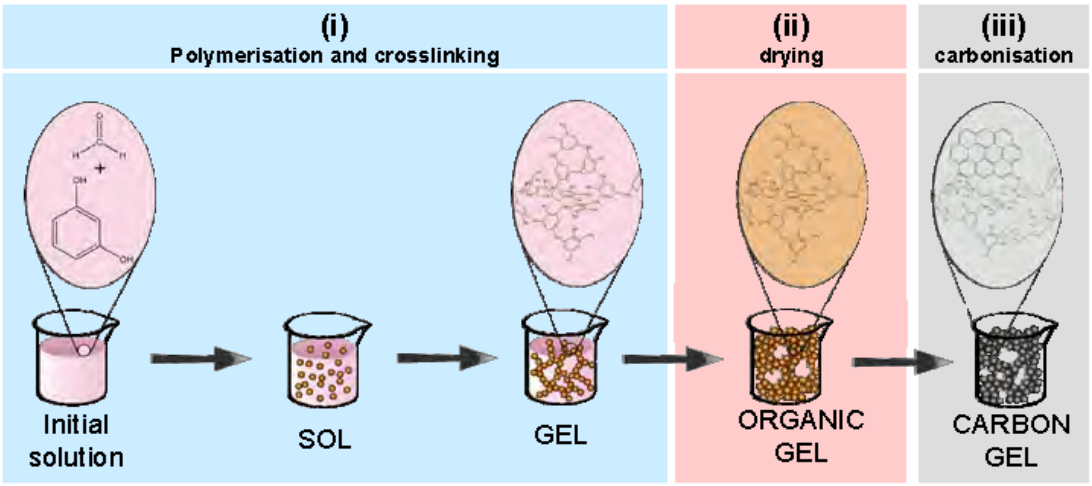

Fig. 3. Different stages involved in the synthesis process of carbon gels.

Figure 3 shows the main stages involved in the synthesis process of carbon gels by means of the polycondensation of a hydroxilated benzene and an aldehyde (resorcinol and formaldehyde in this particular case). These stages are as follows: (i) sol-gel reaction, i.e. the formation and crosslinking of polymeric particles, (ii) drying of the solvent-saturated gel and, finally, (iii) carbonization of the organic gel to yield the final carbon gel.

2.1 Synthesis steps for organic gels

As already mentioned at the beginning of Section 2, the synthesis process of organic xerogels is clearly divided into two main steps: (i) polymerization and crosslinking reactions between resorcinol-formaldehyde aggregates (gelation and curing stages) and, (ii) drying process. Each step plays an important role in determining the final properties of the xerogel, and therefore deserves a detailed description.

2.1.1 Polymerization and crossliking

The polymerisation and crossliking reactions, also referred as the gelation and curing processes, take place during the sol-gel reaction between resorcinol and formaldehyde. According to some published works (Lin & Ritter, 1997; Pekala & Alviso, 1992), the polymerisation mechanism includes two steps: (i) addition reaction to form hydroxymethyl derivatives of resorcinol and, (ii) condensation of hydroxymethyl derivatives to form methylene or methylene ether bridged compounds. After these reactions a polymer is formed and, as a consequence, the initial solution loses fluidity, producing a special material called gel, and the time which it takes for the gel formation is named *gelation time*. The curing step of the gel is an extension of the process whereby the crosslinking of polymeric aggregates previously formed in the gelation stage is favoured, so that a three-dimensional crosslinked polymer is obtained.

As can be seen in the reaction scheme represented in Figure 4, the formation of resorcinol anions via the abstraction of hydrogen is enhanced by the basic media. Resorcinol is a trifunctional fenolic compound that is able to add formaldehyde molecules in three different positions (2, 4 and 6), but these uncharged molecules are less reactive than the corresponding resorcinol anions. Therefore, when there are OH^- anions in the reaction media, the hydrogen of resorcinol molecules is abstracted promoting the formation of hydroxymethyl derivates. In the second stage, the condensation of these hydroxymethyl derivates proceeds via acidic media, generating colloidal particles that start to crosslink producing aggregates with a diameter of around 7-10 nm (Al-Mutasheb & Ritter, 2003).

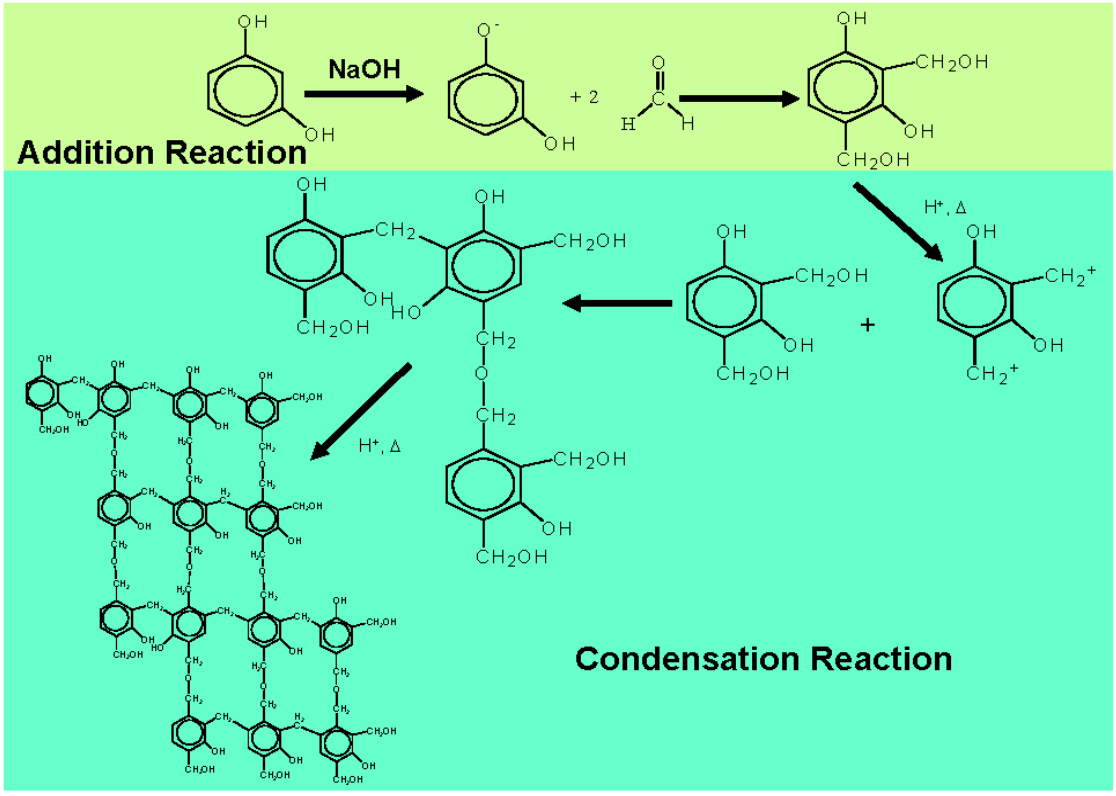

Fig. 4. Mechanism of resorcinol-formaldehyde polymerization (based on reference Al-Mutasheb & Ritter, 2003).

According to this mechanism, the initial pH of the solution is a very important operating condition because it controls the polymerisation, the subsequent crooslinking and therefore, the final porous texture of carbons gels. It is for this reason that some compounds are usually added to the reactants in order to modify the pH of the media. Some authors claim that these compounds are simply pH regulators and therefore not the usually named catalysts (Job et al., 2005) while others postulate that the nature of the compound used (i.e., an ion) is going to have a direct bearing on the pH and therefore it is a real catalyst (Fairén-Jiménez et al., 2006; Tian et al., 2011b). In any case, independently on the nature of the compound used the R/C (resorcinol/catalyst molar ratio), is a parameter usually mentioned in the synthesis receipt and it is directly related with the pH of the reaction media. Therefore, at high catalyst concentrations, i.e. as the pH increases, the first addition reaction is favoured and therefore, very branched and unstable aggregates are formed, leading to smaller more interconnected polymer particles (see Figure 5b). The condensation reaction resulting from such small particles produces materials with smaller pores (Lin & Ritter, 1997; Job et al., 2004). In contrast, when the initial pH decreases, the formation of hydroxymethyl derivates is slow; this results in a smaller number of resorcinol anions. Naturally, polymeric particles have enough time to grow, producing large but weakly branched aggregates. The condensation of such less interconnected polymeric particles leads to higher pore sizes, illustrated in Figure 5c. Therefore, it is possible to affirm that the pH of the precursor solution plays a very important role in the sol-gel reaction because it determines the size of the polymeric particles formed during the gelation and curing stages and, accordingly, the size of the pores in the final carbonaceous material (Calvo et al., 2011a; Lin & Ritter, 1997; Job et al., 2004; Zubizarreta et al., 2008a).

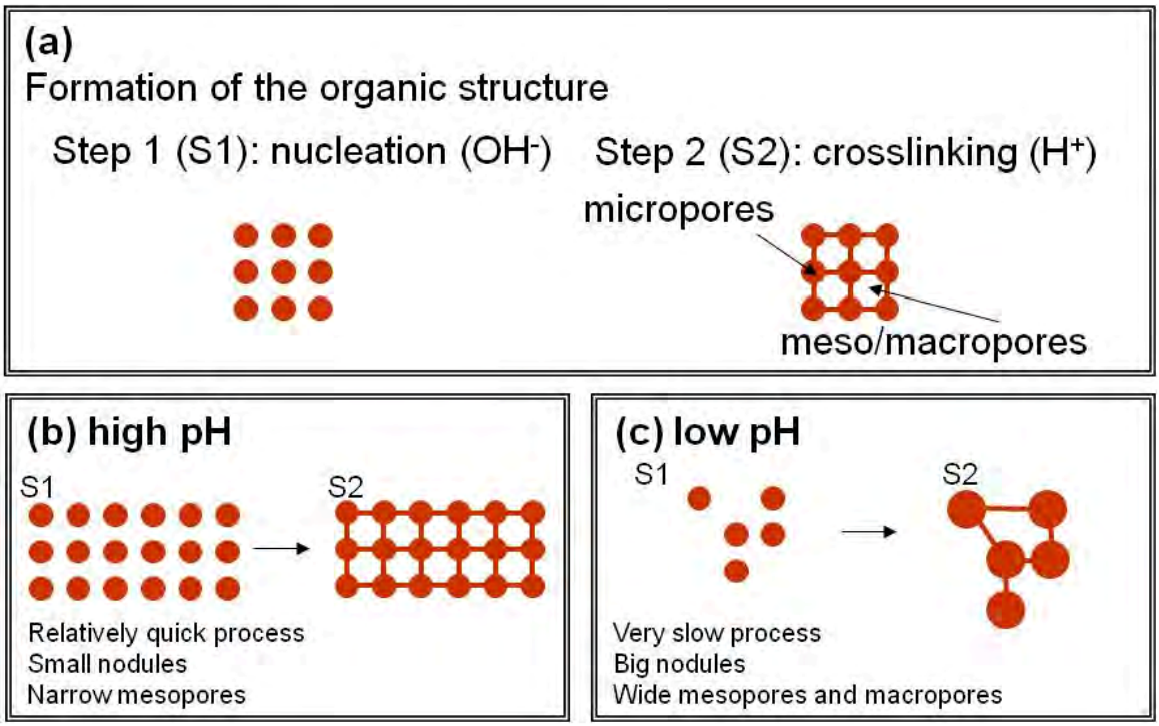

Fig. 5. Schematic representation of the influence of the pH of the precursor solution on the final nanostructure of the carbon gels obtained.

2.1.2 Drying

Once a stable three-dimensional polymer has been obtained, it is necessary to remove the solvent used as the reaction media. There are different types of drying methods, each of which produces materials with different properties. Therefore drying is another synthesis condition that needs to be taken into account when trying to control the final properties of the nanostructure organic gel (Czzakel et al., 2005; Job et al., 2005). The most widely drying methods used are: (i) subcritical drying, i.e. drying the gels by simple evaporation of the solvent (at ambient pressure and temperatures of around 100-150 °C); (ii) supercritical drying, which means eliminating the solvent in supercritical conditions (high pressures and temperatures), and (iii) freeze-drying, i.e. the solvent is frozen and then removed by sublimation. A scheme of the different ways of eliminating the solvent is presented in Figure 6, whilst a more detail description of each of them and their influence on the final properties of the carbon gels is described below.

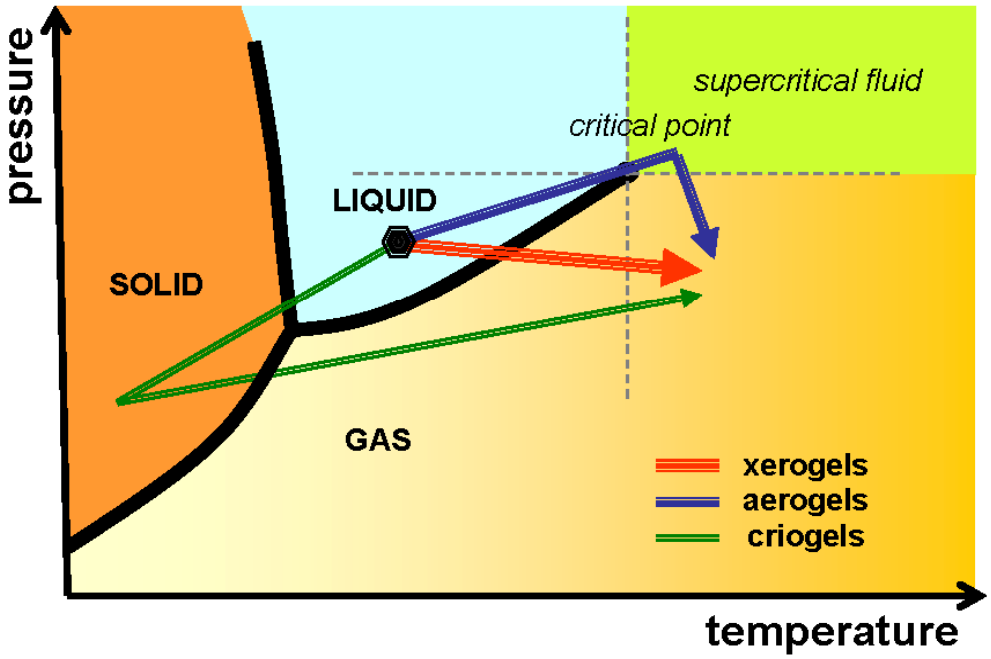

Fig. 6. Scheme of the different ways of removing the solvent used in the synthesis of organic gels.

The drying of organic gels under subcritical conditions is based on the evaporation of the solvent. Unlike other types of drying, by means of subcritical conditions, the formation of a liquid-vapour interface takes place. Therefore, when the solvent inside the pores of the material evaporates, the pores are subjected to high tension which causes the partial collapse of the structure. In order to reduce the capillary forces responsible for the partial destruction of porous texture, according to some pusblished works (Kraiwattanawong et al., 2011; Lee et al., 2010) before performing the evaporation of the water used as solvent, it can be exchanged with another solvent with a lower surface tension. Possible candidates to substitute for water could be, for example, acetone or cyclohexane (the surface tension of water at 20 °C is 72.25×10^{3} Nm^{-1} while in the case of acetone and cyclohexane it is 23.7×10^{3} and 25.5×10^{3} Nm^{-1}, respectively). However, it must be said that in some cases the partial

shrinkage of the structure when water is used as a solvent may not be of any significant if the porous texture desired for a specific application is micro or micro-mesoporosity and an easy and cheap process is required. When the solvent is eliminated by evaporation, the resulting organic gel is called xerogel. This kind of drying is the cheapest and easiest to perform, and usually the process is quite rapid (i.e. hours). Furthermore, according to some recent studies (Calvo et al., 2011a; Job et al., 2006; Leonard et al., 2005; Zubizarreta et al., 2008b) if the different evaporation conditions (i.e. the type of the solvent used, the temperature of evaporation, the carrier gas used during evaporation, use of vacuum, microwave heating, etc.) are correctly selected, it is possible to control the porous texture in order to obtain either microporous, micro-mesoporous or micro-macroporous materials.

Traditionally, although the most widely drying method used is supercritical drying, it is also the most expensive and complicated. Based on the removing of the solvent under high pressure and temperature, it is the best way to preserve the porous texture and structural properties created during the synthesis of the gels. The materials prepared by this method are called aerogels. In order to soften the conditions of supercritical drying, the solvent is usually replaced by CO_2 before its elimination under supercritical conditions. The temperature needed to remove CO_2 is lower than that of any organic solvent due to its lower surface tension, so most of the published studies on carbon aerogels make a preliminary exchange of solvent (Carrot et al., 2007; Liu et al., 2006; Tian et al., 2011a). The main problem is that the most commonly solvent used (i.e., water) needs to be exchange with an organic solvent, prior to be replacing by CO_2, complicating the procedure with several steps. Thus, the aqueous gels must to be placed in an organic solvent (i.e. acetone) for several days to completely remove the water and after that, the organic solvent is exchanged with liquid CO_2 which will finally be removed under supercritical conditions (Carrot et al., 2007). Another option is to remove the organic solvent directly under supercritical conditions, thereby by-passing the CO_2 exchange step (Liang et al., 2000; Wiener et al., 2004). However, although this second procedure avoids one of the steps in the drying process, the process usually requires more drastic operating conditions with respect to pressure and temperature apart from the fact that the aerogels obtained undergo a greater structure collapse and density than aerogels dried following the first recipe. Carbon aerogels are characterized by high pore volumes, which make these materials applicable in a huge number of application fields. However, the main disadvantage of supercritical drying, in addition to the difficulty and extremely high costs associated with the method, is the time needed to obtain dry gels as the solvent exchange steps require several days (Carrot et al., 2007; Job et al., 2005; Liu et al., 2006).

The third drying method, which results in materials called cryogels, is based on the freezing and subsequent removal of the solvent by sublimation. This method is an effective way of preparing gels with a controlled pore structure. The costs associated with freeze-drying are lower than those of supercritical drying, but it is still a more expensive method than drying by simple evaporation of the solvent (Yamamoto et al., 2001). In the case of aqueous gels, it is possible to freeze the water directly by placing the wet gel in a liquid nitrogen bath. Afterwards, the solvent is removed by sublimation under low pressures. This procedure can lead to dramatic changes in the density of the cryogels after freezing and also to the formation of megalopores or voids as a result of the creation of crystals inside the structure of the gels (Job et al., 2005; Kocklenberg et al., 1998). To prevent the formation of crystals which may deform the designed nanostructure of the polymer, the solvent is replaced before drying the gel. The most common solvent used for this purpose is t-butanol (Feaver

& Cao, 2006; Mukai et al., 2005b; Yoshimune et al., 2008), as it causes fewer changes in density than water and the vapour pressure is higher, which reduced the drying time. The advantage of this type of drying process is the possibility of obtaining high mesopore volumes (Yoshimune et al., 2008). As for the disadvantages, it should be highlighted that it is very difficult to prepare monoliths and in addition, in order to avoid the appearance of megalopores, it is necessary to perform a solvent exchange which entails an extra step and therefore and increase in time and costs.

To conclude this section of drying methods, it needs to be affirmed that the choice of drying conditions will determine the textural and structural properties of the final materials. Moreover, none of the drying methods are perfect, all three have their advantages and disadvantages (reported in Table 1), and the choice of method will depend on the requirements of the final applications.

DRYING METHOD	MATERIAL	ADVANTAGES	DISADVANTAGES
SUBCRITICAL	Xerogel	- Simple, rapid and cheap method - High surface areas and pore volumes can be achieved	- Presence of capillary forces that destroy part of the initial porosity
SUPERCRITICAL	Aerogel	- No shrinkage of pore texture	- Requires high temperatures and pressures - Extremely high cost - Long times required - Necessary to perform, at least, one solvent exchange with CO_2
FREEZE	Cryogel	- Low shrinkage - Materials with higher pore diameter	- High cost, long time and complicated method - With aqueous gels, it is essential to exchange the solvent

Table 1. Summary of the main characteristics of the drying methods used in the field of carbon gels.

2.2 Thermal treatments of organic gels

The thermal treatment of the organic gels, i.e. carbonization, allows the removal of non-crosslinked organic chains, labile oxygen and hydrogen surface groups, resulting in thermally stable nanostructured materials formed mainly by carbon. This type of nanostructure endows the materials with a series of electrical, thermal and mechanical properties that are very useful in applications related to catalysts, energy storage, etc. (Al-Mutasheb & Ritter, 2003). The main targets of the carbonization step are to obtain thermally stable carbonaceous materials and promote the development of microporosity in the gels. The nanostructure developed during the synthesis of the organic gel usually remains intact

during the carbonization step, and therefore the meso and macroporosity obtained is preserved as it was previously designed. However, during the carbonization step the elimination of volatiles and labile matter leads to the formation of microporosity, mainly localized in the nodules of the polymer (see Figure 5a). Thus, the meso-macroporosity is controlled during the synthesis of organic gels while the microporosity is controlled independently during the carbonization step, which supposes a great advantage respect to design and control the porous texture of these materials. Usually, organic gels are carbonized by heating the samples in a furnace under inert atmosphere (i.e. N_2, Ar or He) for a specific period of time. Although most of the published works on carbon gels use N_2 or Ar as inert gas during the carbonization step, others use a reactive gas to modify the internal structure of the material. For example, K.Y. Kang et al. (Kang et al., 2008), showed that it was possible to perform the carbonization under an ammonia atmosphere (process known as ammonization). As a result, in addition to develop the microporosity of the samples, nitrogen functionalities are incorporated into the structure.

Like other steps involved in the synthesis process of organic gels, carbonization has also an important influence on the final properties of the material. The most important variables that have a significant influence on the characteristics of carbon gels are: temperature and time of carbonization, type of gas and flow rate used, heating device used, etc. Several authors have studied the influence of carbonization temperature on the porosity of carbon gels. Whereas some of these studies affirm that an increase in carbonization temperature leads to a loss of microporosity (Lin & Ritter, 2000). Others affirm the opposite, i.e. an improvement in microporosity when the temperature increases (Kang et al., 2008). C. Lin and J.A. Ritter (Lin & Ritter, 2008) evaluated the dependence of porous texture with carbonization temperature by performing the carbonization under N_2 flow at several temperatures (600, 750, 900, 1050 y 1200 °C). Their results reflected than the optimum temperature was 600 °C because as the temperature increased, smaller micropore volumes were reported. In addition, the present work shows that carbonization temperature does not influence the mesoporosity of the samples, which corroborates the affirmation that meso-macroporosity is developed during the synthesis of the organic gels while the appearance of micropores occurs during the subsequent carbonization stage (Al-Mutasheb & Ritter, 2003). Other work on the influence of carbonization temperature has also been carried out by K.Y. Kang et al. (Kang et al., 2008) but, in that case, the process was performed at 650, 850, and 950 °C under flows of nitrogen and ammonia. Results showed that higher temperatures promote the development of porosity. The bibliography, therefore, apparently contains contradictions regarding the real influence of the carbonization temperature on microporosity development of carbon gels. The reason for these divergences is probably that many other variables, such as the R/F molar ratio, the pH of the precursor solution, the type of catalyst used, etc., lead to different nanostructure materials that react in a different way with the increase of temperature. The nature of gas used during the carbonization may also have an effect on the porous and structural properties of carbon gels. Starting with the porous texture, most of the literature about carbon xerogels uses N_2 or Ar atmosphere as carrier during carbonization, resulting in materials with specific surfaces areas of approximately 600-700 $m^2\ g^{-1}$ (Calvo et al., 2011a; Job et al., 2004; Matos et al., 2006; Zhu et al., 2007). However, it has been reported that the treatment of organic xerogels with ammonia produces carbon xerogels with specific surface areas above 1000 $m^2\ g^{-1}$ (Kang et al., 2008). Moreover, differences in the chemical characteristics of the samples may also appear due to the nature of the atmosphere. For example, carbon xerogels prepared by

means of ammonia-assisted carbonization contain approximately 6-7 wt. % of nitrogen while in the case of organic xerogels carbonized under nitrogen atmosphere, the amount of nitrogen does not exceed 1 wt. %. These examples show the huge influence of the carbonization process on the final properties of carbon gels and, as in the case of the other synthesis variables, a correct choice of carbonization conditions allows to obtaining a material with the appropriate properties (both porous and chemical) for a specific application.

Carbon gels can be also subjected to activation processes after or during the carbonization step. The aim of activation processes is to increase the surface area and volumes of the pores created during the synthesis, and also to promote their widening, especially in the case of the narrower pores. Therefore, it is very common to activate carbon xerogels, where the porosity is narrower and lower, and they are usually used in applications where besides narrow mesopores a high volume of micropores are needed. It is generally accepted that there are two types of activation methods: physical activation, by means of CO_2, steam, or a combination of both (Lin & Ritter, 2000) and chemical activation, where the activation agent may be KOH (Fang & Binder, 2006; Macia-Agullo et al., 2007; Zubizarreta et al., 2008c), H_3PO_4 (Conceição et al., 2009; Jagtoyen et al., 1993), $ZnCl_2$ (Olivares-Martín et al., 2006), etc. In all cases, it is essential to optimize a number of variables due to their notable influence on the final porosity. Some of these variables are: temperature and time of activation, activating agent and precursor used (i.e., organic or carbon gels as precursor), amount of activating agent, gas flow and heating rate, etc. (Fang & Binder, 2006; Lozano-Castelló, 2002). Chemical activation processes take place in two stages: (i) the precursor is mixed with the activating chemical agent and this can be done in two different ways, by physical mixture, i.e. the two solid products are directly mixed in a mortar, or by wet impregnation, when the sample is mixed with a concentrated solution of the selected chemical agent for a specific time at low temperature (< 100 °C); in the latter case the slurry formed must be subsequently dried before the process is continued; (ii) the mixture is subjected to thermal treatment under an inert atmosphere up to a selected temperature that may range from 300 to 900 °C, depending on the activated agent used. When this thermal treatment is completed, the sample must be washed with water several times in order to remove traces of chemical agent. Finally, the sample is dried. One of the main disadvantages of this type of activation, apart from the higher cost of the activating agents (KOH, H_3PO_4 vs. CO_2 and steam water, for instance), is the washing stage since, in addition to lengthen the process, sometimes it is extremely difficult to completely remove all the traces of the residual activating agent. Despite these drawbacks, chemical activation has several advantages compared to physical activation including the lower temperature and activation time, higher yield and higher development of porosity achieved (Lozano-Castelló, 2002; Molina-Sabio et al., 2004; Teng & Wang, 2000). Physical activation consists of (i) thermal treatment of the precursor in an inert atmosphere and the successively controlled gasification of the carbonaceous material or (ii), the direct activation of the raw material in the presence of the activating gas. The main characteristics of physical activation are: higher temperatures than chemical activation (between 800-1100 °C), a more heterogeneous micropore size and very simple method (Okada et al., 2003). The effect of the type of precursor on the porosity of final materials is well known in the case of chemical activation, whereas in physical activation processes, further studies are needed to determine the relevance of this variable. Published works on chemical activation of organic and carbon gels have shown that in the case of carbon gels, chemical activation produces an increase in micropores volume without modifying the

mesoporous structure formed during the synthesis of the gels. However, when the chemical activation of organic gels is performed, mainly microporous materials are obtained since the mesoporosity created during the synthesis is severely damaged. This phenomenon again shows the versatility of these carbonaceous materials because, by means of chemical activation processes, only by varying the precursor used, it is possible to prepare mainly microporous materials with a small amount of mesopores or materials characterized by a high micropore volume but also by a significant amount of mesopores with a controlled size depending on the pH of the initial solution (Zubizarreta et al., 2008c). In chemical activation, several works in the literature evaluate the influence of the amount of chemical agent used on the final characteristics of the carbon gels. Usually, as the activating agent/precursor ratio increases, a further development of the microporosity takes place. However, it seems that there is a limit to this ratio, above which the specific surface area begins to decline. Thus, Zubizarreta et al. (Zubizarreta et al., 2008c) showed that in the chemical activation of different carbon xerogels with KOH, the activating agent/precursor mass ratio greatly influences (but not always in the same way) the porous texture of the activated carbon xerogels. The authors have used ratio values of 1, 2, 3 and 4 and observed that in some cases the maximum surface area was achieved with a ratio of 3, whilst with other samples the maximum was achieved using a ratio of 4. Different results were obtained depending on the pH of the initial solutions used to synthesize the materials. Highly microporous carbon xerogels can also be prepared by chemical activation with phosphoric acid (Conceição et al., 2009). In this work, several impregnation ratios were used and their influence on the final characteristics on the material was evaluated. It is noteworthy that for all the impregnation ratios employed, the mesoporosity of original samples was destroyed, which is consistent with the findings of other scientific studies (Zubizarreta et al., 2008c). In addition, the higher the impregnation ratio, the greater the development in porosity. However, it should be noted that differences between samples was not very significant, since with ratios of 1, a carbon xerogel with a specific surface area of 1525 m^2 g^{-1} was obtained while if the impregnation ratio was tripled, an increase in specific surface area of barely 200 m^2 g^{-1} was achieved.

From the examples showed in this section 2.2, both in carbonization and activation processes, is clear that the porous texture of carbon xerogels can be designed by modifying several synthesis conditions. This is of huge relevance as it reveals the carbon gels as a nanostructured material with a great potential as it is possible to tailor specific properties of this kind of materials to adequate them for an optimum behavior in a wide variety of scientific fields and applications.

2.3 Another post-synthesis treatments

As already mentioned, the most interesting characteristic of carbon gels is the possibility of tailoring the final properties in order to prepare them for a specific application (al-Mutasheb & Ritter, 2003; Czzakel et al., 2005; Job et al., 2004, 2005; Pekala, 1989; Zhang et al., 2007; Zhu et al., 2007; Zubizarreta et al., 2008a), control and design achieved by selecting the appropriate variables involved in the synthesis. There are many possible *bottoms to be pressed* to obtain the right results. Nevertheless, the porous texture is not the only factor that determines the optimum performance of the carbon gels in a specific application. Surface chemistry also plays a relevant role, due to the interactions between the fluids and the carbon surface (i.e. the possibility of redox reactions, charge transfer, different wettabilities depending on the surface chemistry, the blockage of reactive sites, etc. (Serdich et al., 2008)).

Therefore, there has been an increase in the number of published works focused on the tuning of the surface chemistry of carbon gels in recent years and these processes can be performed in several ways. For example, carbon gel functionalisation can be carried out with post-synthesis treatments, such as oxidation using different oxidizing agents, HNO_3, H_2O_2, air, etc. (Gryzb et al., 2010; Mahata et al., 2008), treatments with compounds such as ammonia, melamine or ammonia borane (Gorgulho et al., 2009; Pérez-Cadenas et al., 2009; Sepheri et al., 2009), with the aim of incorporating nitrogen and borane groups, respectively, into the structure of carbon gels. Alternatively, heteroatoms can be directly added during the synthesis using heteroatom-containing polymeric precursors, i.e. melamine, urea, cellulose acetate, etc. (Gryzb et al., 2010; Long et al., 2008b). Rather than in post-synthesis treatment, this is a modification of the synthesis receipt and therefore, the polymerization process would vary since the initial reactants are different.

Regarding to oxidative processes, oxygenated surface groups are incorporated using liquid-phase oxidants (e.g. nitric acid, hydrogen peroxide, ammonium persulphate) or gas-phase oxidants (i.e. air, steam, oxygen, etc.). The nature of the oxygenated functionalities incorporated depends not only on the type of oxidizing agent used, but also on the conditions in which the oxidative process is carried out. For example, N. Mahata and co-workers (Mahata et al., 2008), studied the type of oxygen surface groups created in carbon xerogel structures by means of three different oxidation treatments (oxygen plasma, nitric acid and diluted air). Of the three oxidative treatments, HNO_3 oxidation produces largest amount of carboxylic acid groups, but the amount of oxygen groups created is difficult to control and besides, high concentrations of HNO_3 are needed. Each of the three processes produces carbon xerogels with different surface chemistry. Consequently, the choice of oxidizing agent should be made according to the application requirements for which the carbon gels are intended. Another work focusing on the oxidation conditions of carbon xerogels with HNO_3 was published by Silva et al (Silva et al.., 2009). In this work, HNO_3-hydrothermal oxidation was carried out using several concentrations of nitric acid (from 0.01 to 0.30 mol l^{-1}) at different operating temperatures (between 120 and 200 ºC) and the results show that both the concentration of HNO_3 and temperature notably influence on the level of oxygen functional groups created on the surface of carbon xerogels. There is a clear correlation between the degree of functionalization and the HNO_3 concentration used. The temperature of functionalisation may also affect the porosity of the final carbon xerogels. Unlike the partial blockage of the pores produced in oxidative processes with concentrated HNO_3, the HNO_3-hydrothermal method not only maintained the porous texture of carbon xerogels but also, when the operating temperature was fixed at 200 ºC, there was even an increase in the specific surface area of carbon xerogels oxidized with a high concentration of HNO_3 solution. Another published study covering several types of carbon xerogels post-treatments, was performed recently by Grzib and co-workers (Gryzb et al., 2010). A series of nitrogen and oxygen functionalised carbon xerogels were synthesized by means of different oxidative processes with HNO_3 and H_2O_2, treatments with gaseous ammonia at high temperature and co-heating of carbon xerogels with melamine. All of these treatments give rise to a wide range of carbon xerogels, with different amounts and type of oxygen and nitrogen groups. This represents a breakthrough for applications that, besides a good porosity development, require materials with a rich surface chemistry. Out of all the post-synthesis treatments studied, it was found that ammonisation produces the most basic carbon xerogels not only because of the incorporation of basic N-groups, but also due to the reduction of acidic oxygen functionalities within the chemical structure of the carbon xerogels. Oxidation with nitric acid or hydrogen

peroxide introduces almost amount of oxygen (about 5 wt. %), while the character of these functionalities is quite different. XPS data reported in this work show that H_2O_2 oxidation mainly produces carbon xerogels with oxygen groups like alcohols and ethers, whereas nitric acid treatment incorporates esters, lactones and carboxylic groups into the structure of the carbon xerogels, results which are consistent with other scientific works.

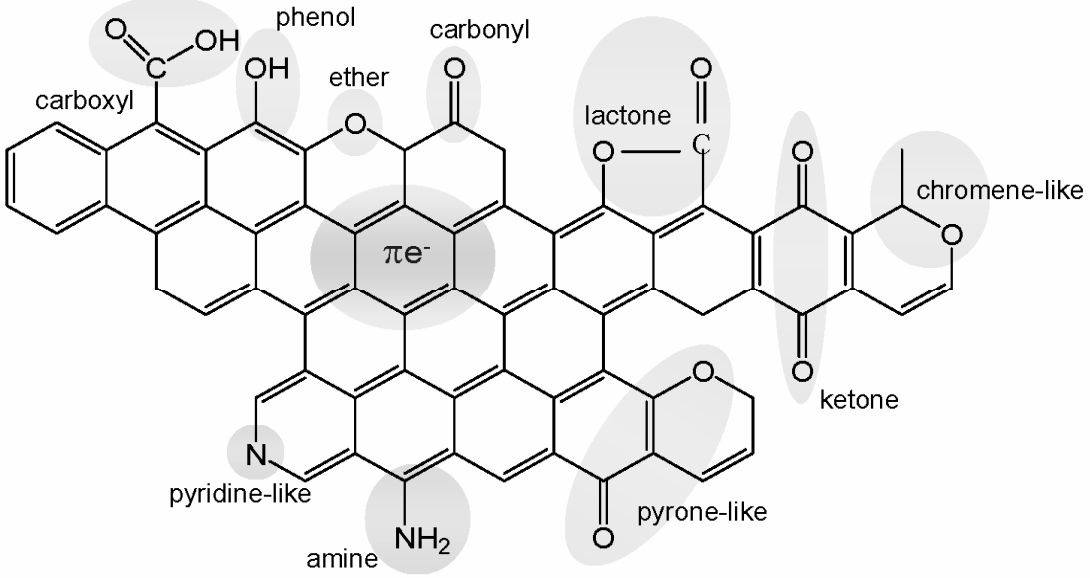

Fig. 7. Main functionality groups that can be incorporated into carbon gels by post-synthesis treatments.

The doping of carbon gels with different metal species (i.e. metals, metal oxides, metal carbides) is another common post-synthesis process in carbon gels, since by means of this technique it is possible to modify their chemical nature, enlarge their surface area and improve their conductivity, thereby increasing the already known potential of this kind of carbonaceous materials. Despite the great interest in carbon gels due to the possibility of tailoring their porous texture, the presence of metal particles acting as active sites is required for specific applications. Consequently, several studies on the doping of carbon gels with transition and non-transition metals have emerged in recent years (Chandra et al., 2011; Job et al., 2007b; Lee at al., 2011; Liu et al., 2006). For example, in the particular case of energy storage in supercapacitors, carbon gels are very promising materials due to their attractive features. Supercapacitors assembled with these carbonaceous materials stores energy mainly because of the formation of a double electric layer on electrodes surface. However, it is well known that specific capacitance can be increased as a result of redox reactions. Hence, in relation to this particular application, numerous studies have emerged on the synthesis of doped carbon gels. The species that are usually incorporated into carbon gel structures to improve their energy capacitance via pseudocapacitive processes are Ni, B, P, Cu, Ca, Co, Mn, etc. (Chandra et al., 2011; Cotet et al., 2006; Job et al., 2007b; Tian et al., 2010). Carbon gels have also received a great deal of attention as hydrogen storage media due to their good adsorption properties that are the result of their remarkable textural development. It has generally been accepted that the hydrogen storage capacity of carbon materials is directly related with their specific surface area and micropore volume (Tian et al., 2010; Zubizarreta et al., 2010). However, the storage

capacity values at room temperature are too low, which is a very serious problem for their application in mobile devices. In order to overcome this limitation, researchers have proposed a doping process of carbon materials to improve the interaction between the hydrogen and the carbon surface and, consequently, to enhance their hydrogen storage capacities. Zubizarreta and co-workers (Zubizarreta et al., 2010), reported the preparation of Ni-doped carbon xerogels by two methods (both post-synthesis treatments): dry impregnation and strong electrostatic adsorption, SEA. Their results showed that both treatments produce Ni-doped carbon xerogels with a small particle size (2-9 nm) and a good nickel dispersion, but dry impregnation method produces carbon xerogels with the higher amount of nickel incorporated. In contrast, the SEA method produces materials with a high interaction between C-Ni and besides, Ni particles with a very homogeneous size (around 2 nm) are obtained. Some of the samples prepared showed very good hydrogen storage capacities, with higher values than those of undoped carbon gels, making Ni-doped carbon xerogels good candidates for hydrogen storage systems. In another study on metal-doped carbon gels performed by Tian et al. (Tian et al., 2010), carbon gels were doped with metallic cobalt particles by means of two methods: (i) the addition of cobalt acetate solution to the carbon gels followed by thermal treatment and a reduction process, and, (ii) ion-exchange method. It was found that the size of the Co particles incorporated into the structure of the materials was between 2 and 8 nm when cobalt acetate solution was used and, besides that, these samples had higher surface area and micropore volume than the Co-doped carbon gels obtained by the ion-exchange method. The hydrogen storage capacity of both types of doped-materials was compared with that of the original undoped material and the results show higher values of hydrogen storage in both of the metal-doped carbon gels, although the process that presented the better results was doping with a solution of cobalt acetate.

All the studies listed in the bibliography point out the huge versatility of carbon gels and the great potential of these materials not only because their tuneable nanostructure but also because their chemical nature can be easily altered by post-synthesis treatments.

2.4 Novel and underdevelopment alternative synthesis conditions

Over the past few decade, a number of works on alternative methods of manufacturing carbon gels by means of different types of electromagnetic radiation (i.e. infrared, ultrasonic or microwave) have been published (Calvo et al., 2008; Kang et al., 2008; Tonamon et al., 2005, 2006; Wu et al., 2004). In some cases, irradiation is applied in order to improve the porous texture of the final products, whereas in other cases, the aim is to shorten the synthesis process, in order to make carbon gels more cost-competitive materials.

Wu et al. (Wu et al., 2004) prepared carbon gels from resorcinol, furfural and hexamethylenetetramine (HMTA), by means of a drying process that combines drying at room temperature, infrared lamp and high-temperature drying. This particular drying method gives rise to low-density carbon gels with a well-developed porosity development. However, although no solvent exchange or high operating pressures are involved, it is still a long drying procedure (about 34 hours). There are many works about polymerization reactions and other types of chemical processes that are accelerated by ultrasonic radiation (Neppolian et al., 2008; Riera et al., 2010; Suslick et al., 1999; Tonamon et al., 2005). Several authors have employed ultrasonic radiation in one or several steps to synthesize carbon gel. Ultrasonic has been found to be very a helpful strategy to increase reaction rates, yields of products and, thereby shortening the reaction time required. One of the studies that applies sonication to carbon gel is that published by Tonamon and co-workers in 2005 (Tonamon et al., 2007). These authors

synthesized resorcinol-formaldehyde carbon xerogels under different catalyst concentrations by means of ultrasonic irradiation using several intensities in order to evaluate the influence of sonication conditions on the porous texture of the materials. First, ultrasounds were applied to the resorcinol-formaldehyde mixture until a highly viscous sample was observed, and then the rest of the gelation and curing stages were completed by heating in a conventional furnace for 7 days. In all the samples prepared, the researchers found that ultrasonic irradiation improved the mesoporosity of the carbon gels, even in samples for which only a minor presence of mesopores could be expected (i.e. S_{BET} = 650 m^2 g^{-1} and V_{meso} = 0.53 cm^3 g^{-1} when the carbon xerogel was synthesized in the absence of sonication vs. 660 m^2 g^{-1} and 0.93 cm^3 g^{-1} if the intensity of the ultrasonic radiation was increased to 106 W cm^{-2}). In addition, it was observed that the higher the ultrasonic intensity, the shorter the gelation times and the higher the mesopore volume. In 2006, the same group of researches introduced a new variable in the synthesis process of carbon gels, i.e., drying by microwave technology (Tonamon et al., 2006). In some cases, the applied ultrasonic radiation to RF aqueous solutions and then they dried the samples by means of microwave radiation (after a water-exchange step using t-butanol in order to minimize the shrinkage of the structure). The results showed that the presence of mesopores was favored when ultrasonic and microwave radiations were combined (i.e. V_{meso} of 0.59 cm^3 g^{-1} and 0.46 cm^3 g^{-1} for resorcinol-formaldehyde carbon gels dried in a microwave oven with and without previous sonication process, respectively). Therefore, one of the conclusions of that work was that microwave drying was a new and efficient drying method for carbon gels because it resulted in time saving without destroying the meso-macroporosity of samples.

Microwave heating has been used to obtain different organic reactions for several years (Kappe, 2004; Menéndez et al., 2010). There are many processes involving carbon materials where microwave radiation is the main heating source used because of the good capacity of most carbon materials to absorb microwaves. The main advantage of microwave-assisted thermal processes is the saving of time, resulting in a reduction in the energy consumed, as a result of the different mechanism involved in the heating process (Menéndez et al., 2010).Thus, microwave radiation promises to be an effective technology in the field of carbon gels allowing their long synthesis time to be reduced and opening up a way to their application to industrial scale. As mentioned above, the first works that combine microwave heating and carbon gels are based on the application of this type of radiation in some stage of the synthesis process, i.e. during the drying stage (Zubizarreta et al., 2008b) or during the gelation and curing stages followed by drying in a vacuum oven (Kang et al., 2008). In all these cases, carbon gels with a good texture development were prepared in a considerably shorter time than by means of conventional heating but even so, the time required for their manufacture were too long. The next step would be the utilization of microwave heating for the entire synthesis process of carbon xerogels, i.e. during gelation, curing and drying stages. The first researchers that used microwave heating in the three stages involved in the synthesis process were Calvo et al. (Calvo et al., 2008), when in 2008 they have showed the possibility of obtaining RF carbon xerogels with similar characteristics to conventionally synthesized xerogels but with a considerable saving of time and energy (i.e. 3-4 hours under microwave radiation compared to several days by conventional heating). In addition, there are several other advantages of using microwave technology to fabricate carbon xerogels. According to a recent publication (Calvo et al., 2011a; Juárez-Pérez et al., 2010), by means of microwave heating is possible to determine the gelation point of the carbon xerogels during the sol-gel synthesis, which is essential for controlling the viscosity of the reaction media in order to obtain the carbon xerogel in an

.

specific form (i.e., sphere, monolith, film, etc.). Another advantage of microwave radiation is the possibility of preparing mesoporous carbon xerogels over a wider pH range than when using conventional methods (Calvo et al., 2011a). It was pointed out that, in addition to time saving and the ability to accurately determine the gelation time, mesoporous materials with a tailored mesopore size can be synthesized in a wider range of pH than in the case of conventional heating. For example, with microwave heating, a pH between 4.5 and 6.5 can be used to produce micro-mesoporous carbon xerogels and micro-macroporous materials when the initial pH is fixed at 3.1, while in the case of conventional methods, only a pH range of 5.8-6.5 serves micro-mesoporous carbon xerogels.

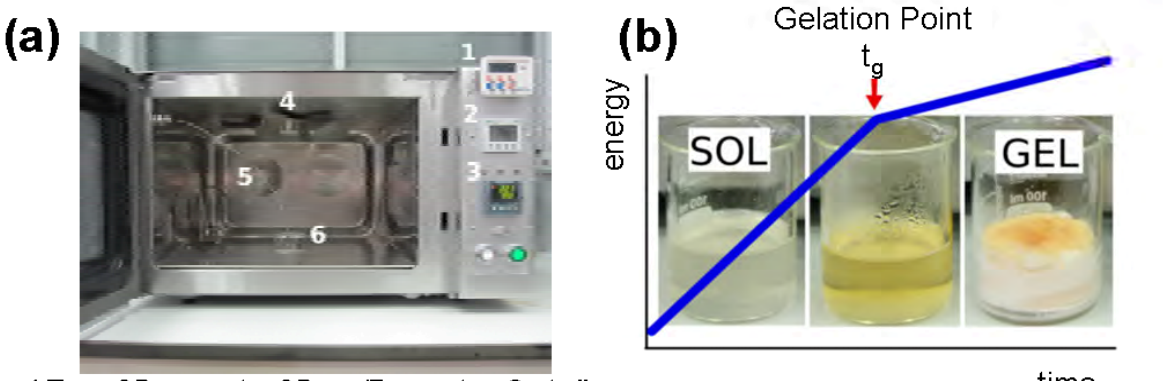

Fig. 8. The microwave device used in the synthesis of carbon xerogels (a) and a scheme showing the determination of the gelation point (b).

3. Properties of carbon gels

As already pointed out, the main advantage of carbon gels lies in the possibility of tailoring their porous texture to accomplish the requirements of the final application, and this can be achieved by selecting the appropriate synthesis conditions. While there is an abundant literature about the effect of the different stages of carbon gel synthesis (i.e. gelation, curing, drying, carbonization and activation) on the surface area, pore volume and pore size distribution (Czzakel et al., 2005, Job et al., 2004, 2005; Lin & Ritter, 2000; Matos et al., 2006; Zubizarreta et al., 2008a), the situation regarding the mechanical and chemical properties is quiet different. Although, in some cases, these parameters may be slightly influenced by the synthesis procedure followed, it is usually necessary to carry out additional processes to produce any significant changes in the mechanical or chemical properties of carbon gels (Gryzb et al., 2010; Gorgulho et al., 2009; Job et al., 2007b; Lee et al., 2011; Pérez-Cadenas et al., 2009; Silva et al., 2009).

In this section, the main factors that have any impact on the final properties of carbon gels are reported. Each of the stages involved in the synthesis process is highlighted and explained. As can be seen in Table 2, there are several variables to be considered in the synthesis of carbon gels, which explains the versatility of these materials since they can be obtained with very diverse characteristics depending on the application which they are intended. However, this also has its downside because there are a large number of variables to consider and control. Moreover, these variables are on many cases interrelated, which

complicates their optimization. A different section will be assigned to each group of characteristics (textural, chemical and structural). Nevertheless, taking into account the information collected in the Table 2, it can be affirmed that: (i) all the variables involved in the different stages of synthesis have a remarkable effect on the porous texture of carbon gels but, in many cases, their influence on the chemistry and structure of these carbonaceous materials remains unknown; (ii) as regards the porosity of carbon gels, it might be said that each stage involved in the synthesis is very selective to a specific pore size. For example , it is possible to modify the macro/mesoporosity of samples by changing the pH of the precursor solution without affecting the development of microporosity, which is conditioned by the carbonization and activation steps (Calvo et al., 2008; Conceição et al., 2009; Job et al., 2004; Lin & Ritter, 2000; Zubizarreta et al., 2008c); (iii) in order to modify the chemistry of carbon gels, for example, by incorporating oxygenated functional groups, it is necessary to perform extra treatments (Gryzb et al., 2010; Silva et al., 2009).

3.1 Porous texture

In this section, the variables that influence the final porous texture of carbon gels are grouped according to the synthesis step and the corresponding operating conditions, in order to clarify the role that each stage plays.

3.1.1 Sol- gel process: pH, RF concentration or temperature and time of gelation and curing

Figure 9 shows a picture of four organic xerogels synthesized from resorcinol-formaldehyde solutions with a different initial pH (between 5.8 and 6.5). Intuitively it may be said that the pH of the precursor solution must be an important factor in the synthesis process of carbon gels because of the different colors of these four materials. Actually, numerous works (Al-Mutasheb & Ritter, 2003; Job et al., 2004; Zubizarreta et al., 2008a) have already established that the pH, or hydroxilated benzene/catalyst molar ratio, is the key factor that determines the meso/macroporous texture of carbon gels. As a general rule, as the initial pH increases, both the volume and the diameter of meso/macropores decrease, while there is no effect on the microporosity of the sample. That it is to say, by means of a slight increase in the initial pH it is possible to go from micro-macroporous to micro-mesoporous materials and from these to exclusively microporous carbon gels (Calvo et al., 2011a; Zubizarreta et al., 2008a).

Fig. 9. Resorcinol-formaldehyde organic xerogels prepared from precursor solutions with different pHs: from left to right 5.8. 6.0, 6.2 and 6.5.

The effect of pH on the porosity of carbon gels can be explained by the polymerization mechanism between hydroxilated benzene and aldehyde molecules. Polymerization reaction between these two species occurs in two different stages: (i) the formation of hydroxymethyl derivatives and (ii) the condensation of these hydroxymethyl derivatives and their clustering. At a high initial pH the first stage is favored, giving rise to the formation of hydroxymethyl derivatives and then to the formation of highly branched clusters. These cross-linked and unstable clusters lead to small and interconnected particles that, after condensation, give rise to the formation of pores, mainly mesopores. On the other hand, a low initial pH leads to the formation of fewer but bigger clusters that finally result in materials with bigger pores in the macropore range (Job et al., 2004; Lee et al., 2010). This is shown in Figure 5.

From the abundant literature that shows the dependence of the porosity of carbon gels on the initial pH (Calvo et al., 2008, 2011a; Job et al., 2004; Zubizarreta et al., 2008a), it would appear that the maximum pH that can be used to synthesize porous carbon gels is about 7.0. What is more, when the carbon gels synthesized in this study were compared, it was observed that variations of only 0.2 units in the initial pH promote significant changes in the size of mesopores. For example, the maximum mesopore diameter for a RF carbon xerogel can change from 26 nm to 14 nm when an initial pH of 5.8 and 6.0 were used. The same trend was observed for two series of carbon xerogels synthesized under microwave and conventional heating (Calvo et al., 2008). In both cases, conventional and microwave-assisted synthesis, carbon xerogels with a higher pH have smaller mesopore size. Moreover, a more recent study (Calvo et al., 2011a) shows that for microwave-assisted synthesis, the pH window used for producing micro-mesoporous materials of different mesopore size is about two units of pH (between 4.5 and 6.5), whereas synthesis in a conventional stove has a smaller pH window (between 5.8 and 6.5). The pore size distributions of these xerogels are collected in Figure 10 in order to see the porous texture in relation to the initial pH and the type of heating device used. This example confirms that there are interactions between the variables involved in the synthesis process. It can be seen that the same variations in initial pH do not produce similar carbon xerogels due to a new variable, i.e. the type of heating device used.

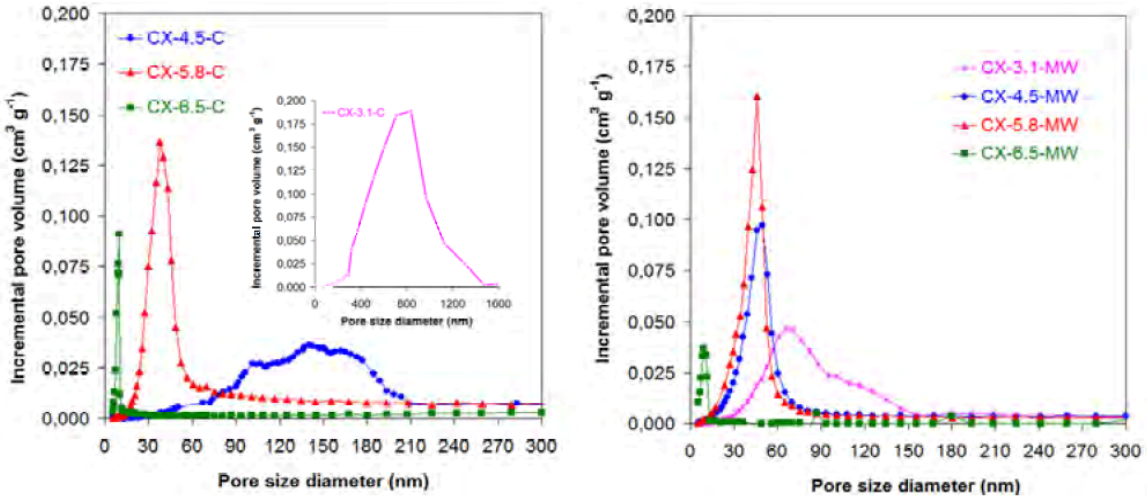

Fig. 10. Pore size distribution of resorcinol-formaldehyde prepared with different pH and heating mechanisms: conventional (a) and microwave radiation (b) (adapted from reference Calvo et al., 2011a).

Conversely, the effect of the concentration of reagents on the porosity of carbon gels has not been studied in depth. Most published works on carbon gels synthesized from resorcinol-formaldehyde mixtures use a molar ratio R/F = 0.5 (Al-Mutasheb & Ritter, 2003; Job et al., 2004; Zhang et al., 2007; Zhu et al., 2007; Pekala, 1989). This is because formaldehyde only has one aldehyde group able to interact with other groups while resorcinol molecules display two hydroxyl groups. Nevertheless, some studies use a lower molar ratio R/F, that it is to say, a more diluted RF solution, leading to carbon gels with smaller particle sizes and, therefore, smaller pore sizes (Al-Mutasheb & Ritter, 2003).
The synthesis procedure of carbon gels found in most of the published literature involves the heating of the monomers solution at temperatures ranging between 70 and 90 °C for 3-5 days in order to perform the gelation and curing stages (Pekala, 1989). The synthesis temperature and time affect the porosity of resulting materials. However, according to the results reported by Job et al. (Job et al., 2006), the effect on the porous structure is not the same in every carbon gel because the most important variable in this sol-gel synthesis, i.e. the initial pH, again comes into play. These authors studied the effect of several combined parameters, gelation and ageing temperature (50, 70 and 90 °C) and ageing time (between 0 and 72 hours), in three series of organic xerogels obtained from precursor solutions with different pH. In all the examples shown, the increase in temperature leads to lower gelation times, which is consistent with other works (Al-Mutasheb & Ritter, 2003; Job et al., 2007a; Kim et al., 2001). Moreover, as the synthesis temperature increases, the ageing time may be shortened (i.e. samples synthesized at 50 °C do not reach stability after 72 hours while in the case of 70 or 90 °C, the polymerization reactions are completed after 24 or 48 hours, depending on the initial pH). In general, it can be said that increasing the synthesis temperature yields narrower pores but this statement does not apply in all cases due to the influence of the pH. If the ageing time is increased, higher surface areas and pores volume are achieved, but once the polymerization reaches stability, the increase in ageing time scarcely has any influence on the porosity of materials. However, it should be noted that it is not easy to establish trends for each of the variables involved in the sol-gel process because a slight change in one variable, like the pH, implies a variation in the effect of other parameters, for example the synthesis temperature.

3.1.2 Drying: Heating device and drying temperature

It is particularly difficult to establish a direct relationship between the drying method and the textural properties of carbon gels because the effects produced by other variables such as the initial pH, synthesis temperature and time can conceal it. However, according to some works in which aero, cryo and xerogels were compared, it was reported that carbon gels with a higher pore size, large mesopores and macropores, are mainly achieved under supercritical and freezing conditions. In contrast, carbon xerogels are susceptible to a high degree of shrinkage of their porous nanostructure due to the surface tensions caused by the solvent upon the vapor-liquid interface (Czzakel et al., 2005; Job et al., 2005; Qin et al., 2001). As a result of the partial collapse of their structure, carbon xerogels possess a smaller pore size than their aero and cryogel counterparts. However, it should be noted that several works suggest that it is possible to prepare meso-macroporous carbon xerogels by employing low values of initial pH, although with lower pores volume than aerogels and cryogels (Calvo et al., 2011a). Subcritical drying is the cheapest, simplest and fastest procedure, since the other two methods require extra processes of solvent exchange and extreme operating conditions. However, in general, the choice of the drying method is conditioned by the requirements of porosity in the final application.

Czakkel and co-workers (Czzakel et al., 2005) published in 2005 a study on carbon gels dried under different conditions, keeping the rest of variables involved in the synthesis process constant. They obtained a S_{BET} of 2650, 1010 and 891 $m^2\ g^{-1}$ and a V_p of 2.05, 0.79 and 0.44 $cm^3\ g^{-1}$, for cryogels, aerogels and xerogels, respectively, and concluded that freeze-drying promotes the formation of materials with a larger textural development. The same trend was also observed in another work in 2005 (Job et al., 2005), where three types of drying methods were studied but in this case, precursor solutions with different pH were used. Carbon cryogels presented a higher specific surface area and pore volume than the other types of carbon gel in three out of the five series studied, those with lower pH. No clear trend was observed in the sizes of the meso and macropores of aerogels and cryogels synthesized. Nevertheless, in the pH range evaluated, carbon xerogels were the materials with the smallest meso and macropores.

In the case of carbon xerogels, some studies report the porous texture differences resulting from evaporative drying under different conditions (Kraiwattanawong et al., 2011; Zubizarreta et al., 2008a). For example, carbon xerogels with a good textural development and significantly reduced synthesis time (up to 98%) were obtained using microwave heating (Zubizarreta et al., 2008b). Furthermore, as illustrated in Figure 11, the microwave process allows the tailoring of the porous texture of the carbon xerogels depending on the initial pH, or R/C.

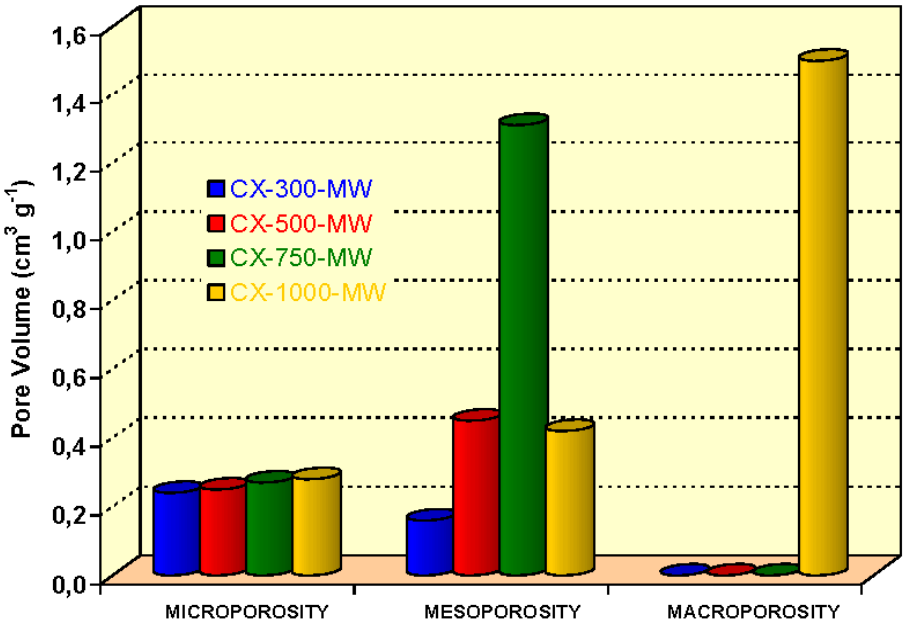

Fig. 11. Influence of R/C molar ratio on the pore size distribution of different carbon xerogels dried by microwave heating (adapted from reference Zubizarreta et al., 2008b).

Another factor to be taken into account is the drying temperature. A number of studies show that the removal of the solvent should be performed with a smooth gradual increase in temperature in order to avoid the collapse of the porosity. In most of the works, the drying stage was carried out at approximately 85-150 °C for the necessary time to remove the solvent inside the structure of the material, but using very slow temperature programs (Job et al., 2005).

3.1.3 Carbonization: Temperature, heating rate and atmosphere used

The aim of the carbonization stage is, on the one hand, to obtain thermally stable materials, mostly composed of carbon atoms and, on the other hand, to develop the microporosity of carbon gels (Al-Mutasheb & Ritter, 2003; Quin & Guo, 2001). Variables such as final temperature or heating rate have a significant influence on the textural properties of carbon gels while the type of atmosphere (inert or reactive), in addition to its impact on porosity, has a notable repercussion on their surface chemistry.

Most published works on the influence of carbonization temperatures on the textural characteristics of carbon gels agree that increasing the temperature leads to materials with a lower surface area and pore volume (Lin & Ritter, 2000). Thus, the microporosity of carbon gels is reduced when the carbonization temperature is increased. However, it is necessary to discriminate between ultramicropores, pores with diameter less than 0.7 nm and supermicropores, in the 0.7-2.0 nm range. Lin and Ritter (Lin & Ritter, 2000), evaluated the effect of carbonization temperature (600, 750, 900, 1050 and 1200 °C) on these two groups of micropores and concluded that the decrease in the surface area at higher temperatures is mainly due to the smaller number of micropores in 0.4-0.7 nm range. The carbon gels reported in this work are also composed of micropores with a diameter between 1-2 nm, whose volume decreases at low temperatures (600-900 °C), while when the carbonization was performed at 1050 and 1200 °C, their volume increased indicating that high temperatures destroy ultramicropores but create a greater amount of larger micropores.

The carbonization temperature is the most important parameter in the pyrolysis processes. However, other factors such as heating rate and carbonization atmosphere have also some influence on the textural properties of carbon gels (Kang et al., 2009). Overall, the heating rates used during pyrolysis are around 5-15 °C (Wu et al., 2004; Yoshimune et al., 2008; Zubizarreta et al., 2008a) since higher heating rates would mean a lower microporosity development, as reflected by several works that evaluate the different conditions in the carbonization processes of several carbon materials (Kuo et al., 2005; Liou, 2004).

Regarding the influence of the carbonization atmosphere, it seems that inert gases produce the materials with the lowest textural development. For example, carbon gels prepared under a N_2 atmosphere usually have specific surface areas about 600-700 $m^2 g^{-1}$ (Calvo et al., 2008; Kraiwattanawong et al., 2011; Zubizarreta et al., 2008a), whereas this parameter can reach 1000 $m^2 g^{-1}$ when the pyrolysis step is carried out under ammonia or CO_2 atmosphere (Kang et al., 2009).

3.1.4 Activation: Physical or chemical activating agent, activating agent/precursor ratio, type of precursor and activation time and temperature

Usually the temperature used for physical activation range between 700-1100 °C for different lengths of time, ranging from few hours (Guo et al., 2009; Lin & Ritter, 2000; Nabais et al., 2008; Zhao et al., 2007) to 24 hours (Contreras et al., 2010). The activation time and temperature are very important variables since they can notably modify the microporosity of the resulting materials, and even the narrower mesoporosity. Usually, increasing the temperature promotes higher development of carbon gel microporosity. As an example, Lin and Ritter (Lin & Ritter, 2000), performed the physical activation of resorcinol-formaldehyde carbon xerogels with CO_2 at 1050 °C for several activation times: 0.5, 1, 2 and 3 hours. The carbon xerogels reported in this study were found to have

significant volume of micropores in the 0.6 nm range, micropores whose diameter is centered at approximately 1.3 nm and also mesopores ranging from 2-10 nm. The increase in the activation time produced a more developed pore structure since the total pore volume increased. The amount of ultramicropores increases until it reaches its maximum value after 2 hours of activation, while the volume of large micropores and smaller mesopores rises consistently with activation time. These results lead to the conclusion that in more prolonged activation processes, not only does the creation of micropores take place but also the destruction of the narrower micropores which are sometimes converted into large micropores and small mesopores. This phenomenon has also been found in another study performed by Contreras and co-workers (Contreras et al., 2010), where physical activation processes with CO_2 at 900 ºC for 4, 8 and 16 hours resulted in carbon xerogels with specific surface areas of 1015, 1365 and 2180 m^2 g^{-1}, respectively, and micropores of size 1.0, 1.1 and 1.4 nm, corroborating the development of porosity and the widening of micropores with the increase in activation time. In the same publication, the influence of another variable involved in the activation processes, i.e. temperature, upon the porosity of materials was evaluated. Two activation temperatures were studied, 800 and 900 ºC, and it was found that the highest temperature produced a greater development in microporosity, as reflected by the increase in S_{BET}, $V_{DUB\text{-}N2}$ and $V_{DUB\text{-}CO2}$. With these examples, it is possible to affirm that the development of microporosity increases with higher activation temperatures and times, i.e. as the burn-off increases, a phenomenon consistent with other works that deal with physical activation processes of different type of materials (Guo et al., 2009; Roman et al., 2008).

As expected, chemical activation processes are also conditioned by many variables such as the activation time and temperature, the amount of activating agent or type of precursor (Conceição et al., 2009; Contreras et al., 2010; Zubizarreta et al., 2007). With regard to the activating agent/precursor ratio, several studies have reported that the increase in the amount of chemical agent leads to materials with a higher textural development, although it should be pointed out that there is a maximum value above which surface area begins to decrease (Zubizarreta et al., 2008c). Conceição et al. (Conceição et al., 2009) published a work on the chemical activation with H_3PO_4 of resorcinol-formaldehyde aerogels using different impregnation ratio values (H_3PO_4/gel = 1, 2 and 3). The increase in the amount of H_3PO_4 leads to a higher total pore volume (i.e. 0.65, 0.94 and 1.41 cm^3 g^{-1} for samples obtained using impregnation ratios of 1, 2 and 3, respectively). The narrower micropores widen and, therefore, the volume of the ultramicropores decreases (i.e. 0.16, 0.15 and 0.13 cm^3 g^{-1}), unlike the volume of supermicropores and narrower mesopores that increases with higher impregnation ratios, a phenomenon similar to that explained in the preceding paragraph regarding the effect of temperature on physical activation processes. This trend was also observed in chemical activation processes of RF xerogels by adding different amounts of KOH (Zubizarreta et al., 2008c). As the activating agent/precursor mass ratio increases, carbon xerogels evolve from exclusively microporous to micro-mesoporous materials when the A/P ratio is 4. As the KOH/precursor mass ratio increases, both the specific surface area and micropore volume increase but sometimes, when A/P > 3, both parameters decrease as a result of the widening of the micropores, which are then conerted to narrow mesopores.

Another noteworthy variable in chemical activation processes is the type of precursor used. According to different works (Calvo et al., 2011b; Zubizarreta et al., 2008c), the chemical activation of carbon gels develops the microporosity notably without modifying

the pristine meso-macroporosity, as a result of the thermal stability of carbon gels. However, when carbonization and activation are simultaneous processes, the reactivity of the organic gels causes the destruction of most of the meso and macropores created during sol-gel synthesis, while the microporosity undergoes intense developed. When chemical activation is performed after the carbonization step, it is possible to synthesize materials with a specific surface area of about 1500 $m^2\ g^{-1}$ and large mesopores volumen (S_{BET} = 1540 $m^2\ g^{-1}$, $V_{DUB\text{-}N2}$ = 0.69 $cm^3\ g^{-1}$ and V_{meso} = 0.25 $cm^3\ g^{-1}$ for a carbon xerogel activated with KOH, (Zubizarreta et al., 2008c)) whereas when organic gels are used as activating precursors, there is an intense development of microporosity, which is reflected by S_{BET} values ranging from 2000 to 3000 $m^2\ g^{-1}$, although this is accompanied by a lower mesopores volume (i.e. S_{BET} = 2037 $m^2\ g^{-1}$, $V_{DUB\text{-}N2}$ = 0.82 $cm^3\ g^{-1}$ and V_{meso} = 0 $cm^3\ g^{-1}$ (Zubizarreta et al., 2008c)).

As mentioned above, during the activation processes narrow mesopores may be created depending on the activation conditions. Therefore, it is important to discriminate between this type of mesopores and the meso- macroporosity that appears during the sol-gel synthesis of organic gels. The latter type of porosity is unable to remain intact when chemical activation of organic gels is carried out. However, in a recent work it has been shown that, under certain conditions, the chemical activation with KOH when microwave radiation is used as a heating source of organic xerogels, leads to materials with the meso-macroporosity of the original samples, in addition achieving remarkable amount of micropores (Calvo et al., 2011b).

Usually, chemical activation processes are performed at lower temperatures than physical activations, i.e. 700-850 °C when metal alkoxides, such as KOH or NaOH, are used as activating agent (Macia-Agulloet al., 2007; Raymundo-Piñero et al., 2005; Zubizarreta et al., 2008c), and temperatures ranging from 450-650 °C in the case of chemical activations with H_3PO_4 (Conceição et al., 2009, Qin et al., 2001). The influence of temperature on the pore structure of carbon gels has been more extensively studied in the case of physical activation processes, although there are also some studies about its effect on chemical activations. As the activation temperature increases, materials with a more developed porosity (i.e. higher surface area, micropore and also mesopore volumes) are formed. However, it is noteworthy that, as with the effect of the amount of activating agent, there is a maximum temperature above which porosity begins to decrease (Niu & Wang, 2008; Okada et al., 2003).

To sum up, by choosing suitable synthesis and post-processing conditions, it is possible to tailor the porosity of carbon gels, discriminating between micropores, mainly produced during carbonization and activation stages and meso-macropores, created during the sol-gel synthesis. It is therefore possible to obtain exclusively microporous carbon gels (suitable for H_2 storage and adsorption applications (Cabria et al., 2007; Mahata et al., 2008)), micro-mesoporous materials (for use as electrodes in supercapacitors (Calvo et al., 2008; Escribano et al., 1998; Frackowiak & Béguin, 2001)) or even meso-macroporous samples (for water treatments (Sanchez-Polo et al., 2007)).

3.2 Chemical properties

Unlike the porous textural properties, which can be easily controlled with the synthesis and processing conditions, the chemical nature of carbon gels is not usually influenced by the synthesis protocol followed during the sol-gel synthesis. Apart from the obvious influence of the chemical nature of the monomers used, it is only possible to create different chemical

characteristics when activation, oxidation or doping processes are employed (Contreras et al., 2010; Silva et al., 2009; Zubizarreta et al., 2008c).

Carbon gels are composed of approximately 92-98 wt. % carbon and the rest of the composition is divided between hydrogen and oxygen, regardless of the synthesis conditions such as initial pH, operating time and temperature, dilution, etc. (Calvo et al., 2011a). However, Zubizarreta et al. (Zubizarreta et al., 2008a) affirm that it is possible to synthesize carbon gels with a larger amount of oxygen by performing the drying step by means of microwave heating. The oxygen content of this type of carbon xerogels was about 6-8 wt. %, probably due to the fact that with microwave radiation, several secondary reactions take place, which would favour greater crosslinkage between organic gel and the more stable oxygenated groups (Caddick, 1995).

Activation processes, both physical and chemical, besides increasing considerably the microporosity, are able to increase the quantity of oxygen present in carbon gels of around 3-4 wt. % and, according to several published works, the higher the temperature and time of activation, the higher the amount of oxygenated groups created (Contreras et al., 2010). However, since the amount of oxygen inside the carbon gel structure is still low, the determination of the nature of these surface groups is no straightforward task (Contreras et al., 2010).

The pH_{PZC}, (i.e. the pH value at which the electrical charge density on the carbon surface is zero), of carbon gels synthesized from resorcinol-formaldehyde solutions generally ranges from 8-9.5, whatever the synthesis conditions used (Calvo et al., 2011a; Zubizarreta et al., 2008a; Lambert et al., 2009). This basic character is may be due to the presence of delocalized π electrons on the surface of the carbon gels, because of their aromatic character (Montes-Morán et al., 1998), and the presence of pyrone or chromene-like structures (Fuentes et al., 1998). When activation and/or oxidation processes are carried out, the point of zero charge is irreversibly modified, increasing or decreasing with respect to the value of the pristine material, depending on the nature of the oxygenated functionalities created (Mahata et al., 2008). Thus, Lambert et al. (Lambert et al., 2009) show that oxidation by nitric acid is able to modify the surface chemistry of resorcinol-formaldehyde carbon gels, by modifying their pH_{PZC} from ca 9.4 to 2.4.

The modification of surface chemistry of carbon gels by doping processes has been widely investigated because of the need for rich chemical nature and good conductivity of these materials in a wide range of areas (e.g. catalysis or energy applications) (Job et al., 2008; Lee et al., 2011; Moreno-Castilla et al., 1999, 2005; Zubizarreta et al., 2010). There are several methods for obtaining metal-doped carbon gels. Basically, they can be classified into three processes: (i) direct dissolution of the metal precursor in the resorcinol-formaldehyde mixture (Chandra et al., 2011; Maldonado-Hódar et al., 2003); (ii) use of a resorcinol derivative containing an ion exchange moiety that can be polymerized by sol-gel reactions (Baumann et al., 2002; Fu et al., 2005), and finally, (iii) deposition of the precursor metal either on organic or carbon gels (Mahata et al., 2008). In addition to the several types of doping processes, factors such as the nature and amount of metal precursor, operating temperature, etc. greatly determined the chemical properties of the resulting materials (Frackowiak & Béguin, 2001; Job et al., 2007b).

The effect of the amount of metal precursor on the final properties of carbon gels has been evaluated by Job et al (Job et al., 2007b), through the synthesis of RF carbon xerogels doped with Cu, Ni, Pd, and Pt, by the addition of complexing agents that react during the sol-gel process. The results of this work showed that the metal particle size varies with the

concentration of the complexing agent, and these metal particles remain inserted into the structure of the materials after the drying and pyrolysis stages. For example, Pd-doped carbon xerogels had metal particle sizes of about 20 nm at low concentrations of metal precursor while the size decreased to 3-5 nm, as the concentration of complexing agent increased. In the case of Cu and Ni-loaded carbon gels, the metal particle size was unchanged with the concentration of complexing agent because they were not incorporated inside the polymeric network of the material and, therefore, they sintered during the pyrolysis stage.

The influence of the processing temperature on the surface chemistry of carbon gels was studied by Maldonado-Hódar (Maldonado-Hódar et al., 2003). In this work, they reported the preparation of tungsten-doped carbon aerogels by means of sol-gel reactions between resorcinol, formaldehyde and ammonium tungsten mixtures. Two carbonization temperatures were selected (500 and 1000 °C), and their influence on the resulting materials was evaluated. By means of SEM images, it was possible to determine the distributions of the metal species created, showing a more homogeneous distribution when the sample was carbonized at 1000 °C. Moreover, the temperature determined the type of tungsten particles inside the carbon structure, since carbonization at 500 °C produced materials composed of needle-like WO_3 particles with a radius of few nanometres, while when the temperature was set at 1000 °C, as well as the same type of particles, a denser species with a certain dendritic character were obtained.

The surface chemistry of metal-doped carbon gels are also conditioned by the pH of the precursor solution (Bekyarova et al., 2000) like the textural properties. Bekyarova and Kaneko (Bekyarova et al., 2000) prepared Ce,Zr-doped carbon aerogels by adding metal salts to the resorcinol-formaldehyde solutions. Two pH values were selected, 3 and 7, results in materials with different features. The TEM images collected in this work showed that in the case of pH 7, the carbon aerogel was composed of bound particles of about 20 nm and, there was a homogeneous distribution of the metal species. However, the sample synthesized from a solution with pH 3 gave rise to spherical particles with diameters of about 3 μm and no doping particles were detected.

3.3 Mechanical properties

Carbon gels are composed of interconnected quasi-spherical nodules, forming a three-dimensional matrix, as reflected by the SEM photograph presented in Figure 12. As already mentioned, the diameter of these nanospheres and, therefore, the pore size is influenced by several synthesis conditions (Czzakel et al., 2005; Silva et al., 2009; Zubizarreta et al., 2008a). As regards to the initial pH, lower microspheres size are obtained as the initial pH increases, corresponding to highly compact structures. Zubizarreta et al. (Zubizarreta et al., 2008a) determined the influence of the pH on the structure of the carbon xerogels, noting that precursor solutions with pH 9 and 7 produced carbon xerogels with a compact and uniform structure while the sample obtained using pH 6 exhibited a low-compact structure and besides, the microspheres have hardly intuit.

The influence of other synthesis variables, such as the drying procedure, on the structure of carbon gels has been determined by several research groups. Regardless of the drying conditions, the structure of carbon gels is composed of interconnected spherical particles, although it is necessary to emphasize that the size of such spheres changes depending on the method used (Czzakel et al., 2005). Sometimes it is difficult to discriminate between the structures of carbon aerogels and cryogels. However, by means of SEM or TEM

photographs, it is possible to appreciate the smaller size of the microspheres of the carbon xerogels, as a result of the shrinkage of the structure (Czzakel et al., 2005).
One of the advantages associated with carbon gels is that they can be made with different morphologies, such as monoliths, although this monolithic shape is notably influenced by the synthesis conditions. There is a scientific work that has demonstrated the effect of the initial pH and the heating device used to evaporate the solvent, on the morphology of carbon xerogels (Zubizarreta et al., 2008a). With microwave heating, it was possible to preserve the monolithic shape of the carbon gel when a precursor solution with a high pH is used, whereas when the pH was low, the monolith broke into pieces as a result of its greater frailty. This confirms that the final carbon gel displays better mechanical properties as the initial pH increases.

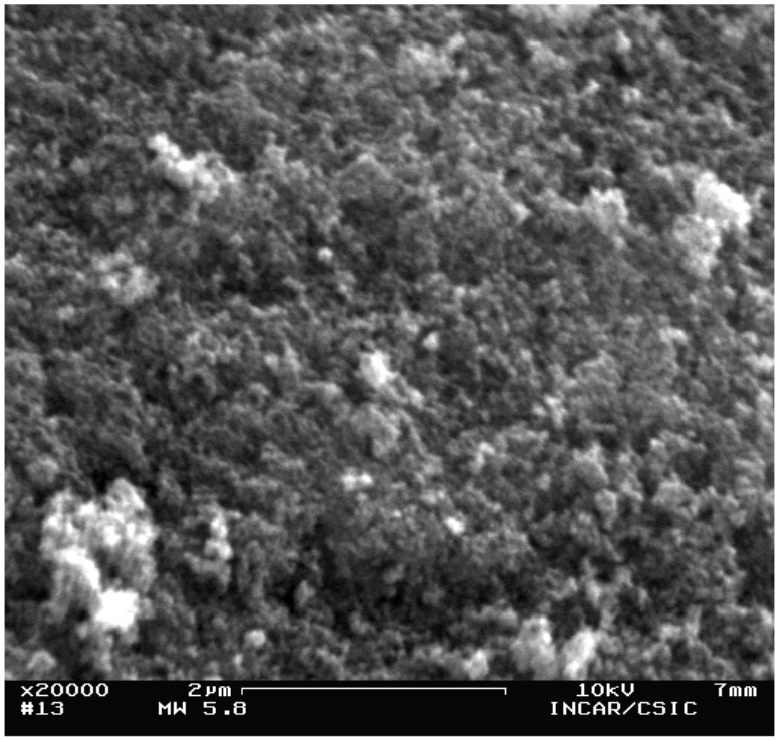

Fig. 12. SEM image of resorcinol-formaldehyde carbon xerogel synthesised in a microwave oven using a precursor solution with a pH of 5.8.

Regarding the effect of the activation processes, both physical and chemical, on the mechanical properties of the resultant activated material, it has been observed that it is possible to obtain monoliths of physically activated carbon gels. However, when chemical activation is used, the process is more severe and it is not possible to retain the monolithic shape.
The porous, chemical and mechanical characteristics of carbon gels are related to the different synthesis steps and the operating variables involved in each stage. As a summary of this section this relationship is reported in Table 2. Although there are many works which deal with the designing of the carbon gel properties and the great potential of these materials, many variables require further study and adjustment with the aim of tailoring the properties of the final material for a specific application.

STEP	VARIABLES	POROUS TEXTURE	CHEMICAL PROPERTIES	STRUCTURAL PROPERTIES
SOLUTION, GELATION AND CURING	pH/catalyst	pH has no influence on microporosity and/or surface area (Calvo et al., 2011a; Job et al., 2004; Lin & Ritter,1997) Increasing pH yields a narrower mesoporosity (Calvo et al., 2011a; Job et al., 2004; Lin & Ritter,1997) Decreasing the pH increases the macroporosity (Zubizarreta et al., 2008a, Calvo et al., 2011a) As the pH increases, the gelation time (t_g) decreases (Calvo et al., 2011a; Juárez-Pérez et al., 2010)	Not influenced (Calvo et al., 2011a, Zubizarreta et al., 2008a)	Increasing the pH increases the mechanical resistance of the carbon xerogels (Zubizarreta et al., 2008a)
	RF concentration	A decrease in the RF concentration leads to a smaller pore size (Al-Mutasheb & Ritter, 2003; Petricevic et al., 2001)	Not influenced	Little studied
	Temperature	Very high synthesis temperatures cause a shrinkage of porosity	Not influenced	Little studied
SUBCRITICAL DRYING	Stove	Causes shrinkage of the pore structure (Al-Mutasheb & Ritter, 2003; Czzakel et al., 2005; Job et al., 2005)	Not influenced	Easy to obtain carbon xerogel monoliths
	Microwave	Slightly higher shrinkage of the pore structure (Zubizarreta et al., 2008b)	Higher oxygen content but few studies on this topic (Zubizarreta et al., 2008b)	It is difficult to obtain carbon xerogel monoliths directly, but the good control of gelation point leads to design the final shape (Calvo et al., 2011a; Mahata et al., 2008)
CARBONISATION	temperature	Increasing the temperature either increases (Husley et al., 1992; Lin & Ritter, 2000) or decreases the surface area and micropore volume (Kang et al., 2009) Little influence on meso or macroporosity	Increasing the temperature reduces the oxygen content (Al-Mutasheb & Ritter, 2003)	Little studied
	Heating rate	A high heating rate reduces the micropore volume (Kuo et al., 2005; Liou, 2004)	Little studied	Little studied
	Atmosphere	A carbonization atmosphere notably influences the porous texture of the carbon gels (Kang et al., 2009; Zubizarreta et al., 2008a)	Depending on the type of carbonisation atmosphere (Kang et al., 2009; Zubizarreta et al., 2008a)	Little studied

STEP	VARIABLES	POROUS TEXTURE	CHEMICAL PROPERTIES	STRUCTURAL PROPERTIES
ACTIVATION	Physical	Increasing activation the temperature and operating times leads to a more developed pore texture (Contreras et al., 2010; Lin & Ritter, 2000)	The oxygen content increases (Contreras et al., 2010)	Possible activation of the monoliths
	Chemical	Activation of the organic xerogels destroys the meso-macroporosity created during the synthesis (except in a MW oven), but increases the microporosity and surface area considerably (Calvo et al., 2011b; Zubizarreta et al., 2008c) Activation of the carbon xerogels increases the microporosity without altering the meso-macroporosity (Al-Mutasheb & Ritter, 2003; Molina-Sabio et al., 2004; Zubizarreta et al., 2008c) The activating agent/carbon ratio influences the micropore volume considerably (Conceição et al., 2009; Zubizarreta et al., 2008c)	The oxygen content increases	The monoliths are usually destroyed (Zubizarreta et al., 2008c)

Table 2. Effect of the synthesis conditions on the properties of resorcinol-formaldehyde carbon gels.

4. Applications of carbon xerogels

All the characteristics already mentioned along this chapter make carbon xerogels very promising candidates for a wide range of applications such as adsorption (Long et al., 2009; Maldonado-Hódar et al., 2007; Ying et al., 2005), water treatment (Girgis et al., 2011; Shánchez-Polo et al., 2007), gas separation (Yamamoto et al., 2004) or enzymes support (Chaijitrsakool et al., 2008). Besides the most common and referenced ones like catalysts support (Job et al., 2008; Lambert et al., 2010; Liu & Creager, 2010; Moreno-Castilla et al., 1999), electrode materials in electric double layer capacitors (Calvo et al., 2008; Frackowiak & Béguin, 2001; Sepheri et al., 2009; Zhang et al., 2007; Zhu et al., 2007) and hydrogen storage (Kang et al., 2009; Tian et al., 2010, 2011a, 2011b; Zubizarreta et al., 2010). In this section a brief review of all these applications of carbon xerogels are reviewed.

4.1 Catalysts support

Catalysis plays a decisive role in many reactions and technologies such as: energy supply by fuel cells, oxidation of organic compounds in liquid effluents, removal of SO_x and NO_x in order to reduce the pollution, synthesis of fine chemistry products, etc (Girgis et al., 2011; Machado et al., 2010; Moreno-Castilla et al., 2005; Pirard et al., 2011). Generally, two types of catalysis are distinguished: homogeneous catalysis, i.e. reactants and catalyst constitute just one phase and heterogeneous catalysis, it is to say, when catalyst is in a different phase respect to the reactants involved in the process. Both kind of catalysts display advantages

and drawbacks. For example, heterogeneous catalysts are much important at industrial scale as a result of their simple preparation procedure, high stability and the possibility of separating them from the reaction media in an easy way. Nevertheless, the disadvantages of heterogeneous catalysis are the presence of two different phases and the control of the active sites nature. On the other hand, regarding to homogeneous catalysis, although reactions take place in a single phase and catalysts can be tailored, their carriage in industrial processes is lower due to their sometimes limited stability and their difficult recovery (Choplin & Quignard, 1998; Djakovitch et al., 2004; Fontecha-Cámara et al., 2011).

Most of published works on carbon gels used in catalysis field are focused on heterogeneous processes and the great interest of carbon gels in this field research is due to their attractive features such as: tailored pore texture, possibility of enriching their surface chemistry by different processes, high packing density, high durability under harsh conditions, etc. (Cotet et al., 2006; Job et al., 2005; Moreno-Castilla et al., 1999; Teng & Wang, 2000). The major challenge in catalysis, together with the reduction of costs is to increase their activity and selectivity. The selectivity is a feature very difficult to manage but catalytic activity has been extensively studied in many publications in order to achieve a relationship between this parameter and the properties of the carbon material. Both surface chemistry and porous texture of carbon gels play an important role on catalytic processes. However, catalytic activity depends on the nature, amount and accessibility of their active sites for the reactants, and it is not always straightforward to correlate it with intrinsic characteristics of carbonaceous materials.

One of the first works found about catalytic performance of metal-doped carbon gels were published in 1999 by Moreno-Castilla and co-workers (Moreno-Castilla et al., 1999). This work was focused on the study of catalytic activity of chromium, molybdenum and tungsten oxide-doped carbon aerogels in the isomerisation reaction of 1-butene and the results showed that the best catalyst for this specific reaction was carbon aerogel based on tungsten oxide because of the higher surface acidity. The isomerization reaction of 1-butene in other structures was a widely investigated process since a hydrocarbon with higher octanoic value can be obtained and therefore, several research groups have performed studies on the effect of using metal catalysts supported on carbon materials for accelerating this reaction (Álvarez-Merino et al., 2000).

Carbon gels have also been explored as metal catalyst support for fuel cell applications. The fact of using carbon supported catalysts in fuel cells allows production costs to be reduced and performance and durability of the electrochemical system to be improved (Arbizzani et al., 2007; Job et al., 2008; Liu & Creager, 2010). One the most recent works in this research field was carried out by Liu and Creager (Liu & Creager, 2010). Resorcinol-formaldehyde carbon xerogels was used as supports for Pt particles, by means of impregnation-reduction method using H_2PtCl_6 as platinum precursor and formaldehyde as the reducing agent. Electrochemical results of the membrane-electrodes fabricated from Pt-deposited carbon xerogels with Nafion as electrolyte, were compared with those of Pt catalyst supported on a commercial carbon black. Pt-carbon xerogel catalysts displayed good intrinsic catalyst activity due to the higher size of Pt particles in these catalysts and besides, the cell performance normalized by Pt loading was slightly higher when Pt particles were supported on resorcinol-formaldehyde carbon xerogels. Job et al. (Job et al., 2008) also prepared Pt-carbon xerogel catalysts for fuel cell applications. The catalysts were synthesized following two different recipes: (i) impregnation of carbon xerogel with Pt precursor solution followed by reduction process and (ii) strong electrostatic adsorption

(SEA method). This latter method produced higher dispersion of Pt particles than the impregnation and consequent reduction, improving the performance of fuel cells in terms of Pt mass activity. Moreover, there are research groups that used bimetallic catalysts for energy production in fuel cells. For example, Figueiredo and co-workers (Figueiredo et al., 2006) evaluated the electrochemical performance of direct-methanol fuel cells (DMFCs) assembled with Pt-Ru catalyst supported on oxidized carbon xerogels and the results reported in that study demonstrated that resorcinol-formaldehyde carbon xerogels were effective as supports for Pt/Ru particles. Pt-Ru bimetallic catalysts were also prepared by Arbizzani and et al (Arbizzani et al., 2007) for their use as anodes in DMFCs. In that case, the carbon supports were mesoporous cryo and xerogel carbons and Pt-Ru catalysts were obtained by impregnation of carbon materials with H_2PtCl_6 and $RuCl_3$ in ethylene glycol and later chemical reduction. The activity of the catalysts were related with structural and morphological properties of carbonaceous supports and electrochemical results of fuel cells were also compared to those obtained with a Pt-Ru supported on a commercial carbon support, showing again the good behaviour of carbon gels as support catalysts.
Other chemical processes and/or reactions catalyzed by carbon gels are for example, oxidation of several organic compounds with the aim of reducing pollution in liquids effluents (Girgis et al., 2011; Maldonado-Hódar et al., 2004), toluene combustion reactions (Gomes et al., 2008; Maldonado-Hódar et al., 2007), growth of carbon nanofilaments and nanotubes (Fu et al., 2003), conversion of D-glucose into D-gluconic acid (Pirard et al., 2011), and a long list since this type of catalysts has infinite number of applications in many different research fields.

4.2 Electric energy storage

A large number of publications can be found in the literature about carbon gels as electrode materials in supercapacitors as a result of being highly porous materials with a good electric conductivity (Kim et al., 2001).
In electrochemical double layer capacitors, EDLC´s, the main mechanism that governs charge storage processes is the formation of the electric double layer in the electrode/electrolyte interface (Frackowiak, 2007; Kötz & Carlen, 2000). Theoretically, as specific surface area increases, higher energy storage capacitance is achieved, but actually the situation changes because the whole surface area of the electrode material is not electrochemically accessible, and therefore useful, when electrodes are immersed in the electrolyte. Many studies about carbon gels and supercapacitors have concluded than charge storage is performed in micropores whereas mesopores with a specific size are needed for a fast diffusion of electrolyte ions (Frackowiak & Béguin, 2001; Salitra et al., 2000; Vix-Guterl et al., 2005). Electrochemical studies on carbon gels with a mesopores size between 3-13 nm have resulted in very high specific capacitance values and also, in a stable capacitive performance of the supercapacitor (Escribano et al., 1998). Therefore, it has been generally accepted that a balanced porosity between micro and mesopores is preferable to reach the optimum performance of the supercapacitor. Carbon gels are very promising materials for this application since besides their high microporosity, mesopores with a specific and tailored size can be obtained varying the synthesis conditions, absent feature in the case of activated carbons. Moreover, carbon gels display other advantages when they are used as electrodes in supercapacitors such as their high conductivity, enabling the removal of the usual additive to promote this property employed with active carbons, possibility of obtaining them in several morphologies directly without the need

of binders, i.e. it would be feasible to prepare carbon gel films in order to directly use as electrodes, and high cycling-life (Pandolfo & Hollenkamp, 2006). It has been found specific capacitance values of carbon gels in aqueous electrolyte between about 100 F g^{-1}, in the case of an untreated carbon gel and 300 F g^{-1}, data corresponding to carbon gels textural and chemically modified by means of several post-synthesis treatments. Some specific capacitance values found in the literature for untreated carbon gels are for example from 153 to 194 F g^{-1} in the case of several resorcinol-formaldehyde carbon xerogels with specific surface areas between 700-800 m^2 g^{-1} (Zhang et al., 2007); 150 F g^{-1} when the electrochemical performance were carried out using a basic aqueous media as electrolyte and RF carbon xerogel dried by microwave heating after a previous solvent exchange with acetone (Halama et al., 2010), or finally, 120 F g^{-1} for a RF carbon xerogel with a S_{BET} of 594 m^2 g^{-1} obtained by microwave-assisted synthesis (Calvo et al., 2011a). It should be noted that despite the lower energy storage capacitance shown in the case of this late carbon xerogel, it is a very promising material because it has been synthesized by microwave heating in few hours compared to several days needed in the other examples cited. Higher capacitance values are reported when activated carbon gels are used as electrode materials in supercapacitors. Zhu and co-workers (Zhu et al., 2007) and Wang et al. (Wang et al., 2008) performed the synthesis of activated carbon gels with KOH and studied their electrochemical performance as electrode materials in supercapacitors with basic aqueous electrolyte, and results reported by both research groups were 244 F g^{-1} (Wang et al., 2008) and 284 F g^{-1} (Zhu et al., 2007), comparable values to those shown by other carbonaceous materials commonly used as electrodes in supercapacitors (Kierzek et al., 2004; Lota et al., 2008; Shi, 1996).

The energy storage mechanism based on charges separation in the electrode/electrolyte interface is not the only mechanism that can carry out in supercapacitors. In fact, there is another type of energy storage, induced by faradaic reactions occurring in electrodes surface, which considerably enhances the capacitance of supercapacitors (Frackowiak & Béguin, 2001). These redox reactions promote so-called pseudocapacitance effects and they are caused due to the presence of heteroatoms in the surface of the carbon electrodes. Some of the heteroatoms which contribute to the energy storage by means of pseudocapacitive effects are, for example, O, N, P, B, some metals, etc. (Frackowiak, 2007; Kang et al., 2008; Tian et al., 2010). Moreover, together with the increase of energy capacitance, surface groups improve the wettability of electrodes in aqueous media, due to electrostatic interactions on the electrode surface with dipole moments of water molecules. There are many examples in the literature about the use of doped carbon gels as electrode materials for supercapacitors. In the case of nitrogen-doped carbon gels, the work presented by Kang and co-workers, mentioned in Section 2 (Kang et al., 2008), reported the preparation of nitrogen enriched carbon xerogels by means of ammonisation processes. In this study, three different carbon xerogels were compared both textural and electrochemically: RF carbon xerogel conventionally synthesized, RF carbon xerogel conventionally synthesized and carbonised under NH_3 atmosphere and, finally, a RF carbon xerogel prepared by microwave-assisted synthesis and carbonised with NH_3. The two samples subjected to NH_3-carbonization display similar nitrogen contents (between 2.6 and 3.2 wt. %), while the porous texture is noticeable different. Microwave assisted sample has around 1700 m^2 g^{-1} of specific surface area opposite to 1080 m^2 g^{-1} for its counterpart synthesized by conventional heating and also, the latter carbon xerogel has lower mesopore volume. This different porosity affects the electrochemical performance

of samples since conventional sample display a specific capacitance of 148 F g^{-1} vs. 185 F g^{-1} in the case of sample with larger porosity development. When these two carbon xerogels were compared to the sample pyrolysed under N_2 atmosphere, it was clearly demonstrated the profitable effects of nitrogen doping since although this last sample has a specific surface area close to 800 m^2 g^{-1}, its energy storage capacitance is very poor as a result of the absence of nitrogen functionalities, i.e. the lack of reversible electrochemical reactions that increase the capacitance due to pseudo-faradaic processes. Other work that shows the improvement of energy storage due to the presence of heteroatoms was performer by Sepheri et al. (Sepheri et al., 2009). In that case, the functionalization was carried out during the synthesis process of organic gels since, once organic gels are synthesized but still wet, they were introduced in ammonia borane/trifluoroacetic acid solution in order to incorporate B and N atoms into the structure of resulting materials. This treatment promotes the presence of functional groups and besides, the increase of mesoporosity since the carbon gel mixed with AB solution possesses a mesopore volume of 1.57 cm^3 g^{-1} opposite to 1.17 cm^3 g^{-1} in the case of untreated carbon xerogel. Results about the chemical nature of these samples, show that the ammonia borane treatment allows the incorporation of borane and oxygen functionalities (2.2 and 11.4 wt. % of boron and oxygen for treated carbon xerogel vs. 0.0 and 3.8 wt. %, respectively, in the case of untreated sample) while nitrogen groups disappear during the carbonization step. The enrichment of surface chemistry together with the enhanced porous texture causes an increase of ca. 30 % in the specific capacitance values and also an improvement in the current density of supercapacitors.

Quin and other researchers (Qin et al., 2011), also reflect the improvement of capacitive performance of supercapacitors by means of nitrogen functionalization of electrodes. Unlike the other two mentioned examples, the electrochemical devices assembled were asymmetric supercapacitors, where $Ni(OH)_2$/$Co(OH)_2$ composite works as anode and an activated carbon gel/melamine resin composite as cathode material, strategy widely used in others research groups (Ganesh et al., 2006; Staiti & Lufrano, 2010). The followed recipe to performer the functionalization of materials was quite different respect to the other two published studies. On the one hand, resorcinol-formaldehyde carbon gel was synthesized and chemically activated with KOH and secondly, a melamine resin was prepared in order to use it as nitrogen source. Both samples were mixed in water with ultrasonic radiation and afterwards, the resulting material was pyrolysed and activated with KOH causing the activated nitrogen enriched carbon/carbon gel composite. Results show that activated organic gel has a specific surface area of 1670 m^2 g^{-1} opposite to 1848 m^2 g^{-1} for the nitrogen enriched composite, demonstrating that, as in previous cases (Kang et al., 2008; Sepheri et al., 2009), treated carbon gels display high porosity development. The composite also has an important amount of heteroatoms since XPS measurements show 2.1 and 13.3 % of nitrogen and oxygen content, for such sample. Electrochemical results reported in this work corroborate the higher energy storage as a result of redox reactions in the electrode surface since specific capacitance values were 103 F g^{-1} in the case of using the activated carbon gel as cathode material and 224 F g^{-1} when the supercapacitor was assembled with the nitrogen enriched composite. The difference in specific surface area between two samples was only 11 % while the electrochemical performance was enhanced about 50 %, indicating that the presence of pseudocapacitive interactions allow the global capacitance of supercapacitor to be increased.

As reflected in Section 2 of this chapter, there are lots of research groups working on doping processes of carbon gels with metal species in order to prepare higher porous and

conductive materials. Therefore, one of the final applications of these metal-doped carbon gels is as energy storage systems. One of the more recent works dealing with doping processes of carbon gels for their use in supercapacitors was published by Lee and co-workers (Lee et al., 2011). The doping method was performed either by impregnation of manganese oxide on carbon gel power or by impregnation onto monolith material and the resulting carbon gels was electrochemically characterized. The best specific capacitance values were found in the case of impregnation of power form (i.e. 135 F g^{-1} for Mn-doped carbon aerogel obtained by impregnation onto power form opposite to 108 F g^{-1} in the best case when the impregnation was carried out with the monolithic material).

4.3 Hydrogen storage

As a result of the scarcity of fossil hydrocarbon resources, hydrogen is becoming a promising substitute for these fossil fuels in mobile applications. In addition to achieve the independence of fossil fuels, the use of hydrogen represents an environmentally friendly technology since allows the production of zero emission vehicles. However, the main requisite to a successful implementation is to store and transport the hydrogen in a safe and easy way (Dillon & Heben, 2001; Schimmel et al., 2004; Zubizarreta et al., 2009). Many researches have showed great attention to solve this hydrogen storage problem by means of several methodologies: high pressure, low temperature, metal or complex hydrides and porous materials, being the latter one of the most attractive solutions. High specific surface areas with narrow micropore size distributions are required for high-efficiency physical adsorption of hydrogen. As already mentioned, the possibility to tailor the micro-mesoporosity of carbon gels besides their surface chemistry makes them suitable materials for hydrogen storage devices (Kabbour et al., 2006; Tian et al., 2010, 2011, Zubizarreta et al., 2010).

There are a large number of published works about carbon gels and hydrogen storage that try to determine the interaction mechanism between H_2 and carbonaceous support and the relationship between adsorption capacities and textural and morphological properties of sorbent material. Regarding to the texture of nanoporous carbon materials, most of the studies conclude that there is a linear relationship between hydrogen storage capacity and surface area and micropore volume, but these are not the only influencing factors, since micropore diameter plays a key role in the final storage capacity. In other words, for hydrogen storage application is so important a high micropore volume as well as a narrow micropore size distribution (De la Casa-Lillo et al., 2002; Gadiou et al., 2005; Jordá-Beneyto et al., 2008). According to several published works (Gadiou et al., 2005; Jordá-Beneyto et al., 2008), micropores with a pore size of approximately 0.7-0.9 nm promotes higher hydrogen sorption capacities. In contrast, regarding to smaller mesopores, there is not a clear relationship between mesopore diameter and process of hydrogen storage. Zubizarreta et al. (Zubizarreta et al., 2009) have published a study based on the hydrogen sorption capacity of several carbon materials, including three resorcinol-formaldehyde carbon xerogels with different porous texture and morphology. In most samples, it has been found that in H_2 adsorption experiments performed at 77 K, the gravimetric storage capacity increases with the narrow micropore volume, analogous results to those reported in the literature about hydrogen storage on other kind of materials such as activated carbon (Akasaka et al., 2011; Cabria et al., 2007; Gadiou et al., 2007; Jordá-Beneyto et al., 2008; Xua et al., 2007) or metal organic frameworks, MOFs (Hirscher & Panella, 2007; Thomas, 2007), for example.

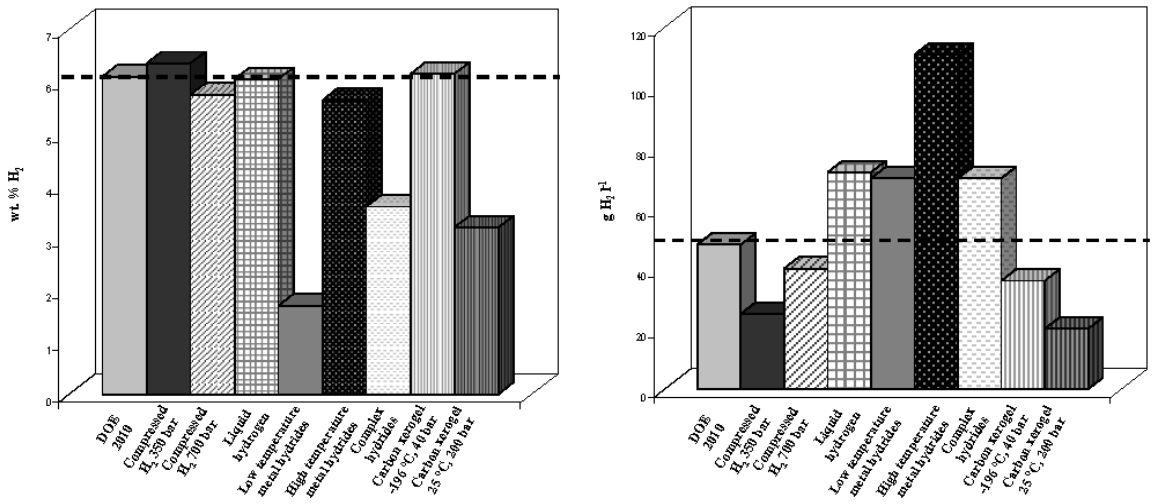

Fig. 13. Gravimetric and volumetric storage capacity of several hydrogen storage systems

For an optimum hydrogen storage capacity in solid materials, besides a well developed porous texture, there is another important feature to take into account, which is their surface chemistry. Experimental results about hydrogen storage on porous materials show that at low temperature, the dominant mechanism in the hydrogen storage process is based on microporous adsorption. However, as the temperature increases or the pressure decreases, chemical structure begins to have noticeable relevance in the mechanism of H_2 adsorption. Therefore, with the aim of changing the hydrogen/carbon interaction and therefore, enhancing the hydrogen storage capacity at room temperature or low pressure, several researches have used doped carbon materials. Some of the heteroatoms used to modify the surface properties and to achieve an enhanced hydrogen adsorption are N, B, Ni, Co, etc. (Kabbour et al., 2006; Tian et al., 2010; Zubizarreta et al., 2010). As already reflected in Section 2, carbon gels can undergo different doping processes, which is a great interest to solve the limitation of poor hydrogen uptake at room temperature. It can be found a remarkable number of studies related to hydrogen storage on doped carbon gels. However, it should be noted that, as a result of the large number of variables involved in the storage process (i.e. temperature and pressure of hydrogen storage, porous texture of carbon gels, amount and particle size of the heteroatom incorporated into the structure of carbon materials, etc.) it is very difficult to find several publications agreeing with the values of hydrogen storage capacity. For example, Kabbour et al (Kabbour et al., 2006) have published in 2006 a study about Co and Ni-doped carbon gels for hydrogen storage. The gravimetric hydrogen storage values reported were 2.1 and 2.3 wt.% for Co and Ni-doped carbon gels, respectively, when the hydrogen sorption experiments were performed at 77 K and low pressure (pressure between 0 and 2.5 bar). Other work about Co-doped carbon gels for H_2 storage shows a value of hydrogen storage capacity of 4.38 wt.% under lower temperature and high pressure conditions (Tian et al., 2010), but it should be said that the carbon gels used as adsorbent material in both works displays very different textural properties (i.e. S_{BET} = 1667 m^2 g^{-1} in 157 versus ca 1000 m^2 g^{-1} in 156), which could explain the notable difference in hydrogen storage capacities. Zubizarreta et al. (Zubizarreta et al., 2010) also investigated the performance of Ni-doped carbon gels in hydrogen storage systems and reported one of the higher values of gravimetric hydrogen storage capacity for this type of

carbonaceous materials. The best Ni-doped carbon xerogel synthesized in that work, whose specific surface area is 1727 m^2 g^{-1} with a Ni content of 2.7 wt.%, exhibits a value of hydrogen storage capacity of 6 wt.% at 77 K and 40 bar. It is very complicate to compare all these results with those found with other doped carbonaceous materials used in hydrogen storage applications (i.e. activated carbons (Akasaka et al., 2011; De la Casa-Lillo et al., 2002; Takagi et al., 2004), nanotubes (Gao et al., 2010; Lamari et al., 2002; Schimmel et al., 2004; Surya et al., 2009) or nanofibers (De la Casa-Lillo et al., 2002; Kim et al., 2008)). The hydrogen storage capacity of Ni-doped carbon gels compared with other hydrogen storage systems is collected in Figure 13. Regarding to the gravimetric storage capacity, the Ni-doped xerogel shows analogous and even higher values to other materials reported in the figure when the experiments were carried out at -196 ºC and 40 bar but, as reflected at the beginning of this paragraph, the increase of the temperature produces an important decrease of the hydrogen storage capacity, thus the Ni-doped carbon xerogel at 25 ºC is far from that the DOE had proposed for the year 2010.

4.4 Other applications

As already reflected in this chapter, the sol-gel reaction allows textural and chemical properties to be tailored but, in addition, it is possible to control other important characteristic of these carbonaceous materials, such as their morphology. As pointed out in Section 1, carbon gels can be synthesized with several shapes: monolith, films, powder, spheres, etc. and morphology may be one of the key factors that could determine the good or bad performance of carbon gels in some specific applications. An example of the relevance of the morphology is the use of carbon xerogel spheres as columns filler for gas separation. A research group from INCAR-CSIC has recently prepared resorcinol-formaldehyde carbon spheres with different sphere size depending on the synthesis procedure followed and has studied their performance as material sieves for separation of N_2/CO_2 gas mixtures (some of their results reported in Figure 14). On the one hand, it can be seen pictures with carbon spheres of different size and on the other hand, N_2 and CO_2 monitoring curves that show that CO_2 can be separated as a result of the porosity and basicity of the carbon xerogel spheres.

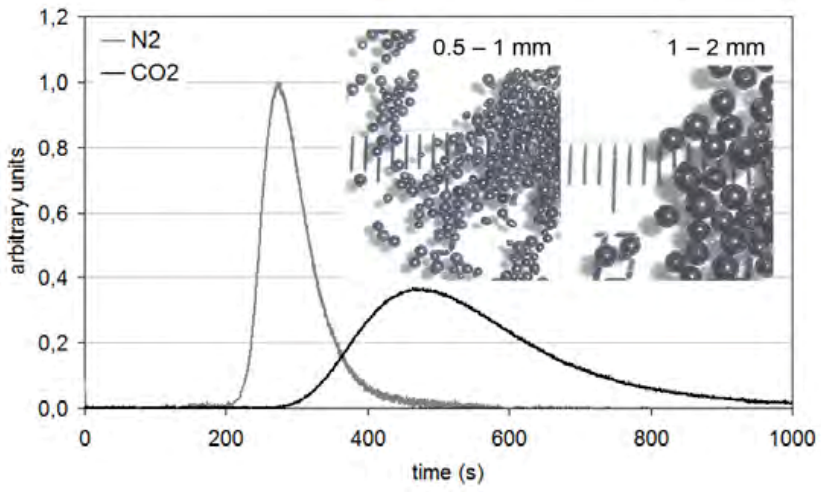

Fig. 14. Carbon xerogel spheres and their potential as fillers for gas separation systems.

In the literature, there is some example about carbon gels designed for gas separation applications. In fact, Zheivot et al. (Zheivot et al., 2010) published in 2010 a study about the production of several phenol-formaldehyde carbon xerogels and their use as adsorption materials in gas chromatography. Results reported showed that microporous carbon xerogels can be prepared varying the synthesis conditions and they can be successfully used as adsorbents to concentrate the impurities of light hydrocarbons and gaseous products of many catalytic reactions. Liquid phase adsorption can also be performed with carbon gels. In 2007, Sanchez-Polo and other researchers (Sánchez-Polo et al., 2007) analyzed the efficiency of Ag-doped carbon aerogels for the removal of several ions (Br^- and I^-) from drinking waters. The doping of resorcinol-formaldehyde aerogels was carried out by the addition of silver acetate as catalyst instead of the commonly used sodium carbonate. The study confirmed that the synthesis of mainly meso and macroporous carbon aerogels with an important amount of Ag particles could be carried out and the resulting materials displayed good adsorption capacities. The performance of carbon aerogels as adsorption materials was compared with the adsorption capacity of a commercial activated carbon that turned out to be lower. Other published work about carbon gels as liquid phase adsorbents was carried out by Girgis et al. (Girgis et al., 2011). In that study, the synthesis of carbon xerogels with difference porous texture was carried out and also the performance as adsorbent materials of two cationic dyes was evaluated. The main conclusion extracted from that publication is that carbon gels are good adsorbing materials in remediation processes since their adsorption capacities towards Methylene blue and Rhodamine B are comparable to conventional activated carbons. There is other recent work that includes the removal of several compounds from liquid effluents by using carbon gels as adsorbent materials (Figueiredo et al., 2011) but in this case, adsorption capacities collected are worse or similar than those shown by activated carbons, indicating that carbon xerogels do not seem to be an feasible option to remove colour from the effluents.

5. Conclusion

Carbon xerogels are nanostructured materials of a huge versatility since they can be synthesized with (i) different porous texture at micro-, meso- and macropore scale, (ii) different surface chemistry and (iii) different final shape. Moreover, all these properties can be tailored by adjusting the synthesis conditions, so it is possible, at least in theory, to obtain nanoporous carbon materials on-demand. However, the main problem to be solved in order to obtain a material with certain predetermined characteristics lies in the large number of variables that is necessary to control during their synthesis and to the fact that some of these variables are not independent. In consequence, one of the main drawbacks for the extensive use of these materials is to define the appropriate synthesis conditions and achieve them in a competitive way in terms of costs and operating time. Despite to the fact that great progress has been done in this sense -for example microwave induced synthesis has reduced the time of the carbon xerogels synthesis from days to hours with an important reduction in the costs of production- there is still need a step forward giving the opportunity to vast research field. Thus, it seems not risked to assure that as investigations on this matter reveals new information the great versatility of the carbon xerogels will make them important members of the family of the nanostructured materials with applications in numerous new, or existing, technologies ranging from electricity storage to drug delivery.

6. Acknowledgment

Authors would like to thanks the Spanish Ministerio de Ciencia e Innovación (Ref. MAT2008-00217/MAT) for the financial support. EGC also acknowledges FICYT for the research grand received.

7. References

Akasaka, H.; Takahata, T.; Toda, I.; Ono, H.; Ohshio, S.; Himeno, S.; Kokubu, T.; Saitoh, H. (2011). Hydrogen storaga ability of porous carbon materials fabricated from coffee bean wastes. *International Journal of Hydrogen Energy*, Vol. 36, (580-585).

Al-Mutasheb, S.A.; Ritter, J.A. (2003). Preparation and Properties of Resorcinol-Formaldehyde Organic and Carbon gels. *Advanced Materials*, Vol. 15 (101-114).

Álvarez-Merino, M.A.; Carrasco-Marín, F.; Moreno-Castilla, C. (2000). Tungsten catalysts supported on activated carbon: II. Skeletal isomerization of 1-butene. *Journal of Catalysis*, Vol. 192, (374-380).

Arbizzani, C.F.; Beninati, S.; Manferrari, E.; Soavi, F.; Mastragostino M. (2007). Cryo and xerogel carbon supported PtFu for DMFC anodes. *Journal of Power Sources*, Vol. 172, (578-586).

Baumann, T.F.; Fox, G.A.; Satcher, J.H.; Yoshizawa, R.; Fu, R.; Dresselhaus, M.S. (2002). Synthesis and characterization of copper-doped carbon aerogels. *Langmuir*, Vol. 18, (7073-7076).

Bekyarova, E.; Kaneko, K. (2000). Structure and Physical Properties of Tailor-Made Ce,Zr-Doped Carbon Aerogels. *Advanced Materials*, Vol. 12, (1625-1628).

Berthon, S.; Barbieri, O.; Ehrburger-Dolle, F.; Geissier, E.; Achard, P.; Bley, F.; Hecht, A.-M.; Livet, F.; Pajonk, G.M.; Pinto, N.; Rigacci, A.; Rochas, C. (2001). DLS and SAXS investigations of organic gels and aerogels. *Journal of Non-Crystalline Solids*, Vol. 285, (154-161).

Burdinova, T.; Ekinci, E.; Yardim, F.; Grimm, A.; Björnbom, E.; Minkova, V.; Goranova, M. (2006). Characterization and application of activated carbon produced by H_3PO_4 and water vapour activation. *Fuel Processing Technology*, Vol. 87, (899-905).

Cabria, I.; López, M.J.; Alonso, J.A. (2007). The optimun average nanopore size for hydrogen storage in carbon nanoporous materials. *Carbon*, Vol. 45, (2649-2658).

Caddick, S. (1995). Microwave Assisted Organic Reactions. *Tetrahedrom*, Vol. 51, (10403-10432).

Calvo, E.G.; Ania, C.O. ; Zubizarreta, L. ; Menéndez, J.A.; Arenillas, A. (2008). Exploring new routes in the synthesis of carbon xerogels for their applications in electric double-layer capacitors. *Energy & Fuels*, Vol. 24 (3334-3339).

Calvo, E.G.; Juárez-Pérez, E.J..; Menéndez, J.A.; Arenillas, A. (2011a). Fast microwave-assisted synthesis of tailored mesoporous carbon xerogels. *Journal of Colloid and Interface Science*, Vol. 357 (541-547).

Calvo, E.G.; Ferrera-Lorenzo, N.; Arenillas, A.; Menéndez, J.A. (2011b). Mesopores role in electrochemical performance of activated organic xerogels obtained by microwave radiation. *III Symposium on Hydrogen, Fuel Cells and Advanced Batteris, Hyceltec*, Abstract Book, p. 465, PO-15 (Zaragoza) 2011, ISBN: 978-84-938668-8-4.

Carrot, P.J.M.; Conceição, F.L.; Carrot, M.M.L.R. (2007). Use of n-nonane pre-adsorption for the determination of micropore volume of activated carbon aerogels. *Carbon*, Vol. 45, (1310-1313).

Chaijitrsakool, T.; Tonamon, N.; Tanthapanichakoon, W.; Tamon, H.; Prichanont, S. (2008). Effects of pore characters of mesoporous resorcinol-formaldehyde carbon gels on enzyme immobilization. *Journal of Molecular Catalysis B: Enzymatic*, Vol. 55, (137-141).

Chandra, S.; Bag, S.; Bhar, R.; Pramanik, P. (2011). Effect of transition and non-transition metals during the synthesis of carbon xerogels. *Microporous and Mesoporous Materials*, Vol. 138, (149-156).

Choplin, A.; Quignard, F. (1998). From supported homogeneous catalysts to heterogeneous molecular catalysts. *Coordination Chemistry Reviews*, Vol. 17, (1679-1702).

Conceição, F.L.; Carrot, P.J.M..; Ribeiro-Carrot,, M.M.L. (2009). New carbon materials with high porosity in the 1-7 nm range obtained by chemical activation with phosporic acid of resorcinol-formaldehyde aerogles. *Carbon*, Vol. 47, (1874-1877).

Contreras, M.S.; Paez, C.A.; Zubizarreta, L.; Leonard, A.; Blacher, S.; Olivera-Fuentes, C.G.; Arenillas, A.; Pirard, J.-P.; Job, N. (2010). A comparison of physical activation of carbon xerogels with carbon dioxide with chemical activation using hydroxides. *Carbon*, Vol. 48, (3157-3168).

Cotet, L.C.; Gich, M.; Roig, A.; Popescu, I.C.; Cosoveanu, V.; Molins, E.; Danciu, V. (2006). Synthesis and structural characteristics of carbon aerogels with a high content of Fe, Co, Ni, Cu and Pd. *Journal of Non-Crystalline Solids*, Vol. 352, (2772-2777).

Czzakel, O.; Marthi, K.; Gueissler, K.; Laszlo, K. (2005). Influence of drying on the morphology of resorcinol-formaldehyde based carbon gels. *Microporous and Mesoporous Materials*, Vol. 86, (124-133).

De la Casa-Lillo, M.A.; Lamari-Darkrim, F.; Cazorla-Amorós D.; Linares-Solano, A. (2002). Hydrogen storage in activated carbons and activated carbon fibers. *Journal of Physical Chemistry*, Vol. 106, (10930-10934).

De Sousa, E.M.B.; Guimares, A.P.; Mohallem, N.D.S.; Lago, R.M. (2001). The effect of thermal treatment on the properties of sol-gel copper silica catalysts. *Applied Surface Science*, Vol. 183, (216-222).

Dillon, A.C.; Heben, M.J. (2001). Hydrogen storage using carbon adsorbents: past, present and future. *Applied Physics A: Material Science Progress*, Vol. 72, (133-142).

Dingcai, W.; Ruowen, F. (2006). Synthesis of organic and carbon aerogels from phenol-furfural by two-step polymerization. *Microporous and Mesoporous Materials*, Vol. 96, (115-120).

Djakovitch, L.; Wagner, M.; Hartung, C.G.; Beller, M.; Koehler K. (2004). Pd-catalyzed Heck arylation of cycloalkenes: Studies on selectivity comparing homogeneous and heterogeneous catalysts. *Journal of Molecular Catalysis A: Chemical*, Vol. 219, (121-130).

Escribano, S.; Berthon, S.; Ginoux, J.L.; Achard, P. (1998). Characterization of carbon aerogels. *In: Extended Abstract, Eurocarbon*, Strasbourg, France (841-842).

Fairén-Jiménez, D.; Carrasco-Marín, F.; Moreno-Castilla, C. (2006). Porosity and surface area of monolithic carbon aerogels prepared using alkaline carbonates and organic acids as polymerization catalysts. *Carbon*, Vol. 44, (2301-2307).

Fang, B.; Binder, L. (2006). A modified activated carbon aerogel for high-energy storage in electric double layer capacitors. *Journal of Power Sources*, Vol. 163 (616-622).

Feaver, A.; Cao, G. (2006). Activated carbon cryogels for low pressure methane storage. *Carbon*, Vol. 44, (590-593).

Figueiredo, J.L.; Pereira, M.F.R.; Serp, P.; Kalck, P.; Samant, P.V.; Fernandes, J.B. (2006). Development of carbon nanotube and carbon xerogels supported catalysts for the electro-oxidation of methanol in fuel cells. *Carbon*, Vol. 44, (2516-2522).

Figueiredo, J.L.; Sousa, J.P.S.; Orge, C.A.; Pereira, M.F.R.; Orfäo, J.J.M. (2011). Adsorption of dyes on carbon xerogels and templated carbons: influence of surface chemistry. *Adsorption*, Vol. 17, (431-441).

Fontecha-Cámara, M.A.; Álvarez-Reinoso, M.A.; Carrasco-Marín, F.; López-Ramon, M.V.; Moreno-Castilla, C. (2011). Heterogeneous and homogeneous Fenton processes using activated carbon for the removal of the herbicide amitrole from water. *Applied Catalysis B: Environmental*, Vol. 101, (425-430).

Frackowiak, E. (2007). Carbon materials for supercapacitor applications. *Physical Chemistry Chemical Physics*, Vol. 9 (1774-1785).

Frackowiak, E.; Béguin, F. (2001). Carbon materials for the electrochemical storage of energy capacitors. *Carbon*, Vol. 39, (937-950).

Fu, R.; Baumann, T.F.; Cronin, S.; Dresselhaus, G. (2005). Formation of Graphitic Structures in Cobalt- and Nickel-Doped Carbon Aerogels. *Langmuir*, Vol. 21, (2647-2651).

Fu, R.; Dresselhaus, M.S.; Dresselhaus, G.; Zheng, B.; Liu, J.; Satcher, J.H.; Theodore, F.B. (2003). The growth of carbon nanostructures on cobalt-doped carbon aerogels. *Journal of Non-Crystalline Solids*, Vol. 318, (223-232).

Fuentes, E.; Menéndez, J.A.; Suárez, D.; Montes-Morán, M.A. (1995). Basic surface oxides on carbon materials: A global view. *Langmuir*, Vol. 19, (3505-3511).

Gadiour, R.; Texier-Mandoki, N.; Piquero, T.; Saadallah, S.; Parmentier, J.; Patarin, J. (2005). The influence of microporosity on the hydrogen storage capacity of ordered mesoporous carbons. *Adsorption*, Vol. 11, (823-827).

Ganesh, V.; Pitchumani, S.; Lakshminarayanan, V. (2006). New symmetric and asymmetric supercapacitors based on high surface area porous nickel activated carbons. *Journal of Power Sources*, Vol. 158, (1523-1532).

Gao, L.; Yoo, E.; Nakamura, J.; Zhang, W.; Chua, H.T. (2010). Hydrogen storage in Pd-Ni doped defective carbon nanotubes through the formation of CH_x (x = 1, 2). *Carbon*, Vol. 48, (3250-3255).

Girgis, B.S.; Attia, A.A.; Fatthy, N.A. (2011). Potential of nano-carbon xerogels in the remediation of dye-contamined water discharges. *Desalination*, Vol. 265, (169-176).

Gomes, H.T.; Machado, B.F.; Ribeiro, A.; Moreira, I.; Rosario, M.; Silva, A.M.T.; Figueiredo, J.L.; Faris, J.L. (2008). Catalytic properties of carbo materials for wet oxidations of aniline. *Journal of Hazardous Materials*, Vol. 159, (420-426).

Gorgulho, H.F.; Gonçalves, F.; Pereira, M.F.R.; Figueiredo, J.L. (2009). Synthesis and characterization of nitrogen-doped carbon xerogels. *Carbon*, Vol. 47, (2032-2039).

Gryzb, B.; Hildenbrand, C.; Berthon-Frabry, S.; Béguin, D.; Job, N.; Rigacci, A.; Achard, P. (2010). Functionalisation and chemical characterization of cellulose-derived carbon aerogels. *Carbon*, Vol. 48, (2297-2307).

Guo, S.; Peng, J.; Li, W.; Yang, K.; Zhang, L.; Zhang, S.; Xia, H. (2009). Effects of CO_2 activation on porous texture strucutres of coconut shell-based activated carbons. *Applied Surface Science*, Vol. 255, (8443-8449).

Halama, A.; Szubzda, B.; Pasciak, G. (2010). Carbon aerogels as electrode material for electric double layer supercapacitors: Synthesis and properties. *Electrochimica Acta*, Vol. 55, (7501-7505).

Hirscher, M.; Panella, B. (2007). Hydrogen storage in metal-organic frameworks. *Scripta Materalia*, Vol. 56, (809-812).

Houmard, M.; Vasconcelos, D.C.L.; Vasconcenlos, W.L.; Berthomé, G.; Joud, J.C.; Langlet, M. (2009). Water and oil wettability of hybrid organic-inorganic titanate-silicate thin films deposited via sol-gel route. *Surface Science*, Vol. 603, (2698-2707).

Husley, S.S.; Alviso, C.T.; Kong, F.M.; Pekala, R.W. (1992). The effect of Pyrolysis Temperature and Formulation on Pore Size Distribution and Surface Area of Carbon Aerogels. *In: Peprint of Lawrence Livermore National Laboratory*, 1992.

Jagtoyen, M.; Groppo, J.; Derbyshire, F. (1993). Activated carbon from bituminous coals by reaction with H_3PO_4 The influence of coal cleaning. *Fuel Proccesing Technology*, Vol. 34, (85-93).

Job, N; Pirard, R.; Marien, J.; Pirard, J.-P. (2004). Porous carbon xerogels with texture tailored by pH control during sol-gel process. *Carbon*, Vol. 42, (619-628).

Job, N.; Marie, J.; Lambert, S.; Berthon-Fabry, S.; Achard, P. (2008). Carbon xerogels as catalyst supports for PEM fuel cell cathode. *Energy Conversion and Management*, Vol. 49, (2461-2470).

Job, N.; Panariello, F.; Marien, J.; Crine, M.; Pirard, J.P.; Leonard, A. (2006). Synthesis optimization of organic xerogels produced from convective air-drying of resorcinol-formaldehyde gels. *Journal of Non-Crystalline Solids*, Vol. 352, (24-34).

Job, N.; Panariello, R.; Crine, M.; Pirard, J.-P.; Leonard, A. (2007a). Rheological determination of the sol-gel transition during the aqueous synthesis of resorcinol-formaldehyde resins. *Colloids and Surfaces A: Physicochemical and Engineering Aspects*, Vol. 293, (224-228).

Job, N.; Pirard, R.; Vertruyen, B.; Colomer, J.-F.; Marien, J.; Pirard, J.-P. (2007b). Synthesis of transition metal-doped carbon xerogels by cogelation. *Journal of Non-Crystalline Solids*, Vol. 353, (2333-2345).

Job, N.; Thery, A.; Pirard, R.; Marien, J.; Kocon, L.; Rouzaud, J.-N.; Beguin, F.; Pirard, J.-P. (2005). Carbon aerogels, cryogels and xerogels: Influence of the drying method on the textural properties of porous carbon materials. *Carbon*, Vol. 43, (2481-2494).

Jordá-Beneyto, M.; Lozano-Castelló, D.; Suárez-García, F.; Cazorla-Amorós, D.; Linares-Solano, A. (2008). Advanced activated carbon monoliths and activated carbons for hydrogen storage. *Microporous and Mesoporous Materials*, Vol. 112, (235-242).

Juárez-Pérez, E.J.; Calvo, E.G.; Arenillas, A.; Menéndez, J.A. (2010). Precise determination of the point of sol-gel transition in carbon gels synthesis using a microwave heating method. *Carbon*, Vol. 48, (3305-3308).

Kabbour, H.; Baumann, T.F.; Satcher, J.H.; Saulnier, J.A.; Ahn, C.C. (2006). Toward new candidates for hydrogen storage: High-Surface-Area Carbon Aerogels. *Chemistry of Materials*, Vol. 18, (6085-6087).

Kang, K.-Y.; Lee, B.I.; Lee, J.S. (2009). Hydrogen adsorption on nitrogen-doped carbon xerogels. *Carbon*, Vol. 47, (1171-1180).

Kappe, C.O. (2004). Microwave Heating in Modern Organic Synthesis. *Angewandte Chemie International Edition*, Vol. 43, (6250-6284).

Kierzek, K.; Frackowiak, E.; Lota, G.; Gryglewick, G.; Machnikowski, J. (2004). Electrochemical capacitors based on highly porous carbons prepared by KOH activation. *Electrochemica Acta*, Vol. 49, (515-523).

Kim, B.-J.; Lee, Y.-S.; Park, S.-J. (2008). A study on the hydrogen storage capacity of Ni-plated porous carbon nanofibers. *International Journal of Hydrogen Energy*, Vol. 33, (4112-4115).

Kim, S.Y.; Yeo, D.H.; Lim, J.W.; Yoo, K.; Lee, K.; Kim, H. (2001). Synthesis and Characterization of Resorcinol-Formaldehyde Organic Aergoel. *Journal of Chemical Engineering of Japan*, Vol. 34, (216-220).

Kocklenberg, R.; Mathieu, B.; Blacher, S.; Pirard, R.; Pirard, J.-P.; Sobry, R.; Van den Bossche, G. (1998). Texture control of freeze-dried resorcinol-formaldehyde gels. *Journal of Non-Crystalline Solids*, Vol. 225, (8-13).

Kötz, R.; Carlen, M. (2000). Principles and applications of electrochemical capacitors. *Electrochimica Acta*, Vol. 45, (2483-2498).

Kraiwattanawong, K.; Tamon, H.; Praserthdam, P. (2011). Influence of solvent species used in solvent exchange for preparation of mesoporous carbon xerogels from resorcinol-formaldehyde via subcritical drying. *Microporous and Mesoporous Materials*, Vol. 138, (8-16).

Kuo, H.H.; Lin, J.H.C.; Pu, C.P. (2005). Effect of carbonization rate on the properties of a PAN/phenolic-based carbon/carbon composite. *Carbon*, Vol. 43, (229-239).

Lamari, F.L.; Malbrunot, P.; Tartaglia, G.P. (2002). Review of hydrogen storage by adsorption in carbon nanotubes. *International Journal of Hydrogen Energy*, Vol. 27, (193-202).

Lambert, S.; Job, N.; D´Souza, L.; Pereira, M.F.R.; Pirard, R; Heinrichs, B.; Figueiredo, J.L.; Pirard, J.-P.; Regalbuto, J.R. (2009). Synthesis of very highly dispersed platinum catalysis supported on carbon xerogels by the strong electrostatic adsorption method. *Journal of Catalysis*, Vol. 261, (23-33).

Lee, Y.J.; Chung, J.C.; Yi, J.; Baeck, S.-H.; Yoon, J.R.; Song, I.K. (2010). Preparation of carbon aerogels in ambient conditions for electric double-layer capacitor. *Current Applied Physics*, Vol. 10, (682-686).

Lee, Y.J.; Jung, J.C.; Park, S.; Seo, J.G.; Baeck, S.-H.; Yoon, J.R.; Yi, J.; Song, I.K. (2011). Effect of preparation method on electrochemical property of Mn-doped carbon aerogel for supercapacitor. *Current Applied Physics*, Vol. 11, (1-5).

Leonard, A.; Job, N.; Blacher, S.; Pirard, J.-P.; Crine, M.; Jomaa, W. (2005). Suitability of convective air drying for the production of porous resorcinol-formaldehyde organic and carbon xerogels. *Carbon*, Vol. 43, (1808-1811).

Li, W.-C.; Lu, A.-H.; Guo, S.-C. (2001). Characterization of the microstructures of organic and carbon aerogels based upon mixed cresol-formaldehyde. *Carbon*, Vol. 39, (1989-1994).

Liang, C.; Sha, G.; Guo, S. (2000). Resorcinol-formaldehyde aerogels prepared by supercritical acetone drying. *Journal of Non-Crystalline Solids*, Vol. 271, (161-170).

Lin, C.; Ritter, J.A. (1997). Effect of synthesis pH on the structure of carbon xerogels. *Carbon*, Vol. 35, (1271-1278).

Lin, C.; Ritter, J.A. (2000). Carbonization and activation of sol-gel derived carbon xerogels. *Carbon*, Vol. 38, (849-861).

Liou, T.-H. (2004). Evolution of chemistry and morphology during the carbonization and combustion of rice husk. *Carbon*, Vol. 42, (785-794).

Liu, B.; Creager, S. (2010). Carbon xerogels as Pt catalyst supports for polymer electrolyte membrane fuel-cell applications. *Journal of Power Sources*, Vol. 195, (1812-1820).

Liu, N.; Zhang, S.; Fu, R.; Dresselhaus, M.S.; Dresselhaus G. (2006). Carbon aerogel spheres prepared via alcohol supercritical drying . *Carbon*, Vol. 44, (2430-2436).

Liu, Z.; Wang, A.; Wang, X.; Zhang, T. (2006). Reduction of NO by Cu-carbon and Co-carbon xerogels. *Carbon*, Vol. 44, (2330-2356).

Long, D.; Qiao, W.; Zhang, L.; Liang, X. (2009). Bimolecular adsorption behaviour on spherical carbon aerogels with various mesopore size. *Journal of Colloid and Interface Science*, Vol. 331, (40-46).

Long, D.; Zhang, J.; Yang, J.; Hu, Z. ; Li, T. ; Chen, G. ; Zhang, R. ; Ling, L. (2008a). Preparation and microstructure control of carbon aerogels produced using m-cresol mediated sol-gel polymerization of phenol and furfural. *New Carbon Materials*, Vol. 23, (165-170).

Long, D.; Zhang, J.; Yang, J.; Hu, Z. ; Cheng, G. ; Liu, X.; Zhang, R.; Zhang, L.; Qiao, W.; Ling, L. (2008b). Chemical state of nitrogen carbon aerogels issued from phenol-melamine-formaldehyde gels. *Carbon*, Vol. 46, (1259-1262).

Lota, G.; Centeno, T.A.; Frackowiak, E.; Stoeckli, F. (2008). Improvement of the structural and chemical properties of a commercial activated carbon for its application in electrochemical capacitors. *Electrochimica Acta*, Vol. 53, (2210-2216).

Lozano-Castelló, D.; Cazorla-Amorós, D.; Linares-Solano, A. (2002). Can highly activated carbons be prepared with a homogeneous micropore size distribution?. *Fuel Proccesing Technology*, Vol. 77, (325-330).

Machado, B.F.; Gomes, H.T.; Serp, P.; Kalck, P.; Figueiredo, J.L.; Faria, J.L. (2010). Carbon xerogel supported noble metal catalysts for fine chemical applications. *Catalysis Today*, Vol. 149, (358-364).

Maciá-Agulló, J.A.; Moore, B.C.; Cazorla-Amorós, D.; Linares-Solano, A. (2007). Influence of carbon fibers crystallinities on their chemical activation by KOH and NaOH. *Microporous and Mesoporous Materials*, Vol. 101, (397-405).

Mahata, N.; Pereira, M.F.R.; Suárez-García, F.; Martínez-Alonso, A.; Tascón, J.M.D.; Figueiredo, J.L. (2008). Tuning of texture and surface chemistry of carbon xerogels. *Journal of Colloid and Interface Science*, Vol. 324, (150-155).

Maldonado-Hódar, F.J.; Moreno-Castilla, C.; Carrasco-Marín, F.; Pérez-Cadenas, A.F. (2007). Reversible toluene adsorption on monolithic carbon aerogels. *Journal of Hazardous Materials*, Vol. 148, (548-552).

Maldonado-Hódar, F.J.; Moreno-Castilla, C.; Pérez-Cadenas, A.F. (2004). Catalytic combustion of toluene on platinum-containing monolithic carbon aerogels. *Applied Catalysis B: Environmental*, Vol. 54, (217-224).

Maldonado-Hódar, F.J.; Pérez-Cadenas, A.F.; Moreno-Castilla, C. (2003). Morphology of heat-treated tungsten doped monolithic carbon aerogels. *Carbon*, Vol. 41, (1291-1299).

Matos, I.; Fernandes, S.; Guerreiro, L.; Barata, S.; Ramos, A.M.; Vital, J.; Fonseca, I.M. (2006). The effect of surfactants on the porosity of carbon xerogels. *Microporous and Mesoporous Materials*, Vol. 92, (38-46).

Mauritz, K.A. (1998). Organic-inorganic hybrid materials: perfluorinated ionomers as sol-gel polymerization templates for inorganic alkoxides. *Materials Science and Engineering: C*, Vol. 6, (121-133).

Menéndez, J.A.; Arenillas, A.; Fidalgo, B.; Fernández, Y.; Zubizarreta, L.; Calvo, E.G.; Bermúdez, J.M. (2010). Microwave Heating processes involving carbon materials. *Fuel Processing Technology*, Vol. 91, (1-8).

Molina-Sabio, M.; Rodríguez-Reinoso, F. (2004). Role of chemical activation in the development of carbon porosity. *Colloids and Surface A: Physicochemical Engineering Aspects*, Vol. 241, (15-25).

Montes-Morán, M.A.; Menéndez, J.A.; Fuentes, E.; Suárez, D. (1998). Contribution of the Basal Planes to Carbon Basicity: An Ab Initio Study of the H_3O^+−π Interaction in Cluster Models. *The Journal of Physical Chemistry B*, Vol. 102, (5595-5601).

Moreno-Castilla, C.; Maldonado-Hódar, F.J. (2005). Carbon aerogels for catálisis applications: An overview. *Carbon*, Vol. 43, (455-465).

Moreno-Castilla, C.; Rivera-Utrilla, F.J.; Rodríguez-Castellón, J. (1999). Group of 6 metal oxide-carbon aerogels. Their synthesis, characterization and catalytic activity in the skeletal isomerization of 1-butene. *Applied Catalysis*, Vol. 183, (345-356).

Mukai, S.R.; Tamitsuji, C.; Nishihara, H.; Tamon, H. (2005a). Preparation of mesoporous carbon gels from an inexpensive combination of phenol and formaldehyde. *Carbon*, Vol. 43, (2628-2630).

Mukai, S.R.; Nishimura, H.; Yoshida, T.; Taniguchi, K.; Tamon, H. (2005b). Morphology of resorcinol-formaldehyde gels obtained through ice-templating. *Carbon*, Vol. 43, (1563-1565).

Nabais, J.N.V.; Nunes, P.; Carrot, P.J.M.; Carrot, M.M.L.R..; García, A.M.; Díaz-Díez, M.A. (2008). Production of activated carbons from coffee endocarp by CO_2 and steam activation. *Fuel Processing Technology*, Vol. 89, (262-268).

Neppolian, B.; Wang, Q.; Jung, H.; Choi, H. (2008). Ultrasonic-assisted sol-gel method of preparation of TiO_2 nano-particles. Characterization, properties and 4-chlorophenol removal application. *Ultrasonics Sonochemistry*, Vol. 15, (649-658).

Niu, J.J.; Wang, J.N. (2008). Effect of temperature on chemical activation of carbon nanotubes. *Solid Stated Sciences*, Vol. 10, (1189-1193).

Okada, K.; Yamamoto, N.; Kameshima, Y.; Yasumori, A. (2003). Porous properties of activated carbons from waste newspaper prepared by chemical and physical activation. *Jounal of Colloid and Interface Science*, Vol. 262, (179-193).

Olivares-Martín, M.; Fernández-González, C.; Macías-García, A.; Gómez-Serrano, V. (2006). Preparation of activated carbon from cherry stones by chemical activation with $ZnCl_2$. *Applied Surface Science*, Vol. 252, (5967-5971).

Pandolfo, A.G.; Hollenkamp, A.F. (2006). Carbon properties and their role in supercapacitors. *Journal of Power Sources*, Vol. 157, (11-27).

Pekala, R.W. (1989). Organic aerogels from the polycondensation of resorcinol with formaldehyde. *Journal of Materials Science*, Vol. 24, (3221-3227).

Pekala, R.W.; Alviso, C.T. (1992). Carbon aerogels and xerogels. *Materials Research Society Symposium Proceedings*, Vol. 270, (3-14).

Pekala, R.W.; Alviso, C.T.; Lu, X.; Gross, J.; Fricke, J. (1995). New organic aerogels based upon a phenolic-furfural reaction. *Journal of Non-Crystalline Solids*, Vol. 188, (34-40).

Pérez-Cadenas, M.; Moreno-Castilla, C.; Carrasco-Marin, F; Pérez-Cadenas, A.F. (2009). Surface chemistry, porous texture and morphology of N-doped carbon xerogels. *Langmuir*, Vol. 25, (466-470).

Petricevic, R.; Glora, M.; Fricke, J. (2001). Planar fiber reinforced carbon aerogels for application in PEM fuel cells. *Carbon*, Vol. 39, (857-867).

Pirard, S.L.; Diverchy, C.; Hermans, S.; Devillers, M.; Pirard, J.-P.; Job, N. (2011). Kinetics and diffusional limitations in nanostructured heterogeneous catalyst with controlled pore texture. *Catalysis Communications*, Vol. 12, (441-445).

Qin, C.; Lu, X.; Yin, G.; Jin, Z.; Tan, Q.; Bai, X. (2011). Study of activated nitrogen-enriched carbon and nitrogen-enriched carbon/carbon aerogel composites as cathode materials for supercapacitors. *Materials Chemistry and Physics*, Vol. 126, (453-458).

Qin, G.; Wei, W.; Guo, S. (2001). Semi-continuous drying of RF with supercritical acetone. *Carbon*, Vol. 41, (851-853).

Qu, R; Wang, M.; Sun, C.; Zhang, Y.; Ji, C.; Chen, H.; Meng, Y.; Yin, P. (2008). Chemical modification of silica-gel with hydroxyl- or amino-terminated polyamine for adsorption of Au (III). *Applied Surface Science*, Vol. 255, (3361-3370).

Quin, G.; Guo, S. (2001). Preparation of RF organic aerogels and carbon aerogels by alcoholic sol-gel process. *Carbon*, Vol. 39, (1935-1937).

Raymundo-Piñero, E.; Azäis, P.; Cacciaguerra, D.; Cazorla-Amorós, D.; Linares-Solano, A.; Béguin, F. (2005). KOH and NaOH activation mechanisms of multiwalled carbon nanotubes with different structural organisation. *Carbon*, Vol. 43, (786-795).

Riera, E.; Blanco, A.; García, J.; Benedito, J.; Mulet, A.; Gallego-Juárez, J.A.; Blasco, M. (2010).High-power ultrasonic system for the enhancement of mass transfer in supercritical CO_2 extraction processes. *Ultrasonics*, Vol. 50, (306-309).

Roman, S.; González, J.F.; González-García, C.M.; Zamora, F. (2008). Control of pore develpment during CO_2 and steam activation of olive stones. *Fuel Processing Technology*, Vol. 89, (715-720).

Salazar-Hernandez, M.M.; Leyve-Ramirez, M.A.; Gutierrez, J. A. (2009). Neutral alkoxysilanes from silica gel and N-phenyldiethanolamine. *Polyhedrom*, Vol. 28, (4044-4050).

Salitra, G.; Soffer, A.; Eliad, L.; Cohen, Y.; Aurbach, D. (2000). Carbon electrodes for double-layer capacitors. Relation between ion and pore dimensions. *Journal of Electrochemistry Society*, Vol. 147, (2486-2493).

Sanchez-Polo, M.; Rivera-Utrilla, J.; Salhi, E.; von Gunten, U. (2007). Ag-doped carbon aerogels for removing halide ions in water treatment. *Water research*, Vol. 41, (1031-1037).

Scherdel, C.; Reichenauer, G. (2009). Carbon xerogels synthesized via phenol-formaldehyde gels. *Microporous and Mesoporous Materials*, Vol. 126, (133-144).

Schimmel, H.G.; Nijkamp, G.; Kearley, G.J.; Rivera, A.; de Jong, K.P.; Mulder, F.M. (2004). Hydrogen adsorption in carbon nanostructures compared. *Materials Science and Engineering B*, Vol. 108, (124-129).

Sepheri, S.; Garcia, B.B; Zhang, Q.; Gao, G. (2009). Enhanced electrochemical and structural properties of carbon cryogels by surface chemistry alteration with boron and nitrogen. *Carbon*, Vol. 47, (1436-1443).

Serdich, M.; Jurcakova, D.H.; Lu, G.Q.; Bandosz, T.J. (2008). Surface functional groups of carbons and the effects on their chemical character, density and accesibility to ions and electrochemical performance. *Carbon*, Vol. 46, (1475-1488).

Shi, H. (1996). Activated carbons and double layer capacitance. *Electrochimica Acta*, Vol. 41, (1633-1639).

Silva, A.M.T.; Machado, B.F; Figueiredo, J.L.; Faira, J.L. (2009). Controlling the surface chemistry of carbon xerogels using HNO_3-hydrothermal oxidation. *Carbon*, Vol. 47, (1670-1679).

Staiti, P.; Lufrano, F. (2010). Investigation of polymer electrolyte hybrid supercapacitor based on manganese oxide-carbon electrodes. *Electrochimica Acta*, Vol. 55, (7436-7442).

Surya, V.J.; Iyakutti, K.; Rajarajeswari, M.; Kawazoe, Y. (2009). Functionalisation of single-walled carbon nanotube with borane for hydrogen storage. *Physica E: Low-dimensional Systems and Nanostructures*, Vol. 41, (1340-1346).

Suslick, K.S.; Price, G.J. (1999). Applications of ultrasound to materials chemistry. *Annual Review of Materials Science*, Vol. 29, (295-326).

Takagi, H.; Hatori, H.; Yamada, Y.; Matsuo, S.; Shiraishi, M. (2004). Hydrogen adsorption properties of activated carbons from modified surfaces. *Journal of Alloys and Compounds*, Vol. 385, (257-263).

Tamon, H.; Ishizaka, H.; Araki, T.; Okazaki, M. (1998). Control of mesoporous structure of organic and carbon aerogels. *Carbon*, Vol. 36, (1257-1262).

Tamon, H.; Ishizaka, H.; Yamamoto, T.; Suzuki, T. (2000). Influence of freeze-drying conditions on the mesoporosity of organic gels as carbon precursors. *Carbon*, Vol. 38, (1099-1105).

Teng, H.; Wang, S.-C. (2000). Preparation of porous carbons from phenol-formaldehyde resins with chemical and physical activation. *Carbon*, Vol. 38, (817-824).

Teng, Z.; Han, Y.; Li, J.; Yan, F.; Yang, W. (2010). Preparation of hollow mesoporous silica spheres by a sol/gel emulsion approach. *Microporous and Mesoporous Materials*, Vol. 127, (67-72).

Thomas, K.M. (2007). Hydrogen adsorption and storage on porous materials. *Catalysis Today*, Vol. 120, (389-398).

Tian, H.Y.; Buckley, C.E.; Paskevicius, M.; Wang, S.B. (2011b). Carbon aerogels from acetic acid catalysed resorcinol-furfural using supercritical drying for hydrogen storage. *The Journal of Supercritical Fluids*, Vol. 55 (1115-1117).

Tian, H.Y.; Buckley, C.E.; Paskevicius, M.; Sheppard, D.A. (2011a). Acetic acid catalysed carbon xerogels derived from resorcinol-furfural for hydrogen storage. *International Journal of Hydrogen Energy*, Vol. 36, (671-679).

Tian, H.Y.; Buckley, C.E.; Sheppard, D.A.; Paskevicius, M.; Hanna, N. (2010). A synthesis method for cobalt doped carbon aerogels with high surface area and their hydrogen storage properties. *International Journal of Hydrogen Energy*, Vol. 35, (13242-13246).

Tonamon, N.; Siyasukh, A.; Tanthapanichakoon, W.; Nishihara, H.; Mukai, S.R.; Tamon, H. (2005). Improvement of mesoporosity of carbon cryogels by ultrasonic irradiation. *Carbon*, Vol. 43, (525-531).

Tonamon, N.; Wareenin, Y.; Siyasukh, A.; Tanthapanichakoon, W.; Nishihara, H.; Mukai, S.R.; Tamon, H. (2006). Preparation of resorcinol-formaldehyde (RF) carbon gels: Use of ultrasonic irradiation followed by microwave drying. *Journal of Non-Crystalline Solids*, Vol. 352, (5683-5686).

Vix-Guterl, C.; Frackowiak, R.; Jurewick, K.; Friebe, M.; Parmentier, J.; Béguin, F. (2005). Electrochemical energy storage in ordered porous carbon materials. *Carbon*, Vol. 43, (1293-1302).

Whang, J.; Yang, X.; Wu, D.; Fu, R.; Dresselhaus, M.S.; Dresselhaus, G. (2008). The porous structures of activated carbon aerogels and their effects on electrochemical performance. *Journal of Power Sources*, Vol. 185, (589-594).

Wiener, M.; Reichenauer, G.; Scherb, T.; Frichke, J. (2004). Accelerating the synthesis of carbon aerogel precursors. *Journal of Non-Crystalline Solids*, Vol. 350, (126-130).

Wu, D.; Fu, R.; Zhang, S.; Dresselhaus, M.; Dresselhaus, G. (2004). Preparation of low-density carbon aerogels by ambient pressure drying. *Carbon*, Vol. 42, (2033-2039).

Xua, W.-C.; Takahashi, K.Y.; Matsuo, Y.; Hattoria, M. (2007). Investigation of hydrogen storage capacity of various carbon materials. *International Journal of Hydrogen Energy*, Vol. 32, (2504-2512).

Yamamoto, T.; Endo, A.; Ohmori, T.; Nakaiwa, N. (2004). Porous properties of carbon gel microspheres for gas separation. *Carbon*, Vol. 42, (1671-1676).

Yamamoto, T.; Nishimura, T.; Suzuki, T.; Tamon, H. (2001). Effect of drying conditions on mesoporosity of carbon precursors prepared by sol-gel polycondensation and freeze-drying. *Carbon*, Vol. 39, (2374-2376).

Yang, K.Y.; Hong, S.J.; Lee, B.I.; Lee, J.S. (2008). Enhanced electrochemical capacitance of nitrogen-doped carbon gels synthesized by microwave-assisted polymerization of resorcinol and formaldehyde. *Electrochemistry Communications*, Vol. 10, (1105-1108).

Ying, D.J.; Haji, Z.S.; Erkey, C. (2005). Dynamics of removal of organosulfur compounds from diesel by adsorption on carbon aerogels for fuel cell applications. *International Journal of Hydrogen Energy*, Vol. 30, (1287-1293).

Yoshimune, M.; Yamamoto, T.; Nakaiwa, M.; Haraya, K. (2008). Preparation of highly mesoporous carbon membranas via sol-gel process using resorcinol and formaldehyde . *Carbon*, Vol. 46, (1031-1036).

Zareba-Grodz, I.; Mista, W.O.; Strek, W.; Bukowska, E.; Hermanowick, K.; Maruszewski, K. (2004). Synthesis and properties of an inorganic-organic hybrid prepared by the sol-gel method. *Optical Materials*, Vol. 26, (207-211).

Zhang, L; Liu, H.; Wang, M.; Chen, L. (2007). Structure and electrochemical properties of resorcinol-formaldehyde polymer-based carbon for electric double-layer capacitors. *Carbon*, Vol. 45, (1439-1445).

Zhao, N.; He, C.; Jiang, Z.; Lin, J.; Li, Y. (2007). Physical activation and characterization of multi-walled carbon nanotubes catalytically synthesized from methane. *Materials Letters*, Vol. 61, (681-685).

Zheivot, V.I.; Molchanov, V.V.; Zaikovskii, V.I.; Krivoruchko, V.N.; Zaitseva, N.A.; Shchuchkin, M.S. (2010). Carbon xerogels: Nano and adsorption textures, chemical nature of the surface and gas chromatography properties. *Microporous and Mesoporous Materials*, Vol. 130, (7-13).

Zhu, Y.; Hu, H.; Li, W.; Zhang, X. (2007). Resorcinol-formaldehyde based porous carbon as electrode material for supercapacitors. *Carbon*, Vol. 45, (160-165).

Zhu, Y.; Hu, H.; Li, W.; Zhao, H. (2006). Preparation of cresol-formaldehyde carbon aerogels via drying aquagel at ambient pressure. *Journal of Non-Crystalline Solids*, Vol. 352, (3358-3362).

Zubizarreta, L.; Arenillas, A.; Dominguez, A.; Menéndez, J.A.; Pis, J.J. (2008a). Development of microporous carbon xerogels by controlling synthesis conditions. *Journal of Non-Crystalline Solids*, Vol. 354, (817-825).

Zubizarreta, L.; Arenillas, A.; Menéndez, J.A.; Pis, J.J.; Pirard, J.-P.; Job, N. (2008b). Microwave drying as an effective method to obtain carbon xerogels. *Journal of Non-Crystalline Solids*, Vol. 354, (4024-4026).

Zubizarreta, L.; Arenillas, A.; Pirard, J.-P.; Pis, J.J.; Job, N. (2008c). Tailoring the textural properties of activated carbon xerogels by chemical activation with KOH. *Microporous and Mesoporous Materials*, Vol. 115, (480-490).

Zubizarreta, L.; Arenillas, A.; Pis, J.J. (2009). Carbon materials for H_2 storage. *International Journal of Hydrogen Energy*, Vol. 34, (4575-4581).

Zubizarreta, L.; Menéndez, J.A.; Marco-Lozar, J.P.; Pirard, J.P.; Pis, J.J.; Linares-Solano, A.; Cazorla-Amorós, A.; Arenillas, A. (2010). Ni-doped carbon xerogels for H_2 storage. *Carbon*, Vol. 48, (2722-2733).

2. Objetivos y Planteamiento de la Tesis

2.1. Objetivos

El presente trabajo surge de la necesidad de encontrar nuevos materiales de electrodo y diferentes configuraciones que den lugar a condensadores electroquímicos capaces de almacenar elevada cantidad de energía y soportar altos voltajes de operación, lo que se traduce en un incremento de los valores de densidad de energía y potencia del dispositivo.

Por ello, el **OBJETIVO GENERAL** de la presente memoria consiste en ***producir xerogeles de carbono a partir de un novedoso método basado en la radiación microondas, para su aplicación como material de electrodo en supercondensadores***. Para alcanzar dicho objetivo general, varios objetivos específicos han sido planteados:

1. Desarrollar un método basado en el calentamiento microondas para la obtención de xerogeles de carbono de manera rápida, sencilla y competitiva industrialmente.

2. Estudiar la influencia de diferentes variables de operación (método de calentamiento y pH) sobre las propiedades porosas, químicas y estructurales de los xerogeles de carbono sintetizados.

3. Incrementar la porosidad de los xerogeles mediante procesos de activación y evaluar la influencia del tiempo y temperatura de activación sobre la textura porosa de los materiales resultantes.

4. Analizar la capacidad de almacenamiento energético de los xerogeles de carbono sintetizados en este trabajo en supercondensadores de distinta configuración y utilizando diferentes tipos de electrolitos.

2.2. Planteamiento de la Tesis

El trabajo realizado durante el desarrollo de esta Tesis Doctoral ha dado lugar a 15 artículos científicos (4 de ellos previos a la obtención del Diploma de Estudios Avanzados, DEA, y otros dos recientemente publicados, cuya información se recoge en el Anexo de la presente memoria). Por ello, esta memoria se presenta como un compendio de algunas de esas publicaciones. Además de la

Introducción, donde se incorpora el capítulo del libro *Nanomaterials,* y una parte experimental, en la que se describen las técnicas de caracterización utilizadas en este trabajo, la presente memoria abarca dos grandes bloques avalados por varios artículos publicados o aceptados en revistas científicas de importante índice de impacto (véase Tabla 2.1).

El primer bloque de publicaciones, recogido en el Capítulo 4 de la presente memoria, atiende a la síntesis de xerogeles de carbono mediante radiación microondas. La relación que existe entre las propiedades texturales y químicas de los geles de carbono con las variables de operación queda evidenciada con la presentación de dos artículos:

- ***Publicación II***: Fast microwave-assisted synthesis of tailored mesoporous carbon xerogels. J. Colloid Interface Sci. 357 (2011) 541-547.

- ***Publicación III***: Microwave synthesis of micro-mesoporous carbon xerogels for high performance supercapacitors. Microporous Mesoporous Mater. 168 (2012) 206-212.

La primera publicación versa sobre la síntesis de xerogeles de carbono mediante dos vías de calentamiento diferentes (horno microondas y eléctrico), a partir de disoluciones resorcinol-formaldehído de distinto pH. En ella se discute ampliamente la repercusión de estas dos variables (pH y mecanismo de calentamiento) sobre la estructura porosa y química de los materiales resultantes y una de las conclusiones más importantes extraídas de este trabajo es la viabilidad de la tecnología microondas para sintetizar xerogeles de carbono con características similares a los producidos mediante rutas convencionales, pero con un ahorro de tiempo más que considerable.

La segunda publicación atiende a procesos de activación. En ella, se realiza un estudio sobre la influencia de la temperatura y tiempo de activación sobre la porosidad de los xerogeles de carbono sintetizados. Además, como consecuencia de la atractiva textura porosa de los xerogeles de carbono producidos (elevada microporosidad y cierta presencia de mesoporos), éstos fueron utilizados como material de electrodo en supercondensadores. Las celdas basadas en los xerogeles de carbono altamente porosos se caracterizaron electroquímicamente y su capacidad de almacenamiento energético se comparó con la capacidad de varios carbones activos comerciales.

La tercera publicación recogida en el Capítulo 4 muestra un novedoso y sencillo método, basado en el calentamiento con microondas, que permite sintetizar esferas de gel de carbono a escala milimétrica. Además, las propiedades fisicoquímicas de estas esferas de xerogel de carbono también se pueden ajustar a partir de las variables de operación.

- ***Publicación IV***: A microwave-based method for the synthesis of carbon xerogel spheres. Carbon 50 (2012) 3553-3560.

La aplicación de los xerogeles de carbono en el campo del almacenamiento energético y, más concretamente, su utilización como electrodos en condensadores electroquímicos se recoge en el Capítulo 5, que a su vez está dividido en dos secciones bien diferenciadas. La primera de ellas, enfocada hacia la búsqueda de materiales de electrodo con propiedades idóneas para su aplicación en supercondensadores, está avalada por las siguientes publicaciones:

- ***Publicación V***: Carbon xerogel and manganese oxide capacitive materials for advanced supercapacitors. Int. J. Electrochem. Sci. 6 (2011) 596-612.

- ***Publicación VI***: Electrochemical behaviour and capacitance properties of carbon xerogel/multiwalled carbon nanotubos composites. J. Solid State Electrochem. 16 (2012) 1067-1076.

- ***Publicación VII***: Carbon xerogel as electrochemical supercapacitors. Relation between impedance physicochemical parameters and electrochemical behaviour. Int. J. Hydrogen Energy 37 (2012) 10249-10255.

En esta sección, se han utilizado supercondensadores basados en xerogeles de carbono con distintas propiedades texturales, sintetizados en el laboratorio, y se ha intentado relacionar su capacidad de almacenamiento energético con el grado de porosidad de los mismos. Además, se han llevado a cabo diferentes estrategias, basadas en combinar xerogeles de carbono con materiales con buenas propiedades conductoras (como los nanotubos de carbono, por ejemplo) o materiales con un comportamiento pseudocapacitivo (un óxido metálico), con el fin de optimizar la cantidad de energía almacenada en estos dispositivos electroquímicos.

La segunda parte del Capítulo 5 está enfocada a analizar el comportamiento electroquímico de supercondensadores basados en un xerogel altamente poroso ante electrolitos de diversa naturaleza, parte que se apoya con dos publicaciones científicas:

- ***Publicación VIII***: Optimizing the electrochemical performance of aqueous symmetric supercapacitors based on an activated carbon xerogel. J. Power Sources (aceptada).

- ***Publicación IX***: Optimizing the energy density of carbon based supercapacitors using protic ionic liquids as electrolytes. Electrochim. Acta (enviada).

Ambas comunicaciones tienen el denominador común de utilizar electrodos basados en un xerogel de carbono con una microporosidad muy desarrollada, que ha sido sintetizado en el laboratorio. No obstante, se diferencian en el tipo de electrolito utilizado, ya que una de ellas hace referencia a la caracterización electroquímica de supercondensadores que emplean electrolitos basados en disoluciones acuosas de diferente pH, mientras que la última publicación se centra en unos novedosos electrolitos basados en líquidos iónicos próticos.

Todas las publicaciones agrupadas en el Capítulo 5 son fruto de la colaboración con tres grupos de investigación de reputado prestigio en el campo del almacenamiento de energía (*Conversión y Almacenamiento de Energía*, INIFTA-UNLP, Argentina; *Sistemi per Tecnologie Energetiche*, CNR-ITAE, Italia; *Matériaux Carbonés – Energie et Environnement*, CNRS, Francia). Además, los dos últimos artículos recogidos en esta memoria han surgido como consecuencia del trabajo realizado durante dos estancias en dichos grupos de investigación.

Tabla 2.1 – Revistas y libros científicos que recogen las publicaciones incluidas en la presente Memoria

Capítulo	Publicación	Índice de Impacto
1. Introducción	Nanomaterials, Chapter 9 (2011) 187-234	—
2. Objetivos y Planteamiento de la Tesis	—	—
3. Técnicas Experimentales	—	—
4. Xerogeles de Carbono y Microondas	Journal of Colloid and Interface Science 357 (2011) 541-547	3.070
	Microporous and Mesoporous Materials 168 (2013) 206-212	3.285
	Carbon 50 (2012) 3555-3560	5.378
5. Xerogeles de Carbono como Electrodos en Supercondensadores	International Journal of Electrochemical Science 6 (2011) 596-612	3.729
	Journal of Solid State Electrochemistry 16 (2012) 1067-1076	2.131
	International Journal of Hydrogen Energy 37 (2012) 10249-10255	4.054
	Journal of Power Sources (aceptada)	4.951
	Electrochimica Acta (enviada)	3.832
6. Conclusiones	—	—
7. Bibliografía	—	—
Anexo	—	—

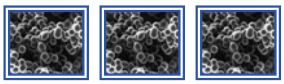

3. Técnicas Experimentales

3.1. CARACTERIZACIÓN POROSA

La porosidad es una de las propiedades más destacables de los geles de carbono ya que, como se ha mencionado en la Introducción de esta memoria, se puede controlar y diseñar en función de las condiciones de síntesis. Por este motivo, los geles de carbono pueden adaptarse perfectamente a los requisitos de la aplicación para la que están destinados.

Antes de entrar de lleno en las técnicas de caracterización porosa utilizadas para el desarrollo de este trabajo, es importante definir una clasificación de poros como por ejemplo la propuesta por Dubinin [DUBININ, 1960] y, posteriormente aceptada por la IUPAC [IUPAC, 1972], basada en la anchura de los mismos. Esta clasificación distingue tres grupos de poros: (i) microporos, poros con una anchura inferior a 2 nm; (ii) mesoporos, cuya anchura se encuentra en el intervalo de 2-50 nm y finalmente; (iii) macroporos, que se refiere a los poros con un tamaño superior a 50 nm. Además de esta clasificación, dentro de la categoría de microporosidad, se pueden distinguir dos tipos de poros: (i) microporos estrechos, también denominados ultramicroporos, que son aquellos con un tamaño inferior a 0.7 nm y, (ii) microporos anchos, cuya anchura se encuentra entre 0.7 y 2.0 nm [DUBININ, 1960].

En principio, no existe ninguna técnica de caracterización capaz de abarcar todo el rango de porosidad, es decir, que pueda detectar desde los microporos más estrechos hasta macroporos de gran tamaño. Por ello, en este trabajo se emplearon varias técnicas de caracterización que, en su conjunto, permiten analizar en profundidad toda la porosidad de los geles de carbono sintetizados.

Las técnicas de caracterización porosa utilizadas en el presente trabajo fueron: (i) adsorción física de N_2 y CO_2 y, (ii) porosimetría de mercurio, técnicas que se describen brevemente a continuación.

3.1.1. Adsorción física de gases

La adsorción física de gases es una técnica ampliamente utilizada para la caracterización textural de sólidos porosos de distinta naturaleza. Las isotermas de adsorción permiten determinar la superficie

específica del sólido (adsorbente), así como obtener información acerca de la porosidad, es decir, volumen y tamaño de poros, accesible a la molécula de gas que se adsorbe (adsorbato).

El trabajo de caracterización de los materiales presentados en esta memoria involucra la determinación de isotermas de adsorción-desorción de dos adsorbatos: nitrógeno a -196 ºC, que permite evaluar los microporos de mayor tamaño y parte de la mesoporosidad, y dióxido de carbono a 0 ºC, que abarca la microporosidad que no es accesible al N_2, es decir, los ultramicroporos (d_{poro} < 0.7 nm). A pesar de que ambos adsorbatos poseen dimensiones moleculares similares (0.33 y 0.36 nm de diámetro cinético para el N_2 y CO_2, respectivamente), la mayor temperatura de adsorción del CO_2 con respecto a la molécula de N_2, hace que el proceso de difusión se vea favorecido cubriendo, por tanto, el rango de microporosidad inaccesible para el nitrógeno.

Los métodos empleados para la determinación de las propiedades porosas (área superficial, volumen y anchura de microporos y distribución de tamaños de poro) fueron: (i) método Brunauer, Emmet y Teller, *BET*, que se basa en que conocida la cantidad de gas adsorbido necesario para formar una monocapa y el área que ocupa una de esas moléculas adsorbidas (0.162 nm^2 para la molécula de N_2), es posible conocer el área superficial de la muestra analizada; (ii) método Dubinin-Radushkevich, *DR*, basado en la teoría de Polanyi [YOUNG, 1962], que se utiliza para determinar el volumen y anchura media de los microporos presentes en una muestra; y, (iii) método *DFT* (Density Functional Theory), que permite calcular la distribución de volúmenes de poro. En la Tabla 3.1 se resumen los distintos métodos aplicados a las isotermas de adsorción de N_2 y CO_2, así como los parámetros texturales obtenidos en cada uno de los casos: S_{BET}, área superficial específica; $V_{DUB\text{-}N2}$, volumen de microporos accesible al N_2 a -196 ºC (0.7 < d_{poro} < 2.0 nm); $V_{DUB\text{-}CO2}$, volumen de microporos accesible al CO_2 a 0 ºC (d_{poro} < 0.7 nm) y PSD, distribución de tamaños de poro.

Tabla 3.1. – Métodos aplicados a las isotermas de adsorción de N_2 y CO_2

Adsorbato	Método aplicado	Parámetro textural
N_2	BET DR DFT	S_{BET} $V_{DUB\text{-}N2}$ PSD
CO_2	DR DFT	$V_{DUB\text{-}CO2}$ PSD

Para llevar a cabo la adsorción física de gases, en primer lugar se procede a desgasificar el adsorbente. Para ello, entre 100-200 mg de muestra se colocan en un bulbo de vidrio, previamente desgasificado a 120 ºC hasta un vacío de 0.1 mbar durante aproximadamente 2 horas. Posteriormente, la muestra es desgasificada durante una noche bajo las mismas condiciones de P y T que los bulbos vacíos. Para

proceder a la realización de las medidas, los bulbos se instalan en el equipo de adsorción, *Micromeritics Tristar 3020*, donde se realizan tanto las isotermas de adsorción-desorción de N_2 como de CO_2.

3.1.2. Porosimetría de mercurio

La porosimetría de mercurio es una técnica que se utiliza para caracterizar el sistema poroso de materiales constituidos por meso y macroporos. Esta técnica de ensayo se basa en el hecho de que, a presión atmosférica, el mercurio no impregna el sólido con el que está en contacto. Por ello, es necesario ejercer una presión para su intrusión en los poros, presión (p) que es inversamente proporcional al tamaño de poro (r), según la ecuación de Washburn [WASHBURN, 1921]:

$$p = \frac{2\sigma \cos\theta}{r} \qquad [3.1]$$

donde σ es la tensión superficial del mercurio, θ corresponde con el ángulo de contacto sólido-líquido y r es el radio del poro que se llena con mercurio suponiendo que su sección transversal es circular (poros cilíndricos o esféricos).

De esta manera, a bajas presiones el mercurio sólo se ve forzado a penetrar en los poros de gran tamaño mientras que a medida que aumenta la presión, el mercurio es capaz de acceder a los poros de menor dimensión.

El ensayo porosimétrico revela información acerca del volumen de mercurio intruido en la muestra analizada y, por lo tanto, de la porosidad de la misma (volumen y distribución de tamaños de poro). Es importante mencionar que dicha técnica se utiliza para determinar la distribución de tamaños de poro en el rango de 5.5 nm – 1 mm, es decir, permite analizar la macroporosidad y casi todo el rango de mesoporos presentes en la muestra. No obstante, combinando la porosimetría de mercurio con adsorción de N_2 y CO_2 a -196 y 0 ºC, respectivamente, todo el rango de porosidad presente en los geles de carbono queda cubierto.

En el presente trabajo, las medidas de porosimetría de mercurio se realizaron en un equipo *Micromeritics AutoPore IV*, limitado a poros con un diámetro medio superior a 5.5 nm. Antes de llevar a cabo el análisis, las muestras (aproximadamente 200 mg) fueron desgasificadas a vacío (0.1 mbar) a una temperatura de 120 ºC durante 2-3 horas.

3.2. CARACTERIZACIÓN QUÍMICA

3.2.1. Análisis elemental

El análisis elemental es una técnica instrumental utilizada para obtener el contenido en C (carbono), H (hidrógeno), N (nitrógeno) y S (azufre), medido en porcentaje en masa, de un amplio abanico de muestras de naturaleza orgánica e inorgánica, tanto sólidas como líquidas. La técnica de análisis se basa en la combustión completa de una muestra que se somete a un tratamiento térmico a alta temperatura, aproximadamente 1000 ºC, y bajo una atmósfera de oxígeno puro. Con ello, se consigue la conversión total de los elementos mencionados previamente en gases simples como CO_2, H_2O, SO_2 y NO_x, que posteriormente es reducido con Cu a N_2. Estos productos de combustión son medidos y procesados mediante un detector de conductividad térmica obteniéndose, al final, el contenido porcentual de cada elemento en la muestra analizada.

En este trabajo, las determinaciones de carbono, hidrógeno y nitrógeno de los xerogeles de carbono sintetizados se llevaron a cabo en un analizador comercial *LECO-CHNS-932*, utilizando para la determinación directa de oxígeno un horno *VTF-900*.

3.2.2. Punto de carga cero

La determinación del punto de carga cero, pH_{PZC}, se lleva a cabo con el objetivo de conocer la química superficial del sólido analizado. El punto de carga cero se corresponde con el pH al cual el número de cargas positivas es igual al de cargas negativas, de manera que la carga superficial total es cero. De forma genérica, cuando el pH del medio es inferior al pH_{PZC} del sólido, la superficie estará cargada positivamente, mientras que si el pH de la solución es mayor que el punto de carga cero del material evaluado, predominarán las cargas negativas [RADOVIC, 2000].

Los materiales de carbono se caracterizan por tener una naturaleza anfótera, es decir, que sobre la superficie del material se encuentran tanto grupos superficiales ácidos como básicos. De esta manera, que un material carbonoso tenga un carácter ácido o básico dependerá tanto de la concentración de sus grupos superficiales como de la fuerza de los mismos.

Los valores de pH_{PZC} obtenidos en este trabajo se evaluaron de acuerdo con el siguiente procedimiento. Inicialmente, 250 mg de muestra se introducen en un tubo de ensayo que contiene un volumen conocido de agua destilada. Transcurrido el tiempo de estabilización (48 horas bajo agitación magnética) se procede a medir el pH de la solución y seguidamente, se reduce la concentración másica de la muestra mediante la adición de un volumen conocido de agua destilada. Esta operación de medida del pH de la solución y adición de distintos volúmenes de agua se repite hasta que el pH se

haya modificado considerablemente. En la Figura 3.1 aparece un ejemplo de la representación gráfica del pH vs. concentración (wt. %) de un xerogel de carbono sintetizado en este trabajo.

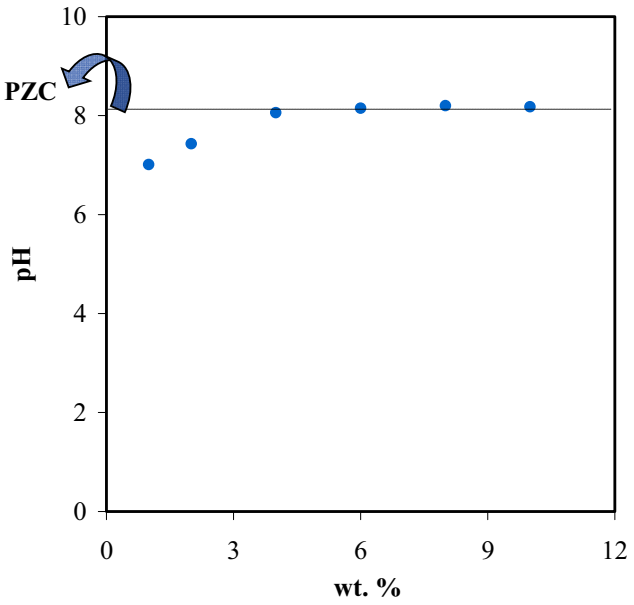

Figura 3.1. Determinación del punto de carga cero.

3.2.3. Desorción térmica programada (TPD)

La desorción térmica programada es una técnica especialmente apropiada para la caracterización de la química superficial de materiales carbonosos, puesto que los grupos funcionales presentes en la superficie de los materiales de carbono dan lugar a diferentes reacciones de descomposición al ser sometidos a un tratamiento térmico en atmósfera inerte. Según diversos estudios, al tratar térmicamente en atmósfera inerte una muestra, algunos grupos funcionales oxigenados desorben como CO_2 mientras que otros se descomponen como CO. Así, es ampliamente conocido que grupos oxigenados tipo ácidos carboxílicos desprenden CO_2 a bajas temperaturas, mientras que las lactonas se desorben como CO_2 a temperaturas más elevadas. Por otro lado, grupos funcionales como fenoles, éteres, carbonilos o quinonas son los responsables de la aparición de CO, si bien es cierto que los fenoles originan monóxido de carbono a temperaturas más bajas [FIGUEIREDO, 1999; HAYDAR, 2000].

En este trabajo, la realización de los experimentos de desorción térmica programada se llevó a cabo utilizando un analizador automático de quimisorción *Micromeritics AutoChem II* acoplado con un espectrómetro de masas, *Onmistar Pfeiffer*. Para ello, las muestras (~ 50 mg) se calentaron a 1000 ºC bajo una atmósfera de argón (50 cm^3 ml^{-1}), utilizando una velocidad de calentamiento de 10 ºC min^{-1}.

3.3. CARACTERIZACIÓN ESTRUCTURAL

3.3.1. Microscopía electrónica

Los microscopios electrónicos permiten obtener imágenes con una resolución mucho mayor que los microscopios ópticos. Este fenómeno se debe a que la fuente de iluminación utilizada es un haz de electrones, y no luz visible como en el caso de la microscopía óptica, y que las lentes son campos magnéticos capaces de desviar la trayectoria de las partículas cargadas eléctricamente. El fundamento de la microscopía electrónica consiste en que un haz de electrones incide sobre la muestra y, como consecuencia de la interacción entre esos electrones y los átomos de la muestra, surgen señales que son captadas por un detector o proyectadas directamente sobre una pantalla.

Dentro de la familia de microscopios electrónicos, los utilizados en este trabajo para la caracterización estructural de las muestras sintetizadas fueron el microscopio electrónico de transmisión (*TEM, Transmission Electron Microscopy)* y el microscopio electrónico de barrido (*SEM, Scaning Electron Microscopy)*. El microscopio electrónico de barrido no tiene la resolución que se alcanza con el microscopio electrónico de transmisión, por lo tanto la información obtenida en cada caso es distinta. El SEM proporciona información sobre la morfología superficial de los materiales (relieve, textura, tamaño y forma de grano), mientras que el TEM permite un estudio de la estructura interna y detalles ultraestructurales.

El microscopio electrónico de barrido utilizado en este trabajo fue el modelo *ULTRA-plus* de la casa Carl Zeiss SMT, mientras que las imágenes de TEM se realizaron en un microscopio modelo *JEOL-2000-EX-II*, disponible en la unidad de Servicios Científico-Técnicos de la Universidad de Oviedo.

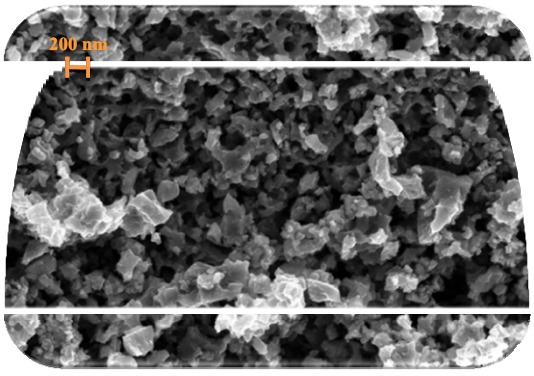

Figura 3.2. Fotografía SEM de un xerogel de carbono sintetizado en el laboratorio.

3.4. ENSAYOS ELECTROQUÍMICOS

Antes de realizar ningún ensayo electroquímico es necesario preparar los electrodos y proceder al montaje de las celdas que se van a caracterizar.

Los electrodos utilizados en este trabajo son de dos tipos, unos con forma de disco de 1 cm^2 y en torno a 6-8 mg de masa (véase Figura 3.3A) y otros electrodos con forma cuadrada (4 cm^2) y aproximadamente 20-30 mg (Figura 3.3B). Estos últimos corresponden con el tipo de electrodos utilizados en el grupo de investigación dirigido por F. Lufrano y P. Staiti (*Sistemi per Tecnologie Energetiche, ITAE-CNR*). El protocolo de preparación de electrodos seguido por cada grupo de investigación con el que se ha colaborado es diferente, pero todos ellos emplean electrodos constituidos por una mezcla de material activo (xerogel de carbono), polímero ligante y, en algunos casos, se utiliza también un aditivo conductor para mejorar las propiedades conductoras de los electrodos.

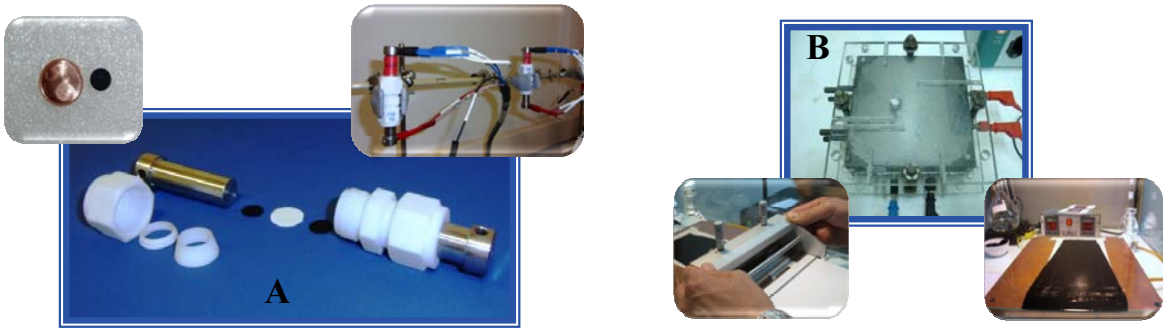

Figura 3.3. Dispositivos electroquímicos utilizados en este trabajo.

Existen dos tipos de dispositivo experimental que permiten llevar a cabo las medidas electroquímicas: celda de dos electrodos (ánodo y cátodo) y configuración de tres electrodos, que consiste en una celda formada por un electrodo de trabajo, un electrodo de referencia y un contraelectrodo [BATANERO, 2003].

Para proceder al montaje de una celda de dos electrodos son necesarios los siguientes módulos/piezas: (i) dos electrodos, (ii) un separador de fibra de vidrio, cuya función es permitir el paso de electrolito a su través pero no el paso de electrones y, (iii) dos colectores de corriente.

La configuración de tres electrodos se emplea habitualmente para caracterizar electroquímicamente un material de electrodo, ya que permite obtener información detallada acerca de los procesos faradaicos que tienen lugar dentro del rango de potencial de trabajo utilizado. En este tipo de sistemas se distinguen los siguientes componentes: (i) electrodo de trabajo, formado por la mezcla de material carbonoso, polímero ligante y aditivo conductor, si fuera necesario, (ii) electrodo de referencia (los electrodos de referencia utilizados en este trabajo han sido Hg/Hg_2SO_4, Hg/HgO y Ag/AgCl) y, (iii) contraelectrodo, como puede ser una barra de grafito (véase Figura. 3.4).

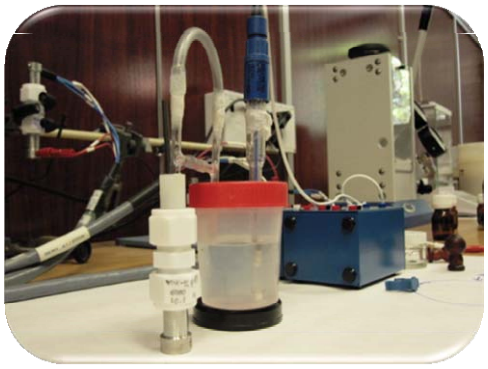

Figura 3.4. Celda electroquímica de tres electrodos.

Una vez construidas las celdas, es necesario llevar a cabo diferentes medidas electroquímicas para obtener información acerca del comportamiento de las mismas. En este trabajo, el comportamiento de los supercondensadores se evaluó mediante cronopotenciometría galvanostática (tests de carga-descarga), voltametría cíclica y espectroscopía de impedancia, técnicas que se describen brevemente a continuación.

3.4.1. Cronopotenciometría galvanostática

La cronopotenciometría galvanostática es una técnica electroquímica basada en la medición del potencial de un sistema en función del tiempo, durante la aplicación de una intensidad de corriente constante [CONWAY, 1999].

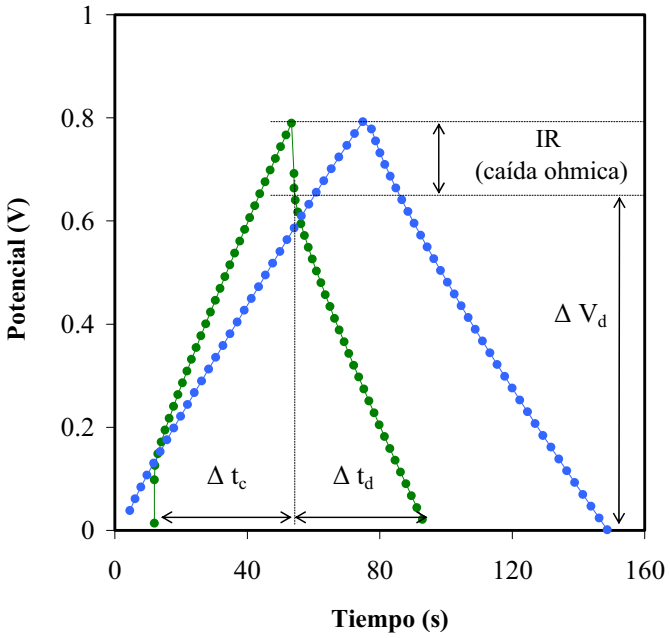

Figura 3.5. Ejemplo de ciclos de carga-descarga (I = 500 mA g^{-1}).

Tal y como se refleja en la Figura 3.5, cuando se aplica una intensidad de corriente determinada, se produce una diferencia de potencial a través de los dos electrodos que varía de forma lineal con el tiempo. La capacidad global del supercondensador puede calcularse, por tanto, a partir del ciclo de descarga según la siguiente ecuación:

$$C = I \frac{\Delta t_d}{\Delta V_d} \qquad [3.2]$$

donde C es la capacidad de la celda (F), I la intensidad de corriente aplicada (A), Δt_d es el tiempo invertido en conseguir la diferencia de potencial ΔV_d (s) y, ΔV_d se corresponde con la ventana de potencial correspondiente a la descarga del supercondensador (V).

La capacidad obtenida a partir de la ecuación 3.2 está asociada con la capacidad total de la célula. No obstante, la capacidad de cada uno de los electrodos que constituyen la celda electroquímica se puede obtener fácilmente a partir de la siguiente expresión:

$$C = \frac{1}{C_a} + \frac{1}{C_c} \qquad [3.3]$$

siendo C_a la capacidad del ánodo y C_c la del cátodo. Por lo tanto, suponiendo que las masas de ambos electrodos son idénticas, la capacidad del condensador se puede expresar como:

$$C = \frac{C_e}{2} \qquad [3.4]$$

En este trabajo, los datos de capacidad se refieren a un electrodo y se expresan como capacidad gravimétrica (F g^{-1}).

Otro parámetro que se puede obtener a partir de los experimentos de carga-descarga galvanostática es la resistencia en serie equivalente (*ESR*) de un supercondensador, que es debida fundamentalmente a tres factores: (i) resistencia de contacto entre los electrodos y los colectores de corriente, (ii) resistencia iónica del electrolito y, (iii) resistencia del electrolito en el interior de los poros del electrodo.

La resistencia en serie equivalente está relacionada con la caída ohmica o caída IR (caída de voltaje observada al inicio de cada ciclo de carga y descarga, véase Figura 3.5), de acuerdo con la siguiente expresión:

$$ESR = \frac{IR}{I} \qquad [3.5]$$

donde *ESR* se expresa en Ω, *IR* se corresponde con la caída ohmica expresada en voltios e I es la intensidad de corriente utilizada a lo largo de todo el experimento (A).

Los experimentos galvanostáticos también permiten obtener fácilmente los valores de energía y potencia específica de un supercondensador, parámetros ampliamente utilizados para representar los *Diagramas de Ragone* (E vs. P). Las ecuaciones utilizadas para obtener los datos de energía y potencia específica son las siguientes:

$$E = \frac{CV^2}{2m} \ (\text{Wh Kg}^{-1}) \qquad [3.6]$$

$$P = \frac{V^2}{4ESR \cdot m} \ (\text{W Kg}^{-1}) \qquad [3.7]$$

3.4.2. Voltametría cíclica

La voltametría cíclica es una de las técnicas más importantes en el campo de la electroquímica, especialmente para estudios de reacciones redox, mecanismos de reacción o determinación de intermedios de reacción. Esta técnica se basa en la aplicación de una perturbación de potencial eléctrico en forma de variación lineal en función del tiempo. Dicho rango de potencial se fija previamente con el objetivo de evitar reacciones no deseadas en el electrolito como es el caso de un electrolito acuoso, ya que si el potencial aplicado es superior a 1.23 V, tiene lugar la descomposición electrolítica del agua y, consecuentemente, el deterioro de los electrodos.

Además de la diferencia de potencial utilizada, también es posible modificar la velocidad de barrido, es decir, el voltaje aplicado por unidad de tiempo (mV s^{-1}). Dicho parámetro es muy relevante puesto que repercute en la cantidad de carga que es capaz de almacenar el supercondensador. Por ejemplo, a mayor velocidad de barrido, menor es el tiempo necesario para llevar a cabo la caracterización. Sin embargo, también será menor la cantidad de energía almacenada ya que los iones de electrolito no tienen tiempo suficiente para acceder a toda la porosidad del material de electrodo.

El registro de la intensidad de corriente del sistema en función del potencial aplicado se denomina voltamograma o voltamperograma (véase Figura 3.6).

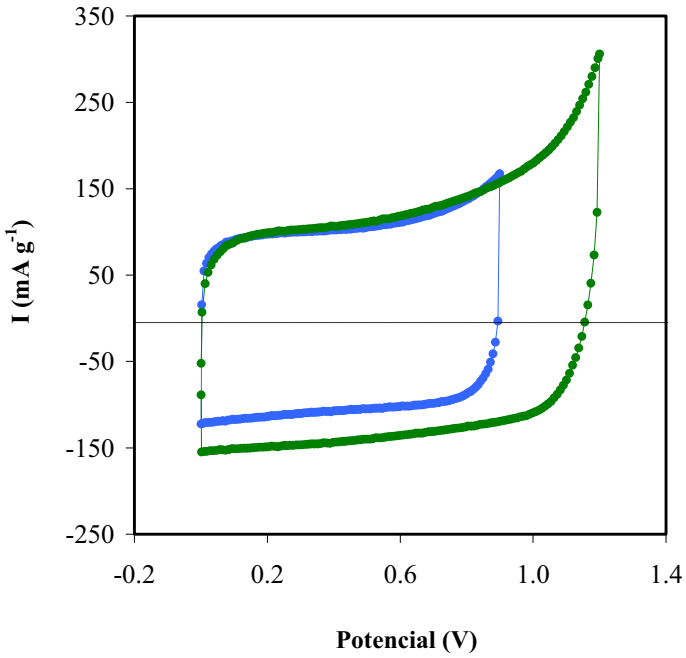

Figura 3.6. Voltamogramas obtenidos con distintas ventanas de potencial (s = 2 mV s^{-1}).

De las curvas voltamperométricas se puede obtener diversa información. Por un lado, aplicando la ecuación 3.8 se obtienen los valores de capacidad del supercondensador y, por otro lado, la morfología de la curva da una idea del mecanismo de almacenamiento de carga. Por ejemplo, un voltamograma con una forma casi rectangular estará asociado con un condensador electroquímico ideal en el que la contribución de fenómenos faradaicos es prácticamente nula, es decir, que el mecanismo de almacenamiento se debe únicamente a la formación de la doble capa eléctrica. Sin embargo, la presencia de picos o jorobas en la curva es indicativa de fenómenos rédox, tales como oxidaciones del material de electrodo y/o descomposición del electrolito.

$$C(F) = \frac{I}{s} \qquad [3.8]$$

3.4.3. Espectroscopía de impedancia

La espectroscopía de impedancia es una técnica electroquímica de corriente alterna que permite cubrir varios órdenes de magnitud en frecuencia (desde MHz hasta μHz). Se define como un método de caracterización de las propiedades eléctricas de los materiales y sus propiedades de contorno [MACDONALD, 1987], información que se consigue al observar la respuesta electroquímica de los electrodos cuando se someten a un estímulo eléctrico. Dicha respuesta depende, sustancialmente, de diferentes factores: microestructura del electrolito, número de iones presentes y porosidad y composición de los electrodos.

La impedancia, Z (f), se define como la relación que existe entre la señal de potencial aplicada y la intensidad de corriente de respuesta del sistema electroquímico, tal y como muestra la ecuación 3.9.

$$Z(f) = \frac{V(t)}{I(t)} \qquad [3.9]$$

Generalmente, la impedancia se suele expresar en forma de números complejos, siendo la parte real Z´ y la parte imaginaria designada como Z". Entre las diferentes representaciones gráficas de los datos de espectroscopía de impedancia, la más común es la representación del Diagrama de Nyquist, donde en el eje de abscisas se sitúan los valores de la parte real de la impedancia (Z´) y en el eje de ordenadas los valores de la parte imaginaria (Z").

En la Figura 3.7 se muestra un Diagrama de Nyquist obtenido experimentalmente en este trabajo con supercondensadores basados en un xerogel de carbono y tres electrolitos acuosos diferentes. En el caso de un supercondensador ideal, el Diagrama de Nyquist está constituido por tres zonas bien diferenciadas: (i) zona de altas frecuencias donde la parte imaginaria de la impedancia tiende a cero, comportamiento resistivo del material; (ii) zona de bajas frecuencias donde la parte imaginaria crece ampliamente, correspondiendo con el comportamiento capacitivo del electrodo; y (iii) zona de frecuencias intermedias donde se produce una inclinación de los valores de impedancia con respecto al eje de abscisas. Un condensador electroquímico ideal se caracteriza por un Diagrama de Nyquist que presenta una rama totalmente vertical en la zona de bajas frecuencias y una inclinación con respecto al eje en el que se representa la parte real de la impedancia de 45º. Sin embargo, en el caso de los supercondensadores reales se suele observar tanto una cierta inclinación de la rama registrada a bajas frecuencias como una especie de semicírculo en la zona de frecuencias altas-medias, probablemente debido a una mayor resistencia del dispositivo y a problemas difusionales del electrolito a través de la estructura porosa del electrodo [GARCÍA, 2011; QIN, 2011].

Tal como ocurre con las otras dos técnicas electroquímicas incluidas en este trabajo (voltametría cíclica y cronoamperometría), la capacidad de un supercondensador también se puede obtener a partir de los resultados de espectroscopía de impedancia, de acuerdo con la siguiente ecuación:

$$C = \frac{-1}{[\omega \cdot Z''(f)]} \qquad [3.10]$$

donde ω corresponde con la frecuencia angular (ω = 2πf) y Z"(f) es el valor de la impedancia en la parte imaginaria para una frecuencia determinada.

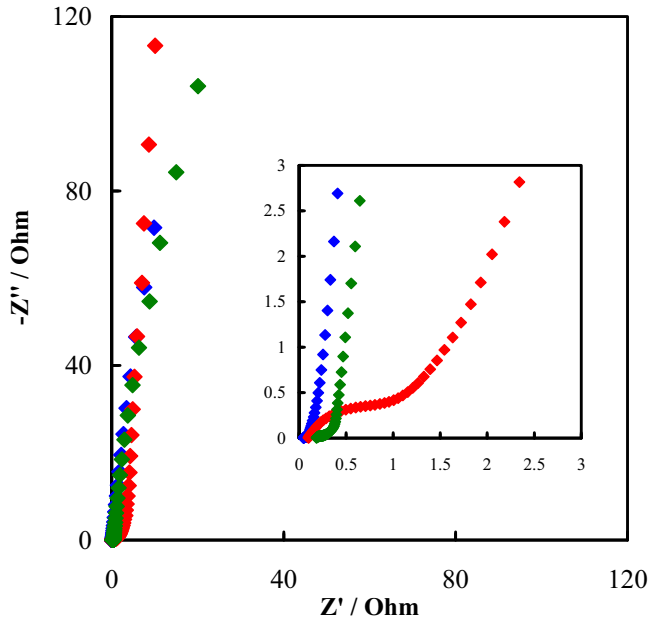

Figura 3.7. Diagrama de Nyquist obtenido en este trabajo (f: 10 MHz-1mHz).

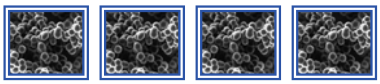

4. Xerogeles de Carbono y Microondas

4.1. Síntesis de xerogeles de carbono asistida con microondas

La utilización a escala industrial de los geles de carbono se encuentra parcialmente obstaculizada por su largo y tedioso proceso de fabricación. En numerosos campos de aplicación, los geles de carbono deben competir con carbones activos, es decir, materiales que presentan una elevada porosidad y se obtienen mediante la activación de precursores de diversa naturaleza. Habitualmente, la materia prima utilizada en estos procesos de activación se basa en residuos agrícolas y/o forestales dando lugar, por tanto, a una serie de materiales de bajo coste y, además, con un efecto positivo para el medioambiente [Ioannidou, 2007; Okada, 2003; Rodríguez-Reinoso, 1992]. Como consecuencia de ello, los geles de carbono no han sido, hasta ahora, unos materiales competitivos en el mercado de los carbones activos.

Dejando a un lado el proceso de síntesis, los geles de carbono presentan ciertas ventajas sobre los carbones activos como son: (i) alta pureza; (ii) textura porosa diseñada en función de las variables de operación; (iii) baja densidad; (iv) buenas propiedades conductoras; (v) diferente morfología (polvo, esferas, monolitos, láminas), etc. [Al-Muhtaseb, 2003; Mahata, 2008; Morales-Tores, 2012; Moreno-Castilla, 2005; Zapata-benabhite, 2012; Zheivot, 2010; Zubizarreta, 2008]. Por ello, con el objetivo de aprovechar al máximo todas estas virtudes, es necesario encontrar rutas de síntesis alternativas que permitan reducir los tiempos y abaratar los costes de producción de los geles de carbono.

Una de las alternativas planteadas por el grupo de investigación donde se ha realizado esta Tesis Doctoral (*MCAT*, *Microondas y Carbones para Aplicaciones Tecnológicas*) se basa en el uso de la tecnología microondas para la producción de este tipo de materiales carbonosos. Las tres fases del proceso de elaboración de un xerogel orgánico (gelación, curado y secado) se llevan a cabo en un horno microondas durante aproximadamente 4-5 horas consiguiendo, por tanto, una notable reducción del tiempo de síntesis.

Experimentos preliminares evidenciaron la posibilidad de sintetizar xerogeles de carbono mediante un método rápido y sencillo permitiendo, además, obtener materiales con un grado de porosidad similar al

de los geles de carbono sintetizados mediante rutas convencionales. Por ello, la síntesis de xerogeles de carbono asistida con microondas ha sido objeto de estudio y discusión en la *Publicación II*, adjuntada al final de este apartado. En esta publicación se presenta la influencia del mecanismo de calentamiento (convencional vs. microondas) y del pH de la mezcla resorcinol-formaldehído sobre la porosidad y química superficial de los geles de carbono.

En la Figura 4.1 se muestra una fotografía del dispositivo experimental utilizado para la síntesis de xerogeles de carbono asistida con microondas. El dispositivo se basa en un horno microondas multimodo que opera a una frecuencia de 2450 MHz y que consta de los siguientes componentes: (1) cronómetro; (2) contador de energía eléctrica que permite hacer un seguimiento del consumo a lo largo de todo el proceso; (3) controlador tipo PID para el monitoreo y control de la temperatura del experimento; (4) distribuidor de microondas; (5) termopar, que permite conocer la temperatura de la mezcla resorcinol-formaldehído en todo momento; y (6) recipiente con la disolución precursora.

Figura 4.1. Fotografía del horno microondas utilizado en este trabajo.

Una de las principales conclusiones extraídas de la *Publicación II* es que **la radiación microondas es una tecnología totalmente viable para la síntesis de xerogeles de carbono porosos**. Los tiempos y, por consiguiente, los costes de producción, se reducen considerablemente, lo que se traduce en materiales altamente competitivos.

Los geles de carbono se caracterizan por poseer unas propiedades definidas por las condiciones de síntesis (pH de la mezcla precursora, por ejemplo). No obstante, puesto que la síntesis de geles de carbono mediante radiación microondas es muy reciente, resulta indispensable comprobar la continuidad de dicha ventaja bajo estas nuevas condiciones de fabricación. Por este motivo, en la *Publicación II* se recoge la preparación de xerogeles de carbono a partir de disoluciones resorcinol-formaldehído de diferente pH, comprendido entre 3.1 y 9.0, tanto por la vía convencional como mediante la utilización de la tecnología microondas.

A partir del estudio de la influencia del pH sobre las propiedades de los xerogeles de carbono sintetizados mediante los dos mecanismos de calentamiento, se obtuvieron varias conclusiones:

❖ El pH influye notablemente en la meso-macroporosidad de los xerogeles de carbono mientras que la microporosidad permanece prácticamente constante. Este fenómeno se cumple tanto en la síntesis convencional como en el proceso asistido con microondas, lo que permite afirmar que el proceso de polimerización es análogo en ambos casos y por tanto, el diseño de la mesoporosidad de estos materiales se puede llevar a cabo perfectamente y de forma más competitiva mediante la radiación microondas.

❖ El pH máximo que da lugar a un xerogel de carbono poroso se sitúa entre 6.5 y 7.0. Cuando el pH de la mezcla resorcinol-formaldehído es superior a 7.0, el material resultante no presenta meso-macroporosidad y la contribución de la microporosidad cada vez es más escasa.

❖ Además del pH, la textura porosa de los xerogeles de carbono se ve ligeramente influenciada por el mecanismo de calentamiento utilizado. Sin embargo, las discrepancias entre ambos métodos de calentamiento se hacen visibles, fundamentalmente, cuando el pH de la mezcla precursora es inferior a 5.8. A pHs bajos, los geles de carbono presentan poros de gran tamaño (meso y macroporos), pero el diámetro de poro está influenciado por el dispositivo de calentamiento utilizado. La síntesis convencional produce xerogeles de carbono micro-macroporosos con un tamaño de macroporo elevado mientras que, bajo las mismas condiciones, la radiación microondas da lugar a materiales formados por un mayor volumen de mesoporos (el contenido en microporos sigue siendo prácticamente idéntico al que muestran los xerogeles producidos convencionalmente).

❖ La rapidez, simplicidad y eficacia del calentamiento con microondas queda demostrada por los resultados presentados en la *Publicación II*. No obstante, la conveniencia de la tecnología microondas frente a métodos tradicionales se decidirá en función de la aplicación final de los xerogeles de carbono. Por ejemplo, para la obtención de materiales micro-mesoporosos, la síntesis asistida con microondas sería un método totalmente viable, mientras que si el uso final de los xerogeles de carbono requiere la presencia de macroporos de gran tamaño, la balanza se decantaría hacia la síntesis convencional.

El dispositivo experimental utilizado en este trabajo permite conocer la energía consumida durante el proceso de síntesis de los xerogeles orgánicos. La representación gráfica de dicha energía vs. tiempo de irradiación da lugar a dos rectas de distinta pendiente, una correspondiente a la fase sol y otra correspondiente a la fase gel (véase Figura 4.2). Además, el punto de corte entre ambas rectas coincide con el punto de gelación (t_g), es decir, momento en el que la disolución pierde fluidez y da lugar a la formación de un gel [JUÁREZ-PÉREZ, 2010].

Como se ha mencionado en la Introducción de esta memoria, para diseñar las propiedades finales de los geles de carbono es necesario llevar a cabo un control y seguimiento del proceso de polimerización, lo que hace que sea de vital importancia conocer el punto de gelación durante la síntesis de los geles de carbono. Sin embargo, los métodos propuestos hasta el momento basados en

medidas directas de la viscosidad y parando el proceso de gelación, no permiten determinar dicho parámetro de forma práctica y precisa y, además, son métodos más complejos que el expuesto en este trabajo. Por ello, el método propuesto en la *Publicación II* es de gran interés puesto que permite determinar el punto de gelación de diferentes muestras, únicamente a través del registro del consumo energético a lo largo del proceso sol-gel, es decir, no requiere de ninguna técnica adicional y no interrumpe el proceso de síntesis.

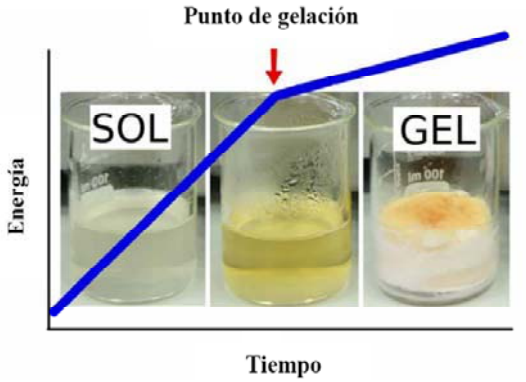

Figura 4.2. Fases involucradas en la síntesis de un xerogel orgánico.

Las conclusiones derivadas de la determinación de la transición sol-gel a partir del consumo energético del microondas se describen a continuación:

- La técnica presentada en este trabajo permite determinar, de manera fiable, el punto de gelación de muestras de diferente pH. A medida que aumenta el pH de la mezcla resorcinol-formaldehído, menor es el tiempo necesario para que se produzca la gelación. Dicho de otra manera, cuanto mayor es la cantidad de catalizador añadida, más se favorece la transición sol-gel.

- La energía consumida depende del estado en el que se encuentra el proceso. Cuando la mezcla se encuentra en el primer estadio del proceso (fase sol), el consumo energético es mayor mientras que, tras producirse la gelación, la energía consumida desciende considerablemente, fenómeno que está relacionado con la cantidad de disolvente residual presente y la estructura porosa desarrollada en cada xerogel de carbono.

Publicación II

FAST MICROWAVE-ASSISTED SYNTHESIS OF TAILORED MESOPOROUS CARBON XEROGELS

Journal of Colloid and Interface Science

357 (541-547)

Año: 2011

Journal of Colloid and Interface Science 357 (2011) 541–547

Contents lists available at ScienceDirect

Journal of Colloid and Interface Science

www.elsevier.com/locate/jcis

Fast microwave-assisted synthesis of tailored mesoporous carbon xerogels

E.G. Calvo, E.J. Juárez-Pérez, J.A. Menéndez, A. Arenillas *

Instituto Nacional del Carbón, CSIC, Apartado 73, 33080 Oviedo, Spain

ARTICLE INFO

Article history:
Received 13 December 2010
Accepted 13 February 2011
Available online 18 February 2011

Keywords:
Microwave-assisted synthesis
Gelation point
Carbon xerogels
Mesoporous materials

ABSTRACT

Resorcinol–formaldehyde carbon xerogels with several initial pH were synthesized using two different heating methods (conventional and microwave heating). The effect of the pH of the precursor solution and the method of synthesis employed on the textural and chemical properties of the final materials was evaluated. It was found that both methods produce tailored carbon xerogels depending on the initial pH and that the pores of the carbon xerogels become larger as the initial pH decreases. High pHs result in exclusively microporous carbon xerogels, while a decrease in the amount of NaOH added, i.e. lower pH, causes the materials to evolve firstly into micro–mesoporous samples and then into micro–macroporous carbon xerogels. The main difference between the two heating methods studied, apart from the duration of the synthesis (i.e. approximately 5 h for the microwave-assisted synthesis as opposed to several days by conventional methods) lies in the meso–macroporosity of the resulting materials, since microwave radiation produces mainly mesoporous carbon xerogels with a specific mesopore size over a wider range of pH than conventional synthesis. For example, the pH range for mesoporous MW samples is 4.5–6.5 while equivalent samples that are conventionally synthesized require an initial pH of between 5.8 and 6.5. This work also illustrates a simple and precise method for determining the gelation point (t_g) of different pH resorcinol–formaldehyde mixtures, based on varying the energy consumed by the microwave device during the synthesis of organic gels, without the need for other more complicated techniques.

1. Introduction

Porous carbon gels synthesized by the polycondensation of resorcinol and formaldehyde in a solvent (i.e. water, acetone, methanol, etc.) followed by drying and pyrolysis have received widespread attention in the literature over the past two decades [1–5]. One of the most important advantages offered by these carbonaceous materials is the possibility of designing their porous texture due to the strong link between the texture and preparation method employed in the synthesis process [6–8]. Because of their tailorability, carbon gels are able to find applications in a wide range of fields as catalyst supports [9–11], supercapacitors [12–14], adsorption materials [15,16], etc., emphasizing that the pore texture required in each case is quite different. Some authors have shown [17,18] that in hydrogen storage applications a good microporosity development together with an appropriate micropore size distribution (pore size of around 0.7 nm) are the key factors governing hydrogen storage capacity. In other cases (e.g. energy storage in supercapacitors), in addition to microporosity, mesopores are required in order to facilitate a good dynamic charge propagation [19,20]. In dynamic adsorption processes, porous carbon materials with a high specific surface area and a substantial amount of large mesopores or macropores with a tailored pore size are very useful, since meso–macroporosity minimizes diffusion limitations inside the carbon supports [10]. In short, carbon gels are very useful materials, since under appropriate synthesis conditions, mainly defined by the pH of the precursor solutions, it is possible to tailor their mesopore and/or macropore texture, while the microporosity remains practically invariable. However, the main drawback to an extensive use of carbon gels is the synthesis method since it is too long and produces more expensive and less competitive materials than other methods currently in use. Therefore, microwave radiation would seem to be a perfectly viable alternative as it would produce carbon gels more quickly and with similar characteristics to those synthesized by conventional methods [12,21].

In this work, microwave radiation was used as a heating source in the synthesis of organic xerogels, enabling all stages (gelation, ageing and drying) were carried out in one simple and fast device. Microwave-assisted synthesis was also employed to determine the gelation point (i.e. the moment when the solution loses fluidity) of several samples obtained from precursor solutions with different pH. The aim of this study was to determine the influence of microwave-assisted synthesis on the pore texture and surface chemistry of carbon xerogels prepared with different pHs and to analyze the main differences between microwave and conventionally synthesized carbon xerogels.

* Corresponding author. Fax: +34 985297662.
E-mail address: aapuente@incar.csic.es (A. Arenillas).

0021-9797/$ - see front matter © 2011 Elsevier Inc. All rights reserved.
doi:10.1016/j.jcis.2011.02.034

2. Experimental

2.1. Preparation of carbon xerogels

Aqueous organic xerogels were synthesized by the polycondensation of resorcinol (*R*) and formaldehyde (*F*) using deionised water as solvent and a sodium hydroxide solution (1 M) as basification agent. The protocol followed to prepare the precursor solutions was the same in all cases but two different heating methods, conventional (C) and microwave heating (MW), were used in the synthesis process.

The precursor solutions were prepared under the following conditions: Resorcinol (VWR International, 99%) was first dissolved in deionised water under magnetic stirring. Then, formaldehyde (Aldrich, 37 wt.% in water, stabilized by 10.7 wt.% methanol) was added to the mixture. In all cases, the resorcinol/formaldehyde molar ratio (*R*/*F*) and the dilution ratio (*D*) were fixed at 0.5 and 5.7, respectively. It should be noted that the dilution ratio (i.e. total solvent/reactant molar ratio) includes the added deionised water and the water and methanol contained in the formaldehyde in the case of "total solvent", while "reactant" refers to the resorcinol and formaldehyde. Seven different precursor solutions were prepared with different initial pH, ranging from 3.1, corresponding to the original pH of the mixture without the addition of NaOH, to 9.0. The pH value of 9.0 was selected to find out the highest pH for obtaining porous carbon xerogels. The resorcinol/formaldehyde solution with an initial pH of 9.0 was found to produce non-porous carbon xerogel and so lower pHs were selected to determine the highest limit of pH able to yield carbon xerogels with a good textural development (the sample prepared using a precursor solution of pH 7.0 was found to have a poorly developed porous texture, see Figs. 2 and 4).

The resorcinol–formaldehyde solutions were divided into several batches and subjected to different thermal treatments (i.e. conventional and microwave heating).

2.1.1. Conventional synthesis

In the case of conventional synthesis (C series), the solutions were placed in sealed beakers which were then introduced in an electrical oven at 85 °C for 72 h to undergo gelation and curing stages. Afterwards, the beakers were opened and the oven temperature was set at 150 °C for 24 h with the purpose of drying the organic gels via evaporation of the solvent. These temperatures were select according to the method proposed by Pekala and Kong [4].

In order to minimize the time required for conventional synthesis, two organic xerogels were prepared using unsealed beakers and two different heating programs. A precursor solution of pH 5.8 (namely CX-5.8-C_1) was added to one beaker which was then placed inside the electrical oven at 85 °C until the processes of gelation, curing and drying of the organic gel had concluded. Once gelation had taken place, the mass loss of the sample was measured in order to determine whether the synthesis had ended. In this particular case, the time required to reach constant mass was approximately 101 h.

A second experiment was performed using the same precursor solution but a different heating program (in this case the sample prepared was labeled CX-5.8-C_2). Initially, the oven temperature was fixed at 85 °C, but once the solution had lost fluidity and the gel had formed, the temperature was increased to 150 °C until constant mass. Under these heating conditions, the time necessary to achieve total synthesis of the organic xerogel was 24 h.

All the organic gels were pyrolyzed at 800 °C under nitrogen flow in a horizontal tubular reactor according to a heating program described elsewhere [22].

2.1.2. Microwave-assisted synthesis

For the microwave-assisted synthesis, the precursor solutions were placed in unsealed glass beakers transparent to microwaves and these were then introduced into a multimode microwave oven. First, the temperature was kept at 85 °C for about 3 h for gelation and part of the curing stage to take place. Then, the power limitation was removed and the microwave device was allowed to operate at maximum power (700 W) until synthesis had been completed. As the solvent is evaporated, the temperature of the organic xerogel, which do not absorb microwaves, comes down until reach ambient temperature. In most of the experiments performed, the total synthesis time of the organic xerogels was around 5 h.

The microwave device used in this work was equipped with a power meter for measuring the amount of energy consumed throughout the process. As described in a previous work [23], the microwave energy consumed (accumulative) depends on the stage of the synthesis, and so representation of the microwave energy consumed with time produces two straight lines of different slope. The first line is associated with the sol stage, whereas the other is related to the energy consumed by the microwave once gelation has occurred. The point of intersection of the two lines allows the gelation point (t_g) of the sample to be determined and, as explained in the results section, this depends to a large extent on the pH of the precursor solution.

The MW organic gels were pyrolyzed at 800 °C using the same procedure as in the case of the conventionally synthesized organic xerogels.

The samples synthesized were designated as follows: the first letters represent the nature of xerogel (OX for organic xerogels and CX for carbon xerogels). These letters are followed by the pH of the resorcinol–formaldehyde solution and, finally, the type of heating used in the synthesis is shown (C for conventional heating and MW for microwave radiation). For example, the label of sample CX-4.5-MW shows that the following sequence was used: preparation of a carbon xerogel by means of microwave heating using a resorcinol–formaldehyde solution with a pH of 4.5.

2.2. Characterization of the samples

2.2.1. Pore texture characterization

The textural properties of the carbon xerogels synthesized were evaluated from N_2 adsorption–desorption isotherms at −196 °C for the study of the microporosity and narrow mesoporosity and by means of mercury porosimetry for the textural characterization of the mesoporous and macroporous samples. The Dubinin–Raduskevich (DR) method [24] was applied to the nitrogen adsorption isotherms to determine the micropore volume (V_{DUB-N2}) and the BET equation was used to calculate the specific surface area, S_{BET} [25]. Nitrogen adsorption has its limitations; it is not precise enough for samples with large mesopores and macropores. For this reason and because the carbon xerogels synthesized in this work display mesopores and even macropores, the textural properties were also evaluated by mercury porosimetry using a Micromeritics Autopore IV. The pore size distribution, average mesopore size ($d_{m,a}$) and mesopore and macropore volume (V_{meso} and V_{macro}) were determined by mercury porosimetry performed over a pressure range of 0.6–230 MPa corresponding to a pore size of 2000–5.5 nm, according to the Washburn's law [26]. It should be noted that V_{meso} obtained by this technique corresponds to a pore volume of width 5.5–49.9 nm whereas V_{macro} corresponds to pores of 50.0–2000 nm.

2.2.2. Surface chemistry characterization

The chemical properties of the samples were studied using point of zero charge (PZC) values [27] and elemental analysis.

The C, N, and H were evaluated on a LECO-CHNS-932 microanalyzer. The oxygen content was determined directly using a LECO-TF-900 furnace.

3. Results and discussion

3.1. Textural properties of carbon xerogels synthesized at pH = 5.8, under different heating conditions

Table 1 provides the textural properties of several carbon xerogels prepared from a precursor solution of pH 5.8 using different devices and heating programs. The first three samples were conventionally synthesized, while the last one, CX-5.8-MW, was obtained by means of microwave heating. As can be seen from the data collected in Table 1, the gelation point (t_g) and total synthesis time of the organic xerogels prepared depends heavily on the heating mechanism used in the synthesis. In the case of conventional heating, it is possible to reduce the synthesis time from 3 days to 1 day, but this results in a poorer textural development of the materials (i.e. V_{meso} of 1.27 and 0.77 $cm^3\ g^{-1}$ for the carbon xerogels CX-5.8-C and CX-5.8-C_2, respectively). On comparing the pore sizes of the materials of series C it is necessary to highlight the differences between the three samples. The carbon xerogel CX-5.8-C presents an average mesopore size of 38 nm, while this parameter is 13 and 18 nm for samples CX-5.8-C_1 and CX-5.8-C_2, respectively. This could be due to the fact that these latter materials undergo greater shrinkage as a result of the synthesis taking place in an unsealed beaker. In this case, the solvent evaporates throughout the entire process producing large capillary forces at the liquid–vapor interfaces that cause the material to shrink [28]. This phenomenon is not observed in the microwave-assisted synthesis because, although an unsealed beaker is also used, the synthesis is much faster so there is not enough time for the polymeric structure to shrink. Despite the reduction of synthesis time achieved in the conventional process, microwave-assisted synthesis is still much faster (i.e. synthesis time of less than 5 h by microwave radiation compared to 24 h by conventional heating) and it produces samples with a greater textural development (for example, V_{meso} of 0.77 and 0.91 $cm^3\ g^{-1}$ and $d_{m,a}$ of 18 and 45 nm for carbon xerogels CX-5.8-C_2 and CX-5.8-MW, respectively).

3.2. Determination of the gelation point using microwave heating

As was mentioned elsewhere [23], plotting the variation of the microwave energy consumed (accumulative) with time allows the accurate determination of the point of gelation in samples of a different nature. Variation of the gelation point as a function of the pH of the precursor solution is represented in Fig. 1. The results obtained show that the speed of the sol–gel transition increases as the pH of the resorcinol–formaldehyde solution increases. In other words, the higher the initial pH, the less time need to carry out the gelation (cf. a t_g of 42.2 min for a precursor solution without any

Table 1
Textural characteristics of carbon xerogels of pH 5.8 and synthesized by different heating methods.

Samples	Gelation point (h)	Total synthesis time OX (h)	S_{BET} ($m^2\ g^{-1}$)	V_{DUB-N2}[a] ($cm^3\ g^{-1}$)	V_{meso}[b] ($cm^3\ g^{-1}$)	$d_{m,a}$[c] (nm)
CX-5.8-C	2.0	102.0	671	0.26	1.27	38
CX-5.8-C_1	2.0	101.0	694	0.26	0.57	13
CX-5.8-C_2	2.0	24.0	671	0.26	0.77	18
CX-5.8-MW	0.4	4.7	637	0.25	0.91	45

[a] Obtained by applying the Dubinin–Raduckevich method to the N_2 adsorption–desorption isotherms.
[b] Mesopore volume determined by mercury porosimetry.
[c] Average mesopore size calculated from mercury porosimetry.

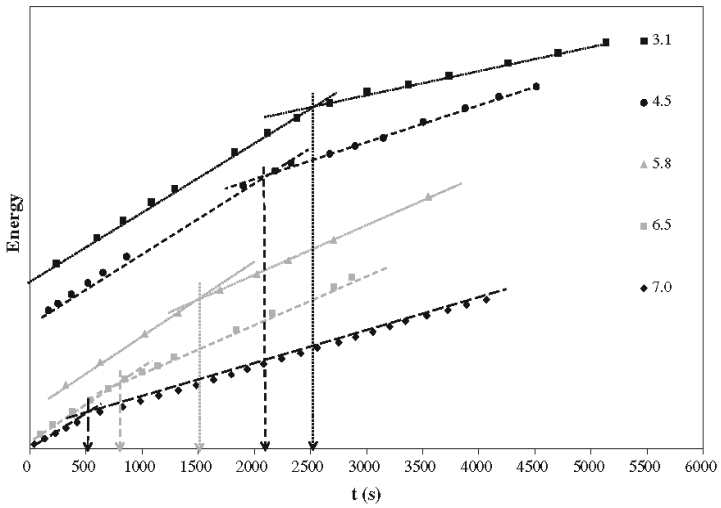

Fig. 1. Representation of the gelation point of several RF xerogels obtained by microwave heating from precursor solutions with different pHs. For a better visualization of the gelation point (i.e. time at which the change in the slope takes place) energy values were displaced along the *y*-axis by adding a constant to the actual values. For that reason no scale is shown in the *y*-axis.

added NaOH, CX-3.1-MW, and 13.4 min for the carbon xerogel prepared with a pH of 6.5). A similar result was obtained by Job et al. [29] who employed a conventional oven to carry out the gelation process and a rheological method to determine the sol–gel transition of carbon gels, but there are important differences between these two studies. The study carried out by Job et al. requires an additional technique to evaluate the t_g, whilst in the present work t_g is determined inside the synthesis device. Secondly, the time required to achieve the gelation of the mixture is much longer than that required by microwave-assisted synthesis.

As can be seen, it is possible to determine the gelation point from the change in the slope and this is probably due to the power consumed by the microwave device to keep the sample at the set temperature (85 °C in the experiments performed) depending on the stage that the process has reached. In fact, the first stage of the process consumes more power than after the formation of the gel, phenomenon probably related to the rate at which the solvent evaporates [23]. The evaporation of the solvent causes a decrease in temperature inside the resorcinol–formaldehyde mixture, so the microwave oven needs to provide more power to keep the mixture at the set temperature. After gelation, the solvent is trapped inside the polymeric structure. Consequently it is less easily evaporated and so less power is required by the microwave device.

If the slopes of the sol (referred to S_{sol}) and gel phases (called S_{gel}) are compared, it can be seen that S_{sol} is very similar in all the cases studied (S_{sol} value of around 220), which would explain because in all cases the mixture of the reactants is the same, only the amount of NaOH added changes slightly. With respect to the slopes of the gel stage (S_{gel}), the differences between the samples are more marked and this is probably due to the fact that once gelation occurs, the formation of the polymeric particles and their crosslinking is markedly influenced by the pH of the precursor solution, resulting in materials with very distinct polymeric and porous structures. In order to relate the microwave energy consumed during the second stage of the process with the porous texture of the materials, two extreme cases were chosen (samples CX-3.1-MW and CX-6.5-MW). Microporosity is virtually identical in both cases (V_{DUB-N2} of 0.24 and 0.23 $cm^3\ g^{-1}$ for CX-3.1-MW and CX-6.5-MW, respectively), whereas they differ in their meso/macroporosity (carbon xerogel CX-3.1-MW consists of large mesopores and even macropores whereas CX-6.5-MW displays small mesopores, as shown in Fig. 3b). As can be seen, the S_{gel} associated with the sample of pH 3.1 is lower than the S_{gel} of the xerogel with a pH of 6.5. In other words, the smaller the initial pH, the smaller the amount of power required by the microwave device to keep the content of the beaker at 85 °C. It could be argued that in the case of the solution with a pH of 3.1, the sample has a structure consisting of large pores filled with solvent that act as thermal spotlights, whereas when the sample is prepared from a solution of pH 6.5, these thermal spotlights are smaller and so they have to heat a larger volume of gel sample. The amount of power required by the microwave device is consequently higher.

3.3. Textural and chemical characteristics of the carbon xerogels obtained (series C and MW)

The N_2 adsorption–desorption isotherms of the carbon xerogels synthesized by conventional heating are shown in Fig. 2a. The shape of the isotherms is markedly influenced by the initial pH, indicating that the pore texture of the carbon xerogels is largely regulated by the pH of the resorcinol–formaldehyde aqueous solution. The sample CX-7.0-C gives rise a type I isotherm according to the BDDT classification [30], which corresponds to exclusively microporous materials. However, as the pH decreases,

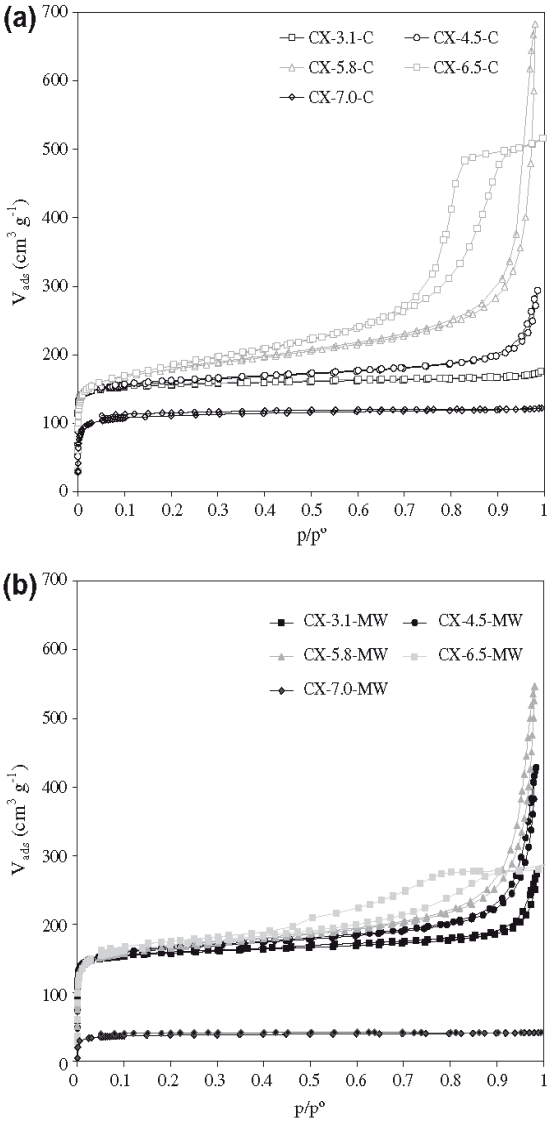

Fig. 2. N_2 adsorption–desorption isotherms of the carbon xerogels studied in this work.

carbon xerogels evolve from microporous to micro–mesoporous materials and this is confirmed by the isotherms of samples CX-6.5-C and CX-5.8-C that are of type I–IV (characteristic of micro–mesoporous materials). The low pH samples (i.e. carbon xerogels with a pH of 3.1 and 4.5) are micro–macroporous solids, a phenomenon corroborated by the mercury porosimetry results shown below. Another point worth mentioning is that, except for the sample labeled CX-7.0-C, the carbon xerogels studied display similar nitrogen adsorption capacities at low relative pressure ($p/p°$), indicating very similar microporosity regardless of the initial pH. This phenomenon is consistent with other published studies [8,12,31] that show the influence of the pH of the precursor solution on the meso–macroporosity of the final carbon xerogels, while the microporosity barely changes.

The carbon xerogels prepared by microwave-assisted synthesis show the same trend as the samples of series C (see Fig. 2b), that it is to say microporosity virtually identical in all cases, whereas

there are notable differences in meso–macroporosity. It is possible to conclude therefore that with microwave heating carbon xerogels with a tailored pore texture can be obtained by adjusting the initial pH.

The results collected in Fig. 2 also reflect that the carbon xerogels prepared using a precursor solution of pH 7.0 (i.e. samples CX-7.0-C and CX-7.0-MW) are exclusively microporous solids. Moreover, this development of microporosity is less marked than in the rest of the samples prepared in this work (Fig. 2 illustrates that the volume of N_2 adsorbed at low relative pressure decreases with respect to the other carbon xerogels studied). The carbon xerogels CX-9.0-C, CX-7.5-C, CX-9.0-MW and CX-7.5-MW are not included in the figure because they are non-porous carbon xerogels. Accordingly, it is possible to affirm that the maximum pH for preparing porous carbon xerogels is between 6.5 and 7.0 both in conventional and microwave-assisted synthesis. This conclusion is in accordance with previous works [1,31] which set the upper pH limit at around 6.5–7.0 in the case of conventional synthesis under specific synthesis conditions (i.e. $R/F = 0.5$ and $D = 5.7$, etc.).

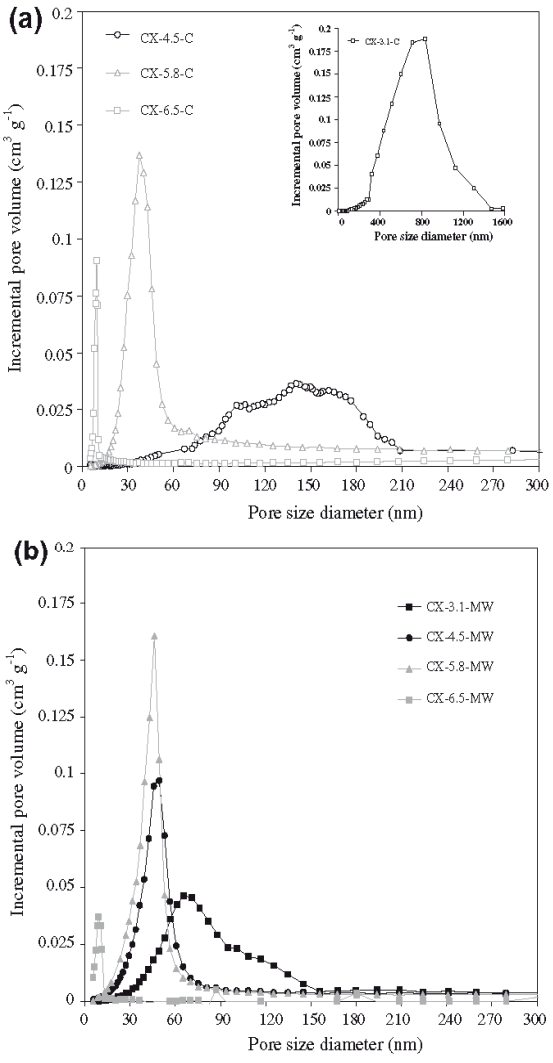

Fig. 3. Pore size distribution of carbon xerogels prepared with different initial pHs and heating methods: conventional (a) and microwave radiation (b).

Fig. 3 illustrates the pore size distribution of the samples obtained by the mercury porosimetry experiments. It includes carbon xerogels prepared by using the two different heating methods and several initial pHs, with the exception of the pH 7.0 samples as they have a much lower pore volume and a pore size of around 1 nm. Both synthesis methods allow the meso–macroporosity of the carbon xerogels to be controlled depending on the initial pH used in their preparation, an observation already reported in previous works in the case of conventional synthesis methods [8,32,33]. It can be observed that, as the initial pH increases, the pore size distribution is displaced to smaller pore sizes and becomes narrower. This can be explained by the polymerization mechanism of resorcinol and formaldehyde, which includes two steps: (i) the formation of hydroxymethyl derivatives (favored by the basic media) and, (ii) the condensation of these hydroxymethyl derivatives and their clustering (catalyzed by H^+). When the initial pH increases, the formation of hydroxymethyl derivatives is favored and therefore highly branched clusters are produced. These cross-linked and unstable clusters give rise to smaller more interconnected polymer particles, and the condensation of such particles resulting in the formation of smaller pores [31].

If Fig. 3a and b are compared, it can be seen that in the case of the conventional method, the resulting materials have larger pores than their microwave counterparts. For example, the carbon xerogels CX-3.1-C and CX-4.5-C show a remarkable macroporosity development, whereas samples CX-3.1-MW and CX-4.5-MW contain pores in the mesopore range and even pores classifiable as macropores (pore size > 50 nm), although they do not reach the sizes of those of the C samples. This is probably due to the much faster synthesis attained in the microwave oven. As the gelation process is faster, there is not enough time for big cluster formation, at the same time that the condensation reactions are accelerated. As a consequence, smaller pores than their counterpart samples synthesized in conventional synthesis are formed. Therefore, microwave-assisted synthesis allows micro–mesoporous samples to be synthesized over a larger pH range than in the case of the conventional heating. For example, with microwave heating a pH range of 4.5–6.5 can be used to produce micro–mesoporous carbon xerogels and micro–macroporous materials provided when the initial pH is fixed at 3.1, whereas in conventional synthesis, it is only possible to prepare micro–mesoporous carbon xerogels when the pH of the precursor solution is between 5.8 and 6.5.

Fig. 4 shows the macropore (Fig. 4a) and mesopore (Fig. 4b) size distributions obtained by means of mercury porosimetry. As mentioned above, this figure confirms the ability of microwave radiation to produce mainly mesoporous carbon xerogels. In the case of conventional synthesis, the macropore volume is much greater than in microwave-assisted synthesis when the initial pH is between 3.1 and 4.5 (V_{macro} of 1.79 and 2.03 $cm^3\ g^{-1}$ for carbon xerogels CX-3.1-C and CX-4.5-C, respectively, opposite to 0.59 and 0.47 $cm^3\ g^{-1}$ for samples CX-3.1-MW and CX-4.5-MW). However, if the pH of the precursor solution is higher than 4.5, this difference is almost negligible. On the other hand, in the mesopore range, the differences between the two heating methods are more obvious (see Fig. 4b). Microwave heating allows the synthesis of mesoporous materials with a tailored mesopore size over a wider range of pH than conventional methods, as well as in a much shorter time.

The chemical properties of the samples studied are presented in Table 2. The elemental analysis data indicate that carbon xerogels consist mainly of carbon (about 97% in all cases) and small quantities of oxygen and nitrogen (between 1% and 2% for oxygen content and around 1% for nitrogen), regardless of the initial pH and heating method employed. In addition, the results show that the carbon xerogels prepared are basic, with a point of zero charge, pH_{PZC}, of around 8 (except sample CX-7.0-C that has a point of zero charge value of 9.3). This basic character may be associated with

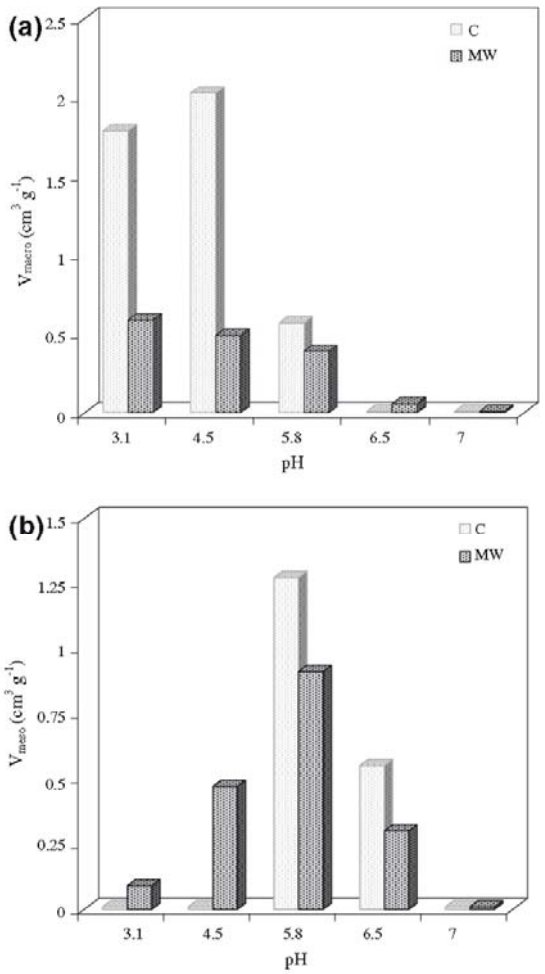

Fig. 4. Macropore and mesopore volume of the carbon xerogels synthesized in this work.

the presence of delocalized π electrons [34] on the surface of the carbon xerogels, due to their aromatic character and to the presence of pyrone or chromene-like structures [35].

Table 2
Chemical properties of the carbon xerogels prepared by conventional (C) and microwave heating (MW).

Samples	Chemical properties				
	Elemental analysis (wt.%, db[a])				PZC
	C	H	O	N	
CX-3.1-C	96.2	0.9	2.3	0.6	8.4
CX-3.1-MW	96.8	1.0	1.5	0.7	8.1
CX-4.5-C	96.8	1.0	1.5	0.7	8.1
CX-4.5-MW	96.4	1.1	1.8	0.7	8.3
CX-5.8-C	96.1	1.2	2.6	0.1	8.4
CX-5.8-MW	96.5	1.0	1.2	1.3	8.4
CX-6.5-C	96.9	1.2	1.7	0.2	8.6
CX-6.5-MW	97.2	1.0	1.0	0.8	8.4
CX-7.0-C	96.9	1.1	1.5	0.5	9.3
CX-7.0-MW	96.2	1.1	2.2	0.5	8.7

[a] Dry basis.

As can be seen in Table 2, all the materials are chemically similar, independently of the pH of the precursor solution or the heating method employed. The main difference between the two heating methods is the size of the pores in the meso–macropore range. The advantages of the microwave assisted method, apart from the speed and simplicity of the process, depend on the final application of the materials. For example, for energy applications, micro–mesoporous materials are preferable to those with macropores [20,36], making carbon xerogels synthesized by microwave radiation more suitable. However, for liquid-phase applications the presence of macropores is important [3,37], making conventional heating the more appropriate method for obtaining carbon xerogels.

4. Conclusions

The microwave-assisted synthesis illustrated in this work allows carbon xerogels to be synthesized in a much shorter time than by conventional methods. Moreover, with this method of synthesis it is possible to identify the exact gelation point (t_g) of different types of sample, since with the microwave device it is possible to control the amount of energy consumed in the sol–gel process. Microwave-assisted synthesis is also a simple and fast method for generating mainly mesoporous carbon xerogels and besides these xerogels display similar chemical properties to those of conventionally synthesized. However, microwave heating allows mesoporous materials to be synthesized with a tailored mesopore size over a wider range of pH than conventional methods, as well as in a much shorter time.

Acknowledgments

The support from the Government of Principado de Asturias PCTI (Ref. IB09-00201) and Ministerio de Ciencia e Innovación (Ref. MAT2008-00217/MAT) is greatly acknowledged. E.G. Calvo also acknowledges a predoctoral research grant from FICYT.

References

[1] C. Lin, J.A. Ritter, Carbon 35 (1997) 1271.
[2] C. Lin, J.A. Ritter, Carbon 38 (2000) 849.
[3] N. Mahata, M.F.R. Pereira, F. Suárez-García, A. Martínez-Alonso, J.M.D. Tascón, J.L. Figueiredo, J. Colloid Interface Sci. 324 (2008) 150.
[4] R.W. Pekala, F.M. Kong, Rev. Phys. Appl. 24 (1989) 33.
[5] R.W. Pekala, C.T. Alviso, Mater. Res. Soc. Symp. Proc. 270 (1992) 3.
[6] C. Scherdel, G. Reichenauer, Microporous Mesoporous Mater. 126 (2009) 133.
[7] L. Zubizarreta, A. Arenillas, A. Domínguez, J.A. Menéndez, J.J. Pis, J. Non-Cryst. Solids 354 (2008) 817.
[8] M.S. Contreras, C.A. Páez, L. Zubizarreta, A. Léonard, S. Blacher, C.G. Olivera-Fuentes, A. Arenillas, J.-P. Pirard, N. Job, Carbon 48 (2010) 3157.
[9] N. Mahata, A.R. Silva, M.F.R. Pereira, C. Freire, B. de Castro, J.L. Figueiredo, J. Colloid Interface Sci. 311 (2007) 152.
[10] N. Job, B. Heinrichs, F. Ferauche, F. Noville, J. Marien, J.-P. Pirard, Catal. Today 102 (2005) 234.
[11] N. Job, B. Heinrichs, S. Lambert, J.-P. Pirard, J.F. Colomer, B. Vertruyen, J. Marien, J. AIChE 52 (2006) 2663.
[12] E. Frackowiak, F. Béguin, Carbon 39 (2001) 937.
[13] E.G. Calvo, C.O. Ania, L. Zubizarreta, J.A. Menéndez, A. Arenillas, Energy Fuels 24 (2010) 3334.
[14] J. Zhou, Y. Ji, J. He, C. Zhang, G. Zhao, Microporous Mesoporous Mater. 114 (2008) 424.
[15] D. Jayne, Y. Zhang, H. Shaker, C. Erkey, Int. J. Hydrogen Energy 30 (2005) 1287.
[16] Y.K. Kang, B.I. Lee, J.S. Lee, Carbon 47 (2009) 1171.
[17] L. Zubizarreta, A. Arenillas, J.J. Pis, Int. J. Hydrogen Energy 34 (2009) 4575.
[18] R. Gadiou, N. Texeir-Mandoki, T. Piquero, S. Saadallah, J. Parmentier, J. Patarin, Adsorption 11 (2005) 823.
[19] E. Frackowiak, Phys. Chem. Chem. Phys. 9 (2007) 1774.
[20] H. Shi, Electrochim. Acta 41 (1996) 1633.
[21] Y.K. Kang, S.J. Hong, B.I. Lee, J.S. Lee, Electrochem. Commun. 10 (2008) 1105.
[22] L. Zubizarreta, A. Arenillas, J.-P. Pirard, J.J. Pis, N. Job, Microporous Mesoporous Mater. 115 (2008) 480.
[23] E.J. Juárez-Pérez, E.G. Calvo, A. Arenillas, J.A. Menéndez, Carbon 48 (2010) 3305.

[24] M.M. Dubinin, J.F. Danielli, M.D. Rosenberg, D. Cadenhead, Progress in Surface and Membrana Science, vol. 9, Academic Press, New York, 1975. pp. 1.
[25] J.B. Parra, J.C. de Sousa, R.C. Bansal, J.J. Pis, J.A. Pajares, Adsorpt. Sci. Technol. 12 (1995) 51.
[26] E.W. Washburn, Proc. Nat. Acad. Sci. 7 (1921) 115.
[27] J.S. Noh, J.A. Schwarz, J. Colloid Interface Sci. 130 (1989) 157.
[28] N. Job, A. Théry, R. Pirard, J. Marien, L. Kocon, J.-N. Rouzaud, F. Béguin, J.-P. Pirard, Carbon 43 (2005) 2481.
[29] N. Job, F. Panariello, M. Crine, J.-P. Pirard, A. Léonard, Colloids Surf., A 293 (2007) 224.
[30] S. Brunauer, T. Emmett, E. Teller, J. Am. Chem. Soc. 60 (1938) 309.
[31] N. Job, R. Pirard, J. Marien, J.-P. Pirard, Carbon 42 (2004) 619.
[32] T. Horikawa, J. Hayashi, K. Muroyama, Carbon 42 (2004) 1625.
[33] T. Yamamoto, T. Sugimoto, T. Suzuki, S.R. Mukai, H. Tamon, Carbon 40 (2002) 1345.
[34] M.A. Montes-Morán, J.A. Menéndez, E. Fuente, D. Suárez, J. Phys. Chem. B 102 (1998) 5595.
[35] E. Enrique, J.A. Menéndez, D. Suárez, M.A. Montes-Morán, Langmuir 19 (2003) 3505.
[36] B.Z. Fang, H.S. Zhou, I. Honma, J. Phys. Chem. B 110 (2006) 4875.
[37] H.T. Gomes, B.F. Machado, A. Ribeiro, I. Moreira, M. Rosario, A.M.T. Silva, J.L. Figueiredo, J.L. Faria, J. Hazard. Mater. 159 (2008) 420.

4.2. DESARROLLO DE LA MICROPOROSIDAD DE LOS XEROGELES DE CARBONO

Como se ha mencionado en la sección anterior, el control de la meso-macroporosidad de los xerogeles de carbono sintetizados en microondas se controla a partir de las condiciones de síntesis y, más concretamente, mediante el ajuste del pH de la mezcla resorcinol-formaldehído. La microporosidad apenas se ve afectada por esta variable, presentando los geles unos volúmenes de microporos, y por consiguiente valores de área superficial específica, análogos en todos los casos (S_{BET} ~ 600 m^2 g^{-1}).

Para ciertas aplicaciones, es necesario disponer de xerogeles de carbono que presenten una elevada microporosidad, como es el caso de su utilización como material activo en los electrodos de supercondensadores. Por ello, la *Publicación III*, que se presenta como parte del contenido de esta Tesis, surge como consecuencia de la necesidad de generar materiales con gran desarrollo textural y así poder conseguir altas capacidades de almacenamiento de energía eléctrica.

Investigaciones previas llevadas a cabo en nuestro grupo de investigación demostraron que es posible activar químicamente con hidróxido de potasio (KOH) tanto xerogeles orgánicos como carbonizados mediante la vía convencional (horno eléctrico horizontal tubular; T = 750 ºC; t = 120 minutos; atmósfera de N_2, 500 cm^3 min^{-1}) [ZUBIZARRETA, 2008B]. No obstante, la porosidad generada en cada uno de los casos es totalmente diferente. Cuando la activación química se realiza tras el proceso de carbonización, se obtienen materiales con una microporosidad bastante desarrollada (valores de S_{BET} en torno a 1500 m^2 g^{-1}) pero se preserva, además, la meso-macroporosidad definida por el pH de la mezcla resorcinol-formaldehído. Por el contrario, si se activa directamente un xerogel orgánico se destruye la meso-macroporosidad creada durante la síntesis, pero se consiguen microporosidades más desarrolladas (S_{BET} > 2000 m^2 g^{-1}). Este hecho no significa que los geles de carbono activados por esta última vía sean exclusivamente microporosos, ya que existe cierta mesoporosidad pero de distinta naturaleza a la formada durante la síntesis del xerogel orgánico (mesoporos creados como consecuencia del ensanchamiento sufrido por los microporos durante el proceso de activación).

Además del mayor volumen de microporos, hay que destacar que la activación directa de los xerogeles orgánicos permite evitar una etapa del proceso de síntesis (fase de carbonización), es decir, la carbonización y activación tienen lugar simultáneamente en un mismo dispositivo, lo que resultaría más idóneo para una producción de geles de carbono a escala industrial.

De acuerdo con estos resultados, y teniendo en cuenta que la aplicación de los geles de carbono como electrodos para supercondesandores no requiere de poros de elevado tamaño (mesoporos grandes ni macroporos), se decidió utilizar un xerogel orgánico como material precursor en los procesos de activación química.

Los prometedores resultados obtenidos con la síntesis de xerogeles de carbono mediante radiación microondas (*Publicación II*), hicieron que esta misma tecnología fuera utilizada durante los procesos

de activación química. El dispositivo empleado en estos experimentos de activación aparece reflejado en la Figura 4.3. Como se puede observar, el sistema consta de una conexión de entrada (tubo conectado a la fuente de gas inerte, N_2) y una de salida que permite la evacuación de la materia volátil y los gases generados durante el proceso de activación. La mezcla de xerogel orgánico + agente activante (hidróxido potásico) se introduce en una navecilla de alúmina y ésta, a su vez, en un reactor de cuarzo. Al igual que el dispositivo descrito en la sección 4.1, este microondas dispone de un controlador tipo PID y un termopar en contacto con la muestra, que permiten controlar la temperatura de activación en todo momento.

Figura 4.3. Horno microondas utilizado en los procesos de activación.

Como se explica detalladamente en la publicación adjuntada a continuación, la activación química mediante calentamiento microondas se llevó a cabo bajo diferentes condiciones de operación (temperatura y tiempo de activación), con el objetivo de hallar las condiciones óptimas que dan lugar a xerogeles de carbono con las propiedades más idóneas para el almacenamiento de energía.

Tras el proceso de síntesis y caracterización textural de los xerogeles de carbono activados, aquellos con las mejores propiedades porosas fueron seleccionados para utilizarse como electrodos en condensadores electroquímicos (experimentos ejecutados con celdas simétricas basados en un electrolito acuoso, H_2SO_4 1 M).

Algunas de las conclusiones más importantes derivadas de este estudio son las siguientes:

- Al contrario que los procesos convencionales, la activación directa de xerogeles orgánicos mediante calentamiento con microondas permite preservar parcialmente la meso-macroporosidad del material precursor, hecho que depende del tiempo de activación utilizado.

- Exposiciones prolongadas a las microondas (45 minutos, por ejemplo), se traducen en una destrucción parcial de la porosidad. Por el contrario, tiempos de activación cortos (6 min) producen materiales con un interesante desarrollo textural (conservan parte de la mesoporosidad originada durante la síntesis del xerogel orgánico y contienen microporos con un tamaño apropiado para garantizar un eficiente almacenamiento de energía en presencia de electrolitos acuosos).

❖ La evaluación del comportamiento electroquímico de estos materiales ha revelado resultados muy interesantes puesto que, en algunos casos, la energía almacenada por los xerogeles de carbono supera los valores obtenidos con carbones activos comerciales y, además, este buen comportamiento se mantiene durante un número muy elevado de ciclos de carga-descarga.

Publicación III

MICROWAVE SYNTHESIS OF MICRO-MESOPOROUS ACTIVATED CARBON XEROGELS FOR HIGH PERFORMANCE SUPERCAPACITORS

Microporous and Mesoporous Materials

168 (206-212)

Año: 2013

Microporous and Mesoporous Materials 168 (2013) 206–212

Contents lists available at SciVerse ScienceDirect

Microporous and Mesoporous Materials

journal homepage: www.elsevier.com/locate/micromeso

Microwave synthesis of micro-mesoporous activated carbon xerogels for high performance supercapacitors

E.G. Calvo, N. Ferrera-Lorenzo, J.A. Menéndez, A. Arenillas *

Instituto Nacional del Carbón, CSIC, Apartado 73, 33080 Oviedo, Spain

ARTICLE INFO

Article history:
Received 17 August 2012
Accepted 15 October 2012
Available online 23 October 2012

Keywords:
Microwave technology
Chemical activation
Porous carbon xerogels
Energy storage

ABSTRACT

This work illustrates the production of porous carbon xerogels by means of a chemical activation method based on microwave radiation. The evolution of textural properties and the electrochemical performance of the materials synthesized, in relation to activation time and temperature, were investigated. The study of the activation time revealed that carbon xerogels with a remarkable micro-mesoporosity development (S_{BET} around 2200 $m^2 g^{-1}$) can be produced in a time range of 6–30 min. However, the prolongation of microwaves exposure, i.e. the increase in the activation time, leads to a decrease in microporosity and reduces the contribution of the precursor material mesoporosity. The results derived from the study of different activation temperatures (i.e. 700, 600 and 500 °C) revealed that the most suitable temperature for synthesizing carbon xerogel with a high surface area is 700 °C. Electrochemical capacitors assembled with carbon xerogels as electrode material and H_2SO_4 (1 M) as electrolyte, were characterized by cyclic voltammetry and galvanostatic techniques. Carbon xerogels synthesized in the laboratory displayed specific capacitance values of about 170 $F g^{-1}$, higher values than those of various commercial activated carbons for this specific application. The best energy storage value was achieved with the xerogel activated for just 6 min, probably as a result of the increase in the volume of ultramicropores from 0.4 to 0.7 nm.

1. Introduction

In recent years, carbon gels have attracted widespread attention for energy applications due to a number of interesting features such as: a unique three-dimensional nano network, a pore texture tailored according to the synthesis protocol, a high electrical conductivity and the possibility of being used without any binding substances [1,2]. Despite these advantages, the main drawback of this kind of carbonaceous material lies in the synthesis process because, by means of conventional methods, at least 24 h are required to produce materials with a significant textural development [3]. The limitation of such slow and uncompetitive synthesis method has recently been solved through the use of microwave technology, as evidenced by several published works [2,3]. These studies demonstrated that it is possible to prepare carbon xerogels analogous to those conventionally synthesized but with a substantial saving of time (about 5 h as opposed to several days in conventional processes).

Another problem that needs to be addressed is the development of carbon xerogels microporosity. The specific surface area of organic xerogels is about 200 $m^2 g^{-1}$, a value that can be increased to 600–700 $m^2 g^{-1}$ after the pyrolysis stage under certain operating conditions [2,4–6]. However, this porosity is well below that exhibited by activated carbons used as electrode material in supercapacitors. Microporosity can be increased to surface area values of almost 2000 $m^2 g^{-1}$ by means of activation processes [7–10] and, in particular, by chemical activation, which is the process studied in this work.

Many variables are involved in chemical activation and this makes it possible to design the porosity of carbon xerogels by selecting specific activation parameters. Variables such as activating agent (A) and precursor (P) used, A/P mass ratio or time and temperature of activation, have a very noticeable effect on the properties of the resulting material [9,11,12]. In this work, both the activating agent (potassium hydroxide) and the precursor material (resorcinol–formaldehyde organic xerogel) used were the same in all cases. Only the activation temperature (T_a) and time (t_a) were modified in order to produce materials with different micro/mesoporosity and evaluate the effect of this porosity on the energy storage capacitance of the carbon xerogels synthesized.

Traditionally, chemical activation processes have been carried out by means of conventional heating mechanisms, at temperatures between 400 and 950 °C and with activation times ranging between 0.5 and 5 h [7,9,12,13]. However, microwave heating has emerged as an alternative activation technique in recent years [14–18]. Some published works report the use of microwaves for producing activated carbons from biomass residues, with a considerable saving of energy and short processing times. For example, Foo and Hameed [16,19,20] have recently published several papers

* Corresponding author. Tel.: +34 985119090; fax: +34 985297662.
E-mail address: aapuente@incar.csic.es (A. Arenillas).

1387-1811/$ - see front matter © 2012 Elsevier Inc. All rights reserved.
http://dx.doi.org/10.1016/j.micromeso.2012.10.008

on microwave-induced activation. By means of microwave heating, they were able to activate different biomass wastes (pistachio nut shells, rice and coconut husks, orange peels, etc.) and produce activated carbons with surface areas higher than 1000 $m^2 g^{-1}$ after irradiation times of only a few minutes. Kubota et al. [18] have also reported the microwave activation using potassium hydroxide as activating agent but, in their case, the precursor was a phenolic resin instead of biomass waste. By means of this process, the authors synthesized materials with a high volume of micropores and a well-developed mesoporosity employing various KOH/raw material ratios and microwave powers. Most of the works reported in the bibliography conclude that prolonged exposure time promotes the development of porosity and produce materials with a S_{BET} greater that 1000 $m^2 g^{-1}$. However, in none of these cases the activation time exceeded the times applied in conventional activation processes.

There is also growing interest in the development of breakthrough materials for enhancing the performance of supercapacitors. The predominant charge storage mechanism in supercapacitors based on carbon electrodes is the formation of the electric double layer, EDL [21,22]. This kind of mechanism requires electrode materials that not only have a considerable degree of microporosity, but also small mesopores to facilitate the diffusion of electrolyte ions [21,22].

Carbon xerogels appear as promising materials for supercapacitors due to their good conductivity and the possibility of tailoring their micro-mesoporosity. The main disadvantage of these carbonaceous materials is that the conventional synthesis processes are both tedious and very costly. Microwave heating is useful not only for obtaining carbon xerogels with a tailored mesoporosity and a considerable saving of time [2,3], but also for applying it in the activation step to achieve the desired microporosity. Therefore, the aim of this paper is to investigate the chemical activation of resorcinol–formaldehyde xerogels by means of microwave heating and to evaluate the capacity of the synthesized materials for use them as electrodes in supercapacitors. Accordingly, organic xerogels were chemically activated under different operating conditions (i.e. activation temperature and time) in order to prepare materials with a micro-mesoporosity suitable for ensuring an efficient electrochemical performance of supercapacitors.

2. Experimental

2.1. Carbon xerogel preparation

The precursor material used in chemical activation processes was an organic xerogel (OX) which was synthesized on the basis of polymerization reactions between resorcinol (R) and formaldehyde (F). Distilled water was used as solvent and a solution 1.0 M of NaOH was also used for pH adjustment (pH = 6.5, in this particular case). Once the resorcinol–formaldehyde mixture has been prepared, it was inserted in an unsealed beaker, which was introduced in the microwave oven. This device has a thermocouple, which is in contact with the sample and connected to a PID controller, thereby enabling that the synthesis temperature is controlled and monitored. First, the temperature was set at 85 °C for about 3 h in order to complete the gelation and part of the curing stages. However, in a second step, the temperature was increased above 100 °C until the complete drying of sample (more details in Refs. [3,23]). The global synthesis of this precursor material was carried out in only 5 h. The organic xerogel synthesized display a specific surface area close to 200 $m^2 g^{-1}$ with a real density of 1.35 g cm^{-3}, and a C content of around 70%, so the remaining material is associated with volatile matter that evolves during the subsequent heat treatment of OX sample.

In all the chemical activations performed, potassium hydroxide (KOH, Aldrich 99%) was used as activating agent and the activating agent/organic precursor mass ratio was 3. Once the reagents had been physically mixed, they were subjected to thermal treatment in a microwave oven under an inert atmosphere (N_2, 500 $cm^3 g^{-1}$). Since the precursor used was an organic xerogel, it could be said that the carbonisation (removal of volatile matter and formation of an essentially carbonaceous structure) and activation (development of microporosity) takes place in just one step.

Both the temperature (T_a) and activation time (t_a) were studied in order to achieve the mildest possible conditions capable of producing materials with an optimal textural development. First, the chemical activations were carried out at 700 °C (the temperature previously used in activation processes based on conventional heating mechanisms) and the activation time was modified accordingly. As a result of the rapidity and efficiency of microwave heating [3,17,24], the activation times applied were shorter than those commonly used in conventional activations, so t_a was set at 6, 20, 30 and finally, 45 min. After optimization of the activation time, the chemical activations were performed at three different temperatures (700, 600 and 500 °C) and the samples were maintained at the maximum temperature for 6 min, in order to evaluate the effect of the temperature on the porosity of resulting materials.

In order to remove any by-products derived from the activation process, all the samples were washed after the heat treatment, with a 5 M solution of HCl and then by distilled water, repeatedly, until the pH of the drained solution reached a value of 6. Finally, to obtain completely dry carbonaceous materials, the samples were placed in an oven at 110 °C overnight.

2.2. Physico-chemical characterization of the carbon xerogels

The specific surface area, S_{BET} was determined from the N_2 adsorption–desorption isotherms at 77 K (Micromeritics Tristar 3020). It was calculated by means of the application of BET equation to the adsorption data in the $p/p°$ range of 0.05–0.10. The micropore volume (V_{DUB-N2}) was calculated by applying the Dubinin–Raduskevich equation [25] to the nitrogen adsorption isotherms and the total pore volume (V_p) was assessed from the amount of nitrogen adsorbed at saturation point ($p/p° = 0.99$). CO_2 adsorption isotherms (273 K) were also performed in order to analyze the ultramicropore region of the carbon xerogels synthesized and, therefore, to assess the influence of this kind of microporosity on their energy storage capacitance:

The chemical properties of the samples were determined by elemental analyses. The C, N and H were evaluated on a LECO-CHNS-932 microanalyzer and the oxygen content was calculated directly using a LECO-TF-900. Their surface morphology was also examined using a Zeiss DSM 942 scanning electron microscope.

2.3. Electrochemical performance

Pelletised electrodes in the form of discs of 1 cm^2 with a thickness between 200–300 μm and a mass of 6–8 mg were manufactured from a mixture of the activated carbon xerogel (75 wt.%), a binder (polyvinylidene fluoride, PVDF, 20 wt.%) and a carbon black (5 wt.%). Electrochemical measurements were performed with a VMP (Biologic) potentiostac/galvanostac, using a solution 1 M of H_2SO_4 as aqueous electrolyte. Cyclic voltammetry (scan rate of 2 mV s^{-1}) and galvanostatic charge/discharge experiments (current density = 200 mA g^{-1}) were carried out to determine the electrochemical properties of the synthesized carbon xerogels. The values of specific capacitance expressed in Farads per mass of one electrode (F g^{-1}) were calculated from galvanostatic charge/discharge cycles in rising voltage windows with a current density of 200 mA g^{-1}. The long-term cyclability of the cells assembled

using the carbon xerogels was studied from galvanostatic tests in a voltage window of 1.0 V and a current load of 500 mA g^{-1}.

3. Results and discussion

3.1. Influence of activation time, t_a, in microwave activation

The effect of the activation time on the textural properties of the carbon xerogels synthesized is presented in Fig. 1. It can be observed that the chemically activated materials display a well-developed porous texture compared to the organic precursor (OX), resulting in specific surface area values, S_{BET}, of above 2000 m^2 g^{-1} in most of the cases studied (see Table 1). Secondly, from the shape of the N_2 adsorption–desorption isotherms, it can be deduced that the samples are micro-mesoporous, although this porosity depends heavily on the irradiation time. For example, the samples activated for 6 and 20 min, MW6 and MW20, respectively, display type I–V isotherms according to the BDDT classification, with a pronounced hysteresis loop related to the presence of mesopores, loop becomes thinner or disappears with longer activation times. This phenomenon is also corroborated by the results collected in Table 1, where the mesopore volume, V_{meso}, is 0.65 and 0.80 cm^3 g^{-1} for the carbon xerogels MW6 and MW20, respectively, while this parameter falls to about 0.40 cm^3 g^{-1} when the activation time is increased. Therefore, it can be affirmed that, by subjecting the samples to short microwaves exposure times, it is possible to partially preserve the original mesoporosity of the precursor, as well as significantly increase the micropore volume. This phenomenon has never been observed before in the case of activation processes in electric furnaces, where the direct activation of organic xerogels severely damages the pore structure, destroying the large-size pores (meso and macro) created during the synthesis of the organic precursor, as evidenced in the work published by Zubizarreta et al. [9]. Fig. 2 shows a SEM photograph of the carbon xerogel MW6. As expected, the morphology of this sample consists of interconnected quasi-spherical nodules, same morphology found in other published works [6,9].

Table 1 also shows textural data of the precursor used (OX sample) and the same precursor carbonised at 700 °C in a nitrogen atmosphere (CX). As can be seen, the heat treatment of OX xerogel in an inert atmosphere (carbonisation process), also produces an increase in microporosity ($V_{DUB\text{-}N2}$ = 0.23 vs. 0.06 cm^3 g^{-1} in the case of OX sample) with a slight increase in mesopore volume. Nevertheless, since any external activating agent was added, the porosity development is not equal to that obtained after activation processes (i.e. S_{BET} = 619 m^2 g^{-1} vs. 2166 m^2 g^{-1} when OX xerogel was submitted to a thermal treatment (N_2 atmosphere) for 6 min in the presence of potassium hydroxide.

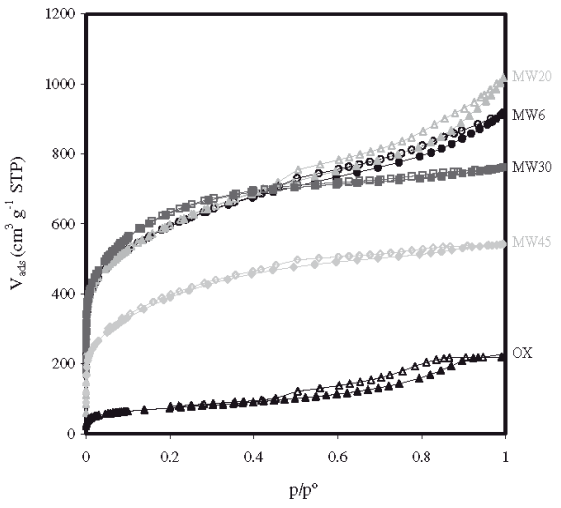

Fig. 1. N_2 adsorption–desorption isotherms of carbon xerogels obtained from different activation times.

Table 1
Textural parameters of the materials synthesized in this work.

Samples	N_2 adsorption (77 K)			CO_2 adsorption (273 K)
	S_{BET} (m^2 g^{-1})	$V_{DUB\text{-}N2}$[a] (cm^3 g^{-1})	V_{meso}[b] (cm^3 g^{-1})	$V_{DUB\text{-}CO2}$[a] (cm^3 g^{-1})
OX	186	0.06	0.29	–
CX[c]	619	0.23	0.39	–
MW6	2166	0.76	0.65	0.41
MW20	2169	0.77	0.80	0.37
MW30	2324	0.78	0.39	0.37
MW45	1398	0.46	0.37	0.15

[a] Obtained from the Dubinin–Raduskevich equation.
[b] $V_{meso} = V_p - V_{DUB\text{-}N2}$, where V_p is the adsorbed volume at saturation point (p/p° = 0.99).
[c] Carbon xerogel obtained from OX treatment at 700 °C in an inert atmosphere (N_2).

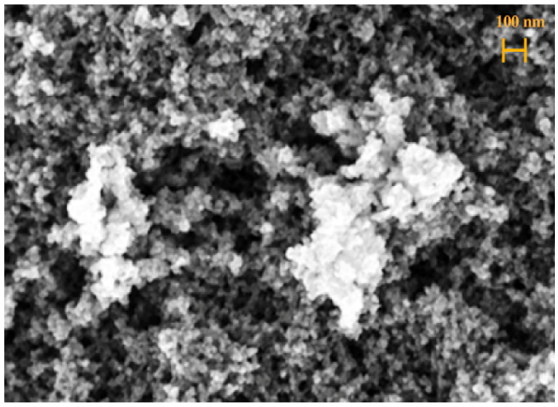

Fig. 2. SEM image of carbon xerogel chemically activated for 6 min (MW6).

The microporosity of the carbon xerogels studied also depends on the duration of the microwave-induced activations. However, as indicated by the N_2 adsorption–desorption isotherms and the textural parameters listed in Table 1, this dependence seems to be only significant when the activation time exceeds 30 min. The samples irradiated for 6, 20 and 30 min display an almost identical micropore volume ($V_{DUB\text{-}N2}$ about 0.77 cm^3 g^{-1}), while the amount of micropores falls sharply when the microwave irradiation extends to 45 min ($V_{DUB\text{-}N2}$ = 0.46 cm^3 g^{-1} for the carbon xerogel MW45). From the micropore size distribution calculated from the CO_2 adsorption isotherms (see Fig. 3), it is possible to perceive slight changes in the narrow microporosity due to variations in the activation time. All of the activated xerogels display ultramicropores of a very similar size (pore diameter between 0.4 and 0.7 nm) and wider micropores whose size and volume increase as the irradiation time decreases. For example, the sample activated for only 6 min exhibits the highest volume of pores between 0.4 and 0.7 nm in addition to a significant amount of micropores whose diameter is centred at ca. 0.9 nm. However, this pore volume becomes smaller and shifts to narrower pore sizes when longer activation times were used. This detrimental impact on the porosity of activated materials after long exposures to microwave radiation has also been observed by other authors using microwave heating to produce activated carbons [15,19,26]. One possi-

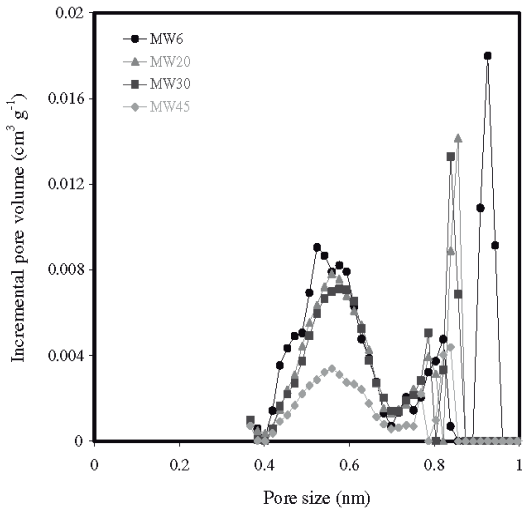

Fig. 3. Pore size distribution of carbon xerogels synthesized, obtained by applying the DFT method to CO_2 adsorption isotherms at 273 K.

ble explanation for this phenomenon could be related with the formation of local hot spots inside the carbonaceous material. The longer microwave heating is applied, the greater is the possibility of the formation of microplasmas leading to the creation of local hot spots [27]. These hot spots may then cause the shrinkage and modification of the internal channels of the carbonaceous structure and the subsequent partial destruction of the porosity.

The results of elemental analysis for the four carbon xerogels synthesized are presented in Table 2. All the samples are mainly composed of carbon (about 90 wt.%), although it is worth noting that the oxygen content increases as the exposure time to microwave radiation is extended (for example, an oxygen content of 7.6 wt%. when the activation time is set at 6 min, as opposed to almost 11 wt.% after 45 min of microwave irradiation).

A possible explanation for the higher oxygen content when microwave radiation is used as heating source or when such treatment is prolonged may be found in the heating mechanism. In microwave heating, the energy is supplied at molecular level through dipole rotation and ionic conduction, resulting in a very efficient internal heating [17,24]. This type of mechanism could lead to the formation of active centres on the surface of materials that, once exposed to an air atmosphere, are stabilized by oxidation, resulting in materials with a higher oxygen content. A similar phenomenon was also observed in a previous work [28] where higher oxygen content was also detected in resorcinol–formaldehyde xerogels subjected to microwave treatments.

3.2. Influence of activation temperature (T_a) on the porosity of carbon xerogels

As the activation process with microwave heating leads to very good results in very short times (6 min), the next step is to optimize the activation temperature, T_a, in order to evaluate whether milder activation processes (i.e. lower temperatures) are also capable of producing similar results regarding the materials porosity. Accordingly, the activation time was set at 6 min and the temperature was reduced from 700 to 500 °C, with the aim of optimizing the activation conditions leading to highly micro-mesoporous materials.

Table 2
Chemical properties of carbon xerogels obtained from different activation times (t_a).

Samples	Elemental analysis (wt.%, db[a])			
	C	H	N	O
MW6	91.4	0.9	0.1	7.6
MW20	89.1	0.9	0.1	9.9
MW30	89.1	0.8	0.1	10.0
MW45	88.2	0.8	0.1	10.9

[a] Dry basis.

As indicated by the results collected in Fig. 4 and Table 3, the activation temperature significantly affects the textural characteristics of the synthesized materials. Regarding the N_2 adsorption–desorption isotherms, it can be seen that the nitrogen adsorption capacity at low relative pressures ($p/p°$) is higher when the activation temperature is fixed at 700 °C, with a S_{BET} value of around 2300 $m^2 g^{-1}$, while the surface area does not exceed 1000 $m^2 g^{-1}$ when lower activation temperatures were used. The V_{meso} values listed in Table 3, show that mesoporosity creation takes place only when the heat treatment was performed at 700 °C. An activation temperature of 500 and 600 °C does not modify the mesoporosity, the mesopore volume is 0.27 and 0.25 $cm^3 g^{-1}$ for the samples treated at 500–600 °C, respectively, almost identical to the value of the precursor material (V_{meso} = 0.29 $cm^3 g^{-1}$). This phenomenon indicates that mesopores were neither created nor destroyed when the activations were performed at the lowest temperatures. Thus, the optimum temperature for producing carbon xerogels with a high micropores volume and a substantial amount of mesopores by means of microwave activation is 700 °C.

Most authors studying the effects of temperature in conventional activations [29–32] or the influence of microwave power in microwave-assisted activations [18,19,33,34] on the textural properties of carbonaceous materials have obtained similar results, that is to say, a higher textural development as the activation temperature is increased. However, it should be noted that there is usually a maximum temperature above which porosity begins to be destroyed. The increase in porosity with the activation temperature seems logical since the higher the T_a, the more favourable the reaction between the organic precursor and the activating agent. Moreover, high temperatures stimulate the release of volatile matter, which also favours the creation of porosity [34,35].

3.3. Supercapacitors performance

Fig. 5 shows the CV-curves recorded with 2-electrode cells using different carbon materials as electrodes and sulfuric acid as

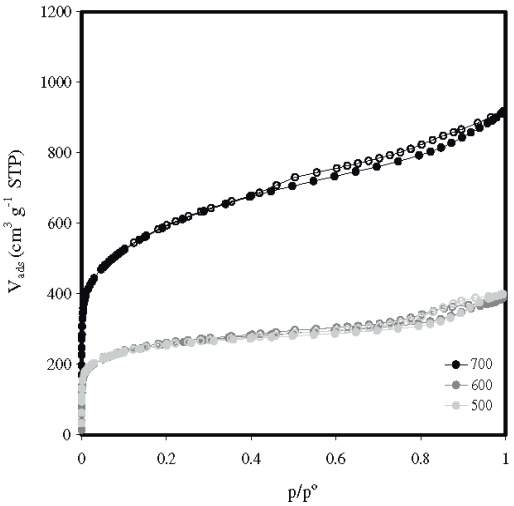

Fig. 4. N_2 adsorption–desorption isotherms of samples treated at different activation temperature (700, 600 and 500 °C).

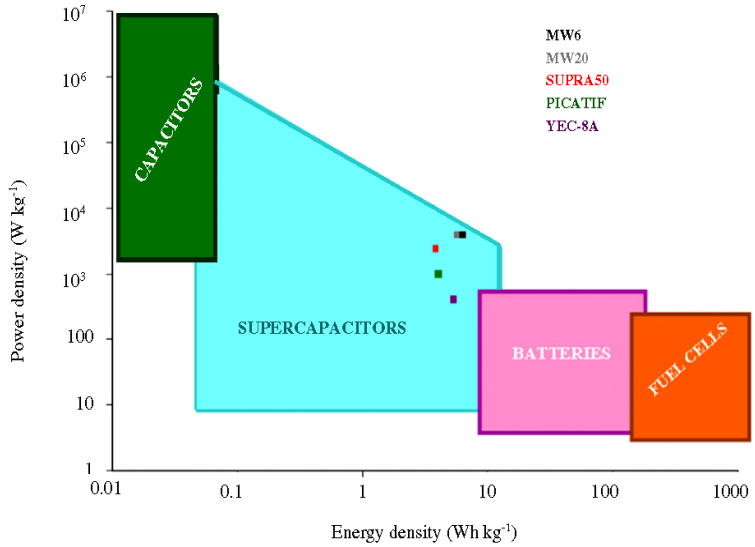

Fig. 6. Ragone plots for supercapacitors assembled with carbon xerogels MW6 and MW20 and the other commercial activated carbons.

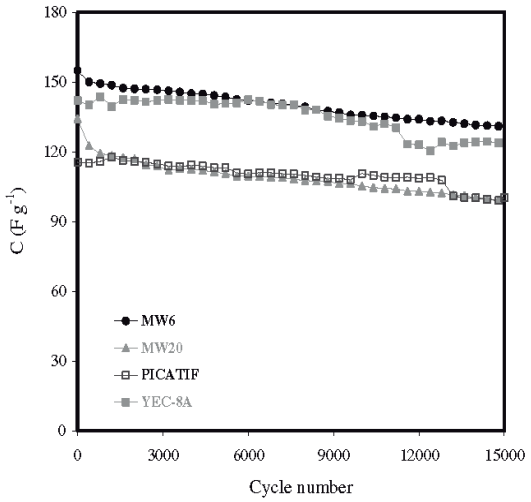

Fig. 7. Evolution of specific capacitance (F g $^{-1}$) with the number of galvanostatic cycles for two carbon xerogels synthesized in this work and two commercial activated carbons (U = 1.0 V; I = 500 mA g $^{-1}$).

Ragone plots of power density (W kg^{-1}) vs. energy density (Wh kg^{-1}) for the electrochemical cells composed of carbon xerogels MW6 and MW20 and the commercial samples studied in this work, are reported in Fig. 6. As can be seen, the supercapacitors assembled with carbon xerogels as electrode material, yield the energy and power density values one would expected of this kind of energy storage devices. Moreover, the plots clearly show the superiority of the cells based on carbon xerogels since, both the amount of energy stored and the power supplied is higher than that of supercapacitors using the commercial activated carbons.

Despite the attractiveness of these specific capacitance values, it is essential to test the viability of these materials for use as electrodes in real devices, since the electrodes must be able to endure a large number of charge and discharge cycles [21,47]. For this reason, the life-cycle of the systems built with the carbon xerogels was evaluated by means of galvanostatic tests at 500 mA g^{-1} in a voltage window of 1.0 V (see Fig. 7). The cyclability of the two commercial activated carbons that showed higher C values was also evaluated with comparative purposes. The energy storage capacitance of the carbon xerogels studied in this work can reach values up to 200 F g^{-1} using a working window above 1.0 V. However, since the cells are in an aqueous medium and the electrolytic decomposition of water takes place at 1.23 V [22], the voltage range chosen for evaluating the cycle durability of the samples was 1.0 V. During the first 400 cycles, there was a sharp drop in the specific capacitance values but once the first hundreds of cycles were overcome, the decline levelled off and in no case did the charge loss exceed 20% (for example, capacitance loss of 13% for the carbon xerogel MW6 and 19% in the case of sample MW20). Therefore, because of the low-cost synthesis process and their attractive electrochemical properties, these carbon materials could be used in commercial supercapacitors with good efficiency.

4. Conclusions

The results obtained in this work show that, by means of microwave technology, highly porous carbon xerogels can be synthesized quickly, efficiently and by means of a low-cost method. Such technology was applied both for the production of organic xerogels and during their subsequent activation with potassium hydroxide.

The effects of the activation temperature (T_a) and time (t_a) on the porosity and, therefore, on the energy storage capacitance of the synthesized materials were evaluated. It was found that when the microwave-induced activation was performed under conditions of a short activation time, 6 min, and at a temperature of 700 °C, the mesoporosity of the precursor material was partially preserved. In addition, a large volume of ultramicropores, i.e. pores that are essential for efficient charge storage, was achieved.

Some of the carbon xerogels synthesized were investigated for use as electrodes in supercapacitors and their electrochemical performance was compared with that of various activated carbons used in commercial devices. The excellent performance of these carbon xerogels as electrode materials was confirmed since, in addition to having a higher charge storage capacity than some

commercial activated carbons, they were able to maintain this energy storage over a large number of charge/discharge cycles.

Acknowledgements

The support from the Government of Ministerio de Economía y Competitividad (Ref. MAT2008-00217/MAT and MAT2011-23733) is greatly acknowledged. E.G. Calvo also acknowledges a predoctoral research Grant from FICYT.

References

[1] C. Schimt, H. Probstle, J. Fricke, J. Non-Cryst. Solids 285 (2001) 277–282.
[2] E.G. Calvo, C.O. Ania, L. Zubizarreta, J.A. Menéndez, A. Arenillas, Energy Fuels 24 (2010) 3334–3339.
[3] E.G. Calvo, E.J. Juárez-Pérez, J.A. Menéndez, A. Arenillas, J. Colloid Interface Sci. 357 (2011) 541–547.
[4] H. Jirglova, A. Pérez-Cadenas, F.J. Maldonado-Hódar, Langmuir 25 (2009) 2461–2466.
[5] K. Kraiwattanawong, H. Tamon, P. Praserthdam, Microporous Mesoporous Mater. 138 (2011) 8–16.
[6] N. Job, R. Pirard, J. Marien, J.-P. Pirard, Carbon 42 (2004) 619–628.
[7] F.L. Conçenciao, P.J.M. Carrott, M.M.L. Ribeiro Carrot, Carbon 47 (2009) 1874–1877.
[8] J.A. Maciá-Agulló, B.C. Moore, D. Cazorla-Amorós, A. Linares-Solano, Carbon 42 (2004) 1367–1370.
[9] L. Zubizarreta, A. Arenillas, J.-P. Pirard, J.J. Pis, N. Job, Microporous Mesoporous Mater. 115 (2008) 480–490.
[10] Y.-Z. Wei, B. Fang, S. Iwasa, M. Kumagai, J. Power Sources 141 (2005) 386–391.
[11] J.A. Maciá-Agulló, B.C. Moore, D. Cazorla-Amorós, A. Linares-Solano, Microporous Mesoporous Mater. 101 (2007) 397–405.
[12] V. Jiménez, J.A. Díaz, P. Sánchez, J.L. Valverde, A. Romero, Chem. Eng. J. 155 (2009) 931–940.
[13] F. Suárez-García, A. Martínez-Alonso, J.M.D. Tascón, Microporous Mesoporous Mater. 75 (2004) 73–80.
[14] H. Deng, G. Li, H. Yang, J. Tang, J. Tang, Chem. Eng. J. 163 (2010) 373–381.
[15] H. Deng, L. Yang, G. Tao, J. Dai, J. Hazard. Mater. 166 (2009) 1514–1521.
[16] K.U. Foo, B.H. Hameed, Biomass Bioenergy 35 (2011) 3257–3261.
[17] J.A. Menéndez, A. Arenillas, B. Fidalgo, Y. Fernández, L. Zubizarreta, E.G. Calvo, J.M. Bermúdez, Fuel Process. Technol. 91 (2010) 1–8.
[18] M. Kubota, A. Hata, H. Matsuda, Carbon 47 (2009) 2805–2811.
[19] K.Y. Foo, B.H. Hameed, Bioresour. Technol. 104 (2012) 679–686.
[20] K.Y. Foo, B.H. Hameed, Chem. Eng. J. http://dx.doi.org/10.1016/j.cej.2011.12.084.
[21] A.G. Pandolfo, A.F. Hollenkamp, J. Power Sources 157 (2006) 11–27.
[22] E. Frackowiak, Phys. Chem. Chem. Phys. 9 (2007) 1774–1785.
[23] E.J. Juárez-Pérez, E.G. Calvo, A. Arenillas, J.A. Menéndez, Carbon 48 (2010) 3293–3311.
[24] C.O. Kappe, Angew. Chem. Int. Ed. 43 (2004) 6250–6284.
[25] M.M. Dubinin, J.F. Danielli, M.D. Rosenberg, D. Cadenhead (Eds.), Progress in Surface and Membrane Science, vol. 9, Academic Press, New York, 1975, pp. 1–70.
[26] H. Deng, G. Zhang, X. Xu, G. Tao, J. Dai, J. Hazard. Mater. 182 (2010) 217–224.
[27] J.A. Menéndez, E.J. Juárez-Pérez, E. Ruisánchez, J.A. Bermúdez, A. Arenillas, Carbon 49 (2011) 346–349.
[28] L. Zubizarreta, A. Arenillas, A. Domínguez, J.A. Menéndez, J.J. Pis, J. Non-Cryst. Solids 354 (2008) 817–825.
[29] H. Teng, S.-C. Wang, Carbon 38 (2000) 817–824.
[30] J.M. Rosas, J. Bedia, J. Rodríguez-Mirasol, T. Cordero, Fuel 88 (2009) 19–26.
[31] T. Kawano, M. Kubota, M.S. Onyango, F. Watanabe, H. Matsuda, Appl. Therm. Eng. 28 (2008) 865–871.
[32] V. Fierro, V. Torné-Fernández, A. Celzard, Microporous Mesoporous Mater. 92 (2006) 243–250.
[33] A.V. Maldhure, J.D. Ekhe, Chem. Eng. J. 168 (2011) 1103–1111.
[34] Q.-S. Liu, T. Zheng, P. Wang, L. Guo, Ind. Crops Prod. 31 (2010) 233–238.
[35] A.C. Lua, T. Yang, J. Colloid Interface Sci. 274 (2004) 594–601.
[36] K. Leitner, A. Lerf, M. Winter, J.O. Besenhard, S. Villar-Rodil, F. Suárez-García, A. Martínez-Alonso, J.M.D. Tascón, J. Power Sources 153 (2006) 419–423.
[37] M.-C. Liu, L.-B. Kong, P. Zhang, Y.-C. Luo, L. Kang, Electrochim. Acta 60 (2012) 443–448.
[38] B. Fang, L. Binder, J. Power Sources 163 (2006) 616–622.
[39] W. Liu, G. Reichenauer, J. Fricke, Carbon 40 (2002) 2955–2959.
[40] X. Lu, J. Shen, H. Ma, B. Yan, Z. Li, M. Shi, M. Ye, J. Power Sources 201 (2012) 340–346.
[41] Y.J. Lee, S. Park, J.G. Seo, J.R. Yoon, J. Yi, I.K. Song, Curr. Appl. Phys. 11 (2011) 631–635.
[42] E. Raymundo-Piñero, K. Kierzek, J. Machnikowski, F. Béguin, Carbon 44 (2006) 2498–2507.
[43] H. Shi, Electrochim. Acta 41 (1996) 1633–1639.
[44] J. Chmiola, G. Yushin, Y. Gogotsi, C. Porter, P. Simon, P.L. Taberna, Science 313 (2006) 1760–1763.
[45] C. Vix-Guterl, E. Frackowiak, K. Jurewicz, M. Fiebre, J. Parementier, F. Béguin, Carbon 43 (2005) 1293–1302.
[46] E. Frackowiak, G. Lota, J. Machnikowski, C. Vix-Guterl, F. Béguin, Electrochim. Acta 51 (2006) 2209–2214.
[47] C. Portet, P.L. Taberna, P. Simon, E. Flahaut, C. Laberty-Robert, Electrochim. Acta 50 (2005) 4174–4181.

4.3. PRODUCCIÓN DE ESFERAS DE XEROGEL DE CARBONO

Con los trabajos expuestos en las secciones anteriores queda patente que la radiación microondas sirve tanto para producir xerogeles de carbono de manera rápida y sencilla como para incrementar su microporosidad, lo que hace que sean más competitivos frente a materiales disponibles actualmente en el mercado. Tras haber conseguido ambos objetivos, el siguiente paso respecto a los geles de carbono consiste en explotar su capacidad de ser sintetizados directamente con diferente morfología, ampliando con ello su campo de aplicación.

Por este motivo, la última publicación del presente capítulo propone un método de preparación de esferas de xerogel de carbono basado en la radiación microondas. Dicho trabajo surge a raíz del hallazgo del método de detección de t_g descrito en la *Publicación II*. La posibilidad de determinar el momento de la transición sol-gel mediante un método sencillo y que está incluido en el dispositivo de calentamiento utilizado durante la síntesis de los xerogeles orgánicos, dio lugar a la idea de preparar este tipo de materiales con diferente morfología.

La elección del xerogel de carbono con forma esférica se hizo en base a las ventajas asociadas a este tipo de morfología, como son buena resistencia mecánica, fácil manejabilidad, buen empaquetamiento en columnas, filtros, etc.

En la bibliografía, se pueden encontrar trabajos que muestran diferentes protocolos que permiten preparar esferas en la escala del micrómetro y nanómetro (deposición química de vapor, CVD, polimerización en emulsión, carbonización hidrotermal) [LI, 2011A; SERP, 2001; YAMADA, 2012]. No obstante, la mayoría de ellos requiere de la presencia de un catalizador, un material que actúe como plantilla o un agente tensioactivo para llevar a cabo el conformado del material.

Las esferas de materiales de carbono con tamaño milimétrico y notable área superficial también han suscitado la atención de varios investigadores debido a su amplio campo de aplicación (separación de gases, adsorción en fase líquida o gaseosa, etc.) [LI 2011B; SUN, 2011]. Sin embargo hasta el momento, no se ha utilizado un proceso de obtención directa de miliesferas de xerogel de carbono. Además de las ventajas inherentes a la morfología esférica, que las esferas sean de un material tan atractivo como los xerogeles de carbono supone un beneficio extra debido a la capacidad de diseño de sus propiedades porosas y estructurales.

Por todo lo expuesto hasta el momento, el objetivo fundamental de la *Publicación IV* fue producir miliesferas de xerogel de carbono con un tamaño y una textura porosa diseñada en función de las condiciones de operación. En la Figura 4.4 aparece un esquema con las etapas involucradas en el proceso de preparación de las esferas de xerogel de carbono. Como se muestra en el trabajo recogido en la *Publicación IV*, de todas las etapas involucradas en el proceso de síntesis, existen dos que son clave puesto que determinan la porosidad y tamaño final del material sintetizado. Estas etapas

cruciales son, (i) el calentamiento de la disolución precursora en el horno microondas hasta el momento del punto de gelación y, (ii) la etapa de agitación y calentamiento de las esferas en un baño de silicona (etapas 1 y 2, respectivamente, mostradas en la Figura 4.4).

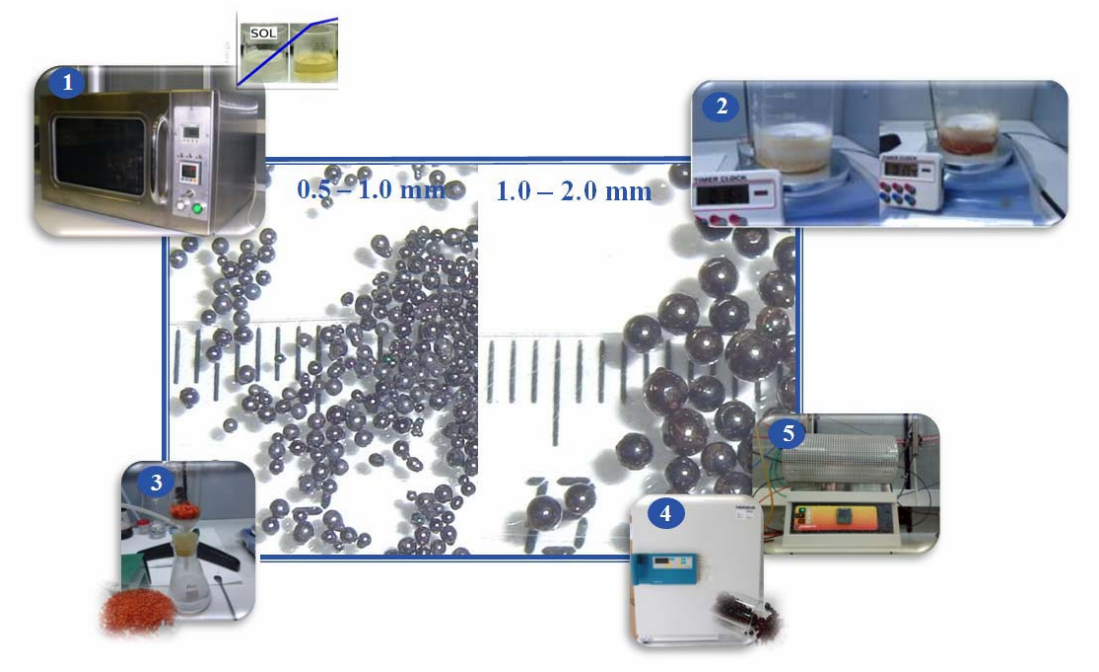

Figura 4.4. Etapas involucradas en la preparación de miliesferas de xerogel de carbono.

Para ver las diferencias existentes entre las esferas producidas, se utilizaron tres disoluciones resorcinol-formaldehído con diferente pH (3, 4 y 5), de tal manera que el tiempo de calentamiento en el horno microondas fue diferente en cada uno de los casos. A partir de las tres disoluciones se obtuvieron esferas de xerogel de carbono de distinto tamaño en el orden de los milímetros y éstas fueron divididas en dos fracciones según su tamaño: 0.5-1.0 mm y 1.0-2.0 mm.

Además de las propiedades porosas, las características químicas de las esferas milimétricas de xerogel de carbono fueron también evaluadas. En todos los casos se obtuvieron esferas formadas principalmente por C (con un contenido superior al 96 %) y un punto de carga cero (pH_{PZC}) en torno a 8, características similares a los geles de carbono recogidos en la *Publicación II*, evidenciando la posibilidad de producir miliesferas de xerogel de carbono con propiedades prácticamente idénticas a las asociadas a xerogeles de carbono en forma de polvo o monolito.

Puesto que en la mayoría de aplicaciones de los materiales esféricos se requiere una alta resistencia mecánica, las esferas de xerogel de carbono fabricadas, junto con varios materiales comerciales, fueron sometidas a unos test de abrasión. El dispositivo utilizado para conocer la dureza de las esferas está basado en dos cilindros de acero inoxidable y cada uno de ellos contiene 12 bolas de acero en su interior. Una vez que las esferas (tamaño comprendido entre 1.0-2.0 mm) se introducen en el cilindro y se mezclan con las bolas, se activa el equipo con el programa fijado que, en este caso concreto,

consiste en hacer rotar los cilindros durante 2 minutos con una velocidad de rotación de 25 rpm. Cuando el experimento termina, se procede a la clasificación y pesada de las muestras para determinar qué cantidad de material ha soportado el experimento sin romperse. En la Figura 4.5 aparecen los porcentajes de esferas recuperadas entre 1.0-2.0 mm de los xerogeles de carbono estudiados y de dos materiales esféricos comerciales utilizados como referencia. De acuerdo con estos resultados se puede decir que la resistencia mecánica de las miliesferas de xerogel de carbono es ligeramente inferior a la de los dos materiales comerciales estudiados. No obstante, en todos los casos, el porcentaje de esferas recuperadas tras los ensayos realizados se encuentra en torno al 90 %.

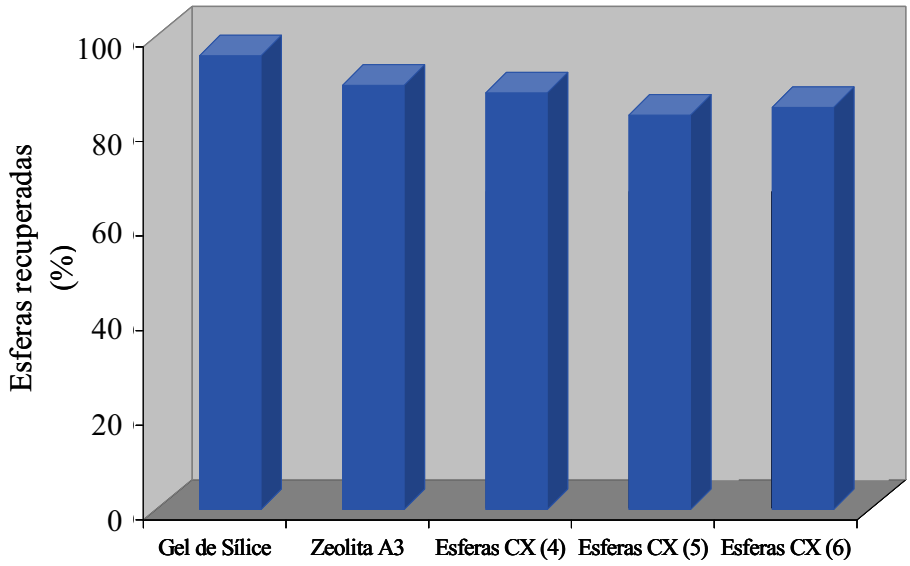

Figura 4.5. Porcentaje de esferas que ha superado el test de abrasión.

Los resultados expuestos en la *Publicación IV* dan lugar a las siguientes conclusiones:

❖ Miliesferas de xerogel de carbono (tamaño entre 0.5-2.0 mm) han sido sintetizadas mediante un método sencillo, basado en la radiación microondas, y que no necesita la adición de ningún tipo de surfactante.

❖ El pH de la mezcla resorcinol-formaldehído determina tanto la porosidad como el tamaño de las esferas de xerogel de carbono. Una disminución en el pH inicial lleva asociada la producción de esferas de menor tamaño, con una distribución de tamaños de poro desplazada hacia diámetros de poro de mayor tamaño. Por ejemplo, con un valor de pH = 4, el 85 % de las esferas de xerogel de carbono sintetizadas tiene un tamaño comprendido entre 0.5-1.0 mm, mientras que para pH = 6, la mayoría de las miliesferas de xerogel de carbono producidas son de 1.0-2.0 mm.

❖ El rendimiento de las miliesferas de xerogel de carbono está notablemente influenciado por el pH inicial y la velocidad de agitación utilizada al poner en contacto la mezcla resorcinol-formaldehído con un aceite de silicona. Así, la cantidad de miliesferas de carbono obtenidas se reduce bruscamente

al disminuir la velocidad de agitación, mientras que un aumento en el valor del pH inicial lleva asociados rendimientos ligeramente superiores.

Publicación IV

A MICROWAVE-BASED METHOD FOR THE SYNTHESIS OF CARBON XEROGEL SPHERES

Carbon

50 (3553-3560)

Año: 2012

CARBON 50 (2012) 3555–3560

Available at www.sciencedirect.com

SciVerse ScienceDirect

journal homepage: www.elsevier.com/locate/carbon

A microwave-based method for the synthesis of carbon xerogel spheres

J.A. Menéndez, E.J. Juárez-Pérez, E. Ruisánchez, E.G. Calvo, A. Arenillas *

Instituto Nacional del Carbón, INCAR-CSIC, Apartado 73, 33080 Oviedo, Spain

ARTICLE INFO

Article history:
Received 22 December 2011
Accepted 13 March 2012
Available online 21 March 2012

ABSTRACT

Carbon xerogel spheres with millimeter-scale diameters were synthesized by a simple process using microwave radiation as the heating source. Using this type of heating it is possible to establish the gelation point of different resorcinol–formaldehyde solutions and stop the gelation step of the material at the exact time of gelation. Organic gel spheres can then be directly obtained by stirring in a silicone bath at 80 °C. Finally, carbonization is performed to obtain carbon xerogels with a spherical shape. The size and porous texture of the spheres can be controlled by adjusting the synthesis conditions.

1. Introduction

Carbon gels have been extensively studied over the last decade due to their unique textural and structural properties and as a result of their simple manufacturing process, at least on a laboratory scale [1,2]. Compared with other carbon materials, the main highlight of carbon gels is the possibility of tailoring their properties during the synthesis process to produce a final material that fits the requirements of a specific application [3,4]. Thus, carbon gels offer great potential in many different fields such as catalysis [5,6], adsorption [7,8], and energy storage [9,10]. Carbon gels can be also produced directly in diverse final forms as monoliths, powder, films or spheres, making them even more attractive for a wide range of applications [3].

Spherically shaped carbon materials of diverse size have been synthesized by different methods due to certain attractive characteristics such as their smooth surface, high mechanical strength, easy manageability and their role as fillers [11,12]. All of these features make them especially suitable in the field of adsorption (i.e. adsorption of pollutants/compounds in gas or liquid phase, gas separation, etc.). These processes are usually based on the use of fixed bed reactors, where the spherical carbon materials are packed in beds, configuration that facilitates the design of the reactor and the control of the operation variables such as pressure drop and residence time [13].

Most preparation methods of carbon spheres reported in the bibliography are based on the use of catalysts, surfactants or templates [14–19]. However, a growing interest has recently appeared focused on alternative methods for carbon spheres production in order to avoid the use of such reagents that tend to complicate the process, thereby increasing production costs and generating less competitive materials.

In the present work, a new method for preparing carbon xerogel spheres with a tailored diameter size (in the millimeter range) and porous texture is described. The originality of the synthesis procedure lies in the fact that there is no need to use any catalyst, template or surfactant for the shaping process. By means of microwave synthesis it is possible to control the gelation process and stop the gelation at the desired point in order to tailor the final shape of the product. It was possible to obtain carbon-xerogel spheres by simply emulsifying the gel mixture at the gelation point (t_g) [20]. The porous and chemical properties of the synthesized materials were controlled by adjusting the usual operating conditions (the pH of the resorcinol–formaldehyde solution, for instance) in the same way as in conventional methods, but with a noticeable saving of time and cost (the synthesis time

* *Corresponding author*: Fax: +34 985297662.
E-mail address: aapuente@incar.csic.es (A. Arenillas).
0008-6223/$ - see front matter © 2012 Elsevier Ltd. All rights reserved.
http://dx.doi.org/10.1016/j.carbon.2012.03.027

can be reduced about 80% when microwaves are used as heating source [21]).

2. Experimental

2.1. Synthesis of carbon xerogel spheres

Details of the preparation of the xerogel spheres are given in the Online supplementary information. The spheres were sorted into different size fractions by standard sieving methods, with all non-spherical material being discarded. The samples were designated MSX (a and b), where X is the pH of the RF solution and (a and b) the diameter range of the spheres in millimeters.

2.2. Characterization of the carbon xerogel spheres

Porous textural characterization was carried out by means of N_2 adsorption–desorption isotherms at −196 °C in the pressure range of 0–1 bar, with a Micromeritics Tristar 3020. The Dubinin–Raduskevich (DR) method [23] was applied to the N_2 adsorption isotherms to determine the micropore volume (V_{DUB-N_2}) and the specific surface area, S_{BET}, was estimated using the Brunauer–Emmet–Teller (BET) equation [24]. The pore size distribution of the samples synthesized was evaluated by applying the DFT method [25].

The chemical nature of the carbon xerogel spheres was evaluated by measuring the point of zero charge (PZC) and from proximate and ultimate analysis. The proximate analysis (i.e. moisture, ash and volatile matter content) was carried out in a LECO TGA-601 thermobalance, and the ultimate analysis (i.e. carbon, nitrogen and hydrogen content) was performed on a LECO-CHNS-932 microanalyzer. The oxygen content was directly measured using a LECO-TF-900. The PZC indicates the acidic or basic nature of the material surface. The procedure for measuring this pH has been described elsewhere [26].

3. Results and discussion

3.1. Yields and diameter size distribution

Table 1 summarizes the yields of the carbon xerogels studied. For comparative purposes, the first row of the table shows the average yield of a non-spherical shape RF xerogel that has been obtained following a similar procedure to that reported in this work for the preparation of the carbon xerogel spheres. In the case of RF xerogel used as reference, a yield value of 12 wt.% may appear too low. However, it should be noted that the yield was calculated from the weight of the precursor solution, including the solvent (distilled water), according to the equation: yield (wt.%) = (mass of the initial solution/mass of the final carbon gel) × 100. Taking into account that distilled water represents approximately 60 wt.% of the initial solution, the yield would be around 30 wt.% on a solvent-free basis. On the other hand, the yield of carbonization stage, on the basis of weight of the organic xerogel, i.e. (mass of organic xerogel/mass of carbon xerogel) × 100 is about 47 wt.%.

The yields (based on the precursor solution) of the total (spherical and non-spherical) carbon xerogels are lower than those of the monolithic carbon xerogel (i.e. 7.3, 8.5 and 10.5 wt.% for samples MS4, MS5 and MS6, respectively, as opposed to 12.0 wt.% in the case of the non-spherical material), probably as a consequence of the loss of material during the stirring and washing processes performed during the synthesis. As can be seen from Table 1, the yields of the carbon xerogel spheres increase as the pH of the precursor solutions increases, As a consequence of this tendency, sample MS6, i.e. carbon gel spheres obtained from a solution with an initial pH of 6, displays a yield of 10.5 wt.%, which is only slightly lower than those associated with the monolithic carbon xerogel used as reference material. The same trend is observed when the yields associated with the production of carbon spheres, i.e. when the non-spherical material has been excluded, are compared (see third column of Table 1). The higher the initial pH, the greater the number of spheres produced (i.e. the smaller the amount of non-spherical material), to the point that they comprise as much as 80 wt.% of all the carbonized material when the precursor solution has a pH value of 6.

Although the effect of the stirring rate was not deeply investigated, the spheres yield shows a significant drop at stirring rates below 1000 rpm, resulting in a yield lower than 20 wt.% when the stirring process was carried out at 300 rpm. For this reason only the carbon spheres obtained at 1000 rpm were characterized and studied.

Besides having an influence on the carbon spheres yield, the initial pH also has a notable effect on the size of the resulting material. The diameters of all carbon spheres obtained lie within the 0.5–2.0 mm range (see Online supplementary information). However, an increase in the pH of the resorcinol–formaldehyde solution results in a greater amount

Table 1 – Yields of the carbon gel spheres obtained under different experimental conditions.

Sample	Total carbon gel yield[b] (wt.% ± 0.5)	Spheres yield[c] (wt.% ± 0.5)
Reference monolith[a]	12.0	–
MS4	7.3	52.2
MS5	8.5	60.2
MS6	10.5	80.3

[a] Carbon gel obtained from the carbonization of a organic gel synthesized under microwave heating for 5 h (removal of stages 3, 4, 5 and 7, described in Section 2) [21]. Note that in this case this yield is independent on the pH of the precursor solution.
[b] Yields calculated from the precursor solution including the solvent (distilled water).
[c] Yields calculated from the total carbon gel obtained.

CARBON 50 (2012) 3555–3560

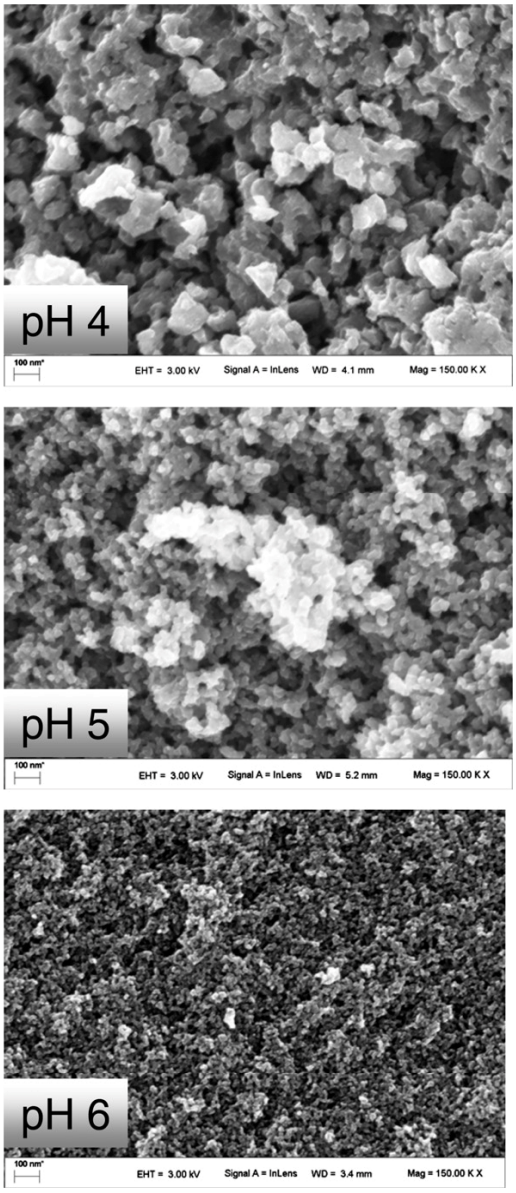

Fig. 1 – FESEM photographs showing the influence of the pH of the precursor solution on the structure of the carbon xerogel (scale bar = 100 nm).

of large-size spheres. Thus, sample MS4 has about 85 wt.% of carbon spheres with a diameter of 0.5–1.0 nm, i.e. only 15 wt.% of the synthesized material lies in the 1.0–2.0 nm range. However, in the case of MS6 spheres the trend has reversed, since 85 wt.% of the spheres obtained have a diameter between 1.0 and 2.0 nm.

The pH of the precursor solution is a very important operating variable because it controls the polymerization and subsequent crosslinking of the polymers. As the pH increases, the first stage of the reaction (addition reaction) is favored, during which a large number of branched and interconnected polymer nodules are formed, leading to smaller and more interconnected polymer particles. The result of this phenomenon is a carbon material with a nanostructure that depends on the pH of the precursor solution used. This fact is corroborated by the FESEM photographs collected in Fig. 1, which shows that the polymeric structure at the nanometer scale is a function of the pH used during the synthesis of carbon xerogel spheres. When the three photographs are compared, it can be seen nodules of smaller size as the initial pH increases.

These differences in carbon structure have a clear influence on the consistency of the final polymer obtained. Thus, as the initial pH increases, small but highly branched particles, resulting in a more viscous incipient gel, are formed. This more viscous gel produces larger carbon spheres (i.e. 85% of the spheres synthesized with pH value of 6 display a diameter between 1.0 and 2.0 mm). In contrast, larger nodules but weakly branched formed at low pH, result in smaller carbon xerogel spheres.

3.2. *Chemical characteristics*

The structural and textural characterization performed suggests that the pH of the precursor solution has a marked influence on the final structure and textural properties of the carbon xerogel spheres but the effect of this variable on their chemical nature is almost negligible. From the chemical characteristics gathered in Table 2, it can be seen that all the carbon spheres synthesized are essentially composed of carbon (more than 96 wt.% in all cases tested). The proximate analysis data indicate that the material has an ash content close to 1.0 wt.%, content probably related to Si (expressed as SiO_2), which probably owes its origin to traces of silicone that have not been completely removed during the washing steps. The volatile matter content of these materials is very low in the three cases studied (i.e. between 0.5 and 1.7 wt.%) and corresponds mainly to residual functional groups (probably oxygen surface groups). Such low content in volatile matter indicates that the carbonization processes have had the desired effect since the main target of the pyrolysis stage is

Table 2 – Chemical properties of the carbon spheres.

	Proximate analysis (wt.% ± 0.5)			Elemental analysis (wt.% ± 0.5)				pH_{PZC} (±0.1)
	Moist	Volatiles[a]	Ash[a]	C[a]	H[a]	N[a]	O[a]	
MS4	2.3	0.5	0.9	96.8	0.8	0.7	0.8	8.6
MS5	2.0	1.5	0.9	96.2	0.8	0.7	1.4	8.6
MS6	2.3	1.7	0.6	96.2	0.9	0.6	1.7	7.6

a Dry basis.

count both the shape of the isotherms and the textural parameters, it can be concluded that, regardless of the initial pH, microporosity is virtually identical in all cases tested, while no case with meso–macroporosity, since the presence of large mesopores and macropores is more evident as decreasing the pH of resorcinol–formaldehyde solution. These textural properties are in agreement with previous studies of the porous properties of resorcinol–formaldehyde carbon xerogels [1,21,22,26].

The tendency of smaller pore size for a higher initial pH is probably associated with the polymerization reaction. As the pH of the initial solution increases, highly branched polymer nodules of small size are formed, resulting in a more condensed carbon structure. Micropores are thought to be present in the nodules of the polymer, and the meso–macropores are due to the spaces between the nodules. For this reason, as the pH increases the mesopores become smaller.

All the spheres have a similar microporosity and therefore a similar specific surface area (S_{BET}) and the mesoporosity can be controlled by the pH of the precursor solution. The micro and mesoporosity are independent of the final form of the carbon xerogel, since the same results were obtained for all spheres, regardless of their size, as for those observed obtained elsewhere in monoliths or grains [21,26]. Independently of the porosity of the carbon xerogels spheres, they present very good wear resistance as shown in the Online supplementary information.

4. Conclusions

Carbon xerogel spheres can be directly obtained without the use of surfactants by microwave-assisted synthesis.

The pore size distribution can be controlled varying the pH of the precursor solution.

The diameter of the spheres can be changed by adjusting the pH of the precursor solution and the stirring rate of the emulsion during the curing step.

Acknowledgements

The support from the Ministerio de Ciencia e Innovación (Ref. MAT2011-23733) is greatly acknowledged. E.G.C. and E.R. also acknowledge the predoctoral research grants from FICYT.

Appendix A. Supplementary data

Supplementary data associated with this article can be found, in the online version, at http://dx.doi.org/10.1016/j.carbon.2012.03.027.

REFERENCES

[1] Lin C, Ritter JA. Effect of synthesis pH on the structure of carbon xerogels. Carbon 1997;35(9):1271–8.
[2] Mahata N, Pereira MFR, Suárez-García F, Martínez-Alonso A, Tascón JMD, Figueiredo JL. Tuning of texture and surface chemistry of carbon xerogels. J Colloid Interface Sci 2008;324(1–2):150–5.
[3] Al-Muhtaseb SA, Ritter JA. Preparation and properties of resorcinol–formaldehyde organic and carbon gels. Adv Mater 2003;15(2):101–14.
[4] Job N, Théry A, Pirard R, Marien J, Kocon L, Rouzaud JN, et al. Carbon aerogels, cryogels and xerogels: influence of the drying method on the textural properties of porous carbon materials. Carbon 2005;43(12):2481–94.
[5] Job N, Heinrichs B, Lambert S, Pirard JP, Colomer JF, Vertruyen B, et al. Carbon xerogel as catalyst supports: study of mass transfers. AIChE J 2006;52:2663–76.
[6] Job N, Heinrichs B, Ferauche F, Noville F, Marien J, Pirard JP. Hydrodechlorination of 1,2-dichloroethane on Pd–Ag catalysts supported on tailored texture carbon xerogels. Catal Today 2005;102–103:234–41.
[7] Jayne D, Zhang Y, Shaker H, Erkey C. Dynamics of removal of organosulfur compounds from diesel by adsorption on carbon aerogels for fuel cell applications. Int J Hydrogen Energy 2005;30(11):1287–93.
[8] Kang YK, Lee BI, Lee JS. Hydrogen adsorption on nitrogen-doped carbon xerogels. Carbon 2009;47(4):1171–80.
[9] Frackowiak E, Béguin F. Carbon materials for the electrochemical storage of energy in capacitors. Carbon 2001;39(6):937–50.
[10] Fang B, Binder LJ. A modified activated carbon aerogel for high-energy storage in electric double layer capacitors. J Power Sources 2006;163(1):616–22.
[11] Wilcox DL, Berg M. Microsphere fabrication and applications: an overview. Mater Res Soc Symp Proc 1994;372:3–13.
[12] Yang J-B, Ling L-C, Liu L, Kang F-Y, Huang Z-H, Wu H. Preparation and properties of phenolic resin-based activated carbon spheres with controlled pore size distribution. Carbon 2002;40(6):911–6.
[13] Girimonte R, Vivacqua V. The expansion process of particle beds fluidized in the voids of a packing of coarse spheres. Powder Technol 2011;213(1–3):63–9.
[14] Quian H-S, Han F-M, Zhang B, Guo Y-C, Yue J, Peng B-X. Non catalytic CVD preparation of carbon spheres with a specific size. Carbon 2004;42(4):761–6.
[15] Xu Z-X, Lin J-D, Roy VAL, Qu Y, Liao D-W. Catalytic synthesis of carbon nanotubes and carbon spheres using Kaolin supported catalyst. Mater Sci Eng B 2005;123(2):102–6.
[16] Jiang X, Ju X, Huang M. Preparation and characterization of porous carbon spheres with controlled micropores and mesopores. J Alloys Compd 2010;509:S864–7.
[17] Tonanon N, Tanthapanichakoon W, Yamamoto T, Nishihara H, Mukai SR, Tamon H. Influence of surfactants on porous properties of carbon cryogels prepared by sol–gel polycondensation of resorcinol and formaldehyde. Carbon 2003;41(15):2981–90.
[18] Yamamoto T, Ohmori T, Kim YH. Preparation and characterization of monodisperse carbon cryogel microspheres. Microporous Mesoporous Mater 2008;112(1–3):211–8.
[19] Yamamoto T, Sugimoto T, Suzuki T, Mukai SR, Tamon H. Preparation and characterization of carbon cryogel microspheres. Carbon 2002;40(8):1345–51.
[20] Juárez-Pérez EJ, Calvo EG, Arenillas A, Menéndez JA. Precise determination of the point of sol–gel transition in carbon gel synthesis using a microwave heating method. Carbon 2010;48(11):3305–8.
[21] Calvo EG, Juárez-Pérez EJ, Menéndez JA, Arenillas A. Fast microwave-assisted synthesis of tailored mesoporous carbon xerogels. J Colloid Interface Sci 2011;357(2):541–7.
[22] Zubizarreta L, Arenillas A, Pirard JP, Pis JJ, Job N. Tailoring the textural properties of activated carbon xerogels by chemical activation with KOH. Microporous Mesoporous Mater 2008;115(3):480–90.
[23] Dubinin MM. Physical adsorption of gases and vapors in micropores. In: Danielli JF, Rosenberg MD, Cadenhead D,

editors. Progress in surface and membrane science. New York: Academic Press. p. 1–70.
[24] Parra JB, De Sousa JC, Bansal RC, Pis JJ, Pajares JA. Characterization of activated carbons by the BET equation – an alternative approach. Adsorpt Sci Technol 1995; 12:51–66.
[25] Jagiello J, Olivier JP. A simple two-dimensional NLDFT model of gas adsorption in finite carbon pores. Application to pore structure analysis. J Phys Chem C 2009;113(45):19382–5.
[26] Job N, Pirard R, Marien J, Pirard J-P. Porous carbon xerogels with texture tailored by pH control during sol–gel process. Carbon 2004;42(3):619–28.

- Supplementary Information –

The synthesis process of the carbon xerogel spheres comprises seven steps as outlined in Fig. S1.

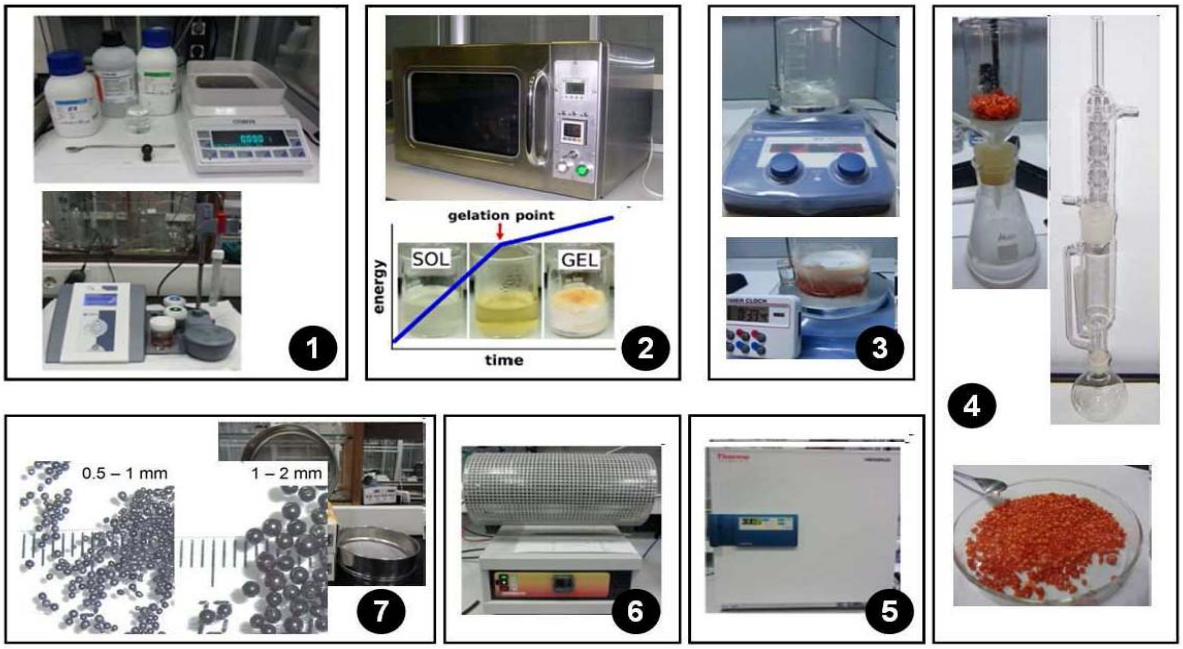

Fig. S1- Preparation of the carbon xerogel spheres.

(1) The aqueous RF solutions were prepared according to a procedure described elsewhere [21, 22] by using a dilution ratio, D, of 0.5 and R/F ratio of 5.7. The pH of each RF solution was adjusted using a 1.0 M NaOH solution, and the pH values employed in this work were 4, 5 and 6.

(2) Once the precursor solution was obtained, it was placed in a glass beaker inside a multimode microwave oven and heated to a temperature of 85 ºC. The temperature was monitored by means of a thermocouple, whose tip is immersed in the solution, and it was connected to a PID controller [20, 21]. During the polymerization reaction between the resorcinol and formaldehyde molecules, the energy consumed by the microwave device was recorded, enabling the exact gelation point was accurately estimated. A complete description of the method used to determine the gelation point, together with a detailed description of the microwave-assisted process used in the synthesis of carbon xerogels (monoliths or powder xerogels, but not spherical) has been reported elsewhere [20, 21]. The times of gelation or gelation points (t_g) of the RF solutions studied in this work were 2472, 1738 and 1368 seconds for pH 4, 5 and 6,

respectively. As can be seen, an increase in the pH of the precursor solution favors the polymerization of the monomers, thereby reducing the time required for gelation.

It must be pointed out that this second step is the most important of all the synthesis process of carbon xerogel spheres since the spheres formation occurs in the next step, it will be only possible if the RF mixture is exactly at, or slightly above, the gelation point. In other words, the mixture must be an incipient gel at this point.

(3) When the solution reached the exact gelation point, it was poured into a beaker containing polydimethylsiloxane oil (Rhodorsil® 47 V 20 from Bluestar Silicones). The formation of small spheres of organic gel is immediately apparent once both species were put in touch. The resorcinol-formaldehyde gel and oil mixture was kept at a temperature of 90 °C for 1 hour under magnetic stirring until the completion of the gelation and curing stages.

(4) Upon completion of curing stage, the organic gel spheres were separated from the silicone baht by vacuum filtration and then, they were subjected to cleaning processes with (i) distilled water, (ii) acetone and, finally, (iii) distilled water again. After such treatments, the organic gel spheres were cleaned again with acetone in a Soxhlet extractor in order to completely remove all possible traces of silicone.

(5) The organic gel spheres were dried overnight in a stove at 90 ºC.

(6) The dried spheres were then carbonized at 800 ºC in a horizontal tubular reactor under a nitrogen atmosphere, following a procedure described elsewhere [22].

(7) Finally, the resulting carbon xerogel spheres were sieved and classified into different diameters. The sample was placed on a sloping surface and the spherical material was collected at the base. The non-spherical material was discarded and assigned to the sphere yield loss.

Diameter size distribution of the carbon xerogel spheres

The pH of the resorcinol-formaldehyde solution has a remarkable impact not only on the porosity of carbon xerogel spheres synthesized but also on their size distribution. The diameter size distributions of the carbon spheres obtained in this work are reported in Fig. S2. The different spheres size obtained are classified in the range of 0.5-1.0 or 1.0-2.0 mm, for the three cases studied with different pH of the precursor solution. Thus, with the lowest initial pH, most of the spheres produced are included in the diameter range between 0.5-1.0 mm, while when an initial pH of 6 is selected, the 85 wt. % of the spheres obtained display a diameter higher than 1.0 mm.

.

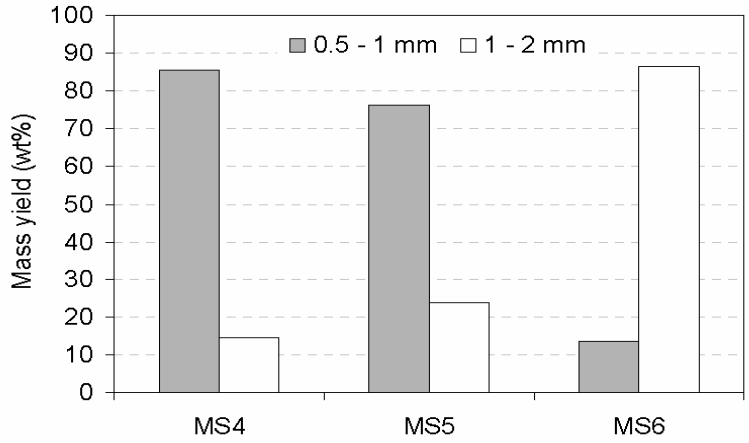

Figure S2. Size distribution (wt. %) of the carbon spheres synthesized at different values of initial pH.

Hardness of the carbon xerogel spheres

An important requirement for the materials used in packed columns or dispersed in stirred tanks (i.e. potential application of the carbon xerogel spheres presented in this work) is that they possess the necessary mechanical strength to be resistant to the abrasion which they will be undergone. Accordingly, the attrition resistances of the 1-2 mm carbon xerogel spheres synthesized in this work were compared with those of other commercial spherical products of the same diameter, such as silica gel and zeolite.

The resistance of this spherical carbon material was measured using a modified version of the Marsh-Ragan method [Ragan S, Marsh H. Carbonization and liquid-crystal (mesophase) development. Microstrength and optical textures of cokes from coal-pitch co-carbonizations. Fuel 1980;60(6):522–8.]. The device used to determine the strength consists of two stainless-steel cylinders, each of which contains 12 steel balls. The carbon spheres were introduced into the cylinders and mixed among the balls. The experiments are based on the rotation of the cylinders at a constant speed of 25 rpm for 2 minutes. The rotation speed was such as to ensure that the entire load (i.e., the samples and the steel balls) extended over the full length of the cylinders. Once the experiment was concluded, the samples were separated into fractions and weighed in order to determine the amount of broken material. The weight percentage that remained in the original size was recorded as R_1. Commercial silica gel and zeolite 3A in the shape of spheres of 1.0-2.0 mm were used as test probes for comparison purposes.

Fig. S3 represents the percentage of the spheres, recovered after the strength tests, with the same diameter as the untreated carbon spheres, i.e. between 1.0-2.0 mm. The results reveal that the carbon xerogel spheres studied in this work display a good hardness since, although the

recovered material is slightly less than the commercial materials, the yield in the three cases evaluated is greater than 80 wt %.

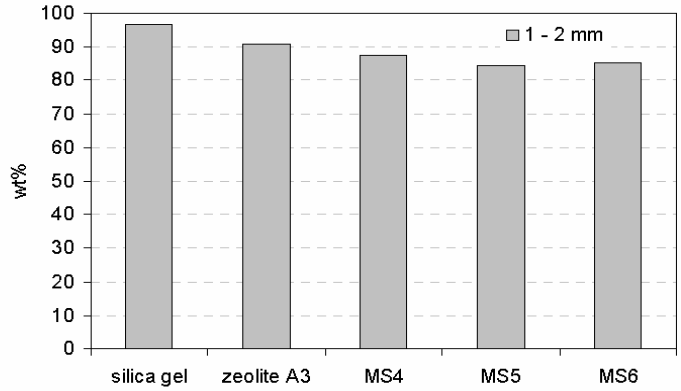

Figure S3. R1 (in wt. %) of the carbon gel spheres (1-2 mm) and commercial spherical particles of the same size (silica gel and zeolite A3).

Los tres trabajos expuestos en este capítulo dan una idea de la importancia de la radiación microondas para la producción de este tipo de materiales carbonosos. Como se ha indicado en la Introducción de esta memoria, los geles de carbono han existido desde comienzos del siglo XX. No obstante, su inserción en el mercado se ha visto entorpecida por el largo, y en ocasiones complicado, método de síntesis, situación que puede variar mediante la utilización de la tecnología microondas. Como evidencian las publicaciones recogidas en este capítulo, la aplicación de la radiación microondas acelera y simplifica el proceso de síntesis de xerogeles de carbono facilitando, por tanto, su fabricación a escala industrial. De hecho, el trabajo presentado en esta memoria ha servido de apoyo para la creación de una spin-off llamada *Xerolutions S.L.* (www.xerolutions.com).

El objetivo fundamental de *Xerolutions* es la producción y comercialización de xerogeles de carbono, con la particularidad de que se ofrecen a la medida del cliente y su aplicación. Como ha quedado reflejado a lo largo de esta memoria, las propiedades finales de los xerogeles de carbono son muy dependientes de las variables de operación, hecho que permite sintetizarlos con unas características muy diversas y diseñarlos para adaptarlos a las necesidades concretas de un gran número de aplicaciones.

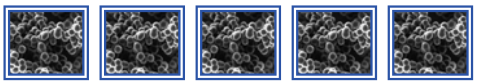

5. Xerogeles de Carbono como Electrodos en Supercondensadores

Este capítulo está dedicado al estudio del comportamiento electroquímico de xerogeles de carbono que se utilizan como electrodos en diferentes tipos de supercondensadores. Todas las publicaciones recogidas en este capítulo muestran la capacidad de almacenamiento energético de supercondensadores basados en xerogeles de carbono sintetizados en nuestro laboratorio. Sin embargo, varias fueron las estrategias adoptadas (combinación de xerogeles de carbono con un óxido metálico, composites xerogel/nanotubos de carbono o uso de electrolitos basados en líquidos iónicos próticos) con el objetivo de definir las mejores condiciones que dan lugar a dispositivos capaces de combinar una elevada capacidad de almacenamiento energético con una excelente ciclabilidad.

Los supercondensadores son dispositivos electroquímicos capaces de suministrar elevadas potencias. Sin embargo, la limitada densidad de energía que ofrecen representa uno de sus principales puntos débiles. Por este motivo, es necesario dar un paso adelante para mejorar dichos valores de densidad de energía. De acuerdo con la ecuación 1.3 recogida en la Introducción de la presente memoria, el diseño de un supercondensador con alta densidad de energía pasa por incrementar la cantidad de carga almacenada (hecho que se puede conseguir mediante el uso de electrodos con elevada superficie activa) y/o utilizar un voltaje de operación elevado, lo que está estrechamente relacionado tanto con el material de electrodo como con el electrolito utilizado [ARBIZZANY, 2008; DEMARCONNAY, 2010; ROBERTS, 2010; SALINAS-TORRES, 2013].

Los artículos incluidos en este Capítulo 5 se agrupan en dos partes bien diferenciadas. La primera de ellas enfocada hacia el estudio del material de electrodo, mientras que la segunda atiende al tipo de disolución empleada como electrolito en los supercondensadores.

5.1. MATERIAL DE ELECTRODO

El material de electrodo es uno de los factores que más influencia ejerce sobre el rendimiento electroquímico de un supercondensador. Por este motivo, existen numerosos estudios centrados en la

búsqueda de nuevos materiales de electrodo capaces de almacenar elevada cantidad de energía y sistemas con diversas configuraciones que permitan mejorar sus prestaciones.

Inicialmente, los principales materiales de carbono utilizados como electrodos para supercondensadores fueron los carbones activos, es decir, materiales de elevada área superficial obtenidos mediante la activación de residuos de diferente naturaleza (madera, carbón, cáscaras de semillas, frutos de distintas especies vegetales, etc.) [OBREJA, 2008; OLIVARES-MARÍN, 2009; WU, 2004]. Sin embargo, en los últimos años, otros materiales carbonosos han suscitado el interés de muchos investigadores debido, principalmente, a ciertas características comunes a este tipo de materiales como su bajo peso, elevada porosidad o posibilidad de modificar la química superficial, favoreciendo el almacenamiento de energía debido a fenómenos faradaicos [FRACKOWIAK, 2007; INAGAKI, 2010; OBREJA, 2008].

En la bibliografía es posible encontrar varios estudios basados en el uso de geles de carbono resorcinol-formaldehído como material de electrodo para condensadores electroquímicos [CALVO, 2010; HALAMA, 2010; RASINES, 2012; TASHIMA, 2009; ZAPATA-BENABITHE, 2012; ZAPATA-BENABHITE, 2013; ZHU, 2007]. Dichos trabajos ponen de relieve la viabilidad de estos materiales carbonosos para almacenar energía eficientemente ya que, además de las ventajas mencionadas en el párrafo anterior, los geles de carbono presentan una porosidad diseñada a medida, buenas propiedades conductoras y son capaces de soportar un elevado número de ciclos de carga y descarga.

La primera sección del Capítulo 5 hace referencia al estudio del comportamiento electroquímico de supercondensadores acuosos basados en xerogeles de carbono sintetizados en el laboratorio. A su vez, este primer bloque se ha dividido en tres partes, según las estrategias llevadas a cabo con el fin de optimizar la capacidad de almacenamiento energético de los supercondensadores: (i) celdas asimétricas que utilizan un xerogel de carbono activado como electrodo negativo y un óxido de manganeso como electrodo positivo (*Publicación V*), (ii) fabricación de materiales de electrodo compuestos, en este caso se utilizaron diferentes mezclas de xerogel/nanotubos de carbono *(Publicación VI)* y, finalmente, (iii) electrodos preparados a partir de xerogeles de carbono que presentan un diferente desarrollo textural (*Publicación VII*).

5.1.1. Supercondensadores asimétricos basados en xerogeles de carbono y MnO_2 como materiales de electrodo

La combinación de un electrodo compuesto por un material con propiedades fundamentalmente capacitivas, como es el caso de los xerogeles de carbono sintetizados en este trabajo, con un electrodo constituido por un óxido metálico que esté involucrado en reacciones redox (MnO_2, por ejemplo),

permite incrementar el voltaje de operación de supercondensadores basados en electrolitos acuosos, lo que se traduce en un aumento de la capacidad de almacenamiento energético.

Diferentes autores han evaluado el comportamiento electroquímico de supercondensadores simétricos que utilizan MnO_2 como material de electrodo, y que son capaces de suministrar valores de capacidad específica en torno a 200 F g^{-1} [DU, 2012; JIANG, 2002; STAITI, 2009]. El rendimiento de este tipo de supercondensadores está limitado por las reacciones de oxido-reducción que sufren ambos electrodos (reducción de Mn(IV) a Mn(II) en el electrodo negativo y oxidación de Mn(IV) a Mn(VII) en el electrodo positivo). Más concretamente, ha quedado demostrado que la reducción de Mn(IV) a Mn(II) que tiene lugar en el ánodo es la etapa limitante del proceso de almacenamiento de carga [RAYMUNDO-PIÑERO, 2005]. Por este motivo, surge la idea de fabricar supercondensadores asimétricos que utilizan MnO_2 como electrodo positivo y otro tipo de material de electrodo para el negativo [HONG, 2002; KHOMENKO, 2006].

El trabajo que aparece reflejado en la *Publicación V* muestra, por un lado, la capacidad de almacenamiento energético de supercondensadores simétricos basados en xerogeles de carbono de distinta porosidad y, por otro lado, sistemas híbridos que combinan MnO_2 y un xerogel de carbono altamente poroso como materiales de electrodo, siendo esta última parte la más novedosa del artículo.

Antes de citar las conclusiones más relevantes derivadas de dicho trabajo, es importante apuntar que en la primera parte del estudio, xerogeles resorcinol-formaldehído producidos mediante síntesis convencional (gelación y curado en estufa a 85 ºC durante 72 h y posterior secado a 150 ºC durante 24 horas) fueron utilizados como material de electrodo. Dichas muestran presentan diferente volumen de meso-macroporos, como consecuencia del distinto pH de la mezcla resorcinol-formaldehído empleada. Además, no muestran microporosidades suficientemente desarrolladas (S_{BET} en torno a 650 m^2 g^{-1}), ya que no fueron sometidos a ningún post-tratamiento que permita incrementar el volumen de microporos. Por este motivo, las capacidades de almacenamiento energético mostradas en la primera parte de la *Publicación V* no son demasiado elevadas.

En el caso de los supercondensadores híbridos, el material carbonoso utilizado como ánodo fue un xerogel de carbono activado mediante H_3PO_4, cuya área superficial S_{BET} se sitúa próxima a 2400 m^2 g^1. Los resultados obtenidos a partir de este estudio dieron lugar a las siguientes conclusiones:

- El uso de sistemas asimétricos basados en MnO_2/xerogel de carbono ha permitido incrementar la diferencia de potencial aplicada en el supercondensador, llegándose a alcanzar voltajes de trabajo de hasta 1.6 V, valor superior al aplicado en supercondensadores simétricos que utilizan disoluciones acuosas como electrolito.

- El mayor voltaje de operación conseguido con el supercondensador asimétrico se traduce en una mayor energía específica (15.1 frente a 3.2 Wh g^{-1} para el supercondensador simétrico que utiliza

el xerogel tratado con H_3PO_4 como material activo en ambos electrodos). Este hecho es crucial en el campo del almacenamiento energético ya que el principal inconveniente de los supercondensadores está relacionado con su limitada densidad de energía, y los resultados recogidos en este trabajo muestran la posibilidad de superar dicho obstáculo mediante el uso de supercondensadores con diferentes configuraciones.

- La pseudocapacidad que tiene lugar como consecuencia de las reacciones redox sufridas por el MnO_2 queda demostrada gracias a los tests de voltametría cíclica y cronoamperometría llevados a cabo en este trabajo. Por un lado, es posible apreciar picos indicativos de fenómenos redox en los voltamogramas obtenidos con el supercondensador híbrido (picos inexistentes en el caso del supercondensador simétrico cuyo almacenamiento de energía se produce exclusivamente como consecuencia de la formación de la doble capa eléctrica). Por otro lado, existe una mayor dependencia de la capacidad específica con la densidad de corriente aplicada en los tests de carga-descarga, indicando un aporte extra de almacenamiento de energía debido a fenómenos faradaicos.

Publicación V

CARBON XEROGEL AND MANGANESE OXIDE CAPACITIVE MATERIALS FOR ADVANCED SUPERCAPACITORS

International Journal of Electrochemical Science

6 (596-612)

Año: 2011

Int. J. Electrochem. Sci., 6 (**2011**) 596 - 612

International Journal of
ELECTROCHEMICAL
SCIENCE
www.electrochemsci.org

Carbon Xerogel and Manganese Oxide Capacitive Materials for Advanced Supercapacitors

F. Lufrano[1,*], *P. Staiti*[1], *E.G. Calvo*[2], *E.J. Juárez-Pérez*[2], *J.A Menéndez*[2], *A. Arenillas*[2]

[1] CNR-ITAE, Istituto di Tecnologie Avanzate per L'Energia "Nicola Giordano", Via Salita S. Lucia, 5 – 98126 Messina, Italy
[2] Instituto Nacional del Carbón, CSIC, Apartado 73, E-33080, Oviedo, Spain
[*]E-mail: xx-yy

Received: 1 November 2011 / *Accepted:* 1 December 2011 / *Published:* 1 January 2011

Symmetric supercapacitors (SSC) and asymmetric supercapacitors (ASC) that use carbon xerogels with different porous textures as negative electrode and manganese oxide as positive electrode were investigated. The electrochemical performance of symmetric supercapacitors with carbon xerogel electrodes was mainly influenced by the textural characteristics of the carbon, pore size distribution being the property that has the strongest influence on the capacitance performance. The asymmetric supercapacitor showed an excellent capacitance performance (i.e. 213 F g^{-1}) when a chemical activated carbon xerogel with a high S_{BET} (i.e. 2360 m^2 g^{-1}) was used as negative electrode and high performing oxide-based manganese as positive electrode, thereby demonstrating that carbon xerogels and manganese oxide have potential applications in supercapacitor devices.

Keywords: Supercapacitors, carbon xerogels, manganese oxide, symmetric supercapacitor, asymmetric supercapacitor

1. INTRODUCTION

Supercapacitors are energy storage devices, which have intermediate characteristics between batteries and traditional capacitors [1-3]. Unlike batteries, the charge/discharge mechanism of electrochemical supercapacitors is mainly of a capacitive type. These devices can be built according to two different configurations: (i) symmetric (SSC), where the two electrodes (positive and negative) are identical, and (ii) asymmetric (ASC), where the two electrodes are different in terms of materials, loading and/or composition. In these supercapacitors two main capacitive storage processes can take place, one based on the formation of a double layer of charges that arises at the interface of the electrode and the electrolyte solution and the other originated from the charge-transfer process in the

active component of the electrode through a reversible redox reaction (faradaic). This reaction causes a change in the state of oxidation of the material (pseudocapacitive process). The use of materials with pseudocapacitive properties in one electrode coupled with materials with purely capacitive properties in the other electrode increases the energy density of the supercapacitor and enlarges the working voltage window up to 2 V in aqueous electrolytes [4-5]. Manganese oxide, a material well known for its pseudocapacitive properties, has attracted growing interest in recent years as a possible alternative to the more costly ruthenium oxide for use in asymmetric (or hybrid) supercapacitors.

Carbon-based active materials with a high surface area are nowadays commonly used in the electrodes of supercapacitors and for this reason they are also known as electric double layer capacitors (EDLCs). These materials are highly competitive due to their relatively low cost and their good electronic conductivity (c.a. 0.1–1 S cm^{-1}), a property that endows the capacitors with a low internal resistance.

Carbon gels are porous materials that are highly sensitive to the conditions in which they are synthesized. They are very easy to tailor in terms of shape, porous texture and surface chemistry [6]. These features, along with their extremely low inorganic matter content, make them more suitable for use in supercapacitors than traditional activated carbons. Moreover, they have a low mass density and a high electrical conductivity which also make them ideally appropriate for use in supercapacitors [6]. Carbon gels can be obtained by different procedures [6], but the preparation basically consists of three steps: (i) gel synthesis, involving the formation of a three-dimensional polymer in a solvent (gelation), followed by a curing period, (ii) gel drying, where the solvent is removed to obtain an organic gel, and finally (iii) pyrolysis under an inert atmosphere to form the porous carbon material, i.e. the so-called carbon gel. Resorcinol-formaldehyde (RF) aqueous gels are among the most studied systems [6]. Most of the published works on RF gels agree that the synthesis and drying processes are the steps that define the size and volume of the mesopores and macropores in the final carbon gels and that the development of the micropores takes place during the subsequent pyrolysis step [7]. The meso- or macroporosity formed during the synthesis is barely altered during thermal stabilization (i.e. the pyrolysis step). The microporosity created during the pyrolysis can be increased through an activation process. These carbon materials are composed of interconnected sphere-like nodules, whose size can be regulated by the synthesis conditions. Consequently, the size of the voids between the nodules can be tailored [7-8]. The micropores are formed within the nodules by removing some of the labile matter during pyrolysis. RF carbon gels usually have surfaces of around 600-700 m^2 g^{-1}, whereas activated carbon surfaces can exceed 2000 m^2 g^{-1}. However, to overcome this limitation, carbon gels can be chemically activated for specific applications where high surface areas are required.

In this work, carbon xerogels with different meso/macropore textures were prepared by varying the initial pH of the resorcinol-formaldehyde aqueous solution. The organic gels were first dried by evaporation of the solvent and then pyrolysed. In order to develop the microporosity and increase the surface area of the final carbonaceous materials, chemical activation with phosphoric acid was performed. The effect of the textural properties of the gels on their performance in the electrodes of supercapacitors was evaluated by electrochemical tests. Although carbon gels have already been studied as active material in double layer capacitors [9-12] and are employed in commercially available supercapacitors, to the best of our knowledge they have not never been used in

asymmetric/hybrid supercapacitors. Here, we report the synthesis of carbon xerogel materials and the development of electrodes for supercapacitors with two possible configurations: a) symmetric (SSC) - where two electrodes of carbon xerogel material were used, and b) asymmetric (ASC) – where carbon xerogel was used as active material in a negative electrode coupled to a manganese oxide-based positive electrode.

2. EXPERIMENTAL

2.1. Preparation of carbon xerogels

Aqueous organic gels were synthesised by the polycondensation of resorcinol (R) with formaldehyde (F) in water (W). Sodium hydroxide (C) was used as basification agent. The resorcinol (99%) by VWR International Eurolab S.L. (Barcelona, Spain), was first dissolved in deionised water in a sealed flask under magnetic stirring. Formaldehyde (solvent: 37% wt. water and 10-15% wt. methanol) was added to the mixture under magnetic stirring and kept under stirring until a homogeneous solution was obtained.

All the gels were synthesised using an R/F molar ratio equal to the stoichiometric value (0.5) and a fixed dilution ratio, D (i.e. the total solvent/reactant molar ratio) of 5.7. It should be noted that the "total solvent" includes the deionised water from the initial solution, and the water and methanol contained in the formaldehyde solution, whilst "reactant" refers to the resorcinol and formaldehyde. Methanol is a stabilizer that prevents the formaldehyde molecules from undergoing polymerisation during storage. Three different organic gels were synthesised under different initial solution pHs (i.e. 5.8, 6.3 and 6.5). In the text these carbon samples are named as CX5.8, CX 6.3 and CX6.5, respectively. The solutions were placed in an oven at 85 ºC for 72 h to undergo gelation and ageing. The aqueous gels obtained were then dried by evaporation, without any pre-treatment, in the same oven at 150 ºC for 24 h. After drying, the gels were pyrolysed at 800 ºC under nitrogen flow in a tubular oven, using the following heating program: (i) ramp at 1.7 ºC min^{-1} to 150 ºC and hold for 15 min; (ii) ramp at 5 ºC $min^{-1}$to 400 ºC and hold for 60 min; (iii) ramp at 5 ºC min^{-1} to 800 ºC and hold for 120 min; and (iv) cool slowly to room temperature.

A carbon xerogel was chemically activated with 75 wt% orthophosphoric acid (from VWR International), using an activating agent/carbon gel mass ratio of 3:1. The mixture was stirred at 85 ºC for 2 h, and then filtered and dried overnight in an oven at 110 ºC. Next the samples were heated under N_2 flow (85 ml min^{-1}) at 5 ºC min^{-1} up to 450 ºC and held at this temperature for 2h. Finally the carbon sample were washed with water until pH 6 and dried overnight at 110ºC. This final sample was denoted as AOX6.5C.

2.2. Characterization of the carbon xerogels

In order to characterize the porous texture of the samples, carbon dioxide adsorption-desorption isotherms at 0 ºC and nitrogen adsorption-desorption isotherms at -196 ºC were performed on a TriStar

3000 Surface Area and Pore Size Analyzer by Micromeritics (Norcross, GA USA). The use of carbon dioxide adsorption at 0 °C for the textural characterisation of narrow micropores has already been established as an effective procedure [13] because carbon dioxide adsorption occurs in pores smaller than 0.7 nm, whereas nitrogen cannot enter in pores of such a small size.

The resulting combination of nitrogen and carbon dioxide adsorption isotherms data provide complementary and relevant information about the full micropore range. The Dubinin-Radushkevich (DR) method [14] was applied to the carbon dioxide and nitrogen adsorption isotherms in order to obtain the narrow micropore volume, $V_{DUB-CO2}$, and the wider micropore volume, V_{DUB-N2}, respectively. The BET surface area was also evaluated from the nitrogen adsorption isotherms. The accessible average micropore width, L_0 (nm), was calculated from the expression L_0 (nm) = V_{DUB-N2} ($cm^3\ g^{-1}$) 2000/S_{mic} ($m^2\ g^{-1}$) [15-16].

However, in the case of the meso-macroporous samples, nitrogen and carbon dioxide adsorption was not used to evaluate the real total pore volume. In this case a mercury porosimeter was employed to determine the pore volume (V_{Hg}) and the mean pore size. The measurements were performed using a Carlo Erba Porosimeter 2000 (Milan, Italy) (after outgassing at 10^{-3} Pa for 2 h. Hg measurements were limited to pores larger than 5.5 nm. The total pore volume, V_T, was considered to be equal to the sum of V_{Hg} and V_{DUB-N2}.

2.3. Preparation of electrodes for symmetric and asymmetric supercapacitors

Both the carbon xerogel and the manganese oxide electrodes were prepared by a casting method. The carbon xerogel based electrodes were prepared by spreading over a glass plate a slurry containing the carbon gel, graphite fibres, poly vinylidene fluoride (PVDF) binder and the N,N-dimethylacetamide (DMA) solvent.

The manganese oxide based electrode was prepared by applying a slurry composed of manganese oxide, carbon black, graphite fibres, PVDF binder and DMA. Both of these self-supporting electrodes were dried at 70°C and then thermally treated at 160 °C for 20 min to improve their mechanical strength. The PVDF (poly vinylidene fluoride) binder (Aldrich) was used as a solution of 2 wt% in DMA. The carbon black (Shawinigan Acetylene Black by Chevron Phillips) with a purity >99.9 % and a surface area of 75 $m^2\ g^{-1}$ was employed as conductive additive material in the MnO_2 electrodes. The graphite fibres were obtained by milling a carbon fabric Avcarb 1071 HCB furnished by Ballard Material Products, Inc. (MA, USA) in a high speed grinder.

The amount of carbon and manganese oxide loaded into the electrodes was similar to that used in real supercapacitors. Thus, 3.6 mg cm^{-2} of MnO_2 was loaded into the positive electrodes whereas 8 ± 2 mg cm^{-2} of carbon gel was loaded into the negative electrodes. The composition of the materials in the electrodes was: 70% MnO_2 – 10% acetylene black – 10% graphite fibres – 10% PVDF, for the positive electrode; 80% carbon gel– 10% graphite fibres – 10% PVDF for the negative electrode [17]. A ready-to-operate 4 cm^2 supercapacitor was prepared by coupling the two electrodes to a porous polymeric film separator (thickness: 50 µm x 2 separators) impregnated with 0.1 M Na_2SO_4.

2.4. Electrochemical characterisation of the symmetric and asymmetric supercapacitors

Electrochemical characterization of electrodes in SSC and ASC was carried out in a two-electrode cell connected to a potentiostat/galvanostat Autolab PGSTAT 30 (Eco Chemie BV, The Netherlands). Cyclic voltammetry (CV) tests and galvanostatic charge/discharge (GCD) measurements were performed at different voltage sweep rates and current densities, respectively by cycling in a voltage window from 0 to +1 V for the SSC and between 0 and +1.6 V for the ASC. The electrolyte used in both supercapacitors was 0.1M Na_2SO_4. The electrochemical impedance spectroscopy (EIS) measurements were performed using a Potentiostat PGSTAT 30 fitted with a FRA2 module at frequencies between 10 MHz and 1 mHz and at open circuit voltage (OCV).

3. RESULTS AND DISCUSSION

3.1. Surface and textural properties of the carbon xerogels

The adsorption-desorption isotherms of all the carbon xerogels studied are presented in Figure 1. They show capillary condensation and a hysteresis loop at high relative pressures (p/p°), indicating the presence of mesoporosity [8,18-19]. Furthermore, at low relative pressures the isotherms of the carbon gels CX5.8, CX6.3 and CX6.5 are very similar, which indicates that the differences between these samples are due mainly to the mesoporosity and not to the microporosity. The BET specific surface area, pore volume, and other micro-textural parameters of the carbons determined by nitrogen adsorption-desorption are summarized in Table 1.

Table 1. Textural properties of the carbon xerogels studied

Sample	pH	S_{BET} ($m^2\ g^{-1}$)	S_{mic} ($m^2\ g^{-1}$)	$V_{DUB\text{-}N2}$ ($cm^3\ g^{-1}$)	$V_{DUB\text{-}CO2}$ ($cm^3\ g^{-1}$)	L_0[a] (nm)	V_{Hg}[b] ($cm^3\ g^{-1}$)	V_T[c] ($cm^3\ g^{-1}$)
CX5.8	5.8	670	500	0.26	0.25	1.04	1.44	1.72
CX6.3	6.3	661	464	0.26	0.24	1.12	0.90	1.16
CX6.5	6.5	651	409	0.26	0.22	1.27	0.57	0.83
AOX6.5C	6.5	2360	706	0.76	0.34	2.1	-	1.56[d]

[a] Calculated from the expression L_0 (nm) = $V_{DUB\text{-}N2}$ ($cm^3\ g^{-1}$) 2000/S_{mic} ($m^2\ g^{-1}$)
[b] Pore volume determined by mercury porosimetry of pores between 5.5 and 100 nm
[c] Total pore volume (V_T) calculated by the sum of V_{Hg} and $V_{DUB\text{-}N2}$
[d] In this case the total pore volume is the volume at the saturation point (p/p^0) in the N_2 adsorption isotherm

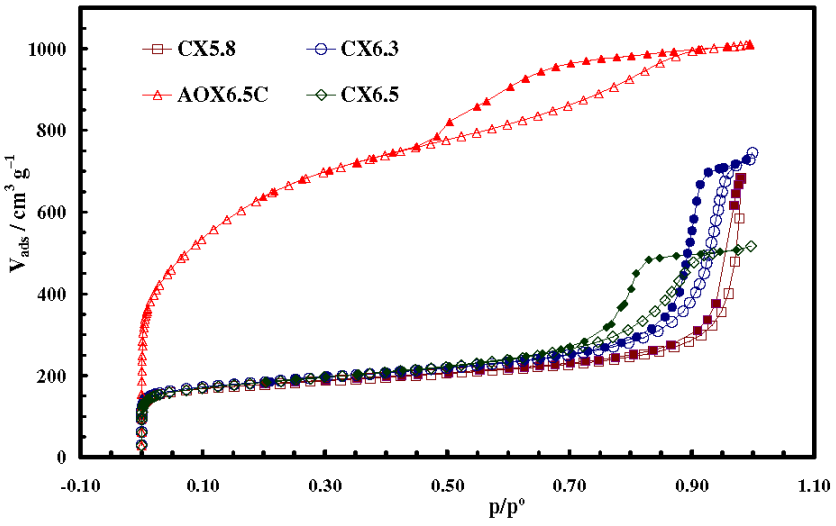

Figure 1. Nitrogen adsorption (open symbol)/desorption (filled symbol) isotherms for synthesized carbon xerogels

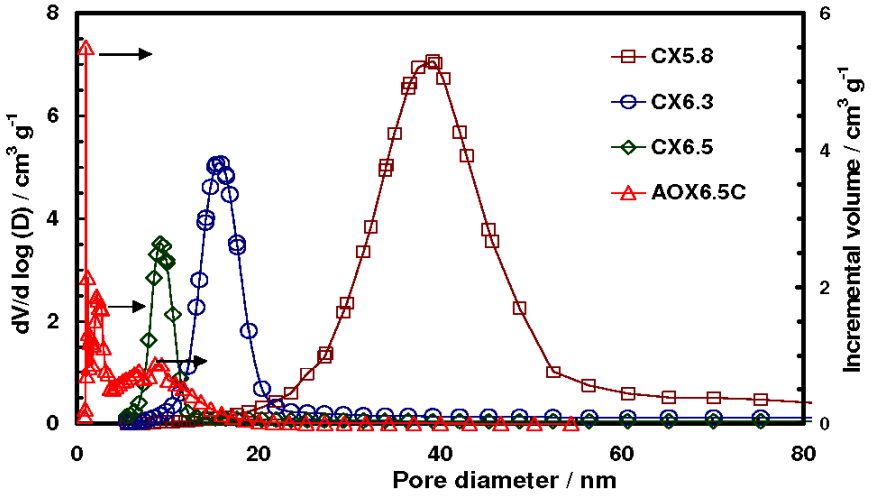

Figure 2. Pore size distributions of the different carbon xerogels.

It can be seen that the S_{BET}, S_{mic} and $V_{DUB-CO2}$ decrease slightly as the pH of the initial solution increases. The accessible average micropore width (L_0) also increases slightly with the pH. This indicates that the used synthesis conditions slightly modify the microporosity and the surface area of the carbon xerogels. The pH of the initial solution mainly affects the meso/macroporosity, as can be inferred from the high relative pressure zones of the N_2 adsorption isotherms and from the mercury porosimetry characterization.

Further differences in the porous texture of the carbon xerogels can be obtained from the mercury porosimetry results. Figure 2 shows the pore size distribution of the carbon xerogels as determined by mercury porosimetry. Although the synthesized xerogels have similar BET surface areas and micropore volumes, their meso/macropore size distribution is clearly correlated to the pH of the initial solutions. Therefore, as the pH increases, their meso/macropore textures start to differ. The average pore diameter decreases as the pH of the precursor solution increases (i.e., 38, 16 and 9 nm for CX5.8, CX6.3 and CX6.5, respectively) and the total pore volume, V_T, as estimated by mercury porosimetry and the DR method ($V_T = V_{Hg} + V_{DUB\text{-}N2}$) also follows the same decreasing trend (i.e., 1.72, 1.16 and 0.83 $cm^3\ g^{-1}$ for CX5.8, CX6.3 and CX6.5, respectively).

Also the chemical activated carbon xerogel AOX6.5C shows high N_2 adsorption capacity at low p/p^0 indicating that this carbon is highly microporous, although the hysteresis loop at high p/p^0 also indicates the presence of mesoporosity. The sample AOX6.5C has a multimodal pore size distribution, as can be seen from Figure 2. Values of mesopores size was found to be at 10 nm and at 2.3 nm indicating that after chemical activation in phosphoric acid the AOX6.5C has preserved the mesoporous features, but increased considerably its microporosity ($V_{mi}DR$ = 0.76 cm^3g^{-1}). The AOX6.5C sample has also a high V_T (1.56 cm^3g^{-1}) and S_{BET} of 2360 cm^2g^{-1} (see Table 1).

3.2. Cyclic voltammetry studies of carbon xerogels in symmetric supercapacitors

Figure 3 shows the curves of specific capacitance (C_s) as a function of the cell voltage for the carbon xerogel based supercapacitors.

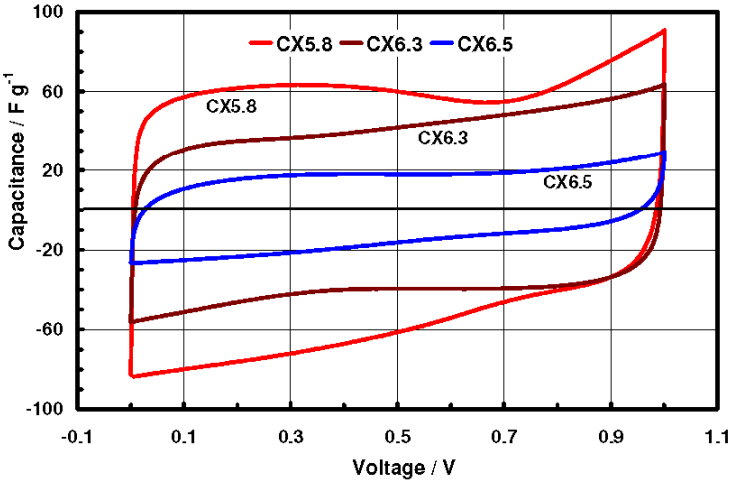

Figure 3. Capacitance curves versus potential for carbon xerogel-based supercapacitors. Voltage sweep rate:10 mVs^{-1}.

These curves show that the CX5.8 based supercapacitor exhibits a higher specific capacitance than the other two carbons. However, the supercapacitors loaded with CX6.3 and CX6.5 produce

voltammograms with more rectangular shapes. In the case of xerogel CX5.8 there is a deviation from pure capacitive behavior with the appearance of a broad peak of uncertain origin in the 0 to 0.4 V range. The presence of this broad peak could be due to parallel redox reactions providing additional pseoudocapacitance to the double layer capacitance, since it is known that surface functional groups present on the surface of carbons can supply strong pseudocapacitance by means of faradaic processes [20]. Whereas the pseudocapacitance derived from oxygenated species is important in acid (H_2SO_4) and basic (KOH) electrolytes, it is absent or very low in neutral aqueous electrolyte [21-22]. It is also well known that the surface chemistry of non graphitic carbons, such as carbon xerogels, can have a strong influence on electronic resistance and consequently on electrochemical performance. The capacitance results obtained for these capacitors show that they bear an evident correlation to the pore size of the xerogels, which in turn depends on the pH of the initial synthesis solution. Higher specific capacitance values were obtained from carbon xerogel CX5.8 (71 F g^{-1}), compared to those of CX6.3 (50 F g^{-1}) and CX6.5 (about 30 F g^{-1}). These values were unexpectedly low in consideration that the surface-texture properties indicated practically the same specific surface area for all the samples (650-670 m^2 g^{-1}). These low values of capacitance are clearly due to the relatively low specific surface area of the carbon samples employed. However, the aim of this work was not to find a breakthrough carbon material but to evaluate the influence of the pore size distribution (PSD) of carbons of similar specific surface area (S_{BET}).

3.3. Electrochemical impedance spectroscopy (EIS) study of carbon xerogels

EIS is an important analytical technique that can be used to establish the characteristic frequency response of supercapacitors from the speed at which the ionic and electronic charges are moving inside the pores of carbon electrodes under one single-sine or multi-sine signal of alternate current (AC).

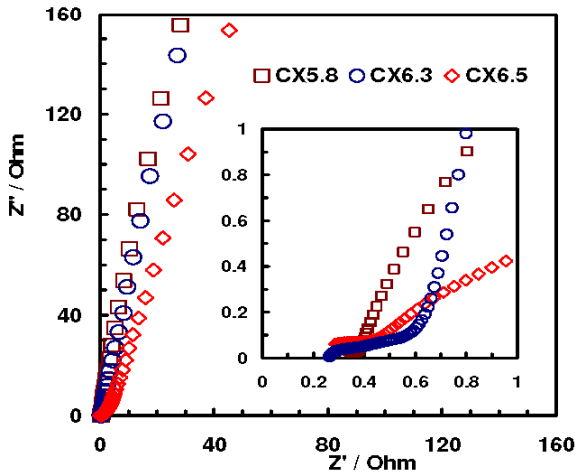

Figure 4. Nyquist plot of the different carbon xerogels. The inset shows the high-frequency region of impedance.

The Nyquist impedance plots corresponding to the different carbon xerogel-based supercapacitors are shown in Figure 4. At low frequencies (mHz range, upper region of large graph), the points depict shapes near to those of ideal capacitors. The inset in the figure shows the impedance behaviour of all the supercapacitors at high frequencies. The impedance plots in the inset have slight loops of different amplitude at high frequency that could be due to the charge transfer process and/or to the different contact resistances [1]. At high frequencies, the resistance characteristics of the supercapacitors are expressed as the so-called electric series resistance (ESR), a term which includes electrolyte resistance, collector/electrode contact resistance and the resistance of the electrode/electrolyte interface. The capacitors loaded with carbon xerogel CX5.8 show lower impedance compared to those loaded with CX6.3 and CX6.5, in agreement with the capacitance results presented in Figure 3.

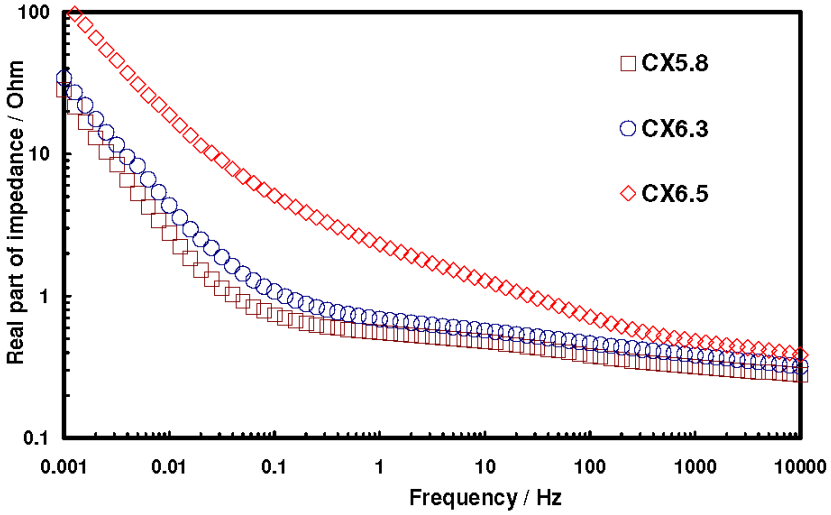

Figure 5. Real part of impedance as a function of frequency for the different carbon xerogel-based supercapacitors.

The differences in impedance behavior are further illustrated in Figure 5, where the real part of impedance, Z', is plotted as a function of frequency. In the high frequency region, kHz, the impedance comes from the resistance of the ionic electrolyte, to which must be added that of the two electrodes and the interface resistance between the electrodes and current collectors.

However, as the frequency decreases other types of resistance appear which cause an increase in the overall supercapacitor resistance. These additional resistances are caused by the penetration of electric signals and the movement of ion species inside carbon pores of different diameter [23-24]. The results in Figure 5 also show that the resistance of sample CX6.5 is very different to that of CX5.8 and CX6.3. The differences between CX5.8 and CX6.3 are also significant. If the resistance behaviour of the xerogels is compared with the potentiometric curves of Figure 3 and the pore-size distribution of

Figure 2 , it can be seen that the highest capacitance is correlated with the lowest resistance and the largest mesopore diameter. The relationship between the capacitance and frequency for the different carbon xerogel electrodes as obtained from the impedance analysis is shown in Figure 6. Table 2 summarizes the characteristics of the electrodes, such as composition, capacitance and ionic resistance. It is surprising to observe such huge differences for carbon xerogel-based supercapacitors even though they were synthesized at different pHs. This is a further confirmation that even if the carbons have a similar BET surface area and microporosity, it is the meso/macropore size distribution that determines the capacitive performance.

Table 2. List of investigated carbon xerogels electrodes with compositions, capacitances and ionic resistances.

Electrode	Xerogel (%)	Carbon loading mg cm^{-2}	Graphite fibres (%)	PVDF (%)	Specific capacitance CV F g^{-1} 10 mV s^{-1}	Specific capacitance, F g^{-1} at 1 mHz	Ionic Resistance Ohm cm^2
CX5.8	80	7.15	10	10	60	71	1.00
CX6.3	80	8.94	10	10	41	50	1.05
CX6.5	80	6.55	10	10	16	29	1.16

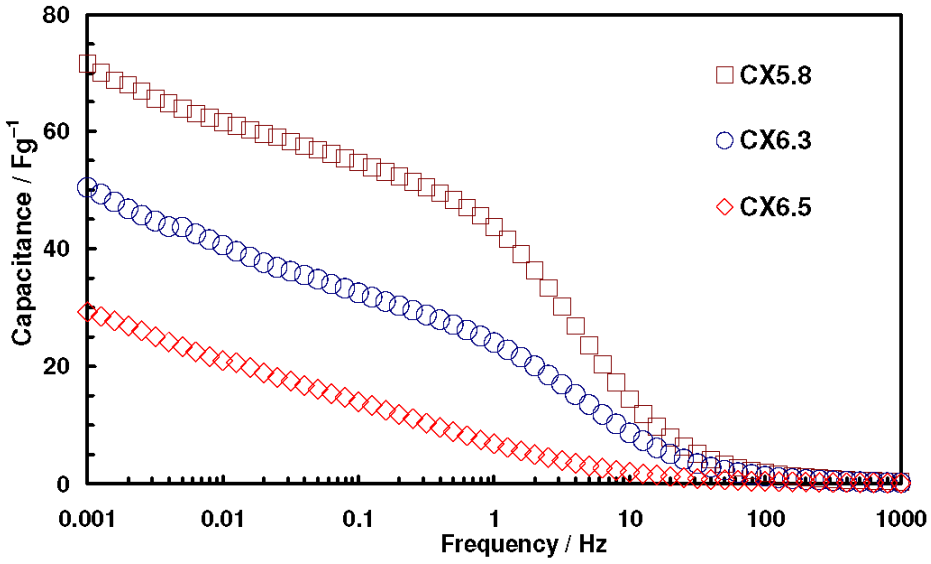

Figure 6. Specific capacitance versus frequency for carbon xerogel based supercapacitors.

Moreover, the impedance analysis of the carbon xerogel-based supercapacitors showed that this analytical technique (EIS) is a quick method for obtaining a great deal of information not only about the electrochemical aspects but also about the textural characteristics of carbons. EIS has already been proposed as a good technique for determining the pore size distributions of carbon materials [25-26].

3.4. Study of chemical activated carbon xerogels in symmetric and asymmetric supercapacitors

Figure 7 shows characteristic voltammograms for SSC and ASC at sweep rates of 5 and 10 mV s^{-1}. The compositions of the electrodes, the capacitance values per electrode and the resistances of the SSC and ASC are presented in Table 3.

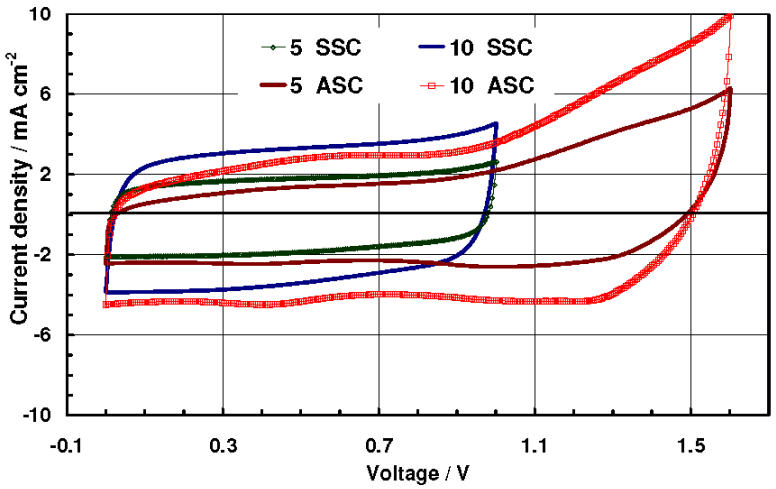

Figure 7. Comparison of the voltammograms of carbon xerogels–based supercapacitors in symmetric (SSC) and asymmetric (ASC) configurations. Voltage sweep rates: 5 and 10 mVs^{-1}. Cell voltage window from 0 to 1 V for SSC and from 0 to 1.6 V for ASC.

The voltammetric behaviour of the symmetric capacitor, AOX6.5C/AOX6.5C, displays almost perfect rectangular shapes, whereas in the voltammograms of ASC, AOX6.5C/MnO_2, there is a deviation from this box-like shape due to the pseudocapacitive behavior of the positive electrode, which provides a higher current at high cell voltages. This behaviour of the positive electrode causes the negative electrode to move towards a more negative potential, where an irreversible reduction process is likely to occur. To prevent the high negative polarization and irreversible faradaic processes an appropriate balance between the positive and negative electrode must be obtained. This is because excessive polarization would lead to the evolution and adsorption of hydrogen in the negative electrode as well as to the evolution of oxygen and excessive oxidation of the manganese oxide toward undesired oxide species in the positive electrode [4-5, 27-29]. A comparison between the two different configurations shows that, at the same sweep rate, ASC is delivering a higher capacitance than the SSC

because of the pseudocapacitance originating from the redox process in the positive electrode. Additional advantages provided by the ASC are a higher energy density, since the increase in energy is proportional to the square of the voltage ($E=1/2\ CV^2$). Yet another advantage is the higher volumetric power (kW cm^{-3}) and energy density (Wh cm^{-3}) resulting from the reduced thickness of the positive electrodes, i.e., approximately 140 µm vs 280 µm for the negative electrode. The difference in thickness is due to the higher density and lower load of MnO_2 material (3.6 mg cm^{-2}) compared to that of the carbon negative electrode (≈ 9.6 mg cm^{-2}).

Table 3. Electrochemical characteristics of the carbon xerogel electrodes in symmetric and asymmetric configuration of supercapacitors

Electrodes	Carbon xerogel (%)	Carbon (MnO_2) loading (mg m^{-2})	Thickness Electrode µm	Graphite Fibres (%)	PVDF (%)	Average capacitance by CV[a] (F g^{-1})	Average capacitance by G-CD[a] (F g^{-1})	Ionic Resistance (Ohm cm^2)
AOX6.5C	80	7.7 (-)	250	10	10	86	90	2.40
AOX6.5C		8.5 (+)	270					
AOX6.5C	80	9.56 (-)	280	10	10	162	118 213	0.28
MnO2		3.62 (+)	140				290	

[a]The capacitance is that for one electrode and is obtained as weighted average between the weights of the negative and positive electrode active material.

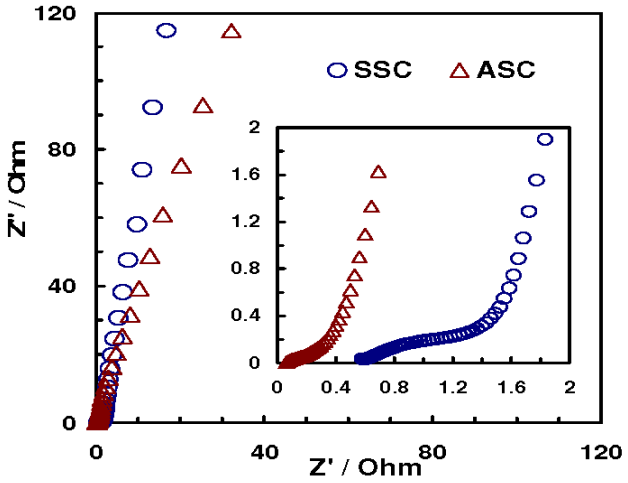

Figure 8. Nyquist plots for the SSC and the ASC in two electrode systems. The inset shows the high frequency region of impedance.

Figure 8 shows the Nyquist plots for the SSC and ASC with an open circuit voltage (OCV). At high frequencies the two plots show small semicircles of different amplitude (inset) and an almost vertical line at lower frequencies (large graph), indicating capacitive behaviour even though the capacitance of the positive electrode is of a faradaic type. Although the impedance plots do not show whether the capacitance in this ASC is capacitive or faradaic, they show that the impedance of ASC is lower than that of SSC, due to the thinner positive electrode in the ASC.

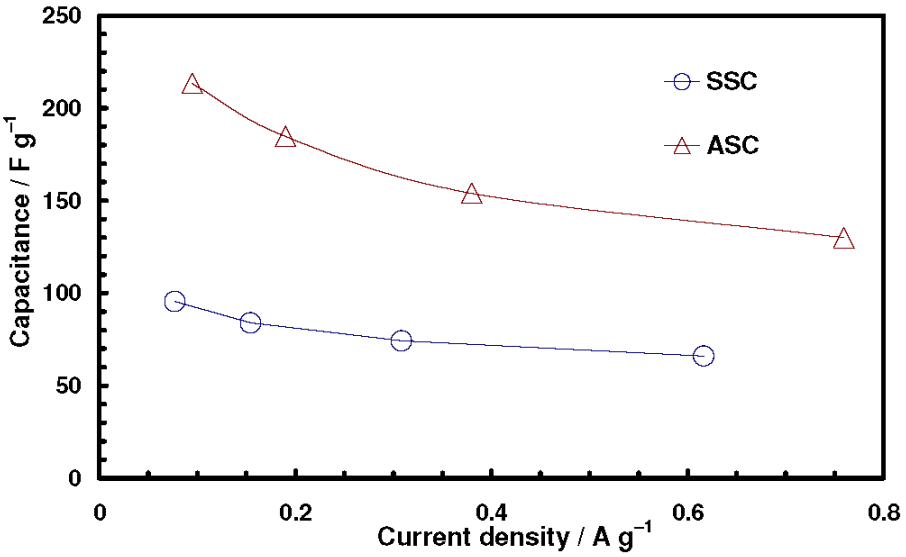

Figure 9. Capacitance behaviour as a function of current density (from G-CD) for the symmetric (SSC) and asymmetric (ASC) supercapacitors.

Figure 9 shows capacitive behaviour as a function of current density in the current range from 0.1 to approximately 0.8 A g^{-1}. These capacitance values were obtained from galvanostatic charge discharge measurements (G-CD) and by calculating the average of the weights of the negative and the positive electrodes (see Table 3), which is considered to be the best way of assessing the specific capacitance (F g^{-1}) of the electrodes of ASCs [30].

The capacitance values (Figure 9) of the ASC are higher than those of the SSC over the entire range of current densities studied. The capacitances of both supercapacitors decrease as the current density increases from 0.1 to 0.8 A g^{-1}. This decrease is about 40% for the ASC, i.e. from 213 to 130 F g^{-1}, whereas that for the SSC is 31%, i.e. from 96 to 66 F g^{-1} for currents varying from 0.08 to 0.6 A g^{-1}. The ASC exhibits a specific energy as high as 15.1 Wh g^{-1}, whereas that of SSC is only 3.2 Wh g^{-1} because of its low window cell voltage (1 V vs 1.6 V). Moreover, it is clear that because the capacitance of the ASC is derived from pseudocapacitance (MnO_2 based positive electrode) it is more dependent on the current density than the SSC capacitor, which has two identical capacitive-type electrodes, so that the charge-discharge processes in the SSC should occur at higher rates.

Table 4. Comparison of carbon/MnO_2 asymmetric supercapacitors from literature data.

	Negative electrode	Positive electrode	Electrolyte	Max cell voltage, (V)	X = mass$^-$/ mass$^+$ (mg cm^{-2})	Specific capacitance (F g^{-1})	Cycling tests (cycles)	Ionic Resistance Ohm cm^2	Ref.
1	Carbon Xerogel 2500 m^2g^{-1}	MnO_2	0.1 M Na_2SO_4	1.6	2.65	213 (+300; -118)	n.d.	0.28	This work
3	AC Maxsorb 2500 m^2g^{-1}	MnO_2	2 M KNO_3	2	2.1	140	1 000	0.54	5
3	AC 2800 m^2g^{-1}	MnO_2	0.1 M K_2SO_4	2.2	n.d	124 (+150; -130)	5 000	n.d.	32
4	AC kuraray 1600 m^2g^{-1}	MnO_2	0.1 M $Ca(NO_3)_2$	2.0	3.17	124 (+314; -80)	1 000	9.0	33
5	AC PICACTIF 2300 m^2g^{-1}	MnO_2	0.1 M K_2SO_4	2	1.65	80 (+72; -95)	195 000	1.30	34
6	AC Ningde Xinseng Chem 2800 m^2g^{-1}	MnO_2	0.5 M K_2SO_4	2	1	153	10 000	3.20	35
7	AC	MnO_2	1 M LiOH	1.0	1	248	< 1500	n.d	36
8	AC Ningde Xinseng Chem 2800 m^2g^{-1}	MnO_2	0.5 M K_2SO_4	1.8	1	215	23 000	n.d.	37
9	AC 1300 m^2g^{-1}	MnO_2	1 M Li_2SO_4	2	1	212	n.d	~ 10-15	38

It is well known that redox phenomena associated with manganese oxide-based positive electrodes play an important role in the final capacitance of an ASC. Moreover, any variation in the pseudocapacitance of the positive electrode influences the capacitance behaviour of the carbon-based negative electrode [4-5, 28, 31]. Therefore, to explain the capacitance behaviour of these electrodes the influence of more parameters, such as the morphology and structure of the manganese oxide, whether it is amorphous or crystalline, the transport of cations (Na^+, H^+) to the pores and electron conduction of the bulk together with the redox reaction process must be taken into consideration [17, 32]. Water of MnO_2 structure is also thought to play an important role in ionic transport, while electronic conductivity is likely to be influenced by the bulk material properties of the electrode.

The results of the present work on carbon/MnO_2 supercapacitors are compared with those of the literature and presented in Table 4 [5, 32-38]. This table includes the composition of the electrodes, the types of electrolyte and the electrochemical characteristics of the ASC. From an analysis of the data, it is evident that the negative electrode is based on activated carbon materials and that the most

frequently used electrolyte was K_2SO_4 or other neutral salts with the exception of those reported by Yuan et al. [36]. They report of using 1M LiOH as electrolyte. Although they claim a high capacitance (~ 250 F g^{-1}) they had to use a cell voltage lower than 1 V because of the limited stability of manganese oxide in a basic aqueous medium [39-40]. Moreover, these authors observed a remarkable loss of capacitance (15-20%) during a cycling test of 1500 cycles. From an analysis of the literature it is evident that our work is the only one to report a good capacitance performance for carbon xerogel-based ASC, whereas the other works report results for supercapacitors based on activated carbon. In fact, the value of 213 F g^{-1} reported in this paper is relatively high compared to those reported by other authors. Another evident advantage of our ASC is its low resistivity, 0.28 Ω cm^2, which is considerably lower than those reported by Qu et al. [37] and Xue et al. [38] even though they reported similar high capacitances (i.e. 215 and 212 F g^{-1}). However, it is not clear from their report how it is possible to obtain these high values of capacitance using ASC of high resistance and with a negative and positive electrode weight ratio of 1:1. In our work we used a weight ratio of 2.65, which is similar (from 1.6 to 3.17) to those reported by other authors [5, 32-34]. Moreover, the manganese oxide-based positive electrode can be expected to provide a higher capacitance than the carbon-based negative electrode because of the high contribution of pseudocapacitance in a neutral aqueous electrolyte.

Analysis of the results of the literature (Table 4) also reveals discrepancies concerning the exact weight ratio between the negative and the positive electrodes. Moreover, the data of Table 4 do not allow evidencing a clear window of cell voltage used for this type of ASC because of the large differences. These points, however, are as important as the resistance of the electrolyte, the resistivity of the electrodes and the cycling stability of the ASC for improving capacitance performance. In short further studies are necessary to find out how the different characteristics of electrodes and electrolytes influence the electrochemical performance of supercapacitor devices. In this work, we have demonstrated that carbon xerogel (AOX6.5C) of a high BET surface area (~ 2300 m^2 g^{-1}) can be used to prepare negative electrodes (load ~ 8 mg cm^2) coupled with manganese oxide in positive electrodes (load of 3.6 mg cm^2) to design an ASC with a low resistivity, high specific capacitance and energy density of 15.1 W h kg^{-1}. This latter is calculated considering the sum of the weight of active material in both electrodes.

Although no conclusive findings were made with respect to the importance of the faradaic and capacitive contributions, a high capacitance value of 213 F g^{-1} was achieved using an ASC with carbon xerogel and manganese oxide. This result indicates that these materials are very attractive for new potential applications in mild aqueous electrolyte-based asymmetric supercapacitors.

4. CONCLUSIONS

Different self-supporting electrodes based on carbon xerogels were prepared and their performance was studied in symmetric supercapacitors in an aqueous electrolyte (0.1 M Na_2SO_4).

The study revealed the important role that meso and macropores play in electrode resistance. It was also found that even when the samples had similar surface areas the capacitances of their supercapacitors differed considerably (from 30 to 70 F g^{-1}).

When a carbon xerogel was chemically activated with H_3PO_4 the surface area increased up to 2360 m^2 g^{-1}. An asymmetric supercapacitor with chemically activated carbon xerogel as negative electrode and manganese oxide as positive electrode made it possible to increase the working voltage from 1 to 1.6 V. The main advantages of using an asymmetric rather than a symmetric supercapacitor are that it provides a higher specific capacitance (213 F g^{-1} vs 90 F g^{-1}); and a higher specific energy (15.1 vs 3.2 Wh g^{-1}).

The capacitance performance of an ASC can be further improved by increasing the capacitance of the carbon material-based negative electrode because of excellent behaviour of MnO_2-based positive electrode, which may achieve a capacitance as high as 300 F g^{-1}. Comparison of the results of this study with those of the literature showed that additional optimizations and improvements are necessary before MnO_2/carbon aqueous ASCs can be considered as a serious alternative to carbon/carbon non-aqueous commercial SSCs. Future optimization will need to consider the materials and the weight ratio for the electrodes as well as the resistivity, window cell voltage and cycling stability of the supercapacitors.

ACKNOWLEDGEMENTS

The authors would like to thank the CNR (Italy) and CSIC (Spain) which have partially financed this work through a bilateral agreement (2009-2010) between the two Institutions. The support from the Government of Principado de Asturias PCTI (Ref. IB09-00201) and Ministerio de Ciencia e Innovación (Ref. MAT2008-00217/MAT) is also gratefully acknowledged. E.G. Calvo also acknowledges a pre-doctoral research grant from FICYT. The authors of CNR of Messina (Italy) acknowledge the Ministero dello Sviluppo Econonomico for the support by the "Accordo di programma CNR – MSE", Project "Sistemi elettrochimici per l'accumulo dell'energia", (Ref. Decreto MAP del 23 Marzo 2006).

References

1. R. Kotz, M. Carlen, *Electrochimica Acta*, 45 (2000) 2483
2. P. Simon, Y. Gogotsi, *Nature Mater.*, 7 (2008) 845
3. E. Frackowiak, F. Beguin, *Carbon*, 39 (2001) 937
4. M. Toupin, T. Brousse, D. Belanger, *Chem. Mater.*, 16 (2004) 3184
5. V. Khomenko, E. Raymundo-Pinero, F. Beguin, *J. Power Sources,* 153 (2006) 183
6. K.Y. Kang, S.J. Hong, B.I. Lee, J.S. Lee, *Electrochem. Commun.*, 10 (2008) 1105
7. L. Zubizarreta, A. Arenillas, J.P. Pirard, J.J. Pis, N. Job, *Micropor. Mesopor. Mater.,* 115 (2008) 480
8. F.L. Conceicao, P.J.M. Carrott, M.M.L. Ribeiro Carrott, *Carbon,* 47 (2009) 1874
9. S.T. Mayer, R.W. Pekala, J.L. Kaschmitter, *J. Electrochem. Soc.,* 140 (1993) 446
10. H. Probstle, C. Schmitt, J. Fricke, *J. Power Sources,* 105 (2002) 189
11. J. Wang, X. Yang, D. Wu, R. Fu, M.S. Dresselhaus, G. Dresselhaus, *J. Power Sources,* 185 (2008) 589
12. E.G. Calvo, C.O. Ania, L. Zubizarreta, J.A. Menendez, A. Arenillas, *Energy Fuels*, 24 (2010) 3334
13. J. Jagiello, M. Thommes, *Carbon,* 42 (2004) 1227.
14. M.M. Dubinin In: J.F. Danielli, M.D. Rosenberg, D. Cadenhead (Eds.), *Progress in Surface and Membrane Science*, vol. 9, Academic Press, New York (1975), pp. 1–70.

15. F. Stoeckli, T.A. Centeno, *Carbon,* 43 (2005) 1184
16. T.A. Centeno, F. Stoeckli, *Electrochimica Acta,* 52 (2006) 560
17. P. Staiti, F. Lufrano, *J. Power Sources,* 187 (2009) 284
18. C. Moreno-Castilla, F.J. Maldonado-Hodar, *Carbon,* 43 (2005) 455
19. F. Lufrano, P. Staiti, *Int. J. Electrochem. Sci,* 50 (2010) 903
20. C.A. Thorogood, G.G. Wildgoose, A. Crossley, R. M. J. Jacobs, J.H. Jones, R.G. Compton, *Chem. Mater.,* 19 (2007) 4964
21. H. A. Andreas, B. E. Conway, *Electrochimica Acta,* 51 (2006) 6510
22. Q. T. Qu, B. Wang, L. C. Yang, Y. Shi, S. Tian, Y. P. Wu, *Electrochem. Commun.,* 10 (2008) 1652
23. L. Zhang; H. Liu, M. Wang, L. Chen, *Carbon,* 45 (2007) 1439
24. F. Lufrano, P. Staiti, M. Minutoli, *J. Electrochem. Soc.,* 151 (2004) A64
25. H.K. Song, J.H. Sung, Y.H. Jung, K.H. Lee, L.H. Dao, M.H. Kim, H.N. Kim, *J. Electrochem. Soc.,* 151 (2004) E102
26. H.K. Song, J.H. Jang, J.J. Kim, S.M. Oh, *Electrochem. Commun.,* 8 (2006) 1191
27. S. Devaraj, N. Munichandraiah, *J. Electrochem. Soc.,* 154 (2007) A80
28. V. Khomenko, E. Raymundo-Pinero, E. Frackowiak, F. Beguin, *Appl. Phys. A-Mater.,* 82 (2006) 567
29. S.H. Kim, Y.I. Kim, J.H. Park, J.M. Ko, *Int. J. Electrochem. Sci*., 4 (2009) 1489
30. Q. L. Fang, D.A. Evans, S.L. Roberson, J.P. Zheng, *J. Electrochem. Soc.,* 148 (2001) A833
31. D. Belanger, T. Brousse, J.W. Long, *Electrochem. Soc. Interface,* 17 (2008) 49
32. T. Cottineau, M. Toupin, T. Delahaye, T. Brousse, D. Belanger, *Appl. Phys. A-Mater.,* 82 (2006) 599
33. C. Xu, H. Du, B. Li, F. Kang, Y. Zeng, *J. Electrochem. Soc.,* 156 (2009) A435
34. T. Brousse, P. L. Taberna, O. Crosnier, R. Dugas, P. Guillemet, Y. Scudeller, Y. Zhou, F. Favier, D. Belanger, P. Simon, *J. Power Sources,* 173 (2007) 633
35. Q. Qu, L. Li, S. Tian, W. Guo, Y. Wu, R. Holze, *J. Power Sources,* 195 (2010) 2789
36. A.Yuan, Q. Zhang, *Electrochem. Commun.,* 8 (2006) 1173
37. Q. Qu, P. Zhang, B. Wang, Y. Chen, S. Tian, Y. Wu, R. Holze, *J. Phys. Chem. C,* 113 (2009) 14020
38. Y. Xue, Y. Chen, M.-L. Zhang, Y.-D. Yan, *Mater. Lett.,* 62 (2008) 3884
39. M. Toupin, T. Brousse, D. Belanger, *Chem. Mater.,* 14 (2002) 3946
40. Q. Zhou, X. Li, Y.-G. Li, B.-Z. Tian, D.-Y. Zhao, Z.-Y. Jiang, *Chinese J. Chem.,* 24 (2006) 835

5.1.2. Comportamiento electroquímico de supercondensadores constituidos por composites xerogel/nanotubos de carbono

Como se ha explicado en la Introducción de la presente memoria, para desarrollar supercondensadores con buenas prestaciones, es necesario disponer de materiales de electrodo altamente y adecuadamente porosos y que presenten buenas propiedades conductoras. Sin embargo, estas dos propiedades (porosidad y conductividad eléctrica) suelen contraponerse por lo que es necesario llegar a una solución de compromiso.

La resistencia intrínseca de un supercondensador viene determinada por tres componentes: resistencia intrínseca del material de electrodo, resistencia iónica del electrolito y resistencia debida al contacto entre los electrodos y los colectores de corriente, cada una de las cuales debe ser minimizada con el propósito de obtener sistemas electroquímicos lo menos resistivos posible.

Existen diferentes alternativas que permiten mejorar la conductividad eléctrica de los electrodos para supercondensadores. La mayoría de ellas se basa en el dopaje de los electrodos con materiales de elevada conductividad eléctrica, como pueden ser nanotubos de carbono o polímeros conductores, siendo el polipirrol, polianilina y politiofeno los polímeros más activamente investigados [BORDJIBA, 2008; LI, 2012; PENG, 2008; TABERNA, 2006; ZHANG, 2011].

Los supercondensadores basados en composites formados por nanotubos de carbono y otro tipo de material carbonoso (un carbón activado, por ejemplo) han sido extensamente estudiados como consecuencia de las propiedades únicas asociadas a los nanotubos de carbono: excelente conductividad eléctrica y elevada estabilidad mecánica y química, entre otras [BORDJIBA, 2008; PENG, 2008; TABERNA, 2006].

Los nanotubos de carbono se clasifican en dos tipos atendiendo al número de capas que poseen: (i) nanotubos de carbono de capa única (Single Walled Carbon Nanotubes, SWNT) que se pueden describir como una lámina de grafeno enrollada formando un cilindro de diámetro nanométrico y, (ii) nanotubos de carbono de capa múltiple (Multi Walled Carbon Nanotubes, MWNT), que son aquellos formadas por capas concéntricas cilíndricas, las cuales están separadas aproximadamente a una distancia similar a la distancia interplanar del grafito (véase Figura 5.1). Los nanotubos utilizados como sustancias dopantes para desarrollar el trabajo recogido en la *Publicación VI* fueron nanotubos de carbono de capa múltiple.

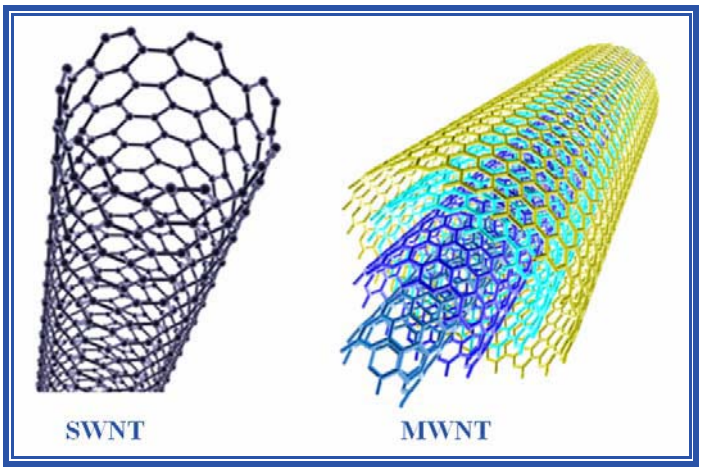

Figura 5.1. Tipos de nanotubos de carbono según el número de capas.

El trabajo que ha dado lugar a la *Publicación VI* consistió en el dopaje de un xerogel de carbono altamente poroso con diferentes cantidades de nanotubos de carbono de capa múltiple (0, 9 y 18 %, en masa) con el objetivo de evaluar su influencia sobre las propiedades eléctricas de los electrodos y, consecuentemente, sobre su capacidad de almacenamiento de energía. El xerogel de carbono utilizado como material activo para la fabricación de los electrodos fue sintetizado en el laboratorio a partir de una disolución resorcinol-formaldehído de pH 6.5, la cuál fue sometida a un tratamiento térmico en una estufa. Además, un proceso de activación con H_3PO_4 utilizado como agente activante fue llevado a cabo para incrementar la microporosidad del xerogel sintetizado (S_{BET} ~ 2300 $m^2\ g^{-1}$). Este mismo protocolo de síntesis fue utilizado para la obtención del xerogel de carbono empleado como ánodo en los supercondensadores asimétricos mencionados en el Apartado 5.1.1. Los nanotubos de carbono utilizados en el proceso de dopaje son materiales comerciales (Aldrich®, Ref. 636525), pero sometidos a un proceso de purificación y activación para disminuir su nivel de impurezas e incrementar la porosidad (etapas desarrolladas por el grupo "*Conversión y Almacenamiento de Energía*" -INFITA-, con el que se ha colaborado en este trabajo).

El estudio de supercondensadores constituidos por electrodos basados en composites de xerogel/nanotubos de carbono en distinta proporción, ha dado lugar a las siguientes conclusiones:

❖ La adición de nanotubos de carbono ha permitido mejorar considerablemente la conductividad eléctrica de los electrodos, afirmación corroborada tanto por los resultados derivados de los tests de voltametría cíclica como de los valores de resistividad, obtenidos a partir del método de Van der Pauw (conocido también como método de 4 puntas). Los voltamogramas recogidos en la publicación muestran una evolución hacia una forma ligeramente más rectangular a medida que aumenta la cantidad de nanotubos de carbono añadida, es decir, se obtienen condensadores electroquímicos menos resistivos.

❖ El dopaje del xerogel resorcinol-formaldehído con nanotubos de carbono ha permitido incrementar la capacidad de almacenamiento de energía (por ejemplo, desde 176 hasta ~ 200 F g^{-1} para una intensidad de corriente de 7.4 mA g^{-1}). Sin embargo, el aumento del contenido de MWNT no lleva asociado un mayor valor de capacidad específica (197 F g^{-1} cuando el contenido en nanotubos de carbono fue igual al 9 % frente a 201 F g^{-1} para el electrodo preparado con un 18 % de MWNT).

Otro punto destacable del estudio recogido en la *Publicación VI* está relacionado con los resultados derivados de las medidas de Espectroscopía de Impedancia Electroquímica (Electrochemical Impedance Spectroscopy, EIS), los cuales fueron utilizados para desarrollar un modelo físico-químico que permite identificar los parámetros estructurales y cinéticos de las celdas electroquímicas evaluadas. El modelo empleado se basa en las siguientes suposiciones: (i) los electrodos son estructuras porosas isotrópicas cuyos huecos están rellenados con el electrolito y (ii) el almacenamiento de energía derivado de reacciones redox es despreciable, es decir, la capacidad del sistema se debe exclusivamente a la formación de la doble capa eléctrica en la interfase electrodo/electrolito.

La aplicación de este modelo ha permitido conocer parámetros tan trascendentes como el área del electrodo que interviene activamente en el proceso de almacenamiento de carga o la conductividad efectiva del electrolito, parámetros que están muy relacionados entre sí. El área superficial S_{BET} obtenida mediante las isotermas de adsorción-desorción de N_2 contiene información acerca de la porosidad global del material analizado. Sin embargo, no toda esta porosidad interviene en el proceso de almacenamiento de carga, hecho que se ha intentado demostrar mediante la aplicación del modelo físico-químico. Los resultados indican que la fracción de material que participa activamente en la formación de la doble capa eléctrica es de 328 m^2 g^{-1} para un electrodo fabricado con el xerogel de carbono poroso, mientras que la fracción electroquímicamente accesible llega hasta 360 m^2 g^{-1} cuando se añadieron los nanotubos de carbono en diferente proporción. En principio, este resultado podría sorprender puesto que la adición de mayor cantidad de nanotubos de carbono lleva asociado un bloqueo parcial de la porosidad del electrodo, ya que el xerogel de carbono posee un S_{BET} de aproximadamente 2300 m^2 g^{-1} mientras que este valor no alcanza los 150 m^2 g^{-1} para los MWNT.

El hecho de que la fracción del material de electrodo que participa activamente en el proceso electroquímico no sólo no disminuye, sino que aumenta con la adición de nanotubos de carbono se puede justificar a partir de los valores de conductividad efectiva de la fase líquida, es decir, del electrolito. Al añadir cierta cantidad de nanotubos de carbono, se produce un incremento en la conductividad efectiva del electrolito, es decir, los iones de electrolito pueden acceder con más facilidad a los poros del electrodo, lo que se traduce en un ligero aumento en la fracción de porosidad del electrodo considerada electroquímicamente activa.

Publicación VI

ELECTROCHEMICAL BEHAVIOR AND CAPACITANCE PROPERTIES OF CARBON XEROGEL/MULTIWALLED CARBON NANOTUBES COMPOSITES

Journal of Solid State Electrochemistry

16 (1067-1076)

Año: 2012

J Solid State Electrochem (2012) 16:1067–1076
DOI 10.1007/s10008-011-1487-4

ORIGINAL PAPER

Electrochemical behavior and capacitance properties of carbon xerogel/multiwalled carbon nanotubes composites

Pablo Sebastián Fernández · Elida Beatriz Castro · Silvia Graciela Real · Arnaldo Visintin · Ana Arenillas · Esther G. Calvo · Emilio J. Juárez-Pérez · Angel J. Menéndez · Maria Elisa Martins

Received: 27 May 2011 / Revised: 15 June 2011 / Accepted: 20 June 2011 / Published online: 12 July 2011

Abstract The electrochemical behavior of carbon xerogel/multiwalled carbon nanotubes composite in a 6 M KOH solution has been investigated. Three different mixtures of teflonized carbons with varying nanotube content were prepared. The electrodes containing multiwalled carbon nanotubes were found to provide enhanced capacities compared with those prepared with only carbon xerogel. Cyclic voltammetry and charge–discharge experiments reveal the presence of a strong resistive component, which decreases as the amount of nanotubes increases. Electrochemical impedance spectroscopy results analyzed in terms of an adequate physicochemical model of the porous electrode, show that an increasing amount of nanotubes enhances both the effective solid-phase conductivity and the effective liquid-phase conductivity, linked to the porosity of the electrodes.

Keywords Electrochemical capacitors · Carbon xerogels · Carbon nanotubes · Electrochemical impedance spectroscopy

Pablo Sebastián Fernández, Elida Beatriz Castro, Silvia Graciela Real, Arnaldo Visintin, and Maria Elisa Martins are ISE members.

P. S. Fernández (✉) · E. B. Castro · S. G. Real · A. Visintin · M. E. Martins (✉)
Instituto de Investigaciones Fisicoquímicas Teóricas y Aplicadas (INIFTA) Facultad de Ciencias Exactas, UNLP,
CCT La Plata-CONICET,
1900 La Plata, Argentina
e-mail: pfernandez@inifta.unlp.edu.ar
e-mail: mmartins@inifta.unlp.edu.ar

A. Arenillas · E. G. Calvo · E. J. Juárez-Pérez · A. J. Menéndez
Instituto Nacional del Carbón, CSIC,
Apartado 73,
33080 Oviedo, Spain

Introduction

It is a well-known fact that energy can be stored electrostatically in electrochemical capacitors (or supercapacitors). A unit cell of an electrochemical capacitor is based on the double-layer capacitance at the solid/electrolyte interface of a high surface area material [1–6].

Electrochemical supercapacitors (ES) are extensively studied due to the increasing demand for a new kind of electrical energy accumulators with a high specific power capacity, i.e., greater than 10 kW kg^{-1} and a long durability (over 10^6 cycles) [1]. The main advantage of this storage system is a high dynamic of charge propagation that can be very useful for short-term pulses in hybrid electrical vehicles, digital telecommunications systems, uninterruptible power supply for computers and pulse laser technique. The development of new materials with very high specific surface areas and the use of carbons with different morphologies introduce new possibilities in a field which is in continuous progress. For this reason, the search of electrode materials suitable for electrochemical capacitors is a subject being continuously studied and developed [7–24].

Carbon gels are very interesting porous materials since their structural characteristics can be appropriately selected by choosing the right conditions for gel synthesis and processing. Carbon xerogels are frequently prepared using resorcinol (R) and formaldehyde (F) as reagents. The gel obtained is subsequently dried by evaporation and finally pyrolysed. The surfaces of RF carbon gels usually exhibit surfaces of 600–700 m^2 g^{-1} but after being activated can exhibit surface areas higher than 2,000 m^2 g^{-1}. Chemical activation is one of the most widely applied techniques for increasing the microporosity of carbon materials. By varying the activation conditions, it is possible to control the micropore development of carbon gels within an

already controlled mesopore/macropore network [25–27]. The activation process allows to obtain carbons of very high surface area, although the connectivity between the carbon particles is poor, giving rise to important internal resistances. On the other hand, interesting properties are given by the presence of multiwalled carbon nanotubes (MWCNT) which exhibit a developed porosity, a high electrical conductivity and a good resilience, all being very important for enhancing the power and cycle life of supercapacitors.

In a previous article, Bordjiba et al. [28] studied the charge storage mechanism of a carbon aerogel/MWCNT composite in acid and basic medium using experimental techniques similar to those employed in the present work. However, in our electrochemical impedance spectroscopy analysis a different basic theoretical approach was followed.

The aim of this work is to provide evidence that composites formed with a very high area carbon as carbon xerogel, and MWCNT, with a good electronic conductivity, can be used to obtain a wide range of capacity–power ES. In addition, from the analysis of electrochemical measurements in terms of a dynamic physicochemical model, the factors which determine the behavior of the electrodes were identified. From a basic point of view, these studies demonstrate the improvement of the performance of the composite electrodes, due not only to the increase of the effective conductivity of the solid but also to the effective conductivity of the electrolyte within the electrode. This worthy finding is scarcely taken into account in the literature dedicated to this research field.

Experimental

Materials

Two different carbon materials were employed, namely, (I) MWCNT (Aldrich® Product Number 636525), with an outer diameter of 10–20 nm, an inner diameter of 5–10 nm, and a length of 0.5–200 μm; carbon content greater than 95%, Fe being the main impurity in the sample. Taking into account the high level of impurities, the MWCNT were purified and activated in boiling concentrated nitric acid for 2 h; (II) high specific surface area in-lab carbon xerogel (AOX). This gel was synthesized using a stoichiometric R/F molar ratio of 0.5 and a dilution ratio, D (i.e., the total solvent/reactant molar ratio), of 5.7. The initial solution had a pH of 6.5 and was placed in an oven at 85 °C for 72 h to undergo gelation and ageing. Afterwards, the aqueous gels obtained were dried by evaporation, without any pre-treatment, in the same oven at 150 °C during 24 h. The gels were then pyrolysed at 800 °C under nitrogen flow in a tubular oven, using the following heating program: (1) ramp at 1.7 °C min^{-1} to 150 °C and hold for 15 min; (2) ramp at 5 °C min^{-1} to 400 °C and hold for 60 min; (3) ramp at 5 °C min^{-1} to 800 °C and hold for 120 min; and (4) cooling slowly to room temperature. Finally, the resultant carbon xerogel was chemically activated with phosphoric acid using a mass ratio of activating agent/carbon gel of 3/1. The mixture was stirred at 85 °C for 2 h, filtered and dried overnight in an oven at 110 °C. The sample was then heated under N_2 flow (85 ml min^{-1}) at 5 °C min^{-1} up to 450 °C and held at this temperature for 2 h. Finally, the samples were washed with water until pH 6 was attained and dried overnight at 110 °C.

Both carbon materials (MWCNT and AOX) were teflonized with 10 wt.% PTFE from DuPont™ Teflon® PTFE TE-3893, an aqueous dispersion fluoropolymer resin; the modified materials being named as MWCNTt and AOXt.

Carbon characterization

The textural characterization of the samples was performed by the physical adsorption of N_2 at −196 °C in a TriStar II from Micromeritics. The micropore volume, $V_{DUB\text{-}N2}$, was achieved by applying the Dubinin–Radushkevich (DR) method to the nitrogen adsorption isotherms [29]. The mean pore size (L_p) was obtained from the Stoeckli equation [30], and therefore the micropore surface was then calculated ($S_{mic}=2V_{mic}/L_p$). The BET surface area was also evaluated from the nitrogen adsorption isotherms [31].

The structure of the samples was evaluated by transmission electron microscopy (TEM). TEM evaluations were performed on JEOL JEM-2000 EX II equipment.

Conductivity measurements were carried out in home-made apparatus at atmospheric pressure by means of a modification of the four-point van der Pauw method [32]. For this purpose the material is pressed between two pistons and a constant current is passed through. Pressure between pistons can be controlled, a fact that allows to perform conductivity measurements in a wide pressure range. Therefore, solid conductivity of our electrodes was obtained raising the applied pressure until a constant conductivity value was reached. As it is explained in the next section, the electrodes were constructed employing the same method used to perform electrochemical measurements but without the Ni mesh.

Electrochemical testing

In order to study their electrochemical behavior, the electrodes were prepared employing 15 mg of AOXt/MWCNTt in different ratios. These teflonized carbons were then pressed onto a nickel mesh under a pressure of 2,000 kg cm^{-2} inside a 0.38 cm^2 transversal area cylindrical die. Three different mixtures were prepared, namely, (1) AOXt (E0), (2) AOXt with 9 wt.% of MWCNTt (E9), and (3) AOXt with 18 wt.%

J Solid State Electrochem (2012) 16:1067–1076

of MWCNTt (E18). With the purpose of obtain well mixed carbons, the AOXt and MWCNTt materials were put in a tube with ethanol and sonicated for 15 min. The suspension was then left to dry overnight.

A three-electrode cell containing 6 M KOH was used to determine the electrochemical performance of the electrodes. The working electrode was placed between two counter-electrodes of large surface area made of a Ni mesh. The electric potentials were measured against an Hg/HgO reference electrode. Electrochemical techniques such as cyclic voltammetry (Princeton Applied Research Potentiostat/Galvanostat Model 273), galvanostatic charge and discharge experiments (Arbin Instruments model BT2000, multiple independent-channel apparatus, which operates as a potentiostat/galvanostat with charging and/or discharging capability) and electrochemical impedance spectroscopy (EIS) (frequency response analyser (FRA) Solartron 1250 and Potentiostat Model PAR 273 coupled to a PC system) were employed. All the experiments were conducted at 25 °C.

Results and discussion

Support characterization

Figure 1 depicts TEM images corresponding to the studied materials. Differences in their structure can be clearly observed. Thus, inspection of the images shows that whereas MWCNT (1a) and MWCNTt (1b) are similar, the sample AOX (1c) is different from AOXt (1d). In addition, Fig. 1a, b shows pure and homogeneous MWCNT where both the internal and outer diameter are clearly visible. Figure 1c exhibits the typical structure of an amorphous carbon in the form of carbon xerogel while in Fig. 1d, it is not possible to make out the porous structure of the gel because PTFE molecules are dispersed over the AOXt surface masking the porous structure.

TEM images corresponding to AOX-MWCNT exhibit a non homogeneous material. Thus, we have found a part of the nanocomposite containing only nanotubes; another one with only AOX; nanotubes "decorated" with AOX, and also MWCNT very well dispersed with carbon xerogel (Fig. 2).

The shape of the isotherm (Fig. 3) shows that both carbon samples (i.e., MWCNT and AOX) have very different textures. AOX is a microporous sample with a high adsorption volume at low relative pressures, while the low microporosity content in MWCNT leads to low values of adsorption. The high relative pressure part of the isotherm gives information of the presence of mesopores in the sample and their relative pore sizes. The hysteresis loop gives an approximate idea of the size and volume of the mesopores. Sample AOX has smaller mesopores (i.e., the position is at lower p/p°) but higher mesopore volumes (i.e., the hysteresis loop is more clearly defined). It is also

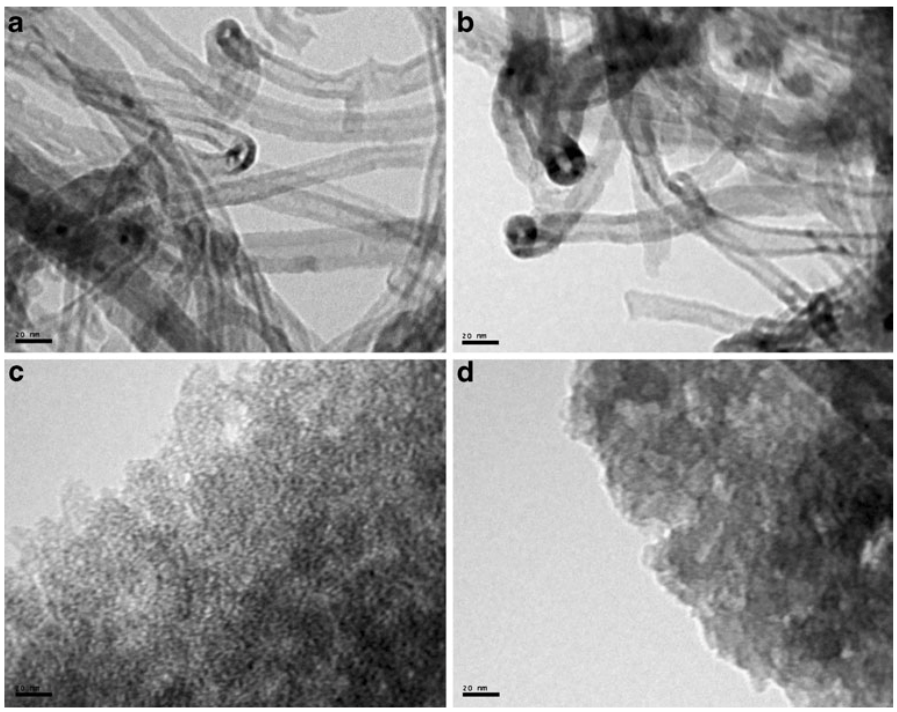

Fig. 1 TEM images corresponding to **a** MWCNT, **b** MWCNTt, **c** AOX, and **d** AOXt

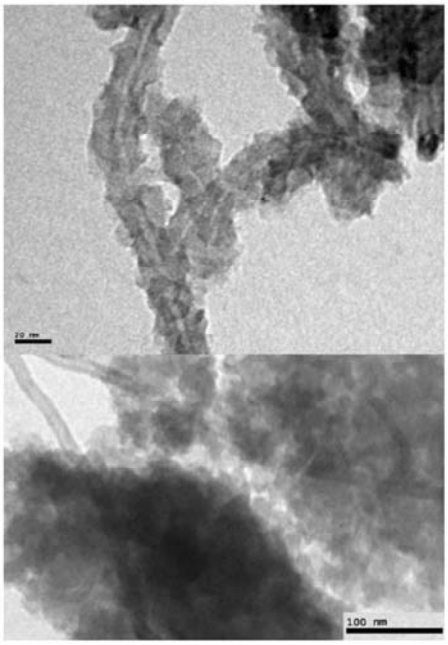

Fig. 2 AOX-MWCNT images for MWCNT "decorated" with AOX (*upper*) and MWCNT dispersed with carbon xerogel (*lower*)

worth noting that the teflonized samples present a slightly lower development in their textural properties (i.e., lower surface area and porosity) than their corresponding pristine samples. A comprehensive summary of the features related to the porosity and surface areas of the carbons is presented in Table 1. As mentioned above, MWCNT has a low porosity development that is reflected in a low BET surface area, 149 $m^2\ g^{-1}$, whereas AOX has a high textural development giving a BET surface area of 2301 $m^2\ g^{-1}$, which is more than one order of magnitude higher. The values of the micropore surface and the micropore volume, S_{mic} and $V_{DUB\text{-}N2}$, respectively, also differ considerably. The mean pore size L_p shows that the pores are wider in the case of MWCNT than in AOX. Comparing the textural values of the initial samples with their teflonized counterparts, it can be observed that in general the textural properties of the former are higher, although these differences are not very significant.

From results of conductivity measurements it can be concluded that an increase of nanotubes content produces an augment of material conductivity, exhibiting a linear behavior when plotted conductivity vs. MWCNT content. Thus, AOXt (E0) has a value of 0.025 S cm^{-1} while those samples containing 9% (E9) and 18% (E18) of MWCNT have values of 0.049 and 0.115 S cm^{-1}, respectively.

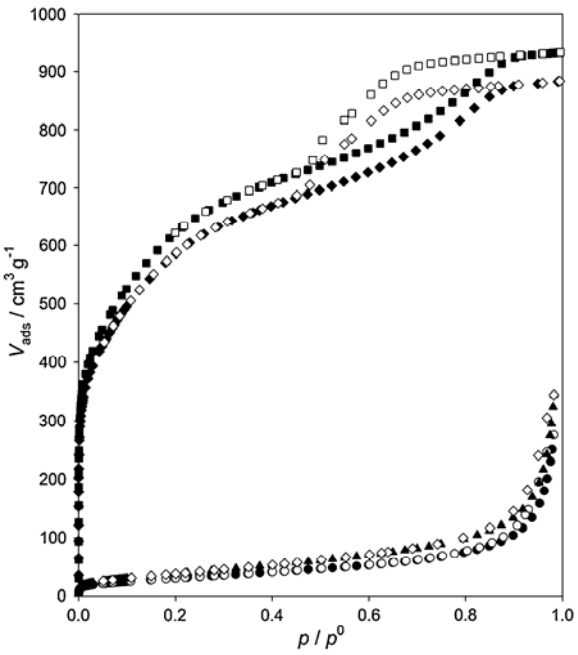

Fig. 3 Adsorption–desorption isotherms of N_2 at −196 °C for: **a** MWCNT (*filled triangles*), **b** MWCNTt (*filled circles*), **c** AOX (*filled squares*), and **d** AOXt (*filled diamonds*)

Electrochemical measurements

Cyclic voltammetry and charge–discharge experiments

Cyclic voltammetry (CV) was conducted performing triangular potential scans at $v=1.10^{-3}$, 3.10^{-3}, 5.10^{-3}, and 1.10^{-2} V s^{-1}. The potential routines were characterized by an upper and a lower potential limits, $E_{sa}=-0.20$ V and $E_{sc}=-1.10$ V, respectively.

Figure 4 exhibits voltammograms run at $v=1.10^{-2}$ V s^{-1} corresponding to all the electrodes used. The voltammograms do not exhibit the typical rectangular shape that is displayed when the electrode behaves as a pure capacitor. This behavior is due to carbon resistivity (solid and electrolyte within the porous structure), electrolyte resistance and the resistivity between carbon and current collectors. In agreement with conductivity measurements, CV results demonstrate that the resistive component increases as the amount of MWCNT decreases. Furthermore, the electrodes that contain MWCNT exhibit higher currents due to the double-layer charge–discharge.

Charge–discharge (CD) measurements were performed within a potential range from −0.20 to −0.90 V. In this work, the electrodes were charged at 7.4 mA g^{-1} and subsequently discharged at 7.4, 37.0, 74.0, and 222.0 mA g^{-1}. These relatively low currents were selected in order to measure very high capacity values and because capacity diminishes to a great extent as the current increases.

J Solid State Electrochem (2012) 16:1067–1076

Table 1 Textural characteristics of the samples studied obtained from N_2 adsorption isotherms at −196 °C

Sample	S_{BET} (m^2 g^{-1})	S_{mic} (m^2 g^{-1})	$V_{DUB\text{-}N2}$ (cm^3 g^{-1})	L_p (nm)
MWCNT	149	22	0.04	3.8
MWCNTt	112	17	0.04	4.3
AOX	2301	710	0.74	2.1
AOXt	2158	711	0.68	1.9

Galvanostatic charge–discharge curves slightly deviate from linearity due to the occurrence of faradaic reactions. Figure 5 shows that for low current values, for instance 7.4 mA g^{-1}, those electrodes containing MWCNTt provide enhanced capacities compared with those made up of only AOXt (E0). E18 and E9 exhibit capacity values in the order of 200 F g^{-1} while E0 gives 176 F g^{-1} at 7.4 mA g^{-1}. This result implies that even at this low current not all the material responds to the current perturbation. As the current increases, the difference in capacity between E0 and E9–E18 becomes larger. Thus, while E9 and E18 have capacities of ca. 130 F g^{-1}, E0 has a capacity of only 99 F g^{-1}. These results indicate the existence of some overpotential, in agreement with the ohmic contribution detected in the voltammetric experiments performed with E0 electrodes.

Rate capability data show that the capacity/power relationship can be set by adjusting the AOXt/MWCNTt ratio. Taking into account the behavior of E9 and E18, it is possible that the later may reach the maximum capacity that can be obtained for this order of current with the AOX-MWCNT nanocomposite.

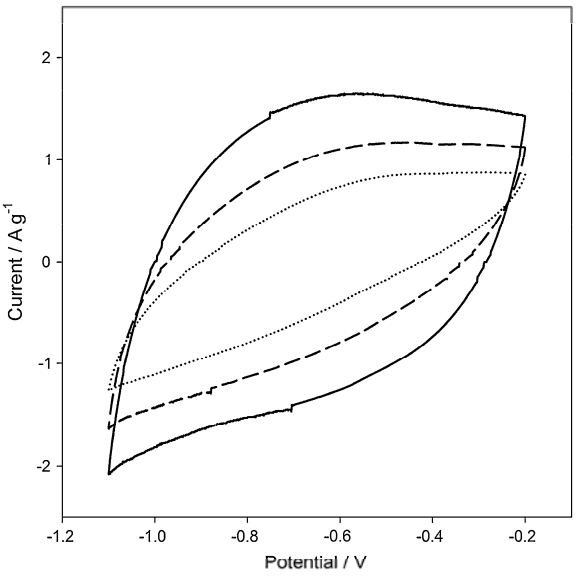

Fig. 4 Voltammograms of: **a** E0 (*dotted line*), **b** E9 (*dashed line*), and **c** E18 (*solid line*). E_{sa}=−0.20 V, E_{sc}=−1.10 V, v=1.10^{-2} V s^{-1}, 6 M KOH; T=303 K

Electrochemical impedance spectroscopy

Electrochemical impedance spectroscopy (EIS) measurements were carried out at −0.3 V by imposing a sinusoidal perturbation of 15 mV in the 0.5 mHz≤f≤50 kHz frequency range. The potential of −0.3 V was chosen with the aim of minimize the pseudocapacitance contribution to the electric double layer in the electrodes. This approach makes it possible to devise a simple electrochemical impedance model with the purpose of deriving the impedance function of the system and drawing direct conclusions from the fitting procedure. This topic is discussed in more detail in the next section.

The typical response of a porous electrode is shown in Fig. 6. At the highest frequencies, a semicircle whose diameter decreases as the amount of MWCNT increases can be seen. This capacitive contribution has been related to poor electrical contact between the solid particles and with the current collector (occurs because of the contact between the carbon particles and also between carbon particles and the current collector) [33]. The diameter of the semicircle decreases with the MWCNT content, probably indicating an improvement in the conductivity of the material, in

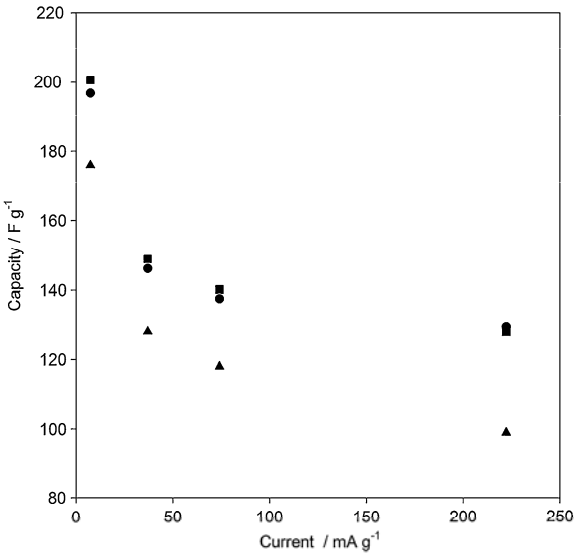

Fig. 5 Rate capability results for E18 (*filled circles*), E9 (*filled squares*), and E0 (*filled triangles*). Charge current, 7.4 mA g^{-1}

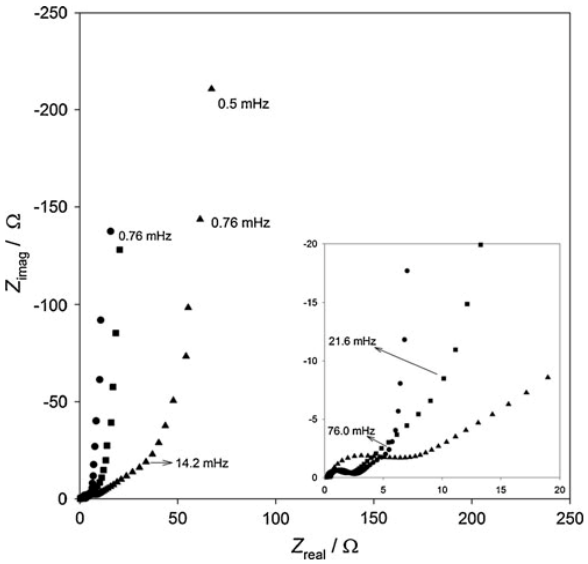

Fig. 6 Nyquist diagrams for electrodes E18 (*filled circles*), E9 (*filled squares*), and E0 (*filled triangles*)

agreement with the conductivity measurements, as mentioned above. In the range of high-medium frequencies, the spectra clearly show a linear behavior with a slope of approximately 45°, and below a characteristic frequency, the value of the angle increases to almost 90°. This type of response is associated with the distribution of potential, due to finite conductivities of the electrolyte and solid phases, within the porous structure [34]. The 45° linear zone becomes shorter as the amount of MWCNT within the electrodes increases.

Theoretical analysis physicochemical model A theoretical analysis of the dynamic electrochemical response of the system is presented and a physicochemical model is derived. In order to identify the structural and kinetic parameters of the different electrodes studied, the impedance function resulting from the model was fitted to the experimental EIS data.

The electrode is modeled as an isotropic porous structure, whose voids are filled with electrolyte. The model, based on the classic theory of porous-flooded electrodes [35, 36], takes into account the porous nature of the material, the solid and liquid conductivities, and the electrochemical processes at the solid material/electrolyte interface.

Fernández et al. carefully explain the development of this model in a previous work [37]. The final expression for the total impedance Z_p may be expressed as:

$$Z_p = \frac{L}{A_p(\kappa+\sigma)}\left[1+\frac{2+\left(\frac{\sigma}{\kappa}+\frac{\kappa}{\sigma}\right)\cosh\nu}{\nu\sinh\nu}\right] \quad (1)$$

where ν is given by:

$$\nu = L\left(\frac{\kappa+\sigma}{\kappa\sigma}\right)^{1/2} Z_i^{-1/2}$$

Z_i is the interfacial impedance per unit volume, A_p is the transverse electrode geometric area, L is the electrode thickness, σ is the effective carbon conductivity, and κ is the effective conductivity of the liquid phase.

κ is related to the porosity (ε) as follows,

$$\kappa = \kappa^T \varepsilon^{1.5} \quad (2)$$

where κ^T=0.55 is the specific conductivity (Ω^{-1} cm^{-1}) of the electrolyte (6 N KOH), and the exponent,1.5, is the tortuosity factor of the system [38, 39].

Interfacial impedance (Z_i) In order to calculate the total impedance Z_p using (1), an expression for Z_i (Ω cm^3) is required. In our case, the interfacial impedance only implies the double-layer capacitance impedance (Z_{dl}),

$$Z_i = Z_{dl} \quad (3)$$

where

$$Z_{dl} = \frac{1}{j\omega C_{dl}} \quad (4)$$

C_{dl} is the double-layer capacitance per unit volume (F cm^{-3}); j is the imaginary number; and $\omega=2\pi f$ (f, frequency of the perturbing signal).

It should be pointed out that our system has two capacitances linked in parallel, namely, the double-layer capacitance and the pseudofaradaic capacitance. The latter was neglected in this model because EIS measurements were conducted at a potential value where the contribution of this capacitance to the total electrode capacity was very low.

Results from the fitting procedure With the aim of identify the parameters of the system, a fitting procedure of the experimental impedance data in terms of the theoretical impedance function, Z_p, was accomplished. A fitting program was developed, based on the Nelder Meade simplex search algorithm. The fitting was considered acceptable when J_p, the cost function, is $J_p<5.10^{-3}$.

$$J_p = \frac{1}{K}\sum_k \left|\frac{Z_e(\omega_k)-Z_p(p,\omega_k)}{Z_e(\omega_k)}\right|^2 \quad (5)$$

where K is the number of frequencies employed in the experiments, and Z_e and Z_p correspond to experimental and theoretical data, respectively, corresponding to the frequency ω_k.

J Solid State Electrochem (2012) 16:1067–1076

As contact between particles is not considered, the higher frequency values were neglected from the fitting procedure.

A comparison of the experimental results and the theoretical Nyquist diagrams derived from the fitting procedure for all the electrodes evidences a good fit (Figs. 7, 8, 9).

Calculation and analysis of electrochemical parameters It must be emphasized that a_i, the interfacial area per unit volume, is a parameter derived after fitting the experimental results and from the electrochemical point of view, it is a measure of the real area that takes part in the electrode reaction. This is a point of extreme importance because the data provided by the BET method for specific area give information about the whole material used in the experiment, while the interfacial area identified from the EIS analysis, is real information about the fraction of material that actually participates in the electrode/solution interfacial process.

The capacity of the electric double-layer per electrode unit volume (C_{dl}) is obtained from the fitting procedure for each electrode. Commonly, charge densities in the double layer at plane electrodes are in the range of $1.6{\cdot}10^{-5}$ to $5{\cdot}10^{-5}$ F cm^{-2} [1]. Assuming an average value of $3{\cdot}10^{-5}$ F cm^{-2} (C^0_{dl}), the interfacial area per electrode unit

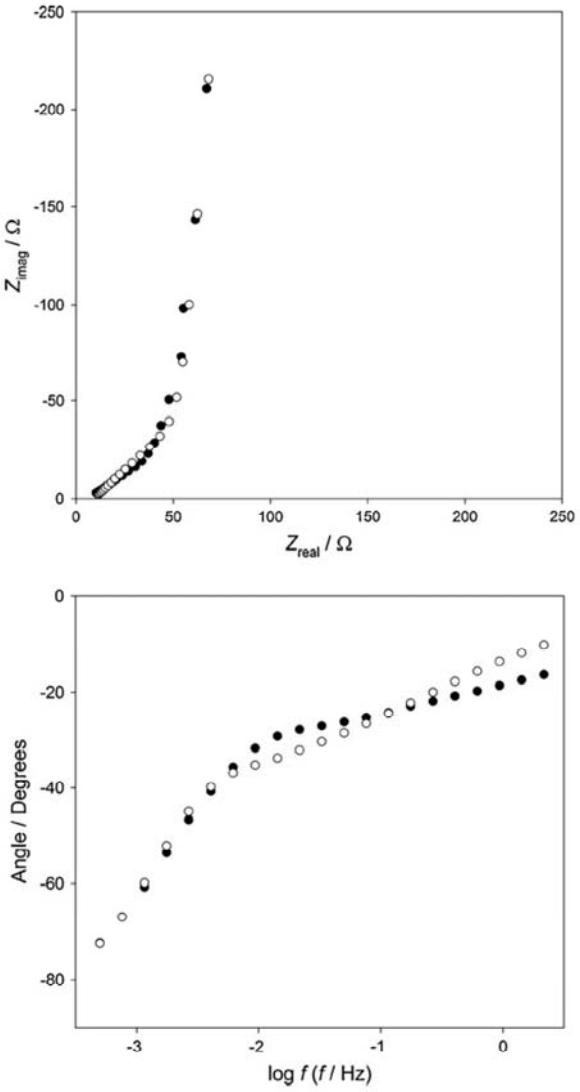

Fig. 7 Nyquist and Bode diagrams, experimental (*filled circles*) and theoretical (*empty circles*) data, for electrode E0

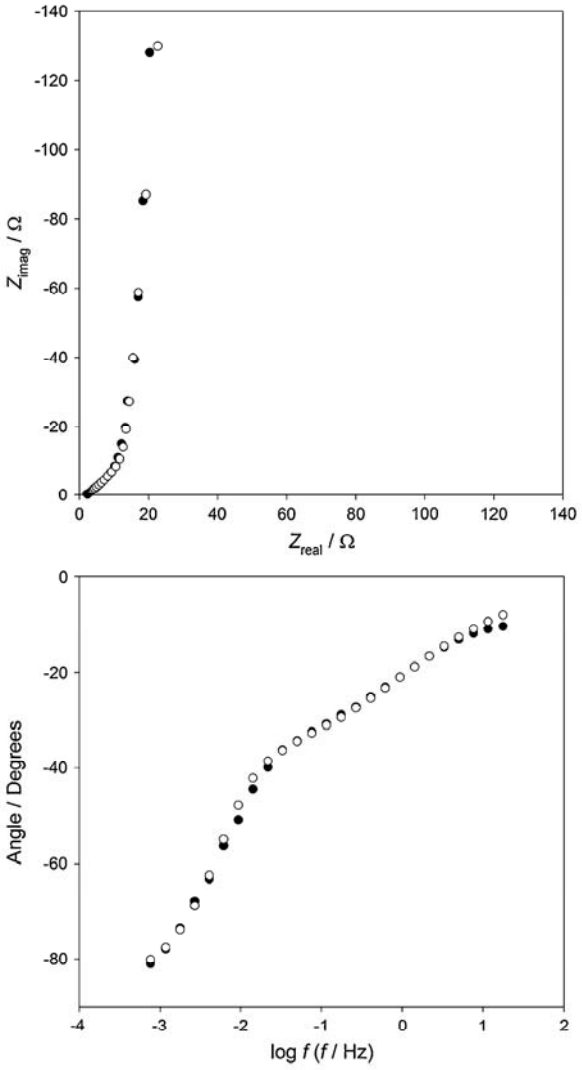

Fig. 8 Nyquist and Bode diagrams, experimental (*filled circles*) and theoretical (*empty circles*) data, for electrode E9

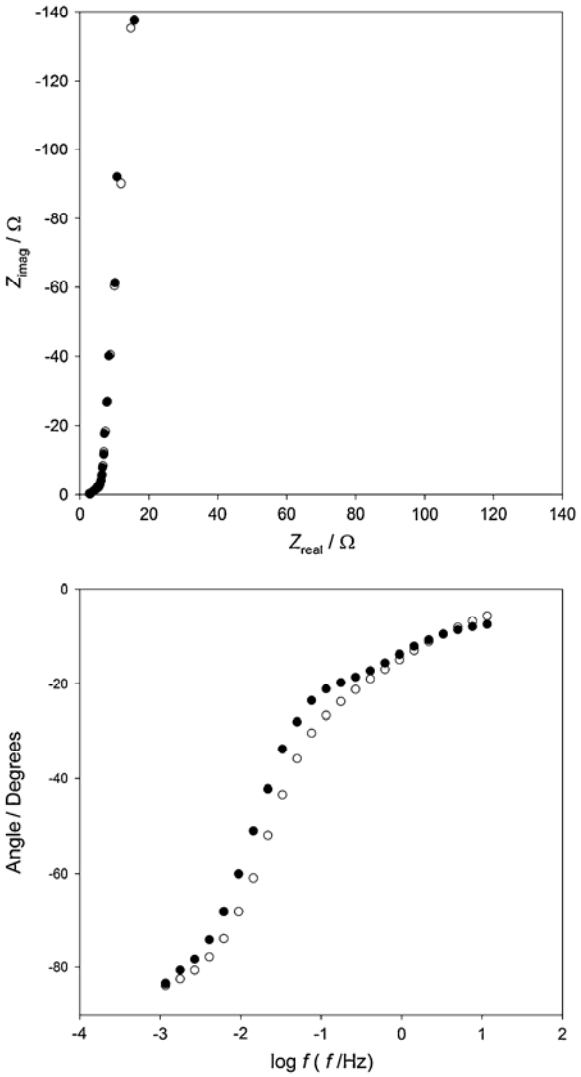

Fig. 9 Nyquist and Bode diagrams, experimental (*filled circles*) and theoretical (*empty circles*) data, for electrode E18

volume (a_i) for each electrode is obtained by means of the following equation,

$$C_{dl} = C_{dl}^{0} a_i \tag{6}$$

Table 2 contains the model parameters derived from the fitting procedure, corresponding to electrodes of different composition. The interfacial areas obtained from this method are quite similar for all the electrodes.

The electrochemically accessible carbon area, S, can be obtained after calculation of a_i,

$$S = \frac{a_i . V}{m} \tag{7}$$

where V is the electrode volume and m is the total carbon mass. Thus, through this parameter and by comparing with the values obtained from the BET measurements it is possible to find out the fraction of the total carbon area that is accessible to the electrolyte. From an inspection of Table 2, it is evident that S values are not so different, demonstrating that the electrolyte can gain access to almost the same fraction percentage of area in all the samples. Nevertheless, the electrodes that contain MWCNT exhibit slightly higher S values.

The most relevant differences can be found in the effective liquid-phase conductivity (κ) and hence in the porosity (ε) of the different electrodes. Percent porosity (ε.100), obtained by using Eq. 2, increases from 2.2% for electrode E0 and reaches 10.5% for electrode E18. This enhancement of the effective liquid-phase conductivity and of the porosity of the electrodes as the amount of MWCNT increases, may account for the decrease in the resistivity component in those electrodes containing MWCNT. These data assist to understand the results obtained from the CV and CD experiments.

It must be emphasized that porosity values obtained by using BET method are different from those calculated employing electrochemical impedance results after applying the developed physicochemical model. Thus, BET results show that porosity of AOX is higher than MWCNT. Due to this fact, the porosity of the AOX/MWCNT composite will decrease as the amount of MWCNT is increased. Furthermore, it must be taken into account that in contrast to BET method where the porosity of the material depends on the amount of nitrogen incoming within the pores, in the electrochemical method the results of porosity values are obtained through a physicochemical model. In the latter method, the porosity of the material is measured or sensed through the electrolyte incoming inside the pores of the electrode, which in turn is responsible of the electric conductivity. From these results, it can be concluded that this carbon xerogel is not good enough as material for supercapacitor due to its pores size distribution that

Table 2 Parameters derived from the fitting procedure

Electrode	C_{dl} (F cm^{-3})	a_i (cm^2 cm^{-3})	k (Ω cm)$^{-1}$	C (F g^{-1})	S (m^2 g^{-1})	ε
E18	39	$1.3 \cdot 10^6$	0.0260	110	366	0.105
E9	39	$1.3 \cdot 10^6$	0.0066	110	366	0.052
E0	35	$1.2 \cdot 10^6$	0.0019	99	328	0.022

impedes that a great part of the micropores could be occupied by the electrolyte.

This fact explains why C_{dl} does not decrease when the amount of MWCNT is increased. Even though the surface area calculated with BET method decreases with the increment of MWCNT, on the other hand, the accessibility of the electrolyte within the porous structure enhances.

For the reasons exposed above, we consider necessary to improve the xerogel synthesis to achieve a better pore distribution with the aim to get higher accessibility of the electrolyte inside the porous material and having enhanced effective liquid-phase conductivity. At the present, we are working on the synthesis of carbons xerogels with a larger mesopore/micropore ratio.

Conclusions

The voltammetric results demonstrate that there is an important resistive component which increases as the amount of MWCNT decreases. Furthermore, those electrodes containing MWCNT exhibit higher currents related to the double-layer charge–discharge mechanism. These results can be attributed to an increase in the electronic conductivity of the solid phase, and, according to the impedance fitting procedure, to an increase in the effective conductivity of the liquid phase as the amount of MWCNT augments.

The rate capability data show that the capacity/power relationship in the capacitor can be set by adjusting the AOXt/MWCNTt ratio. In addition, taking into account the behavior of E9 and E18, it is possible that E18 comes close to reaching the maximum capacity that can be obtained for this order of current with the AOX-MWCNT nanocomposite.

Conductivity measurements and EIS results demonstrate that electrode conductivity is increased by adding MWCNT. This is clearly seen at the highest frequencies in the Nyquist diagram. The decrease in the diameter of the semicircles is attributed to a better conductivity in the carbon materials.

On a basis of a theoretical analysis of the dynamic electrochemical response of the system a physicochemical model has been derived. In order to identify the structural and kinetic parameters of the different electrodes studied, theoretical impedance was fitted to the experimental data. The interfacial areas obtained through this method are slightly similar for all electrodes, demonstrating that the electrolyte can gain access to the same percentage of area in all of the samples tested.

The fitting procedure applied contributed significantly to understand the results found in both the CV and CD experiments. It was found that as the amount of MWCNT increases, an enhancement of effective liquid-phase conductivity associated to a higher porosity of the electrodes occurs. This fact, in addition to the effective solid electric conductivity, accounts for the decrease in the resistive component of those electrodes that contain MWCNT.

Acknowledgments This work was supported by the Consejo Nacional de Investigaciones Científicas y Técnicas of Argentina, the Agencia Nacional de Promoción Científica y Tecnológica, and the Universidad Nacional de La Plata. The financial support received from the Government of Principado de Asturias PCTI (Ref. IB09-00201) and Ministerio de Ciencia e Innovación (Ref. MAT2008-00217/MAT) is also greatly acknowledged. E.G. Calvo also acknowledges a predoctoral research grant from FICYT.

References

1. Conway BE (1999) Electrochemical supercapacitors, scientific fundamentals and technological applications. Plenum, New York
2. Conway BE (1991) Transition from "supercapacitor" to "battery" behaviour in electrochemical energy storage. J Electrochem Soc 138:1539–1548
3. Sarangapani S, Tilak BV, Chen CP (1996) Materials for electrochemical capacitors. J Electrochem Soc 143:3791–3799
4. Burke A (2000) Ultracapacitors: why, how, and where is the technology. J Power Sources 91:37–50
5. Conway BE, Birss V, Wojtowicz J (1997) The role and utilization of pseudocapacitance for energy storage by supercapacitors. J Power Sources 66:1–14
6. Frackowiak E, Béguin F (2001) Carbon materials for the electrochemical storage of energy in capacitors. Carbon 39:937–950
7. Béguin F (2006) Application of nanotextured carbons for electrochemical energy storage in aqueous medium. J Braz Chem Soc 17:1083–1089
8. Qu D, Shi H (1998) Studies of activated carbons used in double-layer capacitors. J Power Sources 74:99–107
9. Björnbom P (2007) Charge/discharge of an electrochemical supercapacitor electrode pore; non-uniqueness of mathematical models. Electrochem Commun 9:211–215
10. Frackowiak E, Jurewicz K, Szostak K, Delpeux S, Béguin F (2002) Nanotubular materials as electrodes for supercapacitors. Fuel Process Technol 77–78:213–219
11. Jurewicz K, Vix-Guterl C, Frackowiak E, Saadallah S, Reda M, Parmentier J, Patarin J, Béguin F (2004) Capacitance properties of ordered porous carbon materials prepared by a templating procedure. J Phys Chem Solids 65:287–293
12. Sullivan MG, Schnyder B, Bärtsch M, Alliata D, Barbero C, Imhof R, Kötzz R (2000) Electrochemically modified glassy carbon for capacitor electrodes. Characterization of thick anodic layers by cyclic voltammetry, differential electrochemical mass spectrometry, spectroscopic ellipsometry, X-ray photoelectron spectroscopy, FTIR, and AFM. J Electrochem Soc 147:2636–2643
13. Vix-Guterl C, Frackowiak E, Jurewicz K, Friebe M, Parmentier J, Béguin F (2005) Electrochemical energy storage in ordered porous carbon materials. Carbon 43:1293–1302
14. Barbieri O, Hahn V, Herzog A, Kötz R (2005) Capacitance limits of high surface area activated carbons for double layer capacitors. Carbon 43:1303–1310
15. Lota G, Grzyb B, Machnikowska H, Machnikowski J, Frackowiak E (2005) Effect of nitrogen in carbon electrode on the supercapacitor performance. Chem Phys Lett 404:53–58

16. Planes GA, Miras MC, Barbero CA (2005) Double layer properties of carbon aerogel electrodes measured by probe beam deflection and AC impedance techniques. Chem Commun 16:2146–2148
17. Raymundo-Piñero E, Leroux F, Béguin F (2006) A high-performance carbon for supercapacitors obtained by carbonization of a seaweed biopolymer. Adv Mater 18:1877–1882
18. Kim JH, Nam K-W, Ma SB, Kim KB (2006) Fabrication and electrochemical properties of carbon nanotube film electrodes. Carbon 44:1963–1968
19. Cebeci FÇ, Sezer E, Sarac AS (2009) A novel EDOT–nonylbithiazole–EDOT based comonomer as an active electrode material for supercapacitor applications. Electrochim Acta 54:6354–6360
20. Niu C, Sichel EK, Hoch R, Moy D, Tennent H (1997) High power electrochemical capacitors based on carbon nanotube electrodes. Appl Phys Lett 70:1480–1482
21. Vix-Guterl C, Saadallah S, Jurewicz K, Frackowiak E, Reda M, Parmentier J et al (2004) Supercapacitor electrodes from new ordered porous carbon materials obtained by a templating procedure. Mat Sci Eng B 108:148–155
22. Malak A, Fic K, Lota G, Vix-Guterl C, Frackowiak E (2010) Hybrid materials for supercapacitor application. J Solid State Electrochem 14:811–816
23. Zhongxue L, Jie C (2008) An impedance-based approach to predict the state-of-charge for carbon-based supercapacitors. Microelectron Eng 85:1549–1554
24. Simon P, Gogotsi Y (2008) Materials for electrochemical capacitors. Nat Mater 7:845–854
25. Zubizarreta L, Arenillas A, Pis JJ, Pirard V, Job N (2009) Studying chemical activation in carbon xerogels. J Mater Sci 44:6583–6590
26. Stoeckli F, Centeno TA (2005) On the determination of surface areas in activated carbons. Carbon 43:1184–1190
27. Dubinin MM (1966) Porous structure and adsorption properties of active carbons. In: Walker PL Jr (ed) Chemistry and physics of carbon, vol 2. Marcel Dekker, New York, pp 51–120
28. Bordjiba T, Mohamedi M, Dao LH (2008) Charge storage mechanism of binderless nanocomposite electrodes formed by dispersion of CNTs and carbon aerogels. J Electrochem Soc 155: A115–A124
29. Dubinin MM (1975) In: Danielli JF, Rosenberg MD, Cadenhead D (eds) Progress in surface and membrane science, vol 9. Academic, New York
30. Stoeckli HF, Ballerini L (1991) Evolution of microporosity during activation of carbon. Fuel 70:557–560
31. Parra JB, de Sousa JC, Bansal RC, Pis JJ, Pajares JA (1995) Characterization of activated carbons by the BET equation-an alternative approach. Adsorpt Sci Technol 12:51–66
32. van der Pauw J (1958) A method of measuring specific resistivity and Hall effect of discs of arbitrary shape. Philips Res Repts 13:1–9
33. Lundqvist A, Lindbergh G (1999) Kinetic study of a porous metal hydride electrode. Electrochim Acta 44:2523–2542
34. de Levie R (1963) On porous electrodes in electrolyte solutions. Electrochim Acta 8:751–780
35. Castro EB, Real SG, Bonesi A, Visintin A, Triaca WE (2004) Electrochemical impedance characterization of porous metal hydride electrodes. Electrochim Acta 49:3879 3890
36. Meyers JP, Doyle M, Darling RM, Newman JJ (2000) The impedance response of a porous electrode composed of intercalation particles. J Electrochem Soc 147:2930–2940
37. Fernández PS, Castro EB, Real SG, Martins ME (2009) Electrochemical behaviour of single walled carbon nanotubes—hydrogen storage and hydrogen evolution reaction. Int J Hydrogen Energy 34:8115–8126
38. De Vidts P, White RE (1995) Mathematical modeling of a nickel-cadmium cell: proton diffusion in the nickel electrode. J Electrochem Soc 142:1509–1519
39. Shung-Ik L, Yun-Sung K, Hai-Soo C (2002) Modeling on lithium insertion of porous carbon electrodes. Electrochim Acta 47:1055–1067

5.1.3. Uso de xerogeles de carbono con distinta porosidad como materiales de electrodo en supercondensadores acuosos

Como se ha comentado en la sección anterior, la utilización de un modelo físico-químico desarrollado a partir de resultados de espectroscopía de impedancia permite relacionar la respuesta electroquímica de un sistema con sus características estructurales y cinéticas. Gracias a dicho modelo, es posible conocer, entre otros parámetros, el grado de porosidad del material de electrodo que está realmente involucrado en el proceso de almacenamiento de carga, factor que puede ayudar a justificar el comportamiento electroquímico de diferentes supercondensadores. Por este motivo, surge el trabajo contenido en la *Publicación VII*, que también es fruto de una colaboración con investigadores del grupo argentino "*Conversión y Almacenamiento de Energía*" y se puede considerar como una segunda parte del trabajo recopilado en la *Publicación VI* adjuntada anteriormente.

El objetivo principal de este trabajo fue evaluar la capacidad de almacenamiento de energía de xerogeles de carbono que presentan diferente desarrollo textural y relacionar su respuesta electroquímica con los parámetros obtenidos a partir del modelo físico-químico. Los materiales de electrodo utilizados fueron xerogeles de carbono altamente porosos obtenidos mediante diferentes procesos de fabricación (véase Figura 5.2), además de un carbón activo comercial utilizado como material de referencia (designado en el artículo como S30). Tal como refleja la Figura 5.2, los cuatro procedimientos de síntesis llevados a cabo incluyen una etapa de activación química con hidróxido potásico, cuyo objetivo es desarrollar notablemente la microporosidad del material resultante. Cada una de las rutas de síntesis produce materiales con una textura porosa determinada, ya que variables como naturaleza del material activado (xerogel orgánico o carbonizado), dispositivo de calentamiento empleado (horno microondas vs. horno eléctrico) ó pH de la mezcla resorcinol-formaldehído (6.5 y 5.8) han sido modificadas. En la Figura 5.2 aparecen también los valores de dos parámetros texturales obtenidos a partir de isotermas de adsorción-desorción de N_2 a -196 ºC (área superficial específica y volumen de mesoporos) que dan idea del tipo de matriz porosa obtenida en cada uno de los cuatro casos. Es necesario apuntar que dichas propiedades texturales no corresponden a los xerogeles de carbono puros sino a la mezcla de xerogel de carbono con PTFE, que es el polímero ligante utilizado para la fabricación de los electrodos. Los valores de área superficial S_{BET} de los xerogeles de carbono sintetizados son más elevados. No obstante, es más conveniente utilizar los datos relativos a la estructura porosa de la mezcla ya que la adición de teflón siempre lleva asociada una ligera reducción de la porosidad.

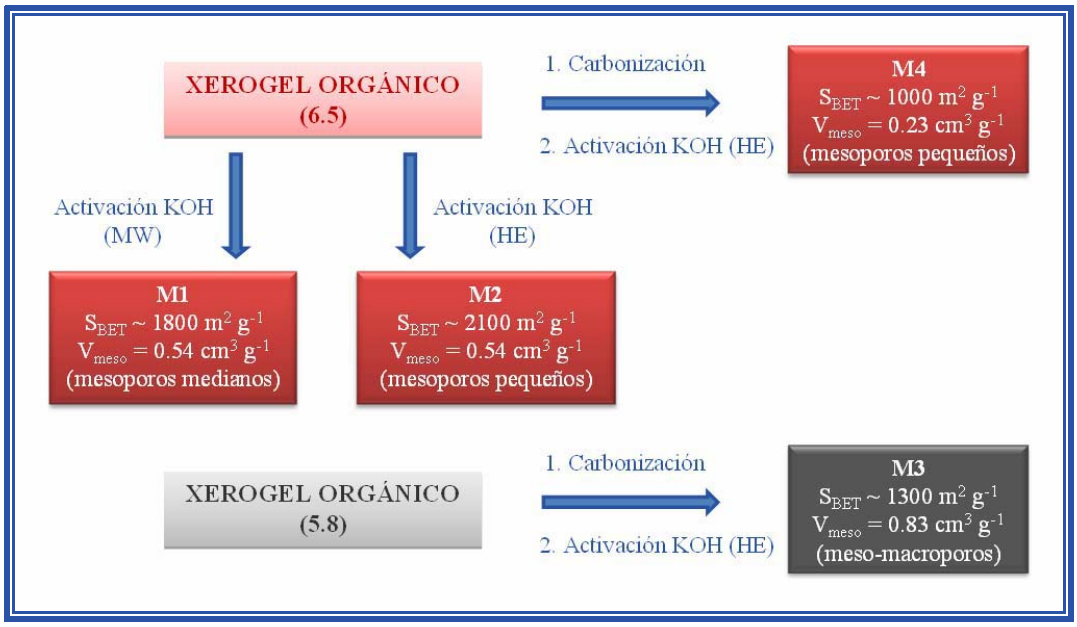

Figura 5.2. Esquema de los métodos de síntesis utilizados en la Publicación VII.

La caracterización electroquímica de los cinco materiales de electrodo estudiados en este trabajo se llevó a cabo mediante tests de voltametría cíclica, cronoamperometría y espectroscopía de impedancia, todas ellas aplicadas sobre una celda de 3 electrodos que utiliza una disolución de KOH 6 M como electrolito. El electrodo de referencia utilizado fue Hg/HgO y como contraelectrodo se empleó una malla de Níquel.

Las principales conclusiones derivadas de este trabajo se muestran a continuación:

❖ Es posible obtener xerogeles resorcinol-formaldehído altamente porosos mediante diferentes vías de síntesis. Todas ellas producen materiales con una microporosidad notablemente desarrollada, característica imprescindible para la aplicación estudiada en esta Tesis Doctoral. No obstante, tanto el volumen como la distribución de tamaños de micro-mesoporos están influenciados por las variables de operación, lo que da una idea de la versatilidad de los xerogeles de carbono ya que es posible ajustar su textura porosa mediante pequeñas modificaciones durante la síntesis.

❖ Todos los xerogeles de carbono sintetizados en este trabajo fueron capaces de almacenar mayor cantidad de energía eléctrica que el carbón activo utilizado como material de referencia (valores de capacidad específica desde 170 a 250 F g^{-1} para los cuatro xerogeles de carbono sintetizados, mientras que el valor asociado al carbón activo S30 fue de 120 F g^{-1}, cuando se llevaron a cabo tests de carga-descarga aplicando una densidad de corriente de 0.34 A g^{-1}).

❖ Todas las técnicas electroquímicas realizadas revelan la importancia de la distribución de tamaños de poro sobre la capacidad de almacenamiento energético de un material. Una mayor proporción de microporos no implica necesariamente una mayor capacidad de almacenamiento

energético (por ejemplo, electrodos preparados a partir del carbón activo S30 llevan asociados valores de S_{BET} y capacidad específica de 1664 m^2 g^{-1} y ~ 130 F g^{-1}, mientras que los xerogeles de carbono designados como M3 y M4 dan lugar a valores de capacidad específica entre 180-190 F g^{-1}, a pesar de poseer un menor volumen de microporos). El volumen y tamaño de mesoporos presentes en el material de electrodo también tiene influencia sobre el proceso de almacenamiento de carga, ya que puede hacer que la fracción de la matriz porosa que participa activamente en la formación de la doble capa aumente, como consecuencia de la mayor accesibilidad de los iones de electrolito hacia los poros del electrodo carbonoso. El carbón activo S30 contiene cierta cantidad de mesoporos, pero son mesoporos muy estrechos, con un tamaño comprendido entre 2-4 nm, lo que puede servir para justificar su peor capacidad de almacenamiento energético ya que esos poros parecen no tener el tamaño adecuado para facilitar la difusión de los iones de electrolito.

❖ A partir del modelo físico-químico se obtuvieron varios parámetros que permiten entender mejor el comportamiento de los diferentes materiales de electrodo estudiados. Por ejemplo, se pudo determinar la fracción del área total del electrodo carbonoso que es accesible electroquímicamente y consecuentemente, un parámetro que se ha denominado parámetro de accesibilidad. Todos los xerogeles de carbono utilizados en este trabajo presentaron un parámetro de accesibilidad superior al del carbón activo comercial, lo que está relacionado, probablemente, con su mayor contenido de mesoporos.

❖ La conductividad efectiva de los materiales de electrodo estudiados se calculó tanto a partir de los resultados de espectroscopía de impedancia como midiendo directamente la resistividad mediante el método de Van der Pauw. Las dos metodologías muestran que la conductividad eléctrica de los xerogeles de carbono es, como mínimo, del orden de la conductividad asociada a carbones activos utilizados como material de electrodo en supercondensadores comerciales.

Publicación VII

CARBON XEROGEL AS ELECTROCHEMICAL SUPERCAPACITORS. RELATION BETWEEN IMPEDANCE PHYSICOCHEMICAL PARAMETERS AND ELECTROCHEMICAL BEHAVIOUR

International Journal of Hydrogen Energy

37 (10249-10255)

Año: 2012

INTERNATIONAL JOURNAL OF HYDROGEN ENERGY 37 (2012) 10249–10255

Available online at www.sciencedirect.com

SciVerse ScienceDirect

journal homepage: www.elsevier.com/locate/he

Carbon xerogels as electrochemical supercapacitors. Relation between impedance physicochemical parameters and electrochemical behaviour

P.S. Fernández [a,*], A. Arenillas [b], E.G. Calvo [b], J.A. Menéndez [b], M.E. Martins [a]

[a] Instituto de Investigaciones Fisicoquímicas Teóricas y Aplicadas (INIFTA), Facultad de Ciencias Exactas, UNLP, CCT La Plata-CONICET, Boulevard 113 y 64, 1900 La Plata, Argentina

[b] Instituto Nacional del Carbón, CSIC, Apartado 73, 33080 Oviedo, España, Spain

ARTICLE INFO

Article history:
Received 25 August 2011
Received in revised form
22 December 2011
Accepted 31 January 2012
Available online 25 February 2012

Keywords:
Electrochemical supercapacitors
Porous electrodes
Electrochemical impedance spectroscopy
Interfacial area

ABSTRACT

The electrochemical behavior of carbon xerogels was studied with the aim of analyzing the performance of the materials used as electrochemical supercapacitors (SC) and to relate with physicochemical parameters. These materials have areas involving 1500–2000 m^2/g measured with the BET equation and a range of pore size distributions.

Conventional electrochemical techniques were used as cyclic voltammetry (CV), which allowed electrochemical characterization of different materials, and chronopotentiometry (CD), in order to determine the charge storage capacity of the xerogel at different currents or discharge rates.

Experimental results using electrochemical impedance spectroscopy (EIS) were interpreted with a physicochemical model that permitted identifying different parameters of the electrode, which explain the differences in the behavior of materials.

1. Introduction

The electrochemical supercapacitors (SC) are devices through which electric charges are stored in the electrical double layer (EDL) for each of the high surface area carbon porous electrodes involved. On the other hand, in the batteries, the charge storage process is essentially faradaic, since electron transfer takes place that changes the chemistry of electroactive compounds. The differences in the processes that occur in each of these devices generate features that are opposed, making them suitable for use in different technologies or working in a complementary manner in a single system [1]. The most striking differences between them are: i) The SC can store a much smaller amount of energy than the batteries (~10 $Whkg^{-1}$ for SC in aqueous electrolyte and 150–250 $Whkg^{-1}$ for a lithium-ion battery). ii) The power densities of the SC are even nine times higher than those of lithium-ion batteries, namely, 6.4 vs. 0.7 $kWkg^{-1}$ [2,3]. iii) A device based on charge and discharge of the EDL involves an entirely reversible process allowing a number of charge–discharge cycles of several orders of magnitude higher than batteries, in which cycle to cycle are produced changes that gradually degrade electrodes irreversibly [1].

In this work, we have synthesized and chemically activated carbon xerogels with high area and a range of pore size distribution. This allowed evaluating the behavior of each

* Corresponding author. Tel.: +54 221 425 7430; fax: +54 221 425 4642.
E-mail addresses: pablosf23@yahoo.com.ar (P.S. Fernández), aapuente@incar.csic.es (A. Arenillas), mariaelisamartins@gmail.com, mmartins@inifta.unlp.edu.ar (M.E. Martins).

0360-3199/$ – see front matter Copyright © 2012, Hydrogen Energy Publications, LLC. Published by Elsevier Ltd. All rights reserved.
doi:10.1016/j.ijhydene.2012.01.154

material as SC and their relationship with physicochemical properties of the carbons. Carbon gels are porous materials interesting for use in this area due to its structural characteristics that can be selected by adjusting the conditions used in the synthesis and subsequent processing of materials [4–6].

While this work can be framed within a specific application, it focuses on discussing basic aspects of electrochemistry that are often neglected, incurring in wrong definitions or assigning a determined behavior to erroneous factors. In this context, there is a very detailed discussion about electrochemical interface area, which is important parameters for all basic electrochemistry areas, especially for electroanalytical chemistry and electrocatalysis discussions.

2. Experimental

Carbon xerogels were used, which were impregnated with PTFE TE-3893® (an aqueous dispersion of a fluoropolymer resin): i) M1 10% PTFE; ii) M2 30% PTFE; iii) M3 15% PTFE; iv) M4 10% PTFE. Moreover, as comparative parameter was used carbon Supra 30 DLC (Norit®) 10% PTFE, designated S30. In all cases a minimum quantity of PTFE were used in order to bring about a minimum change on the properties of the as-prepared carbon material.

The electrodes were prepared by introducing those carbon xerogels impregnated with resin inside a steel pillbox in which had previously placed a Ni wire skeleton, then applying a pressure of 2100 $kgcm^{-2}$.

2.1. Synthesis of carbon Xerogeles

Carbon xerogels used in this work were constructed as follows. First, an organic xerogel (OX) was synthesized using an RF solution through a microwave radiation treatment, according to a procedure described elsewhere [7]. Subsequently, several materials were obtained: i) M1 is an OX prepared with an RF solution (pH = 6.5) and activated with KOH in a microwave oven ($T = 700\ °C$ for $t = 6$ min). ii) M2 was synthesized in the same way as for M1, being activated in a horizontal furnace during 2 h iii) M3 is an OX prepared with an RF solution (pH = 5.8). Then, it was stabilized heating at 800 °C in N_2 atmosphere to obtain a carbon xerogel, which was then activated with KOH in the same way as that for M2. iv) M4 was obtained equally to M3 but RF solution with pH = 6.5.

2.2. Electrochemical system

The electrochemical experiments were performed using a cell of three electrodes in 6M KOH aqueous solution. As working electrode teflonated carbon xerogels were used; the counter electrode was a nickel mesh and as the reference electrode was used Hg/HgO/6M KOH (+0.098 vs. NHE). In the text, the potentials are referred to the electrode employed as reference. All experiments were performed at room temperature.

2.3. Characterization

The textural characterization of the samples was carried out through physical adsorption of N_2 at 77K, using a Micromeritics model TriStar II. The volume of micropores, V_{mic} (cm^3g^{-1}), was achieved by applying the Dubinin-Radushkevich (DR) method [8] to the N_2 adsorption isotherms. From the volume of the micropores and the average size of the pores (L_p) can be obtained the surface area of micropores ($S_{mic} = 2V_{mic}/L_p$) applying Stoeckli equation [9]. The BET area was also evaluated using the N_2 adsorption isotherms [10]. The structure of the samples was assessed using a transmission electron microscope (TEM). The images were taken with a JEOL JEM-2000 EX II.

The conductivity measurements of carbons were carried out at atmospheric pressure, using an apparatus made in the laboratory, which is a modification of the van der Pauw technique [11].

3. Results and discussion

3.1. Carbon characterization

3.1.1. Transmission electron microscopy (TEM)

Fig. 1A and B show images of one of the xerogels with and without Teflon, respectively. Fig. 1A clearly exhibits the structure of a typical amorphous xerogel, whereas the 1B shows the loss of the porous structure characteristic of the material due to masking by the homogeneous deposition of polymer on the surface.

3.1.2. Textural characterization

Fig. 2 shows the isotherms performed with N_2 at 77K for different electrodes. Usually, measurements are made with the carbons in his pristine state. Although we found that the addition of 10% PTFE slightly changes the features of those isotherms, the fact that for the construction of the electrodes is required to apply pressure to the carbons impregnated with Teflon leads to a decrease of the textural characteristics of the materials. For this reason, it was necessary to obtain the isotherms of the electrode materials. These were classified into two groups. Thus, M2 and S30 samples exhibit a type I isotherm, which correspond to the presence of predominantly microporous materials (but also have small mesopores), while M1, M3 and M4 reveal hysteresis cycles, showing isotherms of type I-IV, being characteristic of micro-mesoporous materials [12].

Table 1 shows a summary of the parameters calculated by means of the isotherm measurements, which are related to the porosity and surface area of materials. These are: i) the area calculated by BET equation (S_{BET} in m^2g^{-1}); ii) the volumes represented by mesopores and micropores in cm^3g^{-1}; iii) the average size of micropores, L_P in nm. Moreover, in the last column is placed the solid conductivity measurement, σ, expressed in Scm^{-1}.

3.2. Electrochemical measurements

3.2.1. Cyclic voltammetry (CV) and potentiometry (CD charge and discharge)

VC was conducted by performing triangular potential sweeps at $\upsilon = 1.10^{-3}$, 3.10^{-3}, 5.10^{-3} and $1.10^{-2}\ V^{-1}$. Potential limits were set to show only the region of purely capacitive behavior.

Fig. 3 shows voltammograms for all the carbons utilized, made at $\upsilon = 1.10^{-2}\ V^{-1}$. For these electrodes a clear deviation

INTERNATIONAL JOURNAL OF HYDROGEN ENERGY 37 (2012) 10249–10255

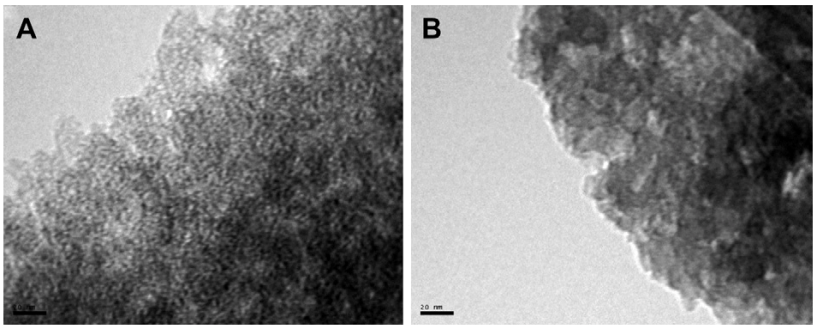

Fig. 1 – TEM images of a xerogel without (A) and with Teflon (B).

from ideal behavior can be observed, since they do not exhibit the typical rectangular shape that is observed for a pure capacitor. Nevertheless, an important part of this deviation is due to the intrinsic resistance of the system employed to evaluate the materials. This fact causes that the parameters measured in these experiments can not be directly compared with those obtained with materials using another system or in a capacitor. Therefore, in order to have a direct parameter for comparison it was purchased commercial coal S30, which is used in the manufacture of SC. While all voltammograms show significant resistive components, in the figure stand out clearly the xerogel M2, which, by reversing the potential sweep in the positive direction reaches the maximum positive current faster. In addition, throughout the entire potential window displays the higher absolute current values being directly related to the charge of the electric double layer. Similarly, electrodes constructed with materials identified S30 and M4 performed better than those made with M1 and M3.

The CDs were carried out between −0.20 and −0.90 V. The electrodes were charged at 88.6 mAg^{-1} and subsequently discharged at different currents.

The potential-time curves demonstrate small deviations from linearity due to the occurrence of charge transfer reactions. Moreover, the variation of capacities with different discharge rates gives an idea of the internal resistance of the system. Because the only change made between measurements is the composition of ET, it is valid to assign the dissimilarities to the different resistive components introduced by the carbons. These are: i) the electronic conductivity of the solid, σ (Table 1) and ii) the effective conductivity of the electrolyte, i.e., the conductivity of aqueous electrolyte within the porous electrode matrix (k).

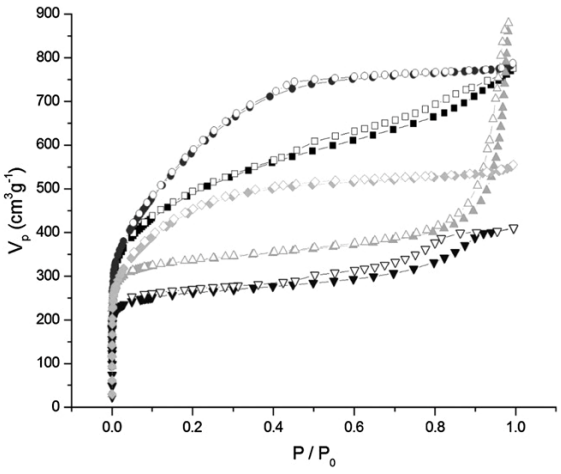

Fig. 2 – Isotherms for M1(■), M2(●), M3(▲), M4(▼), S30(●).

Fig. 4 exhibits the dependence of C with the discharge rate. At low currents, all carbons show higher C than the commercial product S30. Under these circumstances, where the resistances of the system have a secondary role, are prominent those materials with higher specific areas and therefore, as when working with relatively similar materials, exhibit higher interfacial area obtained through BET model. Nevertheless this behavior is not always the same, because the area measured through isotherms depends on access of N_2 to the pores, while for the formation of the EDL is the electrolyte that must be able to join them. It is well known that in experimental conditions N_2 is able to access pores smaller than water molecules [13].

Thus, capacities obtained at low currents are indicative of the interfacial area of the electrode. The fact that M1 (S_{BET}: 1786) has a C markedly higher than that of M2 (S_{BET}: 2089) indicates that the pore distribution of M1 generates greater access of the electrolyte to the porous matrix of this electrode, probably due to the presence of a greater amount of large mesopores and even macropores (the V_{ads} increases even at high pressures). Correspondingly, one can conclude that the aqueous electrolyte is in direct contact with a lesser electrode surface in electrode constructed with S30 than with those

Table 1 – Textural characteristics of the carbons studied, obtained by the N_2 adsorption isotherms at 77K, and conductivity values of the electrodes (active material and binder used).

Muestra	S_{BET}	V_{meso}	V_{micro}	L_p	$\sigma.10^2$
M1	1786	0.54	0.65	1.8	0.42
M2	2089	0.54	0.67	1.8	0.66
M3	1316	0.83	0.52	1.2	0.08
M4	1020	0.23	0.40	1.0	0.09
S30	1664	0.31	0.54	1.6	0.12

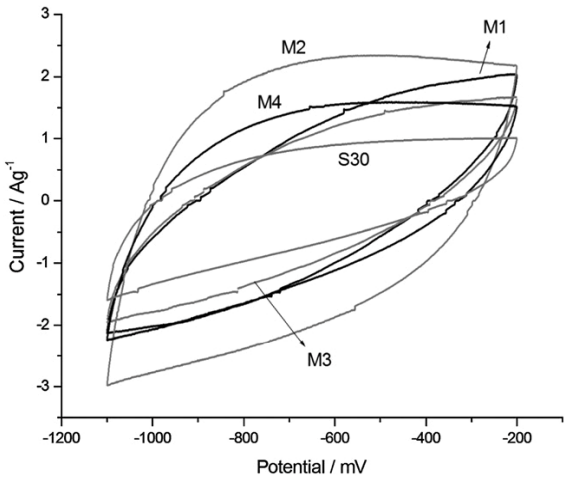

Fig. 3 – Voltammograms performed at $v = 1.10^{-2}\ V^{-1}$ for all the materials employed.

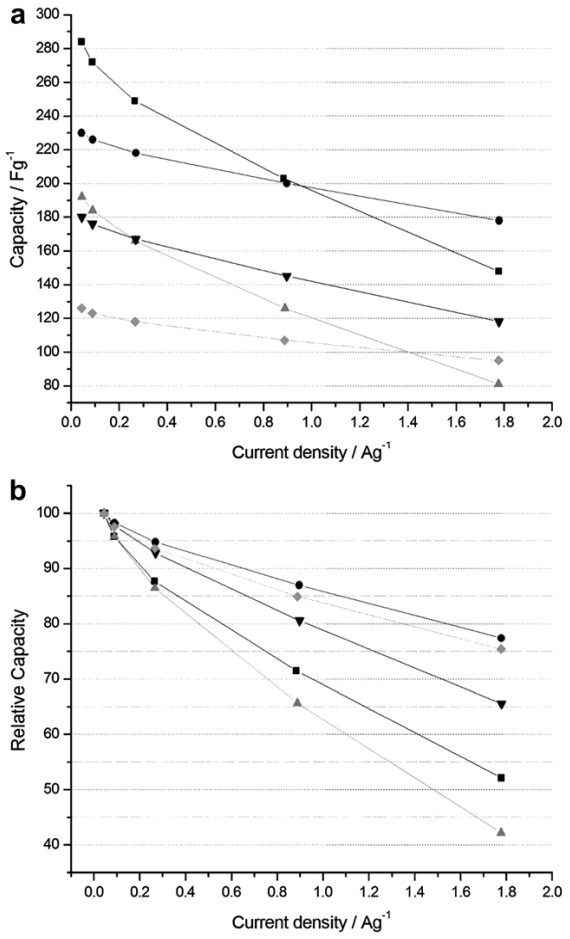

Fig. 4 – Capacity (a); relative capacity (b). M1(■), M2(●), M3(▲), M4(▼), S30(●).

electrodes containing M3 and M4, isotherms shedding a similar conclusion as above. We shall see later through EIS measurements, that one can indirectly measure the accessibility of the electrolyte into the pores of the xerogels.

As the current increases it can be seen a drop in C for all materials, being higher for M1 and M3. In this regard, both M2 and M4 xerogels as carbon S30 are showing the best results, which agree very well with that observed in the VC experiments. Taking into account the values of C at high currents, it can be observed that all the xerogels, excepting M3, outperform S30, being the storage capacity of charge of M2 higher than that of S30 in more than 80 Fg^{-1}.

3.2.2. *Electrochemical impedance spectroscopy (EIS)*

EIS measurements were carried out at −0.3 V by imposing a sinusoidal perturbation of 15 mV in the 0.5 mHz ≤ *f* ≤ 50 kHz frequency range. The potential of −0.3 V was chosen with the aim of minimize the pseudocapacitance contribution to the electric double layer in the electrodes. This approach makes it possible to devise a simple electrochemical impedance model with the purpose of derive the impedance function of the system, and draw direct conclusions from the fitting procedure. This topic is discussed in more detail in the next section.

The typical response of a porous electrode is shown in Fig. 5. At the highest frequencies, a semicircle can be seen. This capacitive contribution has been related to poor electrical contact between the solid particles and with the current collector (occurs because of the contact between the carbon particles and between carbon particles and the current collector) [14].

In the range of high-medium frequencies, the spectra clearly show a linear behavior with a slope of approximately 45°, and below a characteristic frequency, the value of the angle increases to almost 90°. This type of response is associated with the distribution of potential, due to finite conductivities of the electrolyte and solid phases, within the porous structure [15].

3.2.2.1. Theoretical analysis - physicochemical model. A theoretical analysis of the dynamic electrochemical response of

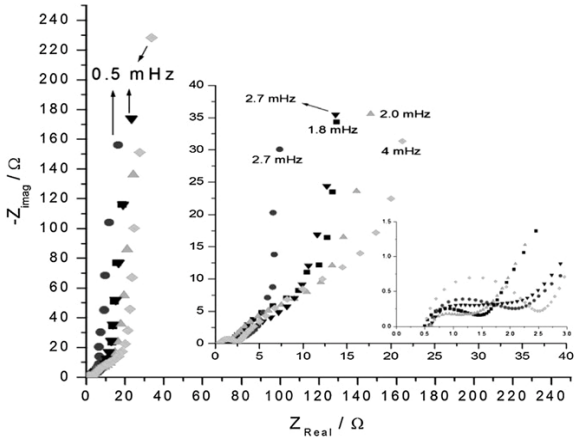

Fig. 5 – Nyquist diagrams. M1(■), M2(●), M3(▲), M4(▼), S30(●). Insert (a) corresponds to behavior at low frequencies and (b) At medium frequencies.

INTERNATIONAL JOURNAL OF HYDROGEN ENERGY 37 (2012) 10249–10255

the system is presented and a physicochemical model is derived. In order to identify the structural and kinetic parameters of the different electrodes studied, the impedance function resulting from the model was fitted to the experimental EIS data.

The electrode is modeled as an isotropic porous structure, whose voids are filled with electrolyte. The model, based on the classic theory of porous flooded electrodes [16,17], takes into account the porous nature of the material, the solid and liquid conductivities and the electrochemical processes at the solid material/electrolyte interface.

Fernández et al. carefully explain the development of this model in a previous work [14]. The final expression for the total impedance Z_p may be expressed as:

$$Z_p = \frac{L}{A_p(\kappa+\sigma)}\left[1+\frac{2+\left(\frac{\sigma}{\kappa}+\frac{\kappa}{\sigma}\right)\cosh\nu}{\nu\sinh\nu}\right] \quad (1)$$

where ν is given by:

$$\nu = L\left(\frac{\kappa+\sigma}{\kappa\sigma}\right)^{1/2} Z_i^{-1/2} \quad (2)$$

Z_i is the interfacial impedance per unit volume, A_p is the transverse electrode geometric area and L is the electrode thickness. The conductivities previously defined have units of $\Omega^{-1}cm^{-1}$.

3.2.2.2. *Interfacial impedance (Z_i).* In order to calculate the total impedance Z_p using (1), an expression for Z_i (Ωcm^3) is required. In our case, the interfacial impedance only implies the double layer capacitance impedance (Z_{dl}),

$$Z_i = Z_{dl} \quad (3)$$

where

$$Z_{dl} = \frac{1}{j\omega C_{dl}} \quad (4)$$

C_{dl} is the double layer capacitance per unit volume (Fcm^{-3}); j is the imaginary number; and $\omega = 2\pi f$ (f, frequency of the perturbing signal).

It should be pointed out that our system has two capacitances linked in parallel, namely, the double layer capacitance and the pseudofaradaic capacitance. The latter was neglected in this model because EIS measurements were conducted at a potential value where the contribution of this capacitance to the total electrode capacity was very low.

3.2.2.3. *Fitting procedure.* With the aim of identify the parameters of the system, a fitting procedure of the experimental impedance data in terms of the theoretical impedance function, Z_p, was accomplished. A fitting program was developed, based on the Nelder-Meade simplex search algorithm [18,19]. The fitting was considered acceptable when J_p, the cost function, is $J_p < 5.10^{-3}$.

$$J_p = \frac{1}{K}\sum_k \left|\frac{Z_e(\omega_k) - Z_p(p,\omega_k)}{Z_e(\omega_k)}\right|^2 \quad (5)$$

where K is the number of frequencies employed in the experiments, and Z_e and Z_p correspond to experimental and theoretical data, respectively, corresponding to the frequency ω_k.

As contact between particles is not considered, the higher frequency values were neglected from the fitting procedure.

A comparison of the experimental results and the theoretical diagrams derived from the fitting procedure for all the electrodes evidences a good fit. Experimental and theoretical, Nyquist and Bode diagrams for M2 electrode are shown in Fig. 6.

3.2.2.4. *Calculation and analysis of electrochemical parameters.* It must be emphasized that S_{EIE}, the interfacial area per unit gram, is a parameter derived after fitting the experimental results and from the electrochemical point of view, it is a measure of the real area that takes part in the electrode reaction. This is a point of extreme importance because the data provided by the BET method for specific area give information about the whole material used in the experiment, while the interfacial area identified from the EIS analysis, is real information about the fraction of material that actually participates in the electrode/solution interfacial process.

The capacity of the electric double layer per electrode unit volume (C_{dl}) is obtained from the fitting procedure for each electrode. This parameter can be related to the values of C, obtained from CD measurements, when multiplied by the volume of each of the electrodes (LA_p). Thus, Table 2 shows the values of capacity obtained by CD and through the adjustment of the impedance measurements. C_{EIS} values are compared with those obtained at the lower currents used in this work, since C_{dl} is obtained from EIS measurements, in which it is determined the total interfacial area available. As can be seen, the tendency of both values match very well. The fact that the results are different is not strange, because the fitting procedure gives a value that represents the charge storage on the EDL and that obtained by CD features contributions from the electric double layer and faradaic charge transfer generated by surface groups of the carbons. Besides, the parameter L was not measured with a high precision.

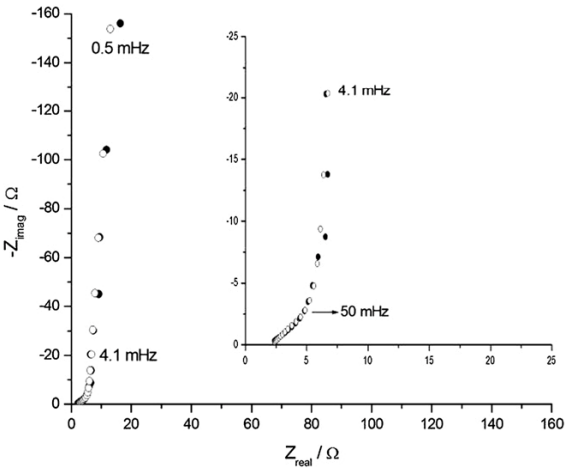

Fig. 6 – Experimental (●) and theoretical (○) spectra for M2 electrode. The insert shows the high-medium frequency range.

Table 2 – Capacity values obtained by CD and through the adjustment of the impedance measurements.

Muestra	C/Fg^{-1}	C_{EIS}/Fg^{-1}
M1	284	197
M2	230	174
M3	192	139
M4	180	133
S30	126	98

Commonly, charge densities in the double layer at plane electrodes are in the range of 1.6 10^{-5} to 5.10^{-5} Fcm^{-2} [1]. Assuming an average value of 3 $\times$ 10^{-5} Fcm^{-2} (C^0_{dl}), the interfacial area per electrode unit volume (a_i) for each electrode is obtained by means of the following equation,

$$C_{dl} = C^0_{dl} a_i \quad (6)$$

Table 3 contains the model parameters derived from the fitting procedure, corresponding to electrodes of different composition. The interfacial areas obtained from this method are quite similar for all the electrodes.

The electrochemically accessible carbon area, S_{EIE}, can be obtained after calculation of a_i,

$$S_{EIE} = \frac{a_i V}{m} \quad (7)$$

where V is the electrode volume and m is the total carbon mass. To find out the fraction of the total carbon area (sensed by N_2) that is accessible to the electrolyte, we define the accessibility parameter, A_c, as

$$A_c = S_{EIS}/S_{BET} \quad (8)$$

Table 3 exhibits the values of A_c obtained for each electrode. This parameter allows clarifying the differences in the capacities at low currents of each of the electrodes. The fact that C for M1 is higher than M2, the last with an interfacial area measured by BET significantly higher is because the electrolyte can access a much larger fraction of the porous matrix of M1 than to M2. While S30 has an area BET greater than the M3 and M4, the accessibility of the electrolyte to the porous matrix is much smaller, which leads to the fact that it is the carbon with lower C at low currents. In the same way can be explained the results for M3 and M4. While the latter has a significantly lower S_{BET}, the highest value of A_c generates similar capacities.

In addition, it must be pointed out the effective conductivity of the solid and of the electrolyte. Table 4 shows σ experimentally measured and σ_{EIS} and k_{EIS} determined with the adjustments of the impedance diagrams.

Table 3 – Values of A_c, S_{BET}, S_{EIS} and C_{dl} for all the electrodes.

Muestra	S_{BET}	C_{dl}	S_{EIS}	A_c	C
M1	1786	56	657	0.37	284
M2	2089	43	581	0.28	230
M3	1316	43	464	0.35	192
M4	995	45	422	0.42	180
S30	1664	35	345	0.21	126

Table 4 – Conductivity values obtained experimentally (σ) and from adjustment of impedance measurements (σ_{EIS} and k_{EIS}).

Muestra	$\sigma.10^2$	$\sigma_{EIS}.10^2$	$k_{EIE}.10^2$
M1	0.42	0.82	5.4
M2	0.66	1.7	5.4
M3	0.08	0.67	19.6
M4	0.09	0.52	1.3
S30	0.12	0.42	3.8

Results of solid conductivity values obtained by van der Pauw method and through EIS experiments show the same tendency. Because both, σ and κ, are expressed in Scm^{-1}, in order to make a direct comparison between the electrodes, σL and κL are the parameters that must be taken into account. Unluckily, the uncertainty on the measurement of the parameter L, make it impossible to analyze small differences between the electrode conductivities. On the other hand, these measurements allow concluding that in these materials, σ is the main responsible of the whole electrode resistivity, exhibiting in all electrodes less value than κ. However, for the electrode containing M4 and especially for that made of M2 is not possible to neglect any contribution to the total resistivity. As both of them have values of the same order, they contribute to the dynamic behavior of the electrode.

4. Conclusions

Carbon Xerogels with different pore size distribution were successfully obtained. Through basic electrochemical measurements, the dynamic behavior of every one electrode was evaluated. All xerogels, except for M3, showed higher capacities than the purchased carbon S30 for the currents employed in this work. Chronopotentiometry experiments performed at different discharge rates showed that M2 and S30 have similar behaviors; this fact allow concluding that the marked differences in C between these electrodes should be maintained using larger discharge currents. Electrochemical results show that through these carbons synthesis techniques it is possible to obtain very good materials to act as an SC.

Through a theoretical physicochemical model developed for porous electrodes, it was possible to obtain several parameters which permit to explain the different behavior of the electrodes. By comparing areas values obtained by BET method and from the EDL capacity obtained performing EIS experiments, the parameter A_c was proposed. It allows making a comparison of the electrolyte accessibility to the porous frame in each electrode, clearing up the differences in C at low currents.

Acknowledgments

This work was supported by: CONICET, Consejo Nacional de Investigaciones Científicas y Técnicas of Argentina, the Agencia Nacional de Promoción Científica y Tecnológica and the Universidad Nacional de La Plata. The financial support

received from the Government of Principado de Asturias PCTI (Ref. IB09-00201) and Ministerio de Ciencia e Innovación (Ref. MAT2008-00217/MAT) is also greatly acknowledged. E.G. Calvo also acknowledges a predoctoral research grant from FICYT.

REFERENCES

[1] Conway BE. Electrochemical supercapacitors. Scientific Fundamentals and Technological Applications. New York: Kluwer Academic/Plenum Publishers; 1999.
[2] Obreja VVN. On the performance of supercapacitors with electrodes based on carbon nanotubes and carbon activated material—A review. Physica E 2010;40:2596–605.
[3] http://www.panasonic.com/industrial/batteries-oem/oem/lithium-ion.aspx.
[4] Zubizarreta L, Arenillas A, Pis JJ, Pirard V, Job N. Studying chemical activation in carbon xerogels. J Mater Sci 2009;44:6583–90.
[5] Stoeckli F, Centeno TA. On the determination of surface areas in activated carbons. Carbon 2005;43:1184–90.
[6] Dubinin MM. Porous structure and adsorption properties of active carbons. In: WalkerJr PL, editor. Chemistry and physics of carbon, vol. 2. New York: Marcel Dekker; 1966. p. 51–120.
[7] Calvo EG, Juárez-Pérez EJ, Menéndez JA, Arenillas A. Fast microwave-assisted synthesis of tailored mesoporous carbon xerogels. J Colloid Interf Sci 2011;357:541–7.
[8] Dubinin MM. In: Danielli JF, Rosenberg MD, Cadenhead D, editors. Progress in surface and Membrane Science, vol. 9. New York: Academic Press; 1975.
[9] Stoeckli HF, Ballerini L. Evolution of Microporosity during activation of carbon. Fuel 1991;70:557–60.
[10] Parra JB, de Sousa JC, Bansal RC, Pis JJ, Pajares JA. Characterization of activated carbons by the BET equation-an alternative approach. Adsorpt Sci Technol 1995;12:51–66.
[11] van der Pauw J. A method of measuring specific resistivity and Hall effect of discs of arbitrary shape. Philips Res Repts 1958;13:1–9.
[12] Sing KSW. Reporting physisorption data for gas/solid systems with Special reference to the determination of surface area and porosity. Pure Appl Chem 1985;57:603–19.
[13] Rodríguez J, Elola D, Laria D. Confined Polar Mixtures within Cylindrical Nanocavities. J Phys Chem B 2010;114:7900–8.
[14] Fernández PS, Castro EB, Real SG, Martins ME. Electrochemical behaviour of single walled carbon nanotubes – Hydrogen storage and hydrogen evolution reaction. Int J Hydrogen Energy 2009;34:8115–26.
[15] de Levie R. On porous electrodes in electrolyte solutions. Electrochim Acta 1963;8:751–80.
[16] Castro EB, Real SG, Bonesi A, Visintin A, Triaca WE. Electrochemical impedance characterization of porous metal hydride electrodes. Electrochim Acta 2004;49:3879–90.
[17] Meyers JP, Doyle M, Darling RM, Newman JJ. The impedance response of a porous electrode composed of intercalation particles. J Electrochem Soc 2000;147:2930.
[18] Nelder JA, Mead R. A simplex method for function minimization. Comput J 1965;7:308–13.
[19] Visintin A, Castro EB, Real SG, Triaca WE, Wang C, Soriaga MP. Electrochemical activation and electrocatalytic enhancement of a hydride-forming metal alloy modified with palladium, platinum and nickel. Electrochim Acta 2006;51:3658–67.

5.2. ELECTROLITO

Como se ha mencionado en la Introducción de la presente memoria, existen diferentes tipos de electrolitos para supercondensadores, y la elección de uno u otro condiciona el voltaje de celda utilizado. Los electrolitos basados en disoluciones acuosas son unos de los más extensamente estudiados para este tipo de dispositivos electroquímicos debido a su bajo coste, fácil manipulación y mayor conductividad iónica que los electrolitos orgánicos, por ejemplo [CHAE, 2012; PANDOLFO, 2006; KHOMENKO, 2010; YANG, 2011]. Además, las disoluciones acuosas constituyen el medio que más favorece las reacciones redox que tienen lugar entre los grupos superficiales del material de electrodo y el electrolito, incrementando, por tanto, la capacidad del supercondensador debido a fenómenos faradaicos [EVANS, 1966; SIVAKKUMAR, 2007]. Pese a sus importantes prestaciones, el principal inconveniente de los electrolitos acuosos es el reducido voltaje de operación que ofrecen, ya que está limitado por la descomposición electrolítica del agua que tiene lugar a ~ 1.23 V [PANDOLFO, 2006; YANG, 2011]. La problemática del reducido voltaje de trabajo se resuelve mediante el uso de electrolitos de naturaleza orgánica. Sin embargo, dichos electrolitos llevan asociados una mayor resistividad, lo que supone un empeoramiento en el comportamiento electroquímico del dispositivo, mayores costes de fabricación de los módulos y, además, que a menudo no cumplan los requisitos de compatibilidad medioambiental y de seguridad exigidos, debido a la generación de vapores, inflamabilidad y toxicidad de los disolventes orgánicos [BURKE, 2000; WU, 2013].

Como consecuencia de las limitaciones asociadas a los electrolitos acuosos y orgánicos, recientemente han surgido nuevas líneas de investigación cuyo interés va dirigido hacia el reemplazo de las disoluciones comúnmente utilizadas por un nuevo tipo de electrolito basado en líquidos iónicos. Los líquidos iónicos permiten incrementar el voltaje de operación a valores cercanos a 3 V, lo que supone un significativo incremento en la capacidad de almacenamiento energético. Además, son electrolitos que presentan una elevada estabilidad térmica, baja inflamabilidad y reducida volatilidad, por lo que están considerados como una de las alternativas más prometedoras para conseguir supercondensadores con elevadas prestaciones y compatibles con el medioambiente [ARBIZZANY, 2008; BALDUCCI, 2004].

De los tres tipos de electrolitos líquidos disponibles para supercondensadores, en este trabajo se han utilizado tanto disoluciones acuosas como líquidos iónicos próticos, en combinación con xerogeles de carbono altamente porosos (microporosidad notablemente desarrollada y cierta presencia de mesoporos).

5.2.1. Electrolitos acuosos

El estudio del comportamiento electroquímico de supercondensadores basados en un xerogel de carbono activado (CO_2 como agente activante) y disoluciones acuosas de diferente pH utilizadas como

electrolito aparece reflejado en la *Publicación VIII* adjuntada al final del presente apartado. Dicho trabajo, desarrollado durante una estancia en el grupo de investigación *Sistemi per Tecnologie Energetiche* (CNR-ITAE), dirigido por los Dres. P. Staiti y F. Lufrano, tiene dos objetivos claramente diferenciados: (i) evaluar la capacidad de almacenamiento energético de un xerogel de carbono altamente poroso mediante el uso de dos tipos de electrodos (obtenidos a partir de diferentes protocolos de preparación) y celdas electroquímicas de diferente dimensión y, (ii) determinar la influencia del pH del electrolito sobre los mecanismos de almacenamiento de energía eléctrica (doble capa eléctrica y/o pseudocapacidad) y, consecuentemente, sobre el comportamiento electroquímico de la celda.

A diferencia de otras publicaciones recogidas en este capítulo, los electrodos utilizados en este trabajo están compuestos por un xerogel de carbono obtenido mediante un proceso de activación que emplea CO_2 como agente activante. Los procesos de activación química (KOH, H_3PO_4, $ZnCl_2$, etc.) precisan una etapa de lavado final cuyo objetivo es eliminar los restos de agente activante. Generalmente, son necesarias sucesivas etapas de lavado y, además, no siempre se puede obtener el material activado totalmente libre de impurezas [CONTRERAS, 2010; MACIÁ-AGULLÓ, 2004]. Por ello, en este trabajo se ha optado por llevar a cabo un proceso de activación física ya que, además de ser un método de activación más sencillo y rápido, produce xerogeles de carbono con una estructura porosa muy desarrollada (elevado volumen de microporos y presencia de mesoporos con un diámetro comprendido entre 2-18 nm).

Como se ha comentado en líneas superiores, dos han sido los objetivos perseguidos con la realización de este trabajo. Por ello, el estudio electroquímico mostrado en la *Publicación VIII* se encuentra dividido en dos partes: (i) caracterización electroquímica de dos tipos de celdas compuestas por electrodos (basados en un xerogel de carbono activado) fabricados mediante dos métodos diferentes (H_2SO_4 1 M como electrolito) y, (ii) evaluación de la capacidad de almacenamiento energético de una celda electroquímica con tres disoluciones acuosas de diferente pH (H_2SO_4, Na_2SO_4 y KOH).

Antes de dar paso a las conclusiones más importantes extraídas de este trabajo, es importante puntualizar los dos tipos de protocolos utilizados para la fabricación de los electrodos (uno de ellos empleado en el grupo *Microondas y Carbones para Aplicaciones Tecnológicas,* INCAR-CSIC, y el otro desarrollado en el grupo de investigación *Sistemi per Tecnologie Energetiche*, CNR-ITAE). Los electrodos producidos en el Instituto Nacional del Carbón se componen de una mezcla de xerogel de carbono (90 %) y polímero ligante, PTFE, (10 %). Por contra, el otro tipo de electrodos estudiados contienen, además, una cantidad determinada de fibras de grafito cuyo objetivo es mejorar sus propiedades mecánicas y conductoras (80 % xerogel de carbono, 10 % polímero ligante, PVDF, y 10 % fibras de grafito). Además, la mezcla se somete a un tratamiento térmico que da lugar a electrodos con todavía mejores características mecánicas y eléctricas.

En cuanto al primer objetivo propuesto en la *Publicación VIII*, la principal conclusión derivada del estudio electroquímico es la siguiente:

❖ El procedimiento seleccionado para la elaboración de los electrodos tiene cierta relevancia sobre el comportamiento final del supercondensador. Los electrodos denominados E4 (electrodos constituidos por una mezcla de xerogel de carbono + polímero ligante + fibras de grafito, con un tamaño de 4 cm^2) son capaces de almacenar mayor cantidad de energía eléctrica. Además, de acuerdo con los resultados derivados de los ensayos de voltametría cíclica, las celdas ensambladas con este tipo de electrodos presentan una menor resistividad, probablemente como consecuencia de las mejores propiedades mecánicas y eléctricas asociadas a los electrodos E4.

El xerogel de carbono utilizado como material de electrodo en este trabajo presenta cierta cantidad de funcionalidades oxigenadas (contenido en O = 2.1 %). Con el objetivo de definir el carácter de dichos grupos oxigenados se realizaron ensayos de TPD, los cuales evidenciaron el carácter fundamentalmente básico (grupos tipo carbonilo y quinona, véase Figura 5.3) de los grupos superficiales encontrados en el xerogel de carbono. Como consecuencia del carácter ligeramente básico del material de electrodo utilizado, se seleccionaron disoluciones acuosas de diferente pH para evaluar la relación que existe entre el pH del medio y la actividad de los grupos presentes en la superficie del electrodo y, por tanto, la consecuencia que esto tiene sobre la capacidad de almacenamiento energético del dispositivo.

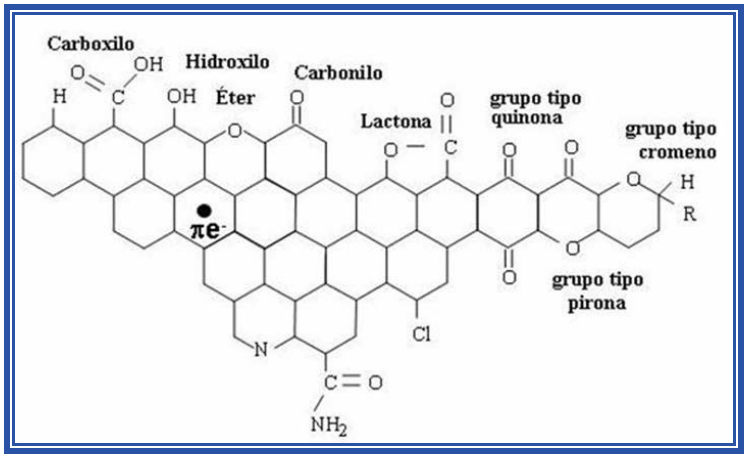

Figura 5.3. Principales grupos funcionales que se pueden encontrar en la superficie de un material carbonoso.

Para poder llevar a cabo el segundo objetivo se construyeron celdas electroquímicas con electrodos tipo E4 y electrolitos basados en disoluciones de H_2SO_4, Na_2SO_4 y KOH (1 M). Se realizaron diferentes ensayos electroquímicos, tests de voltametría cíclica, cronoamperometría y espectroscopía de impedancia, y todos ellos dieron lugar a las siguientes conclusiones:

❖ Tanto el pH del electrolito como la química superficial del material de electrodo son factores que determinan la capacidad de almacenamiento energético de los dispositivos evaluados. De esta manera, se ha podido observar como el medio ácido lleva asociado un almacenamiento de energía más elevado (C en torno a 200 F g^{-1}), fundamentalmente como consecuencia de su mayor conductividad iónica y mayor contribución de fenómenos pseudocapacitivos. Esta última afirmación está relacionada con la actividad de los grupos funcionales oxigenados presentes en la superficie del xerogel de carbono. Las funcionalidades oxigenadas encontradas son, mayoritariamente, de carácter básico y, de acuerdo con los resultados obtenidos, hay evidencias de que estos grupos son más activos cuanto menor es el pH del electrolito utilizado.

❖ La celda electroquímica formada por el par xerogel de carbono/KOH da lugar a un almacenamiento de energía de origen puramente electrostático. La técnica de cronoamperometría revela una independencia de la capacidad de almacenamiento de energía con la densidad de carga aplicada, sugiriendo la ausencia total de fenómenos de oxido-reducción entre la superficie del electrodo y el electrolito.

❖ La evaluación de la respuesta electroquímica del xerogel de carbono con las tres disoluciones acuosas de distinto pH da una idea de la viabilidad de estos electrolitos para ser aplicados en un dispositivo real. Pese al mayor almacenamiento de carga conseguido en medio ácido, el carácter corrosivo del ácido sulfúrico limita seriamente su aplicación en supercondensadores comerciales. Por ello, y puesto que el Na_2SO_4 también promueve el almacenamiento de energía eléctrica a niveles elevados (capacidad específica próxima a 150 F g^{-1}), supercondensadores basados en este tipo de electrolito serían más adecuados tanto desde un punto de vista de la seguridad como de la conservación de los componentes de la celda electroquímica.

Publicación VIII

OPTIMIZING THE ELECTROCHEMICAL PERFORMANCE OF AQUEOUS SYMMETRIC SUPERCAPACITORS BASED ON AN ACTIVATED CARBON XEROGEL

Journal of Power Sources

(aceptada)

Año: 2013

Optimizing the electrochemical performance of aqueous symmetric supercapacitors based on an activated carbon xerogel

E. G. Calvo[1,2], F. Lufrano[2], P. Staiti[2], A. Brigandì[2], A. Arenillas[1*], J.A. Menéndez[1]

[1] Instituto Nacional del Carbón CISC, Apartado 73, 33080 Oviedo, Spain

[2] CNR-ITAE, Istituto di Tecnologie Avanzate per L´Energia "Nicola Giordano", Via Salita S. Lucia, 5, 98126 Messina, Italy

Abstract

A highly porous carbon xerogel was synthesized by means of physical activation. The precursor used was an organic xerogel obtained from resorcinol and formaldehyde polymerization. The activated carbon xerogel, which displayed a well-developed porous texture (high microporosity and a remarkable V_{meso}), was employed as electrode material in different supercapacitors. In assessing the performance of the supercapacitors, special attention was paid to their dimensions and the type of electrolyte used. The same xerogel was employed in all the electrochemical cells. However, both the method of electrode manufacture (rolling and punching of 1 cm^2 pellets and casting by means of a film applicator to produce 4 cm^2 electrodes) and the type of supercapacitor (swagelok system vs. cell with graphite plate current collectors) were evaluated. The results reveal that the cells with larger electrodes were able to store higher amounts of energy. In addition to the cells, the electrochemical characteristics of the carbon xerogel-based electrodes in aqueous electrolytes with a different pH were studied (H_2SO_4, Na_2SO_4 and KOH, 1 M). The highest capacitance values were achieved with sulfuric acid (196 F g^{-1} as opposed to 140 and 106 F g^{-1} for Na_2SO_4 and KOH, respectively), probably due to its higher ionic conductivity and the basic nature of the oxygen functionalities found on the surface of the carbon xerogel. Nevertheless, because of the corrosive character of sulphuric acid, Na_2SO_4 would be a more suitable electrolyte.

Keywords: Carbon xerogel; Supercapacitor; Electrode manufacturing process; Aqueous electrolyte.

*Corresponding author. Tel.: +34 985 11 90 90; Fax: +34 985 29 76 62.

E-mail address: aapuente@incar.csic.es (A. Arenillas).

1. Introduction

Electrochemical capacitors, also known as supercapacitors, have attracted the interest of the scientific and industrial community due to a series of advantages including their high power density, long durability and maintenance-free operation [1-5]. These unique features make them suitable devices for a wide range of applications as hybrid electric vehicles, telecommunications systems, portable electronic applications or solar/wind power plants, all of which require a rapid storage and release of energy at high power rates [1,2,5]. Electric energy storage in carbon material-based supercapacitors is mainly based on the separation of charged species by means of the electric double-layer (EDL) formed at the electrode/electrolyte interface (purely electrostatic energy storage). However, charge storage capacity can be enhanced by redox reactions between electrolyte ions and electrode surface functionalities [1,4-7]. Both electric double-layer formation and pseudocapacitance are interfacial phenomena, so electrodes for this type of electrochemical device need to be composed of materials with a high specific surface area (S_{BET} > 2000 m^2 g^{-1}). Furthermore, when the charge storage is the result of faradaic reactions, electroactive species must be present on the electrode surface (i.e. O, N, B, P, etc.) in combination with aqueous electrolytes [4-7].

Aqueous solutions have several advantages over organic electrolytes since, firstly, they allow oxidation/reduction processes between electrolyte ions and the electrode surface, thereby facilitating extra energy storage and, secondly, they are cheaper, environmentally friendly and more conductive [8-11]. However, although aqueous solutions are more favourable, their main limitation is a reduced energy storage capacitance due to their low operating voltage (theoretical stability window of water = 1.23 V). In recent years, several strategies have been proposed to increase the working voltage in aqueous supercapacitors (for example, the use of asymmetric systems based on dissimilar electrode materials [12-16]). Furthermore, as mentioned above, specific capacitance can be increased by means of pseudo-faradaic reactions. These reactions occur between ions from the aqueous solution and functionalities in the electrode material. Thus, the type and pH of the electrolyte and cation/anion size have a considerable impact on the pseudo-faradaic processes. Several studies relating to the use of different aqueous solutions as electrolyte in supercapacitors can be found in the literature [8-11,17]. Zhang et al. [11] prepared carbon based-supercapacitors with aqueous solutions with a different pH and they achieved higher gravimetric capacitance values using a solution of KOH, 6 M (supercapacitor capacitance ~ 60 F g^{-1}). Andreas and co-workers [17] also evaluated the effect the electrolyte pH on the charge-storage capacitance of a carbonaceous electrode (highly porous C-cloth) and they obtained a much higher energy storage by using an acidic media (H_2SO_4 1 M), as a result of the pseudocapacitance of the quinone-type surface functionalities. These two examples show that pseudocapacitance is not only directly related to the pH of the electrolyte but also to the surface

chemistry of the carbon electrode, since each type of surface functionality is oxidised/reduced under different pH conditions.

It is well known that highly porous carbon electrodes are required for superior performance supercapacitors. Microporosity is especially important since it is in the micropores where charge storage takes place. However, larger pore sizes (mesopores) also favour the process as a faster diffusion of electrolyte ions into the micropores is thereby achieved [1,18,19]. For this reason, one of the most promising carbon materials for charge storage is carbon gel. This carbonaceous material is characterised by: (i) a porous structure tuneable according to the synthesis and processing conditions, (ii) a high surface area and porosity, (iii) a high electrical conductivity and finally, (iv) an excellent cycling behaviour, all properties that make them ideal materials for electrochemical applications [12,20-25]. Another required characteristic of any electrode material for supercapacitors is an acceptable production cost. Until recently, carbon xerogels did not satisfy this requirement since they were obtained from a long, tedious and, therefore, rather expensive procedure. However, this problem was solved in 2009 when Arenillas and co-workers [26] showed that it was possible to design and produce carbon xerogels by means of a faster, easier and cheaper synthesis process based on microwave radiation.

Thus, the objective of the present work is to produce high-performance carbon xerogel-based electrodes and evaluate their energy storage capacitance in different types of aqueous supercapacitors. For this purpose, a resorcinol-formaldehyde carbon xerogel was fabricated by means of microwave-assisted synthesis followed by an activation process (using CO_2 as activating agent) in order to increase the microporosity of the final material and thereby improve its charge storage capacity. The electrochemical behaviour of the carbon xerogel was studied in electrochemical cells of diverse dimensions. The electrodes were produced by using two different preparation methods. Furthermore, in order to investigate the effect of the pH media on the electrochemical performance and, more specifically, on the pseudo-faradaic phenomena of the carbon electrode, three aqueous solutions with different pH were employed as electrolyte (H_2SO_4, Na_2SO_4 and KOH, 1M).

2. Experimental

2.1. Preparation of the carbon xerogel

The precursor material used in the activation process was an organic xerogel obtained from the polymerisation of resorcinol and formaldehyde. The pH of the resorcinol/formaldehyde mixture was adjusted to a value of 6.5 by adding drops of a sodium hydroxide solution (1 M). Once the precursor solution was prepared, it was subjected to microwave heating in order to induce and accelerate polymerization reactions between the two types of monomers. More details on the microwave-assisted

synthesis of organic xerogels can be found in Ref. [27] and [28]. The organic xerogel (OX) obtained had a specific surface area, S_{BET}, of around 200 m^2 g^{-1} and a helium density of 1.3 g cm^{-3}.

The OX sample was crushed and sieved to between 1 and 2 mm before the physical activation. The device used for the activation process was a vertical tubular reactor, previously purged with nitrogen for approximately 20 minutes. The activation temperature was 1000 ºC, the heating rate 50 ºC min^{-1} and the sample was kept at this maximum temperature for 2 hours.

2.2. Physicochemical characterization of the activated carbon xerogel

The textural characteristics of the activated carbon xerogel, ACX, were evaluated from the N_2 adsorption-desorption isotherms recorded at 77 K (*Micromeritics Tristar 3020*). The specific surface area, S_{BET}, was calculated by means of the BET equation and the micropore volume (V_{DUB-N2}) was determined by applying the Dubinin-Raduskevich (DR) method to the N_2 adsorption isotherm. The pore size distribution was obtained by applying the DFT method and the total pore volume (V_p) was ascertained from the amount of nitrogen adsorbed at saturation point ($p/p^o = 0.99$).

The chemical properties of the ACX sample were evaluated by elemental analysis. The C, N and H content was determined on a *LECO-CHNS-932* microanalyzer and the amount of oxygen with a *LECO-TF-900*. The surface chemistry characterization was carried out by temperature-programmed desorption (TPD) measurements and from the point of zero charge (PZC). TPD experiments were performed on a *Micromeritics AutoChem II* analyzer, by heating the samples up to 1000 ºC in an Argon flow (50 cm^3 min^{-1}) at a heating rate of 10 ºC min^{-1}. The amount of CO, CO_2 and H_2O desorbed was monitored on a mass spectrometer (*OmniStar Pfeiffer*).

2.3. Electrode preparation

To conduct the experiments shown in this study, two types of electrode were prepared: (i) 1 cm^2 disc-shaped electrodes with a thickness of 200-300 μm and, (ii) 4 cm^2 square- shaped electrodes with a thickness of 250-300 μm.

The disc-shaped electrodes were prepared by mixing the activated carbon xerogel (90 wt. %) and polytetrafluoroethylene (PTFE) binder (10 wt. %). The PTFE binder was a solution 60 wt. % in H_2O (Aldrich). Once a homogeneous mixture of both compounds was obtained, the slurry of the mixture was rolled out in order to form a thin film. Electrodes were manufactured by punching pellets (diameter = 1 cm) from the composite based paste. Afterwards, they were pressed and dried before being inserted into the electrochemical cells. The weight of the 1 cm^2 electrodes ranged between 5-6 mg.

The larger size electrodes (4 cm^2, square in shape) used for this study were prepared using a casting procedure. A slurry was obtained from mixing the ACX sample (80 wt. %), graphite fibers (10 wt. %), polyvinylidene fluoride (PVDF) binder (10 wt. %) and the solvent N,N-dimethylacetamide (DMA). In this case, the binder used was a solution 2 wt. % PVDF in DMA. The slurry was then spread over a glass plate by means of a film applicator and left to evaporate at 50 ºC for at least 15 h. The composite electrode thus formed was further dried at 70 ºC and then thermally treated at 160 ºC for 20 min to improve the mechanical strength of the electrodes. The electrodes mass ranged between 20-30 mg, but due to their large size, the densities were very similar to those of the previous electrodes (~ 6 ± 1 mg cm^{-2}).

For purposes of identification, the electrodes were denoted as E1 (1 cm^2 pelletised electrodes) and E4 (4 cm^2 electrodes).

2.4. Electrochemical measurements

Electrode material characterization was performed using a two-electrode cell configuration. This configuration was selected because it provides the most accurate measurements of electrode material performance in supercapacitors. Two supercapacitors with different dimensions were assembled in order to evaluate the electrochemical performance of activated carbon xerogel. One of these was a Teflon Swagelok ® two-electrode cell filled with stainless steel current collectors, a fibre glass separator (400 μm) and two E1 electrodes. The other cell was composed of two 4 cm^2 electrodes (E4) separated by a porous paper of around 60 μm thickness (NKK-Japan) and graphite plate current collectors. The electrolytes employed in both of the assembled cells were: H_2SO_4, Na_2SO_4 and KOH solutions (1 M).

The electrochemical measurements were carried out using a potentiostat/galvanostat *Autolab PGSTAT 30* (Eco Chemie, BV, The Netherlands) and the following techniques: (i) cyclic voltammetry at different voltage sweep rates (from 2 to 100 mV s^{-1}) in a voltage window of 1.0 V; (ii) galvanostatic charge/discharge measurements at several current densities (in the range of 0.2-1.0 A g^{-1}) with U = 1.0 V and, (iii) impedance spectroscopy at frequencies ranging between 10 MHz and 1 mHz and with open circuit voltage. The impedance measurements were performed using a potentiostat PGSTAT 30 equipped with a FRA2 module. Due to the different ACX ratios used in each type of electrodes, the specific capacitance values (calculated from the galvanostatic charge/discharge cycles) were expressed in Farads per mass of active material per electrode (F g^{-1}).

3. Results and discussion

3.1. Physicochemical properties of ACX xerogel

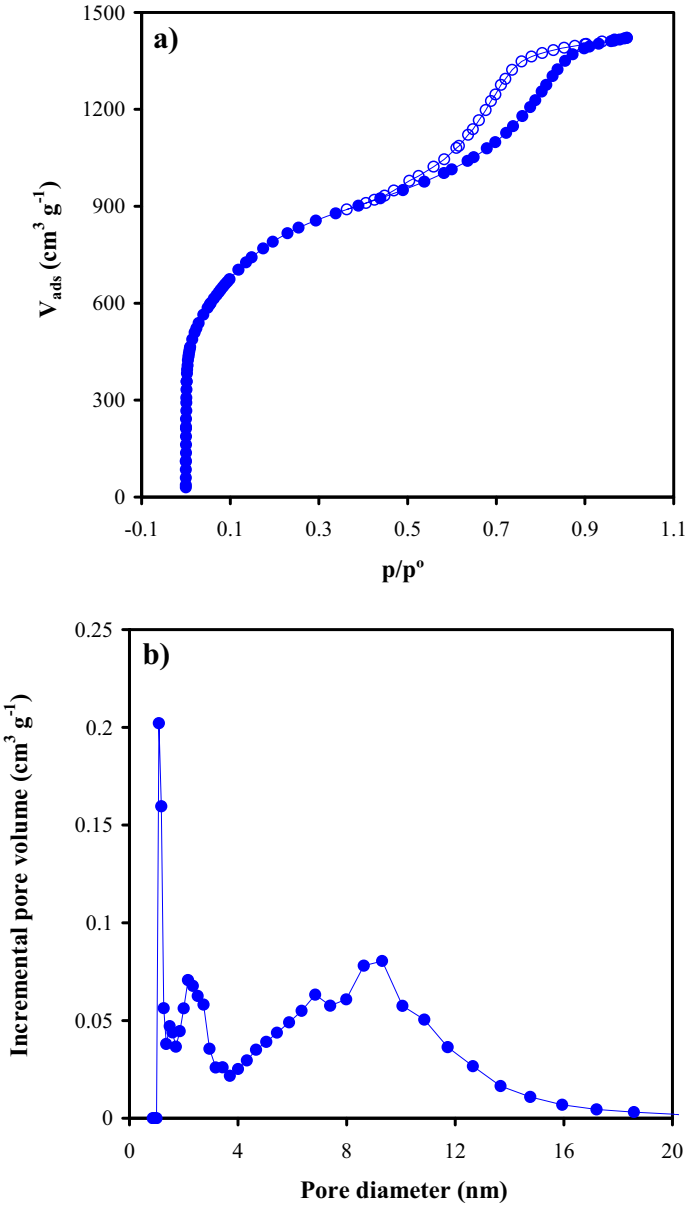

Figure 1. N_2 adsorption-desorption isotherm (a) and pore size distribution (b) for the activated carbon xerogel used as electrode material.

The N_2 adsorption-desorption isotherm of the carbon xerogel (Fig. 1a) is a combination of type I and type IV isotherms (micro-mesoporous materials) according to the IUPAC classification [29]. It displays a remarkable hysteresis loop (p/p^o ranging from 0.5 to 0.9), which is related to the presence of medium size mesopores, as is evidenced by the pore size distribution (PSD) shown in Fig. 1b. From this PSD, it can be seen that this activated carbon xerogel has a well-developed porosity. On the one hand, there is an ample volume of micropores (i.e. V_{DUB-N2} close to 1 cm^3 g^{-1}), whose diameter is

approximately 1.5 nm, and, on the other hand, there are two different mesopore groups (narrow mesopores with a pore diameter between 2 and 4 nm, and medium size mesopores with a pore diameter that does not exceed 16 nm). All of the information provided by Fig. 1, is corroborated by the pore data collected in Table 1.

Table 1 – Physico-chemical characteristics of the activated carbon xerogel synthesized

N_2 adsorption (77 K)			Elemental analysis (wt. % db[b])				PZC
S_{BET} ($m^2\ g^{-1}$)	V_{DUB-N2} ($cm^3\ g^{-1}$)	V_{meso}[a] ($cm^3\ g^{-1}$)	C	H	O	N	
2876	0.97	1.28	97.5	0.3	2.1	0.1	8.3

[a] $V_{meso} = V_p - V_{DUB-N2}$, where V_p is the adsorbed volume at saturation point ($p/p^o = 0.99$)
[b] Dry basis

Table 1 also contains data concerning the chemical characterization of the ACX sample. As can be seen, the carbon xerogel is mainly composed of C (around 97 wt. %) with a small amount of oxygen (i.e. O = 2.1 wt. %). Although the presence of oxygen is only slight, it was necessary to identify the type of oxygen functionalities observed on the carbon xerogel surface. For this purpose, the point of zero charge (pH_{PZC}) was calculated and temperature programmed desorption experiments were carried out. The basic pH_{PZC} (with a value of 8.3) indicates that the oxygen groups have a slightly basic nature, which is corroborated by the TPD results collected in Fig. 2. From the profiles of CO and CO_2 vs. temperature, it can be seen that the presence of oxygen functionalities desorbing as CO_2 (carboxylic acids, anhydrides, lactones [20-32]) is lower and only one peak close to 300 ºC is observed. The profile of CO presents a maximum peak at around 850 ºC, which can be attributed to carbonyl and quinone-like groups, but a small peak that appears at a temperature of approximately 300 ºC can also be observed. Both the pH_{PZC} value and the TPD spectra confirm the basic character of the carbon xerogel synthesized in this work. Three aqueous solutions with a different pH were used as electrolyte and therefore, electrode-electrolyte interface of different nature are expected.

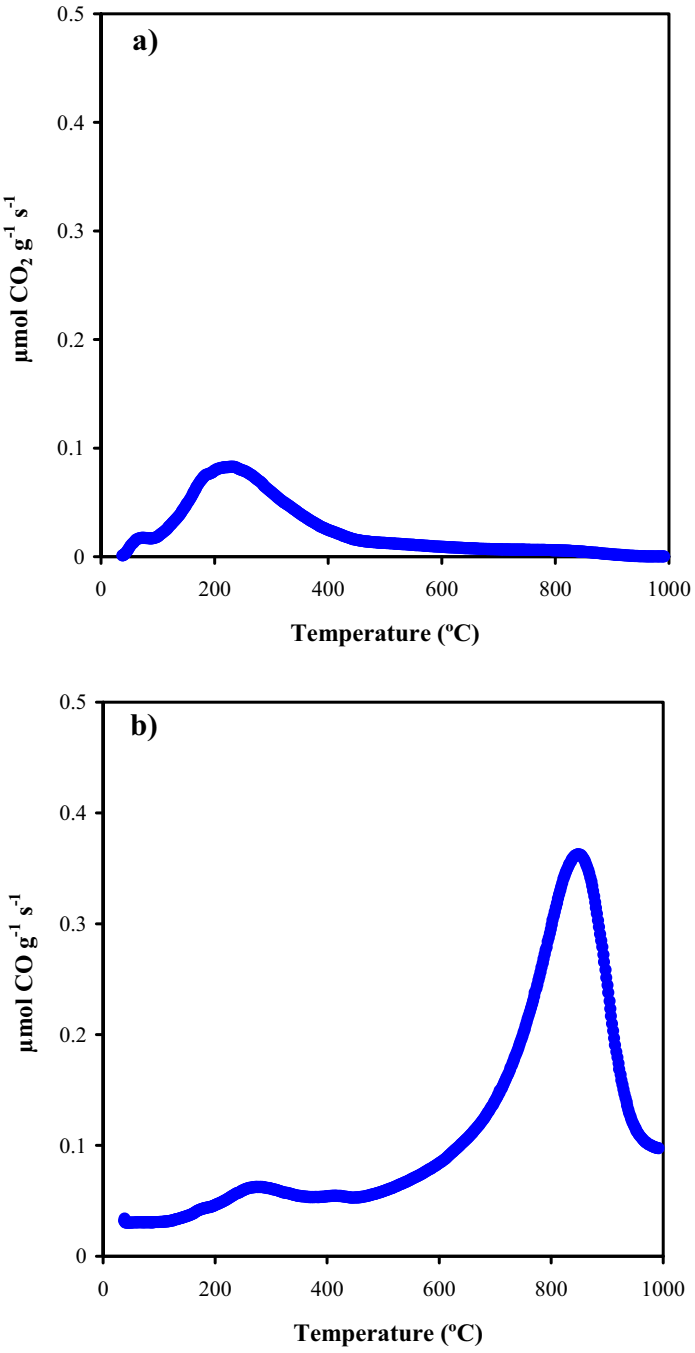

Figure 2. CO_2 (a) and CO (b) profiles obtained by TPD experiments for ACX sample.

3.2. Supercapacitor performance

3.2.1. Electrochemical behaviour of supercapacitors with different dimensions

As mentioned in the experimental section, the two types of electrodes were prepared using a specific manufacturing procedure and a particular electrode size (1 and 4 cm^2). Furthermore, the cells used in each case for the electrochemical tests were also different (a Swagelok® cell fitted with stainless steel collectors vs. graphite plate current collectors).

Cyclic voltammograms of the electrochemical cells with H_2SO_4 1M as electrolyte and E1 (grey circles) and E4 (black circles) type electrodes are presented in Fig. 3 (voltage range of 1.0 V and scan rate = 10 mV s^{-1}). No significant contribution was observed from the redox reactions involving oxygen functionalities, due to the limited amount of oxygen contained in the carbon xerogel that was used as electrode material (O = 2.1 wt. %). However, although both voltammograms present the typical rectangular behaviour expected for an ideal supercapacitor with quick charge propagation, a slight distortion can be appreciated in the curve obtained with the 1 cm^2 two-electrode cell (E1), possibly as a result of the contact resistance between the electrodes and current collectors (the ionic resistance of the electrolyte solution, H_2SO_4, is assumed to be the same in both cases) and the method of preparing the electrodes. The addition of carbon fibers and the heat treatment to which the 4 cm^2 electrodes were subjected, were intended to enhance their mechanical and electrical properties and, according to the results presented in this section, it seems that little improvement was achieved.

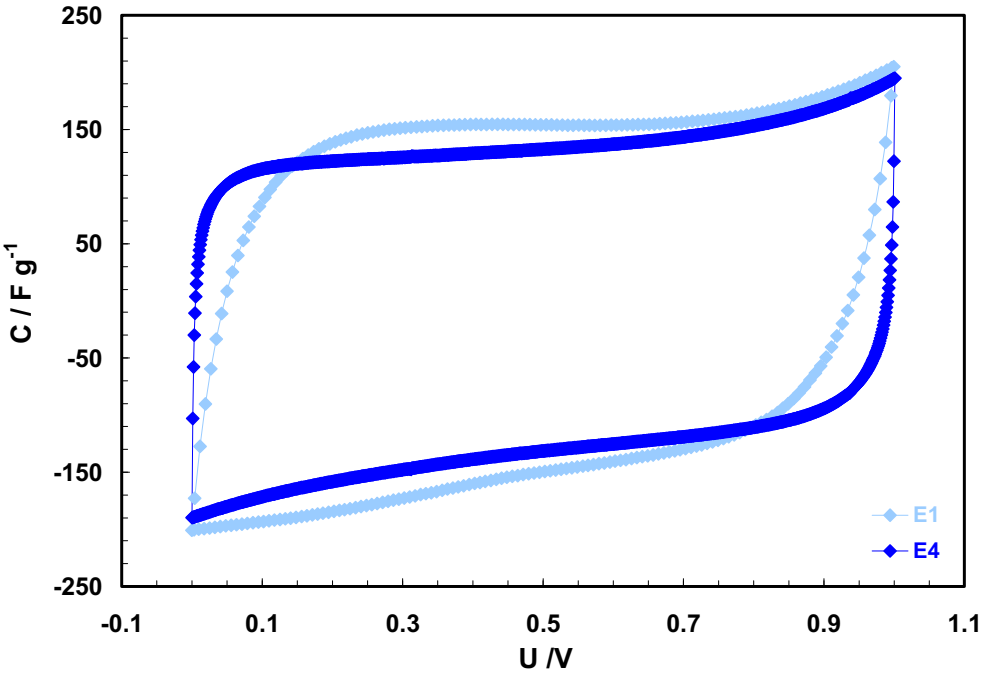

Figure 3. Cyclic voltammograms for supercapacitors using H_2SO_4 1.0 M as electrolyte and carbon xerogel-based electrodes of different size (scan rate = 10 mV s^{-1}).

Fig. 4 shows the specific capacitance values for the carbon xerogel-based electrode (E1 as opposed to E4) as a function of current density. The data were derived from the galvanostatic charge/discharge profiles obtained using different current loads (from 0.2 to 1.0 A g^{-1}) in a voltage window of 1.0 V. As expected, energy storage capacitance decreases as the current density increases, from 196 to 173 F g^{-1} for the type E4 electrodes and from 179 to 147 F g^{-1} for the 1 cm^2 electrodes. However, the most interesting feature of these results concerns the high energy storage capacitance achieved with the carbon xerogel (values close to 200 F g^{-1}). Also, worthy of note are the excellent electrochemical performance of the E4 type electrodes (i.e., those with an electrode surface of 4 cm^2 and better

mechanical properties), and the high carbon loadings (~ 5 mg cm^{-3}), which suggests that with electrodes based on carbon xerogels and produced on an industrial scale (optimized manufacturing process), energy storage devices with a high specific capacitance can be obtained.

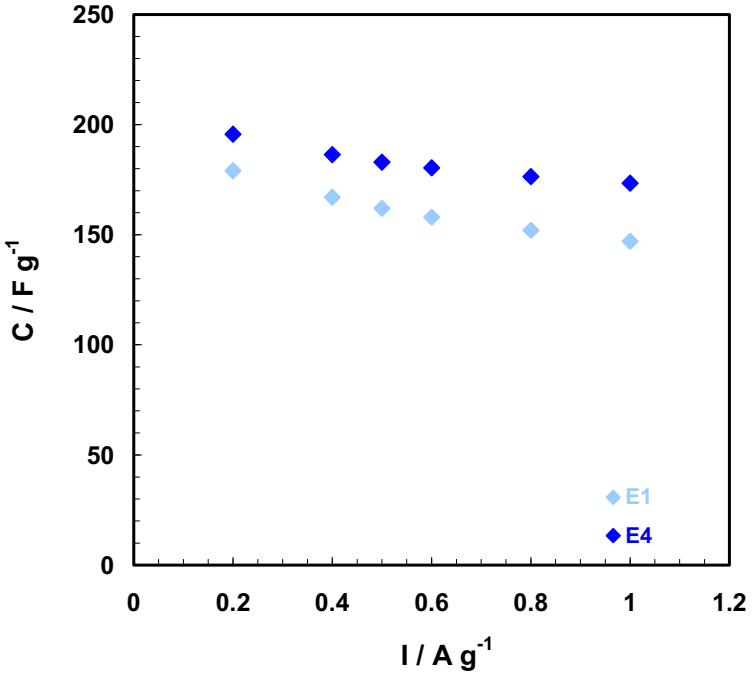

Figure 4. Variation of specific capacitance (F g^{-1}) with current density for cells built with 1 and 4 cm^2 electrodes and H_2SO_4 1M as electrolyte (maximum voltage = 1.0 V).

3.2.2. Influence of the electrolyte pH on the energy storage capacitance of activated carbon xerogel

The carbon xerogel synthesized in this work was tested as supercapacitor electrode material (electrode surface: 4 cm^2) in aqueous solutions with a different pH (H_2SO_4, Na_2SO_4 and KOH). It is well known that the nature of the electrolyte influences the charge storage capacity of the electrode material via: (i) the ionic radius of the electrolytes (free and solvated ion electrolyte), (ii) the conductivity of the ions and, (iii) ion mobility [11]. The radiuses of the solvated anions and cations in bulk solution for the electrolytes used in this study are: 3.58 Å (Na^+), 3.31 Å (K^+), 2.80 Å (H^+), 3.79 Å (SO_4^{2-}) and 3.00 Å (OH^-) [11,33]. In addition to the different ionic radiuses, which affect the access of the ions to the pores of the electrode material, ionic conductivity is also a crucial factor that affects the performance of the supercapacitor. The molar conductivities of the ions used in this work are: 50.1 $cm^2\ \Omega^{-1}\ mol^{-1}$ (Na^+), 73.5 $cm^2\ \Omega^{-1}\ mol^{-1}$ (K^+), 349.8 $cm^2\ \Omega^{-1}\ mol^{-1}$ (H^+), 79.8 $cm^2\ \Omega^{-1}\ mol^{-1}$ (SO_4^{2-}) and 198 $cm^2\ \Omega^{-1}\ mol^{-1}$ (OH^-) [11]. These data suggest that a different energy storage capacitance can be expected for each electrolyte and this diverse electrochemical performance may be closely related to the conductivity and mobility of the ions and the surface chemistry of the electrode material.

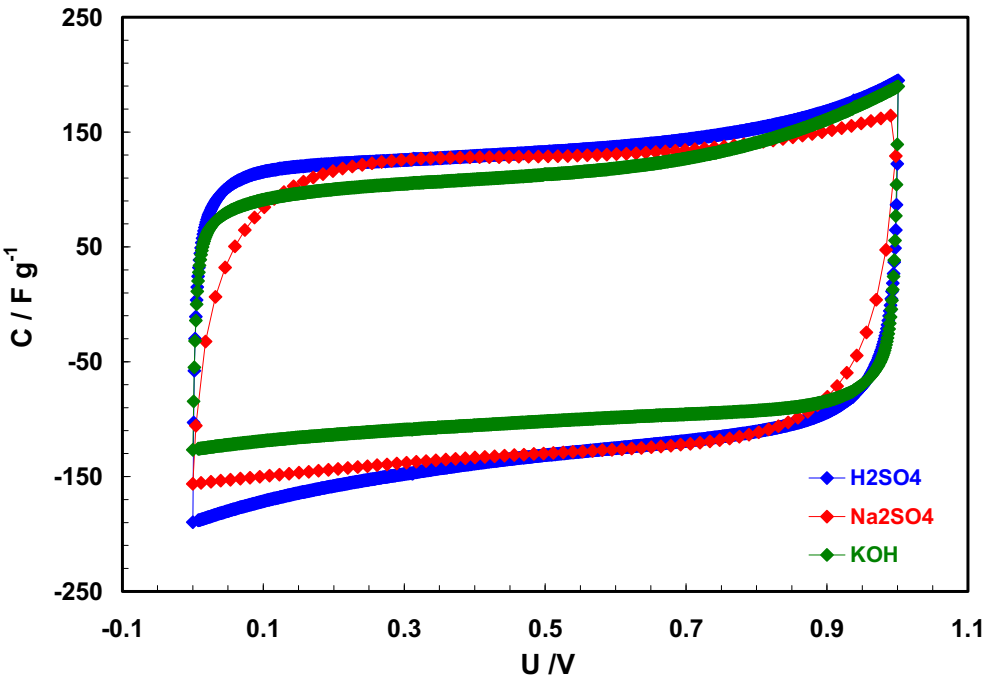

Figure 5. Cyclic voltammograms obtained in 2-electrodes cells (4 cm^2) and three electrolytes with different pH (H_2SO_4, Na_2SO_4 and KOH).

Fig. 5 compares the cyclic voltammograms of the supercapacitors assembled with ACX xerogel in various aqueous media (voltage range from 0 to 1 V; scan rate = 10 mV s^{-1}). As can be seen, the three solutions produce an almost box-shaped curve, reflecting the quasi-capacitive behaviour of the devices studied. Moreover, the figure evidences the largest specific capacitance obtained in the acidic medium, probably due to its higher ionic conductivity, which is consistent with the literature data [15,17,34]. The Na_2SO_4-based electrolyte produces almost the same electrochemical response as sulphuric acid. However, its higher resistivity, evidenced by a slight deviation from the box-like behaviour of the voltammogram, leads to a lower charge storage capacitance, as is confirmed by the galvanostatic charge-discharge results reported in Fig. 4.

The working voltage used in the cyclic voltammetry tests (U = 1.0 V) prevents water electrolysis (1.23 V) and, therefore, faradaic processes from occurring between the electrode material and electrolyte. One possible way to identify the presence of redox reactions, without appreciable peaks in the voltammograms, is to observe the dependence of energy storage on the scan rate or current density. Therefore, charge-discharge tests from 0 to 1 V were carried out using increasing current densities (from 0.2 to 1.0 A g^{-1}).

Table 2 – Specific capacitance (F g^{-1}) as a function of current density for ACX electrode in the three aqueous solutions

Electrolyte	Current density (A g^{-1})						C reduction (%)
	0.2	0.4	0.5	0.6	0.8	1.0	
H_2SO_4	196	186	183	180	176	173	11.7
Na_2SO_4	140	135	132	129	127	124	11.4
KOH	106	106	106	105	104	103	2.8

The gravimetric capacitance values (Farads per gram of ACX xerogel in one electrode) as a function of current density for the three media tested are listed in Table 2. When a neutral and acidic solution was used as electrolyte, there was a decrease in energy storage capacitance (a C reduction of 11.7 and 11.4 % for Na_2SO_4 and H_2SO_4, respectively, when the current load was increased from 0.2 to 1.0 A g^{-1}), suggesting the possible contribution of pseudo-capacitance to the charge storage [12, 35]. Both electrochemical systems were equally influenced by the current density. However, a higher specific capacitance was achieved with the H_2SO_4 electrolyte (i.e. 183 F g^{-1} as opposed to 132 F g^{-1} in the neutral electrolyte when the current density was 0.5 A g^{-1}), probably as a result of its higher conductivity, faster H^+ mobility in comparison to sodium cation (Na^+) and the greater activity of the basic oxygenated groups found on the surface of the electrode material in this acidic medium. Pseudocapacitive effects probably do not have the same origin in these two media since, in the case of H_2SO_4, pseudocapacitance is the result of redox reactions involving oxygen surface groups on the electrode material whereas in the case of the sodium sulphate electrolyte, it may also be in mind the contribution of extraction/insertion processes of Na ions contained in the solution [36], although the latter is believed to be minimised in the case of carbon materials.

In the alkaline electrolyte (KOH 1 M), there is virtually no dependency on the current load since the gravimetric capacitance is maintained at ca. 105 F g^{-1} throughout the range of currents studied. This reflects the strictly capacitive behaviour of the device. In other words, the oxygenated functionalities present on the electrode material surface are inactive in the basic medium. Consequently, the specific capacitance values are lower than those obtained with the other two electrolytes (e.g., 106 F g^{-1} when the current load was 0.5 A g^{-1} vs. 183 and 132 F g^{-1} for the other two solutions used). According to these results, a superior electrochemical performance was achieved with the H_2SO_4 solution due to its greater ionic conductivity, H^+ mobility and the activity of oxygen groups in the activated carbon xerogel. However, because of special requirements of commercial supercapacitors where a non-corrosive electrolyte is desired, Na_2SO_4 would be preferable to permit further scale-up, even though its slightly lower energy storage capacitance than the H_2SO_4 solution.

The electrochemical impedance spectroscopy (EIS) data were analyzed by means of Nyquist plots, in which imaginary impedance vs. real impedance as a function of frequency is plotted. The Nyquist diagram can also be used to obtain a better insight into the electrochemical behaviour of supercapacitors in different aqueous electrolytes. Because the carbon xerogel has surface oxygen functionalities, these can be expected to show different behaviours depending on the pH of the solution. The Nyquist plot of the AXC cells for the three aqueous electrolytes studied is shown in Fig. 6, with an enlarged view of the high frequency provided in the inset. All the devices display an almost pure capacitive behaviour because of the vertical data point distribution over the entire range of frequencies. A slight deviation (from vertical points) is observed for the supercapacitor equipped with the KOH (1M) electrolyte. The series resistances (high frequency region) of the devices are equivalent at 0.28, 0.37 and 0.68 ohm cm^{-2} for H_2SO_4, Na_2SO_4 and KOH electrolyte, respectively. These series resistance values are attributed to the ionic resistance of the electrolyte and the contact resistances between the electrode and current collector. The latter was assumed to be constant for all the devices because the same amount of carbon was added in the electrodes and the same current collectors were applied. It is remarkable that, because of the higher ionic conductivity, the supercapacitor with the 1M H_2SO_4 electrolyte shows the lowest real impedance at all of the frequencies (the Figure is not provided here), but at values close to 1 mHz the resistance of the Na_2SO_4 electrolyte (10.1 ohm) approaches that of H_2SO_4 (9.87 ohm), which indicates that neutral electrolyte can also be an effective electrolyte for this kind of carbon xerogel. These results are in agreement with recent literature findings on the development of high energy supercapacitors based on neutral aqueous electrolyte (e.g. Na_2SO_4 and Li_2SO_4), which are able to work up to 1.6-2 Volt [13,16,37-39].

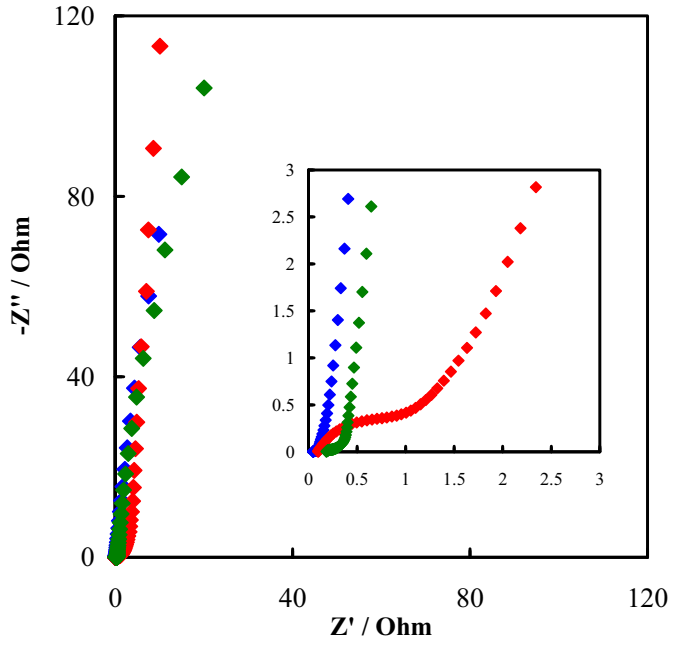

Figure 6. Nyquist plots for 4 cm^2 two-electrode cells and three different aqueous electrolytes. The insert shows the high frequency region of impedance.

The specific capacitances of the supercapacitors in different aqueous electrolytes were calculated from the impedance analysis employing the imaginary component of impedance. Fig. 7 reports the behaviour of specific capacitance as a function of frequency. The specific capacitance for one electrode is obtained using the equation C = 4(−(1/2πfZ''m)), where *f* is frequency in Hz, *Z''* is the imaginary component of impedance and *m*, the mass of xerogel calculated for one electrode. At a frequency of 1 mHz, the values of capacitance for H_2SO_4, Na_2SO_4 and KOH were 250, 190 and 145 F g^{-1}, respectively, which are higher than the values shown in Table 2, calculated for a current load of 0.2 A g^{-1} using galvanostatic charge and discharge (G-CD) measurements. The differences may be attributed to the different conditions in which the measurements were taken. The impedance was carried out at OCP in alternating current and the G-CD are measurements performed using a continuous current and they are performed at different voltages (from 0 to 1 V). It is thought that by extrapolating the current from G-CD to zero, capacitance could achieve that of impedance at a frequency of 1 mHz. Moreover, it must be borne in mind that the capacitance from impedance analysis is derived from a series-RC circuit model. The capacitances of 250, 190, and 145 F g^{-1} at 1 mHz should be considered as limiting values for these devices in conditions of 0 V. Nevertheless, high values can be obtained with supercapacitors based on electrodes of a large enough size (4 cm^2) and a large enough carbon load (5±1 mg cm^{-2}). In short, the electrodes we have developed using an activated carbon xerogel and a casting procedure are fully scalable and almost ready for use in automatized production lines.

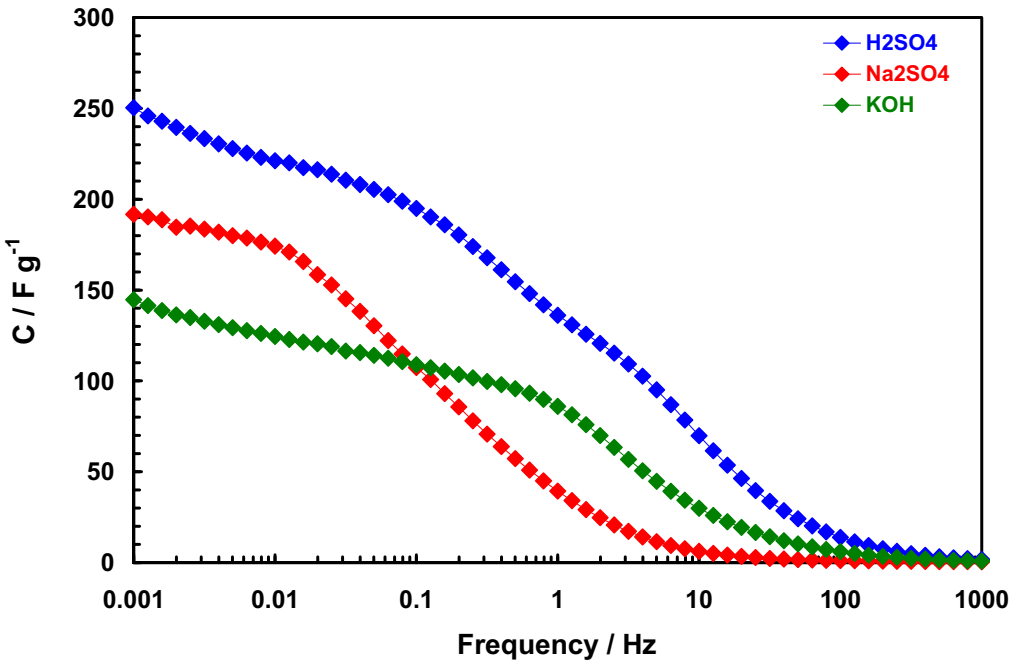

Figure 7. Gravimetric capacitance (F g^{-1}) as a function of the frequency (Hz) for the supercapacitors assembled with the three aqueous solutions studied.

All the electrochemical tests performed in this work demonstrate the superior electrochemical performance of an electrochemical cell composed of an ACX sample-sulphuric acid pair. The higher energy storage achieved with this device is basically due to the higher ionic conductivity of H_2SO_4 and the more facile diffusion of the protons (H^+) into the pores of the electrode material. However, the chemical nature of the ACX sample, used as electrode material, is also an important factor to be considered. According to the literature [40, 41], the point of zero charge (PZC) is the pH at which the total surface charge assumes the value of zero, i.e., when the positive and negative charges compensate each other. Carbon xerogels are characterized by their amphoteric nature [21]; they can be electron donors/acceptors, depending on the pH medium. For this reason, the nature of aqueous electrolyte used in supercapacitors is important since, depending on the type of the electrolyte, the electric charge of the electrode surface can be adjusted in order to permit different energy storage capacitances. When a solution of H_2SO_4 is used as electrolyte (i.e. when the pH_{PZC} of the electrode material is higher than the electrolyte pH) there is a predominance of positive charges in the surface of the carbon material. These may be involved in redox reactions, thereby increasing the capacitance of the electrochemical cell due to pseudo-faradaic phenomena. In a similar way, the use of the basic electrolyte (i.e., KOH) gives rise to a difference between the pH_{PZC} and pH_e but, in this particular case, the surface has an excess of negative charges, which, might be indicative of a different pseudo-faradaic contribution. However, the results obtained from chronoamperometry (complete independence of gravimetric capacitance with current density), suggest that a basic electrolyte promotes charge storage via a purely electrostatic mechanism so, in these operating conditions, it seem that negative charges probably do not play a major role in pseudocapacitive processes.

4. Conclusions

Carbon xerogels can be tailored to have a substantial micropore volume and well-defined mesoporosity. In this study, an activated carbon xerogel with a tailored porosity was used as active material in supercapacitors. The combination of this promising electrode material with three aqueous electrolytes (H_2SO_4, Na_2SO_4 and KOH, 1 M solutions) and supercapacitors of different dimensions (a Swagelok® cell with 1 cm^2 electrodes vs. graphite plate collectors using 4 cm^2 square electrodes) was evaluated in order to optimize the electrochemical behavior of the supercapacitor.

A supercapacitor built with large carbon xerogel electrodes with superior properties exhibited a higher energy storage capacity than the counterpart device composed of 1 cm^2 electrodes (196 F g^{-1} vs. 173 F g^{-1} for E4 and E1 electrodes, respectively). This finding could be useful for the scaling up of electrodes. If a highly porous carbon xerogel is used for the production of electrodes on an industrial scale, the good behaviour of the device can be ensured.

The influence of the pH of electrolyte on the electrochemical response of supercapacitors based on activated carbon xerogel was also investigated. It was found that the surface chemistry of the active material in combination with the pH of the medium may have a strong influence on pseudocapacitance. It has been shown that the highest gravimetric capacitance is obtained with H_2SO_4, probably due to its better conductivity and proton mobility and the superior activity of the oxygen functionalities on the carbon xerogel surface. The impedance analysis showed that when f = 1 mHz, gravimetric capacitance reached 250 F g^{-1} with H_2SO_4 as electrolyte, while this value was only 190 and 145 F g^{-1} for the Na_2SO_4 and KOH electrolytes, respectively, and with the activated carbon xerogel as electrode material. Because of the corrosive nature of acid electrolyte and the high energy storage capacitance demonstrated by Na_2SO_4, a neutral solution would seem an attractive alternative for aqueous supercapacitors environmentally friendly. The results of this study also show that the combination of an activated carbon xerogel and a basic electrolyte (KOH 1 M) produces a supercapacitor with no pseudocapacitive reactions and, therefore, substantially lower gravimetric capacitance values.

Acknowledged: This work was financially supported by the Ministerio de Economía y Competitividad (Ref. MAT-2011-23733), the Ministero dello Sviluppo Economico within the framework of "Accordo ti programma CNR-MSE", project "Sistemi elettrochimici per l´accumulo dell´energia) and with funding from COST Organization (COST Action MP1004: Hybrid Energy Storage Devices and Systems for Mobile and Stationary Applications). E.G. Calvo also acknowledges a predoctoral research grant from Ficyt (Spain). The authors also thank *Xerolutions* for its help in the carbon xerogel synthesis.

References

[1] A.G. Pandolfo, A.F. Hollenkamp, J. Power Sources 157 (2006) 11-27.

[2] E. Raymundo-Piñero, K. Kierzek, J. Machnikowski, F. Béguin, Carbon 44 (2006) 2498-2507.

[3] M. Inagaki, H. Konno, O. Tanaike, J. Power Sources 195 (2010) 7880-7903.

[4] R. Kötz, M. Carlen, Electrochim. Acta 45 (2000) 2483-2498.

[5] Y. Zhang, H. Feng, W. Wu, L. Wang, A. Zhang, T. Xia, H. Dong, X. Li, L. Zhang, Int. J. Hydrogen Energy 34 (2009) 4889-4899.

[6] E. Frackowiak, Phys. Chem. Chem. Phys 9 (2007) 1774-1785.

[7] E. Raymundo-Piñero, F. Leroux, F. Béguin, Adv. Mater. 18 (2006) 1877- 1882.

[8] J.H. Chae, G.Z. Chen, Electrochim. Acta 86 (2012) 248-254.

[9] V. Khomenko, E. Raymundo-Piñero, F. Béguin, J. Power Sources 195 (2010) 4234-4241.

[10] V. Ruíz, R. Santamaría, M. Granda, C. Blanco, Electrochim. Acta 54 (2009) 4481-4486.

[11] X. Zhang, X. Wang, L. Jiang, H. Wu, C. Wu, J. Su, J. Power Sources 216 (2012) 290-296.

[12] F. Lufrano, P. Staiti, E.G. Calvo, E.J. Juárez-Pérez, J.A. Menéndez, A. Arenillas, Int. J. Electrochem. Sci. 6 (2011) 596-612.

[13] L. Demarcomay, E. Raymundo-Piñero, F. Béguin, Electrochem. Commun 12 (2010) 1275-1278.

[14] M.S. Hong, S.H. Lee, S.W Kim, Electrochem. Solid State Lett. 5 (2002) A227-A230.

[15] M.P. Bichat, E. Raymundo-Piñero, F. Béguin 48 (2010) 4351-4361.

[16] X. Zhang, Y. He, G. Jiang, X Liao, Z. Ma, Electrochem. Commun 13 (2011) 1166-1169.

[17] H.A. Andreas, B.E. Conway, Electrochim. Acta 51 (2006) 6510-6520.

[18] E. Frackowiak, G. Lota, J. Machnikowski, C. Vix-Guterl, F. Béguin, Electrochim. Acta 51 (2006) 2209-2214.

[19] W. Li, G. Reichenauer, J. Fricke, Carbon 40 (2002) 2955-2959.

[20] C. Moreno-Castilla, M.B. Dawidziuk, F. Carrasco-Marín, E. Morallón, Carbon 50 (2012) 3324-3332.

[21] E.G. Calvo, J.A. Menéndez, A. Arenillas, Nanomaterials, Mohammed Muzibur Rahman Editorial, 2011, pp. 187-234

[22] E.G. Calvo, N. Ferrera-Lorenzo, A. Arenillas, J.A. Menéndez, Micro. Meso. Mater. 168 (2013) 206-212.

[23] G. Rasines, P.Lavela, C. Macías, M. Haro, C.O. Ania, J.L. Tirado, J. Electroanal. Chem. 671 (2012) 92-98.

[24] K. Y. Kang, S.J. Hong, B.I. Lee, J.S. Lee, Electrochem. Commun. 10 (2008) 1105-1108.

[25] Y.-M. Chang, C.-Y. Wu, P.-W. Wu, J. Power Sources 223 (2013) 147-154.

[26] A. Arenillas, J.A. Menéndez, L. Zubizarreta, E.G. Calvo, Patent ES-2000930256 (2009).

[27] E.G. Calvo, E.J. Juárez-Pérez, J.A. Menéndez, A. Arenillas, J. Colloid Interface Sci. 357 (2011) 541-547.

[28] E.J. Juárez-Pérez, E.G. Calvo, A. Arenillas, J.A. Menéndez, Carbon 48 (2010) 3293-3311.

[29] IUPAC Recommendations, Pure Appl. Chem. 57 (1985) 603-619.

[30] D. Lozano-Castelló, D. Cazorla-Amorós, A. Linares-Solano, S. Shiraishi, Carbon 41 (2003) 4351-4361.

[31] J.L. Figueiredo, M.F.R. Pereira, M.M.A. Freitas, J.J. Órfao, Carbon 37 (1999) 1379-1389.

[32] N. Mahata, M.F.R. Pereira, F. Suárez-García, A. Martínez-Alonso, J.M.D. Tascón, J.L. Figueiredo, J. Colloid Interface Sci. 324 (2008) 150-155.

[33] Q.T. Qu, B. Wang, L.C. Yang, Y. Shi, S. Tian, Y.P. Wu, Electrochem. Commun. 10 (2008) 1652-1655.

[34] C.-C. Hu, C.-C. Wang, J. Power Sources 125 (2004) 299-308.

[35] A. Malak-Polaczyk, C. Matei-Ghimbeu, C. Vix-Guterl, E. Frackowiak, J. Solid State Chem. 183 (2010) 969-974.

[36] O.A. Vargas, A. Caballero, L. Hernán, J. Morales. J. Power Sources 196 (2011) 3350-3354.

[37] K. Fic, G. Lota, M. Meller, E. Frackowiak, Energy Environ. Sci. 5 (2012) 5842-5850.

[38] P. Staiti, A. Arenillas, F. Lufrano, J.A. Menendez, J. Power Sources 214 (2012) 137-141.

[39] Q. Gao, L. Demarconnay, E. Raymundo-Pinero, F. Beguin, Energy Environ. Sci. 5 (2012) 9611–9617.

[40] L.R. Radovic, I.F. Silva, J.I. Ume, J.A. Menéndez, C.A. León y León, A.W. Scaroni, Carbon 35 (1997) 1339-1348.

[41] P. Burg, D. Cagniant, Chemistry and Physics of Carbon, R.L. Radovic Editor, 2008, pp. 130-169.

5.2.2. Líquidos iónicos próticos

Los líquidos iónicos son sales formadas por iones asimétricos de gran tamaño (fundamentalmente cationes de naturaleza aromática con átomos de nitrógeno en el anillo y aniones constituidos por diferentes elementos químicos), de manera que las fuerzas de atracción que existen entre las especies catiónicas y aniónicas son bastante débiles, provocando que sean líquidos en un amplio rango de temperaturas, incluyendo a temperatura ambiente. Además de su bajo punto de fusión, los líquidos iónicos se caracterizan por su baja inflamabilidad debido a su baja presión de vapor, baja o nula volatilidad, extenso intervalo de estabilidad química y térmica y, finalmente, amplia ventana de potencial [ARBIZZANY, 2008; BALDUCCI, 2004; KUMAR, 2010]. No obstante, es justo apuntar que los líquidos iónicos muestran ciertas debilidades como son el todavía elevado coste de fabricación que llevan asociado y la peor mojabilidad que existe entre los electrodos y los líquidos iónicos debido a su viscosidad, hecho que puede mejorar aumentando ligeramente la temperatura de operación. A pesar de sus puntos débiles, el campo de estudio de los líquidos iónicos está creciendo vertiginosamente debido a las numerosas aplicaciones para las que pueden ser destinados: electrolitos para la industria electroquímica, lubricantes, productos farmacéuticos, membranas líquidas iónicas soportadas, disolventes líquidos para reacciones químicas, etc.

La necesidad de desarrollar nuevos electrolitos seguros y medioambientalmente benignos ha propiciado que los líquidos iónicos se hayan considerado candidatos perfectos para su aplicación en el campo de los supercondensadores. Además, debido a sus únicas propiedades físico-químicas, los dispositivos electroquímicos basados en líquidos iónicos presentan elevados niveles de densidad de potencia/energía y excelente durabilidad, cualidades exigidas para cualquier sistema de almacenamiento de energía.

Existen diferentes estudios que combinan electrolitos basados en líquidos iónicos con electrodos compuestos por materiales carbonosos capaces de acumular una gran cantidad de carga. No obstante, la mayoría de estos estudios emplean líquidos iónicos apróticos (AILs), por ser los primeros líquidos iónicos investigados [BALDUCCI, 2004; LEWANDOWSKI, 2010; XU, 2006]. Varios estudios han demostrado que los líquidos iónicos próticos (PILs) pueden ser más adecuados para su aplicación como electrolitos en sistemas electroquímicos [ANOUTI, 2012; MYSYK, 2010], ya que presentan una menor toxicidad y mayor conductividad iónica que los AILs pero, además, contienen un protón que puede estar involucrado en reacciones redox, lo que hace que la capacidad del supercondensador pueda verse incrementada debido a fenómenos pseudocapacitivos.

Por este motivo, el trabajo recogido en la *Publicación IX* se basa en el estudio de la respuesta electroquímica de supercondensadores que utilizan un xerogel de carbono poroso como material de electrodo y líquidos iónicos próticos de diversa naturaleza como electrolito (véase Figura 5.4). En lo

que respecta a los líquidos iónicos, los objetivos planteados en el trabajo han sido varios: (i) obtener elevados valores de densidad de energía mediante el uso de líquidos iónicos próticos en supercondensadores basados en xerogeles de carbono y, (ii) evaluar la influencia tanto del pH como del contenido en agua del líquido iónico sobre la capacidad de almacenamiento de energía del supercondensador.

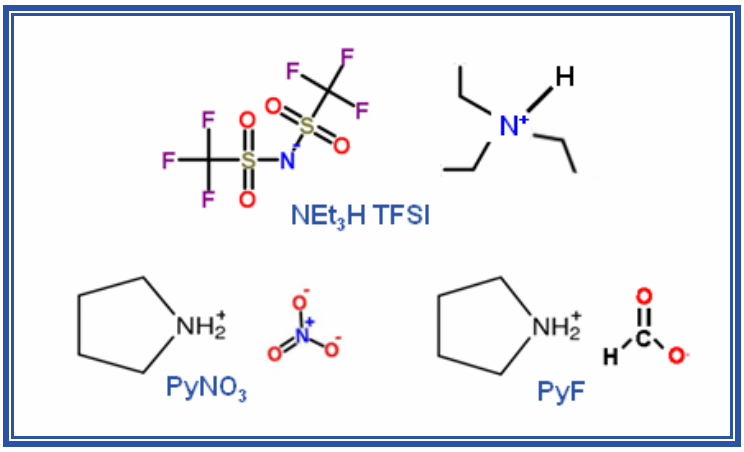

Figura 5.4. Ilustración esquemática de la estructura molecular de los Líquidos Iónicos Próticos (PILs) utilizados como electrolito en la Publicación IX.

Como se ha indicado en la Introducción de la presente memoria, existen evidencias de que los materiales micro-mesoporosos favorecen el proceso de almacenamiento de carga, ya que los mesoporos pueden actuar como canales permitiendo una mejor difusión de los iones de electrolito hacia los poros de menor tamaño [ESCRIBANO, 1998; FRACKOWIAK, 2007; PANDOLFO, 2006]. Por este motivo, en la *Publicación IX*, además del xerogel de carbono, supercondensadores basados en un carbón activo comercial fundamentalmente microporoso han sido preparados con objeto de evaluar la influencia de la textura porosa del material de electrodo sobre su capacidad de almacenamiento de energía. Las isotermas de adsorción-desorción de nitrógeno a -196 ºC de ambos materiales de electrodo se recogen en la Figura 5.5. Como se puede apreciar, ambos materiales dan lugar a isotermas con diferente forma. Por un lado, el carbón activo comercial presenta una isoterma tipo I de acuerdo con la clasificación de la IUPAC [IUPAC, 1985], indicando que se trata de un sólido prácticamente microporoso (valor de área superficial S_{BET} ~ 2200 m^2 g^{-1}). Si bien, es necesario matizar que la forma de la rodilla más abierta sugiere la existencia de microporos anchos y el ligero aumento del volumen de N_2 adsorbido a presiones relativas superiores al llenado de los microporos se relaciona con la existencia de una pequeña cantidad mesoporos de reducido tamaño. Por su parte, la isoterma de adsorción-desorción del xerogel de carbono sintetizado en el laboratorio parece evolucionar ligeramente hacia una combinación de isotermas tipo I y IV, asociadas con materiales micro-mesoporosos. En el caso del xerogel de carbono, el volumen de nitrógeno adsorbido a bajas presiones relativas es mayor, dando lugar a un área superficial S_{BET} próxima a 2800 m^2 g^{-1}. La presencia de

mesoporos queda evidenciada por el incremento del volumen de nitrógeno adsorbido a elevadas presiones relativas y por la existencia del ciclo de histéresis observado a presiones relativas entre 0.4 y 0.7, lo cuál corresponde con mesoporos cuyo diámetro está comprendido entre 2-7 nm aproximadamente.

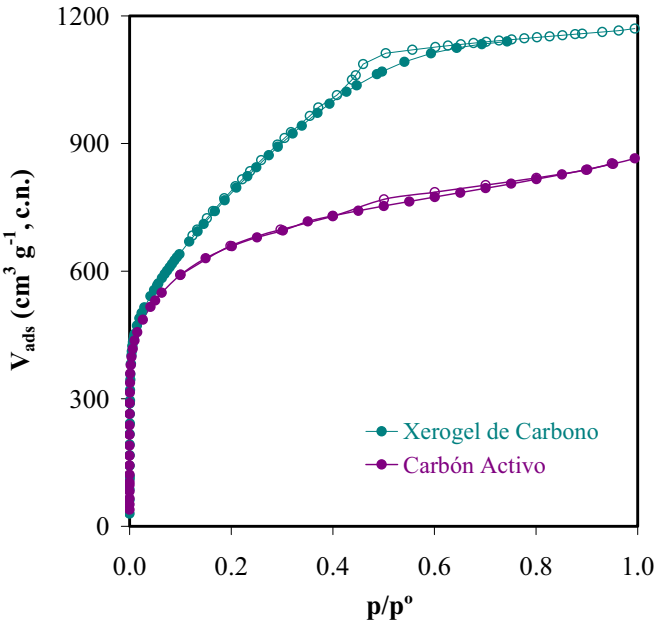

Figura 5.5. Isotermas de adsorción-desorción de N_2 de los materiales de electrodo utilizados en la Publicación IX.

Una vez presentados los diferentes materiales de electrodo y líquidos iónicos empleados para alcanzar los objetivos planteados en la *Publicación IX*, las principales conclusiones derivadas de este trabajo son las siguientes:

❖ En lo que respecta a la textura porosa del material de electrodo, mayores valores de capacidad específica se alcanzaron con los supercondensadores basados en el xerogel de carbono sintetizado en el laboratorio. Es decir, al igual que ocurre con los electrolitos acuosos y orgánicos, en el caso de los líquidos iónicos, el proceso de almacenamiento de carga también está favorecido por la presencia de mesoporos.

❖ El pH del líquido iónico empleado como electrolito tiene notable repercusión sobre el comportamiento de la celda electroquímica. Hay que destacar que un aumento en el pH del líquido iónico $PyNO_3$ supone un incremento en la capacidad de almacenamiento de energía (por ejemplo, en el caso de utilizar el xerogel de carbono activado como material de electrodo, valores de capacidad de 201 y 121 F g^{-1} se obtuvieron cuando el pH del $PyNO_3$ fue igual a 11 y 7, respectivamente). Sin embargo, este incremento no es tan pronunciado al utilizar electrodos basados en el carbón activo. Todo parece indicar que la mejoría en la capacidad gravimétrica puede deberse a una contribución de

la pseudocapacidad, consecuencia de reacciones redox que tienen lugar entre el electrolito y los grupos oxigenados presentes en la superficie del xerogel de carbono. Los resultados de análisis elemental y desorción térmica programada mostraron que el carbón activo comercial utilizado como electrodo contiene una menor cantidad de grupos oxigenados que el xerogel de carbono, lo que podría explicar la menor dependencia de la capacidad con el pH del electrolito (147 y 109 F g^{-1} con el electrolito $PyNO_3$-11 y $PyNO_3$-7, respectivamente)

❖ La presencia de agua en los líquidos iónicos determina la ventana de potencial de trabajo del supercondensador. Así, en el caso de utilizar los líquidos iónicos $PyNO_3$ y PyF, el voltaje de trabajo no fue superior a 1.2 V, es decir, valor similar al utilizado en supercondensadores compuestos por disoluciones acuosas, mientras que el sistema electroquímico fue capaz de operar con un voltaje máximo alrededor de 2.5 V en presencia de un líquido iónico que contiene una cantidad de agua casi despreciable (NEt_3H TFSI, 200 ppm).

Publicación IX

OPTIMIZING THE ENERGY DENSITY OF CARBON BASED SUPERCAPACITORS USING PROTIC IONIC LIQUIDS AS ELECTROLYTES

Electrochimica Acta

(enviada)

Año: 2013

Optimizing the energy density of carbon based supercapacitors using Protic Ionic Liquids as electrolytes

L. Demarconnay[1], E. G. Calvo[1,2], Laure Timperman[3], E. Raymundo-Piñero[1], M. Anouti[3], D. Lemordant[3], A. Arenillas[2], J.A. Menéndez[2] and F. Béguin[1]*

[1]Centre de Recherche sur la Matière Divisée (CRMD), FRE 3520 CNRS, 1b Rue de la Férollerie, 45071 Orléans Cedex, France.

[2] Instituto Nacional del Carbón CISC, Apartado 73, 33080 Oviedo, Spain

[3] Université François Rabelais, Laboratoire PCM2E, Parc de Grandmont 37200 Tours, France.

Abstract

Protic ionic liquids (PILs) were tested as electrolytes for carbon/carbon supercapacitors. Activated carbons with different porous texture were applied as electrode material. The carbon material with the largest specific surface area and highest amount of narrow mesopores (pore diameter: 2-7 nm) was found to be the most efficient sample for energy storage compared to other microporous material. With the pyrrolidinium nitrate ($PyNO_3$) and pyrrolidinium formate (PyF) ionic liquids, high specific capacitances were recorded. However, it should be noted that when the pH value of these ionic liquids was around 11, higher specific capacitances were achieved, revealing a better electrochemical performance of carbon electrodes in basic media (i.e., capacitance values of 121 and 208 F g^{-1} for an electrolyte based on $PyNO_3$ with a pH value of 7 and 11, respectively). These ionic liquids contained a small amount of water, which restricted the maximum voltage of symmetric capacitors to a value of 1.2 V, even after the $PyNO_3$ electrolyte had been partially dried (H_2O content around 1110 ppm). Therefore, in order to expand the potential window used, a dried PIL was prepared (triethylammonium bis((trifluoromethyl)sulfonyl)amide (NEt_3H TFSI); 200 ppm water). The results obtained with this ionic liquid suggest that maximum voltages as high as 2.5 V can be achieved. This clearly shows that the presence of water in PILs has a negative effect on the performance of supercapacitors.

Keywords: Protic ionic liquids; Supercapacitors; Activated carbon; Water; High voltage.

*Corresponding author. Tel.: +33 2 38 25 53 75; fax: +33 2 38 63 37 96.

E-mail address: beguin@cnrs-orleans.fr (F. Béguin).

1. Introduction

Electrochemical capacitors are promising systems for applications requiring high power densities. At the moment, most industrial modules are built with porous carbon-based electrodes in a non-aqueous medium, as these provide high operating voltages [1]. The use of organic solvents such acetonitrile or propylene carbonate increases the cost of such modules and, in addition, they are also environmentally unfriendly. In order to overcome these problems, aqueous media have been considered as alternative electrolytes for supercapacitors. Although aqueous solutions are more affordable, their main drawback is the lower energy density stored due to the theoretically low stability window of water (1.23 V). Recently, several solutions have been proposed in order to improve the performance of such systems, e.g., asymmetric configurations [2-6]. However, even if some of the proposed solutions are on the right track, the maximum voltage with aqueous electrolytes still remains between 1 and 2 V, depending on the nature of the aqueous solution and the materials used to prepare either one or both electrodes.

Aprotic Ionic liquids (AILs) have often been proposed as alternative electrolytes. AILs are molten salts at ambient temperature. They have been studied on a large scale and they are employed in very diverse applications such as "Green solvents" for extraction [7-8], catalysis [9], fuel cells [10-12], electrochemical synthesis [13], pharmaceutical applications [14], etc. As electrolytes for supercapacitors, they have given rise to encouraging results specially by providing a large stability potential window when used with non-porous electrodes [15]. Moreover, inflammability and the low vapor pressure of ILs are great assets for safety, as an example for systems operating in hybrid-electrical vehicles [16]. These electrolytes were first studied in hybrid systems comprising a carbon based material as negative electrode and a polymer based material as the positive one [17, 18]. Carbon/carbon systems operating with AILs have also been evaluated [15, 19] and similar performances to those obtained with organic electrolytes have been achieved, though only at high temperatures i.e. 60 °C. The main disadvantages of AILs are their low ionic conductivity and high viscosity, making it necessary to increase the temperature for an improved operation [20]. This, however, has a negative effect on the cyclability of the electrochemical device.

Like AILs, Protic Ionic Liquids (PILs) offer the advantage of a high stability potential window when used with non-porous materials [21]. Moreover, they display a higher conductivity than AILs in all temperature ranges [22]. PILs also possess a proton that is available for redox processes. The occurrence of pseudo-faradic reactions at the electrode-electrolyte interface was first observed when a pseudocapacitive oxide as RuO_2 was used as electrode material [23]. In a previous work [24], we showed that when porous carbons were employed as electrode material, pseudofaradaic reactions involving the surface oxygen functionalities and the available proton of the electrolyte give rise to

high values of specific capacitance. However, the amount of energy stored is still far from that obtainable with organic electrolytes.

The aim of the present study is to improve the energy density of carbon based supercapacitors using PILs as electrolytes. By calculating the energy density (E) from the following equation (1):

$$E = \frac{1}{2} C U^2 \quad (1)$$

where *C* is the capacitance and *U* the system's maximum voltage, it is evident that it is necessary to improve C and/or U in order to obtain a high energy density. For this purpose, two carbon materials with a high surface area, different mesoporosities and a moderate amount of surface groups were used as electrode materials with three different electrolytes based on Protic Ionic Liquids. PILs composed of diverse anions and cations, with different pH values and water content were chosen in order to identify the most promising medium for such systems. Of all the previously cited variables, the water content of PILs has the most noticeable effect on the performance of supercapacitors (maximum voltage and capacitance values). Although the drying process is relatively easy in the case of AILs [25], it is more difficult with PILs due to the strong hydrogen bond between the water molecules and the anions of the PILs, therefore reach water contents of few hundred ppm is still a challenge.

2. Experimental

An organic xerogel with an initial pH of 6.5 was synthesized by means of microwave heating (synthesis time about 6 hours) [26]. The sample was chemically activated with KOH (activating agent/precursor mass ratio 3:1) in a horizontal tubular furnace at 750 °C for 6 minutes. The resulting active material (AOX), was used as active material for the supercapacitor electrodes and its electrochemical performance was compared to that of a high purity commercial activated carbon (MWV, MWV-E510A from MeadWestvaco, USA).

The porous texture of the activated carbons was analysed by N_2 and CO_2 adsorption at 77 K and 273 K, respectively (Autosorb-1, Quantachrome Instruments). Before the analysis, the samples were degassed (Flo Vac Degasser, Quantachrome Instruments) overnight at 200 °C. The specific surface area was calculated from the N_2 adsorption isotherm by applying the BET equation. The micropore volume was determined by applying the Dubinin-Radushkevich equation to the adsorption data up to $p/p^o \leq 0.015$ for N_2 and $p/p^o < 0.1$ for CO_2. Thermoprogrammed desorption, e.g., TGA (Netzsch STA 449 C) coupled to a mass spectrometer (Netzsch QMS 403 C) was used in order to evaluate the surface chemistry of the active carbons (ACs). The device was calibrated by using calcium oxalate (CO, CO_2, H_2O).

The ionic liquids based on pyrrolidinium nitrate and formate were synthesized by proton exchange between pyrrolidine and nitric or formic acid. Next, water was removed by azeotropic distillation with dichloroethane (DCE). The water content of $PyNO_3$ was estimated to be about 1110 ppm H_2O. Triethylammonium bis(tetrafluoromethansulfonamide) was synthesized using a metathesis method. First, triethylammonium chloride (22.06 g; 0.16 mol) was prepared by mixing triethylamine and hydrochloric acid solution (37 wt. %). Next, the resulting triethylammonium chloride was mixed with a solution of LiTFSI in water, thus obtaining two different phases. In order to separate these two phases, approx. 10 mL of chloroform was added. In this way, the PIL diluted in chloroform was separated from the aqueous phase. In order to remove the chloride, the PIL was washed with water, and finally, it was dried under high vacuum using a trap with liquid nitrogen for 2-3 days. The water content of NEt_3H TFSI was analyzed by coulometric Karl-Fisher titration. Immediately after the drying stage, the H_2O content was observed to be approximately 200 ppm compared to 400-600 ppm at equilibrium (i.e. in normal conditions outside the glove box). PILs with a low water content were kept inside a glove box (Jacomex) under an inert atmosphere (Ar).

A paste was prepared by mixing the active material (MWV or AOX, 80 wt. %), acetylene black (Pure Black, Superior Graphite Co., USA, 10 wt. %) and PTFE binder (10 wt. %). The composite was rolled out in order to obtain a film. Electrodes were prepared by punching pellets (1 cm diameter) in the composite based paste. The mass of the electrodes was between 5-6 mg. The punched electrodes were pressed before assembling the cells. Two-electrode cells were assembled using a Teflon Swagelok® system with gold current collectors and a glassy fibrous separator. Three-electrode cell experiments were carried out in closed cells in order prevent the ionic liquids from becoming contaminated with water. A pellet ($\geq$ 15 mg) of activated carbon with a high specific surface area was used as auxiliary electrode and a solid Ag/AgCl electrode acted as reference electrode. The cells prepared with PILs of low water content were prepared in the glove box. A VMP2 (Biologic, France) multichannel potentiostat/galvanostat was used for the cyclic voltammetry measurements and galvanostatic charge/discharge cycling.

3. Results and discussion

3.1. Influence of the carbon porosity and pH media on specific capacitance

To improve the capacitance of the supercapacitors, two different strategies were followed: i) the porosity of the carbon electrode was modified in order to find the best suited to the size of the ions and, ii) the effect of the electrolyte pH was investigated.

As PIL, $PyNO_3$ was chosen because of its high conductivity (σ = 50.1 mS cm^{-1}) and low viscosity (η = 5.1 mPa s). Moreover in our previous work [24], capacitances of around 100 F g^{-1} were achieved when $PyNO_3$ was used as electrolyte in a supercapacitor with a microporous carbon (S50, Norit) as

active electrode material. This S50 carbon has a moderate surface area (i.e. S_{BET} = 1481 m^2 g^{-1}) and is made up almost exclusively of micropores.

Table 1 – Adsorption and TPD data for activated carbons MWV, AOX and S50

Sample	Adsorption				TPD	
	S_{BET} (m^2 g^{-1})	V_{DUB-N2} (cm^3 g^{-1})	$V_{DUB-CO2}$ (cm^3 g^{-1})	V_{meso} (cm^3 g^{-1})	n_{CO} (µmol g^{-1})	n_{CO2} (µmol g^{-1})
AOX	2800	0.91	0.34	0.89	889	314
MWV	2244	0.79	0.83	0.45	460	150
S50	1481	0.60	0.57	0.17	-	-

In order to determine the impact of porosity on the performance of the ionic liquid-based supercapacitors, an activated carbon with a large amount of micropores (MWV) and a carbon xerogel with a large amount of mesopores (AOX) were tested. Data concerning the physico-chemical characterization of MWV and AOX are presented in Table 1. The textural parameters of the S50 activated carbon have also been added for comparative purposes. AOX exhibits the highest specific surface area (2800 m^2 g^{-1}), but also displays a significant amount of mesopores with a pore diameter ranging between 2-7 nm (i.e. V_{meso} of 0.89 cm^3 g^{-1} for the AOX xerogel as opposed to 0.45 and 0.18 cm^3 g^{-1} for MWV and S50, respectively). The MWV carbon has a slightly smaller specific surface area than AOX but a higher volume of ultramicropores (V_{CO2}= 0.83 cm^3 g^{-1}).

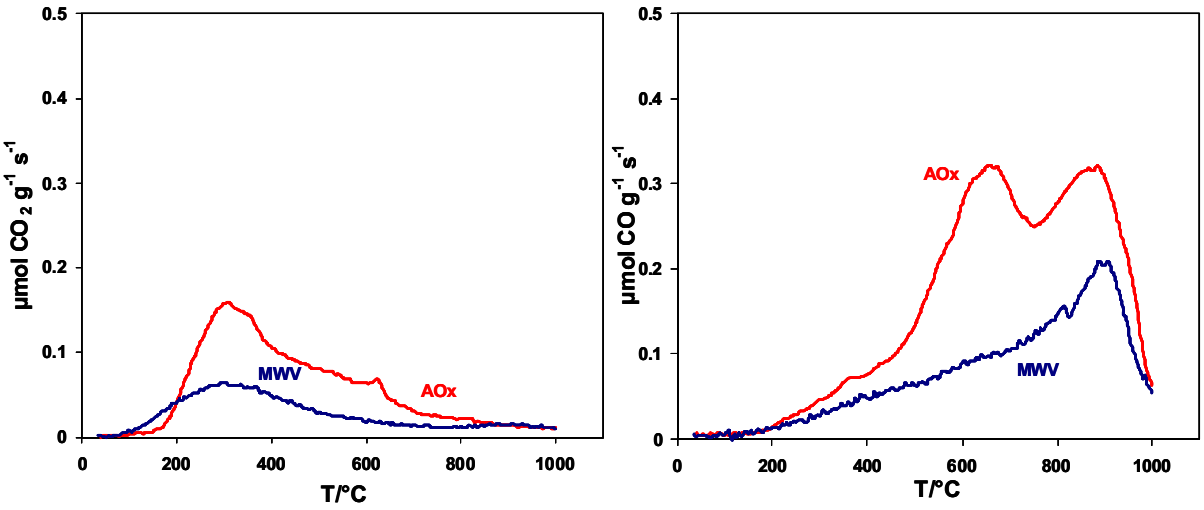

Fig. 1. CO_2 (A) and CO (B) profiles obtained by TPD experiments with AOX and MWV samples.

Furthermore, the surface functionalities of the electrode materials were characterized by TPD/MS experiments. The amounts of CO and CO_2 molecules detected are reported in Table 1 and the profiles of CO and CO_2 released vs. temperature for both electrode materials are shown in Fig. 1. Both the AOX xerogel and the MWV carbon display quite low oxygen contents, reaching ~1.6 wt. % for MWV

and ~3.1 wt. % for AOX. In both carbons, the presence of surface groups desorbing as CO_2 is very low and only one peak located at around 300 °C can be observed. The CO profile of AOX is characterized by two peaks at high temperature (670 and 900 °C). The peak appearing at 900 ºC is analogous to that found in the CO profile of the MWV sample, but the peak at 600 ºC is only characteristic of the AOX xerogel and, judging from the release temperature, it can be attributed to quinone-like groups. The presence of this type of oxygenated functions on the surface of AOX is promising as they can provide pseudocapacitive reactions in the presence of electrolytes capable of such reactions.

Cyclic voltammograms (CV) obtained in a 3-electrode cell with AOX as active material and $PyNO_3$ (pH 7) as electrolyte are presented in Fig. 2A. The vertical line corresponds to the theoretical potential for dihydrogen generation (around -0.6 V). The CVs show a redox couple of peaks located at around -0.05 V vs. Ag/AgCl, which could be attributed to the activity of oxygenated functions found on the AOX surface (as in the case of the S50 and S50ox carbons reported in ref. [24]). From the results shown in Fig. 2A, it can be inferred that the stability potential window of the electrolyte is around 1.2 V ([-0.6; 0.6] V vs. ref). Fig. 2B shows the CVs recorded for a symmetric 2-electrode cell with AOX as electrode material in $PyNO_3$-pH7. The shape of the CV is almost rectangular when U < 1 V. Nevertheless, some distortions, recorded during the positive potential scan in the highest voltage windows, are probably due to the generation of dihydrogen.

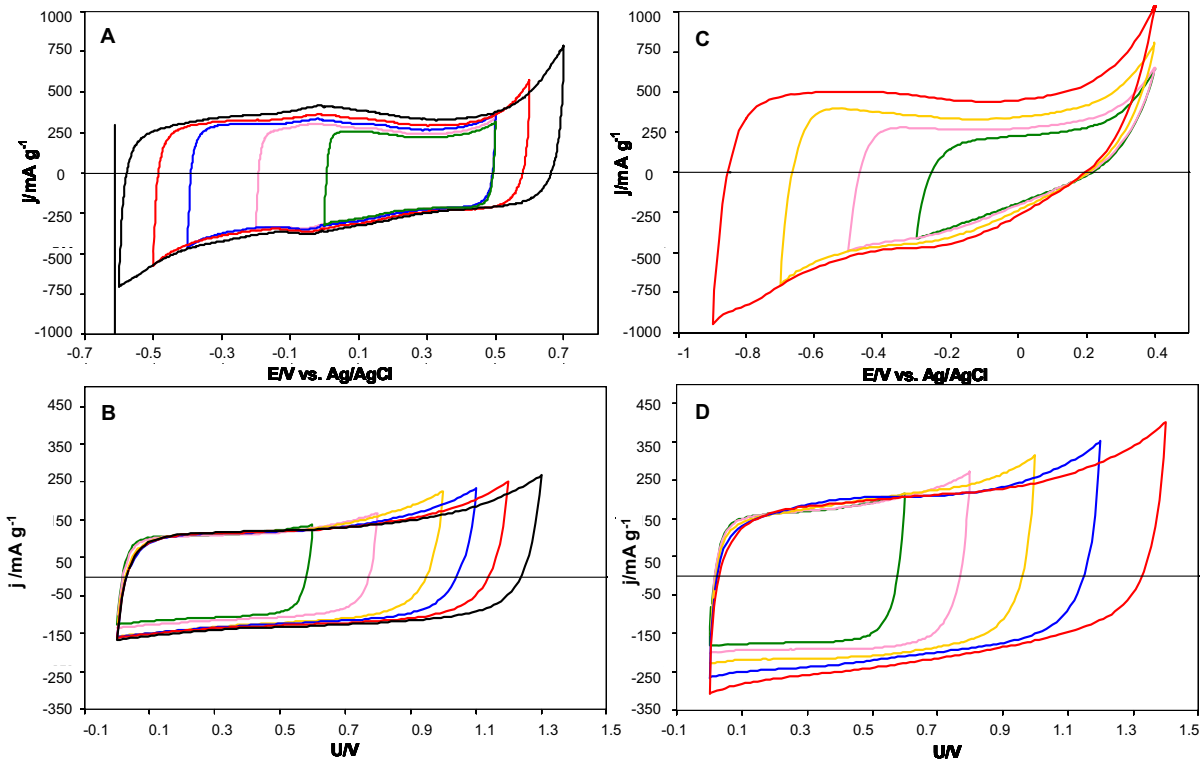

Fig. 2. 3-electrode (A) and 2-electrode (B) cyclic voltammograms of AOX in $PyNO_3$-pH7 and $PyNO_3$-pH 11 (C and D); scan rate 2 mV s^{-1}.

The specific capacitance (Cs) of this symmetric supercapacitor was determined by galvanostatic charge/discharge cycling, according to equation (2):

$$C_S = \frac{4\,C}{M} \tag{2}$$

where C_s is the capacitance of the cell and M the total mass of the two electrodes. The values calculated during the discharge of the supercapacitors for a maximum cell voltage of 1.2 V are presented in Table 2. The data obtained for the symmetric capacitors built with MWV or S50 (extracted from [24]) as electrode material and $PyNO_3$-based electrolytes have also been included. In $PyNO_3$, the specific capacitance of the AOX symmetric system is 121 F g^{-1}, which is higher than in the case of S50 (99 F g^{-1}) and slightly higher than for the MWV system (109 F g^{-1}). These results confirm, as in the case of the aqueous and organic electrolytes, that the capacitance of PIL-based systems is improved when the capacitors are based on activated carbons with a more developed porosity (i.e. a high micropore volume and a significant amount of narrow mesopores).

It is well known that in the case of aqueous electrolytes, the pH of the solution greatly affects the capacitance values. Thus, higher capacitances are found with acidic or basic electrolytes than with neutral ones [4, 5, 27]. The reasons given in the literature are that protons or hydroxyl ions are mobile species with a better ion diffusion inside the pores than other ionic species. As PILs are protic electrolytes, the pH can also be expected to have an effect on the capacitance of the systems.

The pH of $PyNO_3$ was increased from 7 up to 11 by adding a small excess of pyrrolidine during the synthesis. A comparison of the CVs obtained in a three-electrode cell with AOX carbon in $PyNO_3$-pH 7 (Figure 2A) with those obtained in the presence of $PyNO_3$-pH 11 (Figure 2C), confirms that capacitance improves when the pH increases. Moreover, in the case of pH 11, the shape of the CVs reveals an important contribution of pseudocapacitive reactions, implying a greater energy storage capacitance. Nevertheless, the stability potential window seems to be as for pH 7: 1.2 V.

From the construction of the two capacitors with the different carbon materials and two electrolytes ($PyNO_3$ pH 7 and 11), it can be seen that the use of an alkaline protic ionic liquid results in higher specific capacitance values, particularly when AOX was the electrode material (i.e. 208 vs. 121 F g^{-1} for AOX with $PyNO_3$ pH 11 and 7, respectively, whereas the improvement is less pronounced in the case of sample MWV, 147 F g^{-1} as opposed to 109 F g^{-1}, for a pH of 11 and 7, data collected in Table 2). These results show that the most efficient supercapacitor is the one composed of electrodes based on AOX xerogel and $PyNO_3$-pH 11 as electrolyte. Capacitance values of around 200 F g^{-1} were obtained with an electrolyte based on a solution of potassium hydroxide (pH value greater than 14). Therefore, an electrolyte based on $PyNO_3$ with a pH value of 11 would be preferable since it is a less corrosive medium. Moreover, the main drawback with aqueous basic electrolytes is their low

maximum voltage [28], whereas $PyNO_3$-based PILs exhibit better stability potential windows and a maximum cell voltage of 1.2 V [24]. The improvement achieved by increasing the pH of the electrolyte is not the same with the two electrode materials. Wit the pH 11 electrolyte, the specific capacitance of the carbon xerogel increases by 70 % while in the case of MWV sample the increase is only 35 %. This could be due to the nature of this high purity carbon and to the absence of oxygenated surface groups (particularly quinone groups), which are particularly active in an alkaline medium [29].

According to these results, it can be concluded that, in order to achieve higher capacitances using PILs such as $PyNO_3$, highly porous activated carbons containing a certain amount of narrow mesopores and electrolytes with basic properties are probably the most appropriate.

Table 2 – C (F g^{-1}) obtained with MWV and AOX electrodes and different $PyNO_3$ electrolytes (maximum cell voltage = 1.2 V)

Sample	Specific Capacitance (F g^{-1})		
	pH 7	pH 11	1110 ppm H_2O
AOX	121	208	116
MWV	109	147	103
S50	99*	-	-

* Data for S50 have been extracted from Ref. [23].

3.2. Influence of the water content of PILs on the cell voltage

As mentioned above, in order to increase the energy density of supercapacitors, the cell voltage needs to be as high as possible. As shown in Section 3.1, the maximum cell voltage achieved with the two electrolytes studied was only 1.2 V. Therefore, it must be increased if the performance of supercapacitors is to be improved. Such cell voltage values correspond to the theoretical maximum cell voltage expected with aqueous electrolytes, which is related to the thermodynamic stability potential window of water (1.23 V). $PyNO_3$ electrolytes contain several thousands ppm of water, which may explain their narrow potential window. In order to clarify this point, the $PyNO_3$ electrolyte with a pH of 7 was dried as thoroughly as possible, which is a rather complicated procedure since alkylammonium nitrate ionic liquids form aggregated structures where the water remains trapped. Indeed, Greaves et al. [30] have demonstrated that water may be predominately present either as individual water molecules bound to anions or as aggregates of water molecules. After drying, the final water content of the $PyNO_3$ (pH = 7) was 1110 ppm.

Fig. 3A and 3B show the CVs recorded with a 3-electrode cell and a symmetric 2-electrode cell, respectively. The cells were assembled with the dried $PyNO_3$ (pH = 7) as electrolyte and electrodes based on sample AOX. Unlike the case of Fig. 2A, in the voltammograms reported in Fig. 3A there are

no peaks attributed to the activity of oxygenated surface groups. This would seem to indicate that, in the absence of a large amount of water, pseudocapacitive reactions are not involved in the electrochemical measurements (in the case of an electrode material with a low amount of oxygenated surface groups) and also that the water remaining in the electrolyte is probably not free. It should also be noted that the stability potential window of the systems improved when the dried PIL was used as electrolyte. In particular, the positive potential limit shifted towards higher values of at least 200 mV. For the 2-electrode cell, the CVs are rectangular up to a maximum voltage of 1.3 V. Some distortions can be perceived when the cell voltage reaches higher values (U > 1.2 V) but, by comparison with Fig. 2B, the shape of the curves is more rectangular, which is indicative of a pure capacitive behavior of the system. These observations confirm that most of the pseudo-faradaïc charge transfers between the electrolyte and activated carbons (dihydrogen generation, oxygen generation, redox processes) observed with PILs are due to free water. The specific capacitance determined at 1.2 V in $PyNO_3$ (1110 ppm) for the symmetric capacitors with AOX or MWV as active material are given in Table 2 (i.e. C values of 116 and 103 F g^{-1} for AOX and MWV, respectively). Such values are slightly lower than those obtained with the initial electrolyte (116 as opposed to 121 F g^{-1} for the xerogel AOX and 103 vs. 109 F g^{-1} for MWV), indicating that the removal of individual water molecules from the electrolyte may have forestalled the appearance of pseudocapacitive effects. However, this slight decay in capacitance could be compensated for an increase in the maximum voltage used, since it seems that as the water content decreases, the stability potential window increases.

The drawback with $PyNO_3$ is that, even after extensive drying, an appreciable amount of water (~1000 ppm), still remains. Thus, in order to take full advantage of the theoretical potential window of such electrolytes and to obtain good performances in terms of energy stored and power density, a different ionic liquid with very low water content should be used as electrolyte.

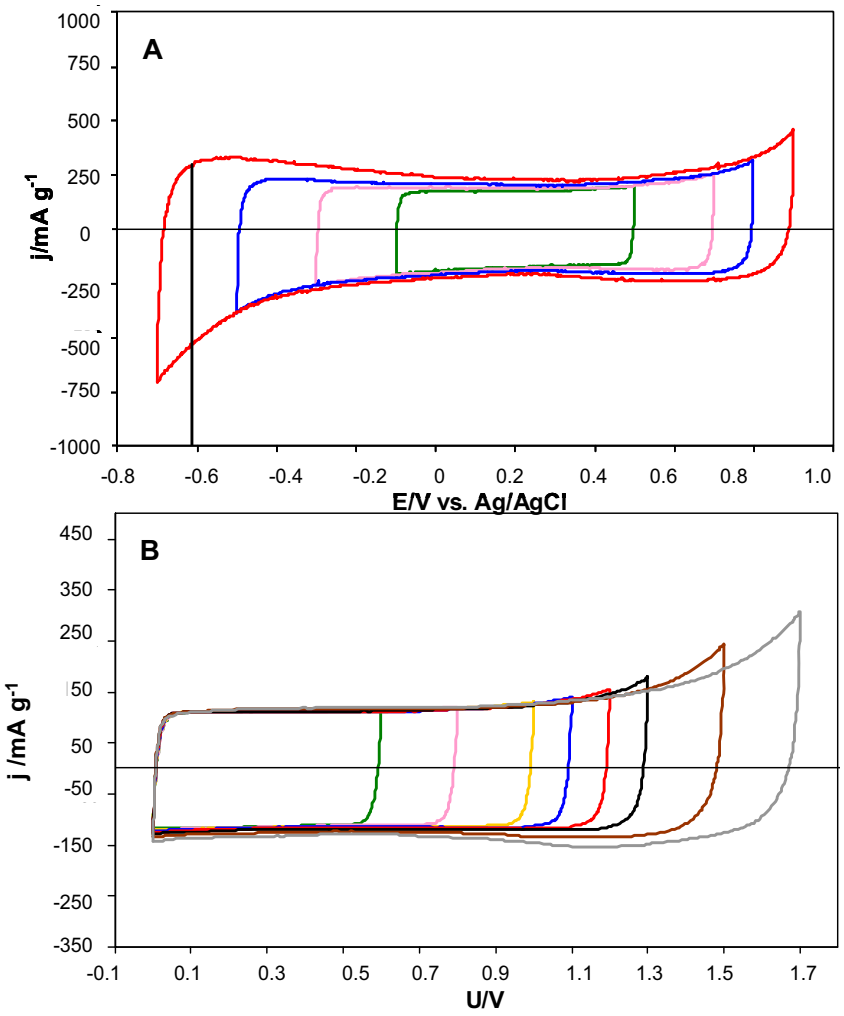

Fig. 3. 3-electrode (A) and 2-electrode (B) cyclic voltammograms of AOX in $PyNO_3$ with 1110 ppm water; scan rate 2 mV s^{-1}.

Triethylammonium bis(trifluoromethanesulfonyl)imide (NEt_3H TFSI) ionic liquid (σ = 5 mS cm^{-1}, η = 39 mPa s) might be a good candidate for this application since it can be dried until the water content is as low as 200 ppm. CVs recorded in a 3-electrode cell for a working electrode of MWV with NEt_3H TFSI-dry as electrolyte are presented in Fig. 4. The vertical line located at around -0.6 V vs. Ag/AgCl corresponds to the theoretical potential for the generation of dihydrogen. The voltammograms exhibit a quasi-rectangular behavior in a potential window as large as [-0.8; 1.6] V vs. Ag/AgCl (the brown curve), suggesting that a maximum cell voltage of at least 2.4 V can be applied. When the lower potential limit is shifted towards more negative values, a redox process begins to appear. This is probably due to the hydrogen storage process [31] (during the negative potential scan) coupled to its oxidation (during the positive scan) coming from the reversible decomposition of the cation. On the black curve, when the lower limit reaches -1.4 V vs. Ag/AgCl, some distortions can be observed, an oxidation wave for the highest potential and a reduction one which reaches its maximum at around 0.25 V vs. ref. Such distortions have not yet been assigned, but they might correspond to an

irreversible degradation of the electrolyte. It should also be noted that a similar behavior was observed when the working electrode was composed of AOX xerogel.

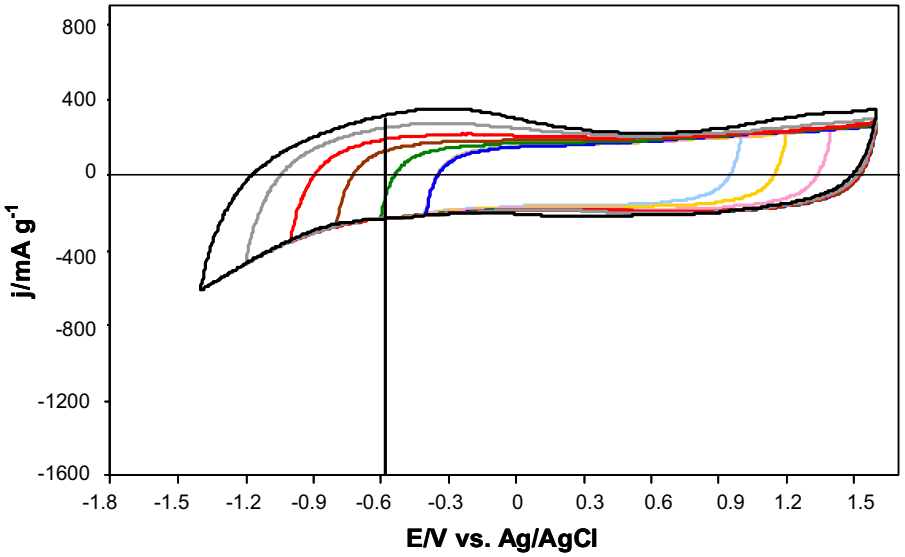

Fig. 4. 3-electrode cyclic voltammograms of MWV with NEt_3H TFSI (200 ppm water); scan rate 2 mV s^{-1}.

In order to evaluate the effect of water contained in this ionic liquid, a 3-electrode cell with MWV as electrode material and an electrolyte based on NEt_3H TFSI (water content of around 5000 ppm) was prepared. The results are presented in Fig. 5 where certain differences stand out when compared to the results in Fig. 4. As expected, several distortions can be observed, even for the narrow potential window, and there is a very pronounced reduction wave at around -0.4-0.5 V vs. Ag/AgCl. Moreover, when the lower limit is shifted towards more negative values, the hydrogen storage process and, possibly dihydrogen generation, becomes apparent at -0.6 V (for NEt_3H TFSI 200 ppm H_2O, this starts when E < -0.8 V). The charge involved in the hydrogen process is also more intense (j is more negative when the electrolyte contains a larger amount of water), indicating a more pronounced process. These phenomena confirm the presence of water in the electrolyte and suggest that water reduces/limits the stability potential window of the electrolyte. Thus, NEt_3H TFSI seems to be a promising electrolyte since it can be dried until it contains very low levels of water (200 ppm).

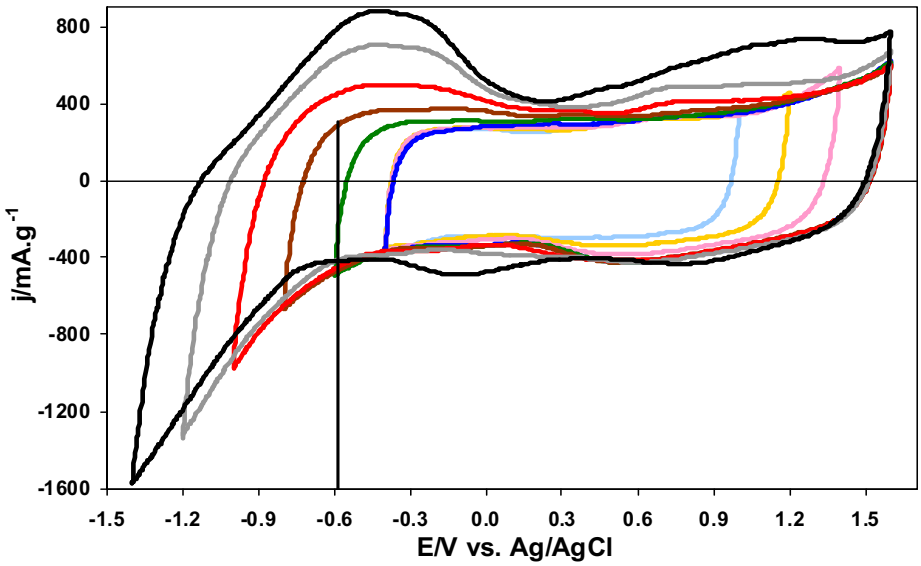

Fig. 5. 3-electrode cyclic voltammograms of MWV recorded in NEt_3H TFSI with 5000 ppm water; scan rate 2 mV s^{-1}.

The effect of the water content of NEt_3H TFSI on the electrochemical properties of the supercapacitors was also evaluated by applying charge-discharge tests to a 2-electrode cell with MWV as electrode material. Fig. 6 shows the values corresponding to specific capacitance and efficiency (parameter related to the reversibility of the systems) vs. the maximum voltage used for two cells based on Net_3H TFSI with a different water content (200 ppm, green line and 5000 ppm, blue line). Efficiency was calculated by means of Eq. (3):

$$\eta = \frac{t_d}{t_c} \tag{3}$$

where t_d and t_c are the discharge and charge time, respectively. As can be seen in Fig. 6, efficiency is higher in the case of the dried electrolyte. In the case of the electrolyte containing 5000 ppm of water, redox processes linked to water reduction/oxidation, even at low voltages, result in a poorer efficiency. As a result of these redox reactions, the specific capacitance of the system is increased but, on the other hand, a marked decrease in reversibility is observed. Therefore, the maximum voltage used in the presence of 5000 ppm of H_2O is similar to that obtained with capacitors based on a neutral aqueous medium (1.6 – 2.0 V) [5, 32], whereas when an almost dried electrolyte is used, voltages as high as 2.4-2.5 V can applied.

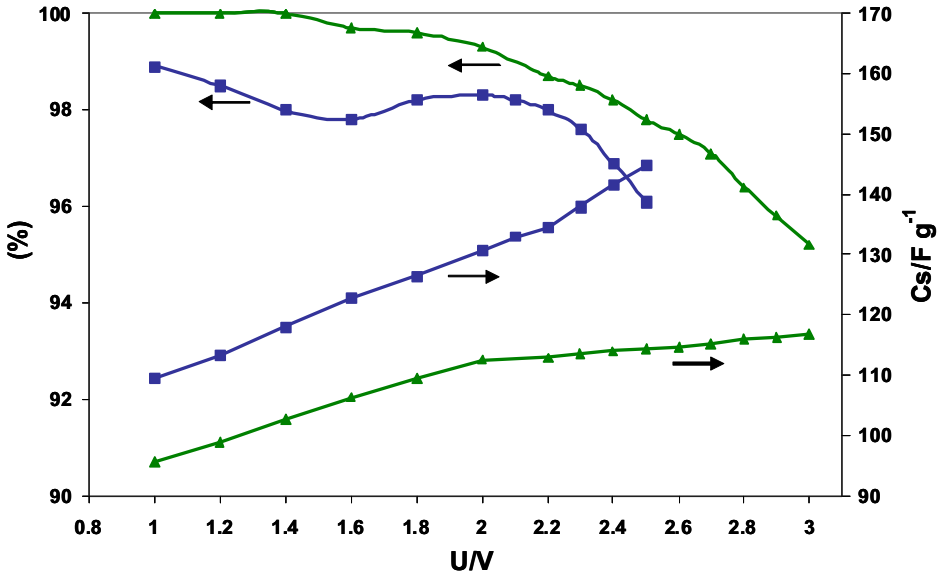

Fig. 6. Efficiency and specific capacitance at various maximum voltages recorded for symmetric 2-electrode cells with MWV as active material and NEt_3H TFSI as electrolyte. Effect of water content: 200 ppm (green) or 5000 ppm (blue).

It can be seen from Fig. 7 that the CVs recorded on a two electrode-cell capacitor with MWV exhibit a quasi-rectangular shape at voltages higher than 2.5 V. As further confirmation of capacitive behavior, Fig. 8A shows that the galvanostatic charge-discharge curves for supercapacitors based on MWV or AOX carbons have an almost isosceles triangle shape whatever the cell voltage applied. In short, cell voltages as high as the ones obtained with organic electrolytes can be reached when almost dry PILs are used.

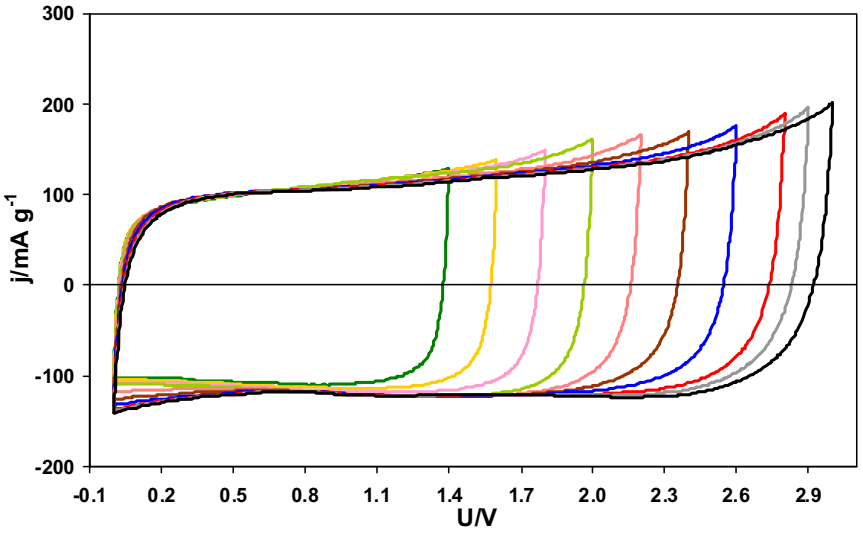

Fig. 7. Cyclic voltammograms obtained in a symmetric 2-electrode cell built using NEt_3H TFSI 200 ppm water and MWV as active material.

The capacitance values collected in Fig. 8B confirm that specific capacitance is higher in AOX-based supercapacitors. In particular, approximately 150 F g^{-1} can be achieved at a cell voltage of 2.5 V.

These results confirm that, whatever the PIL used, the presence of a more developed microporosity and small mesopores favors the diffusion and trapping of electrolyte ions and therefore, a greater specific capacitance.

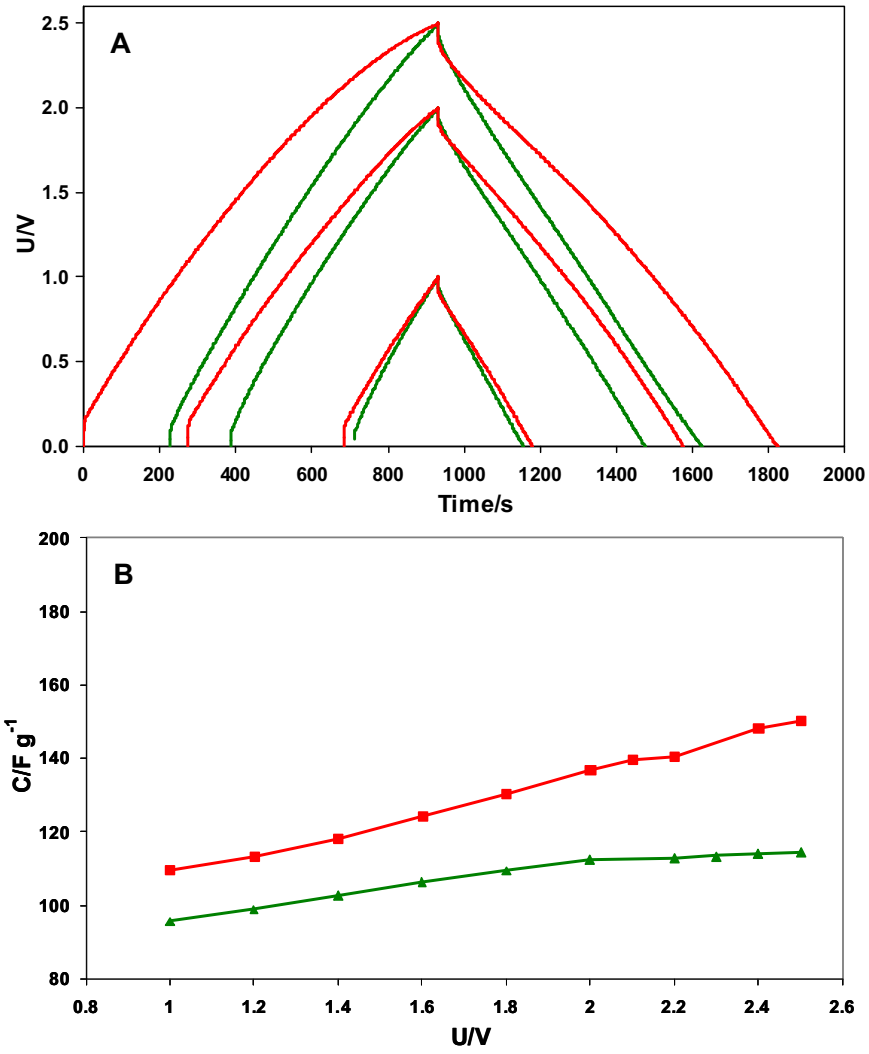

Fig. 8. Galvanostatic characteristics (j = ±200 mA g^{-1}) obtained at different maximum voltages (A) and specific capacitance versus maximum voltage (B) recorded with symmetric 2-electrode cells built in NEt_3H TFSI 200 ppm water with AOX (red) or MWV (green).

The ionic liquids can be mixed with organic solvents in order to increase the conductivity of the electrolyte. This approach has been tried by various research groups. For example, AILs have been mixed with acetonitrile [33] or propylene carbonate [34] and PILS have been mixed with acetonitrile [21]. These mixtures are promising for applications in supercapacitors since high performances (great energy and power densities) and good cyclability have been reported. Accordingly, we prepared a mixture of NEt_3HTFSI/PC (1:1) and used it as electrolyte for electrochemical capacitors. This mixture displays a water content of around 300 ppm. Fig. 9 shows the CVs recorded with a symmetric 2-electrode cell with MWV as active material in the mixed electrolyte. Compared to the CVs obtained

with the pure electrolyte, the shape of the voltammograms is more rectangular in the case of the cells assembled with the mixture NEt_3H TFSI/PC, which indicates that this electrolyte is more conductive. This is confirmed by the conductivity measurements, since the ionic conductivity for the PIL with no solvent is 5.7 mS cm^{-1} while this value is 12.5 mS cm^{-1} in the presence of PC. In the case of the charge passed through each system, the current densities appear to be of the same order, revealing that, whichever electrolyte is employed (with or without solvent), the specific capacitance of the system obtained with MWV is not affected.

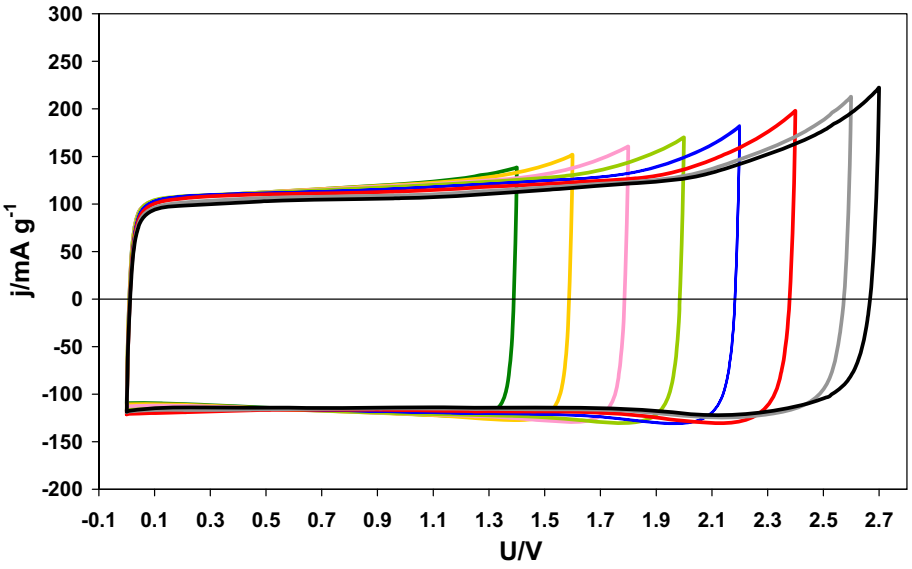

Fig. 9. Cyclic voltammograms obtained in a symmetric 2-electrode cell built using NEt_3H TFSI / PC with MWV as active material.

Fig. 10 shows the values of specific capacitance and efficiency obtained using a symmetric capacitor operating with the mixed electrolyte (red curves). For comparison, the data collected with the pure electrolyte have been added (green curves). It can be seen that the addition of PC to NEt_3H TFSI does not favor the performance of the supercapacitors. Indeed, in the presence of organic solvent, the efficiency of the system is slightly lower while the specific capacitance is not improved. In short, for this type of PILs, there is no indication that adding PC is a good method of improving the performance of the system, even if the ionic conductivity of the electrolyte is increased.

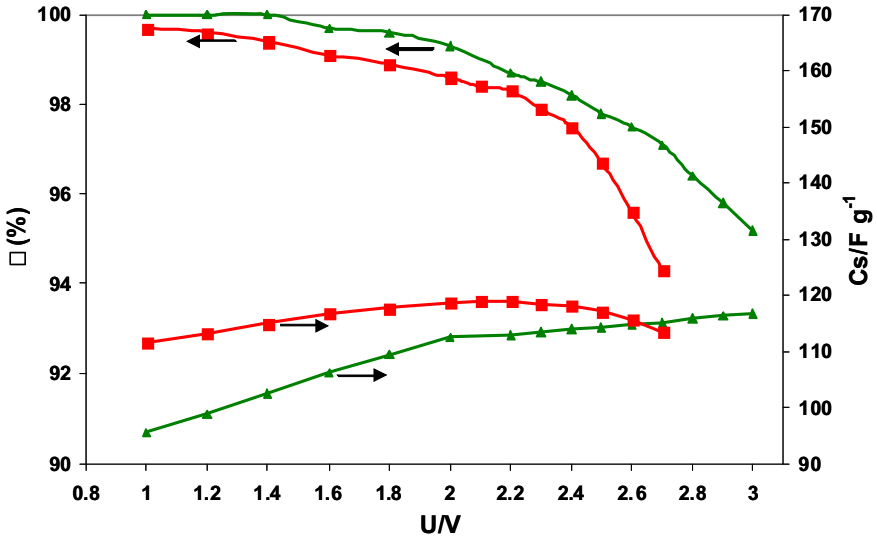

Fig. 10. Efficiency and specific capacitance at various maximum voltages recorded for symmetric 2-electrode cells with MWV as active material. Effect of the nature of the electrolyte: NEt_3H TFSI (green) or NEt_3H TFSI/PC (1:1) (red).

4. Conclusions

PILs are very promising electrolytes as they are cheap, "green", easy to synthesize, thermally and electrochemically stable, more conductive than AILs and they possess protons able to undergo redox processes with the surface functionalities of electrode materials.

In the present study, different strategies have been employed in order to improve the capacitance and/or the cell voltage of carbon-based supercapacitors using PILs as electrolytes with the aim of enhancing the energy density.

Capacitance can be optimized, independently of the PIL, by using a nanoporous carbon containing a sufficient amount of small mesopores (pore diameter between 2-7 nm). However, the strongest effect on capacitance is observed when the pH of the electrolyte is modified, as in the case of aqueous electrolytes. A symmetric carbon-carbon cell operating with a PIL of basic pH as electrolyte delivers 70 % more capacitance than the same cell based on the PIL of neutral pH.

In addition, it has been shown that the cell voltage of carbon-PIL supercapacitors is affected by the presence of water in the electrolyte. If the electrolyte contains certain amount of H_2O, the cell voltage is not able to exceed the potential window of water, i.e. 1.2 V. Therefore, only water-free PILs are suitable for generating a high cell voltage and for developing high energy systems. Supercapacitors built with dry NEt_3H TFSI (less than 200 ppm of H_2O) are able to operate at cell voltages of 2.5 V and, therefore energy densities comparable to those obtained with organic electrolytes can be achieved but with a cleaner electrolyte.

Acknowledgments: This work was financially supported by the "Conseil Général de la Région Centre" (project Sup'Caplipe) and Ministerio de Economía y Competitividad, Spain (project MAT-2011-23733). E.G. Calvo also acknowledges a predoctoral research grant from Ficyt (Spain).

References

[1] A. Burke, R&D considerations for the performance and application of electrochemical capacitors, Electrochim. Acta 53 (2007) 1083.

[2] V. Khomenko, E. Raymundo-Piñero, F. Béguin, Optimisation of an asymmetric manganese oxide/activated carbon capacitor working at 2 V in aqueous medium, J. Power Sources 153 (2006) 183.

[3] T. Brousse, P. L. Taberna, O. Crosnier, R. Dugas, P. Guillemet, Y. Scudeller, Y. Zhou, F. Favier, D. Bélanger, P. Simon, Long-term cycling behavior of asymmetric activated carbon/MnO_2 aqueous electrochemical supercapacitor, J. Power Sources 173 (2007) 633.

[4] V. Khomenko, E. Raymundo-Piñero, F. Béguin, A new type of high energy asymmetric capacitor with nanoporous carbon electrodes in aqueous electrolyte, J. Power Sources 195 (2010) 4234.

[5] L. Demarconnay, E. Raymundo-Piñero, F. Béguin, A symmetric carbon/carbon supercapacitor operating at 1.6 V by using a neutral aqueous solution, Electrochem. Comm. 12 (2010) 1275.

[6] G. Lota, K. Fic, E. Frackowiak, Alkali metal iodide/carbon interface as a source of pseudocapacitance, Electrochem. Comm. 13 (2011) 38.

[7] J. Liu, G. Jiang, Y. Chi, Y. Cai, Q. Zhou, J. Hu, Use of Ionic Liquids for Liquid-Phase Microextraction of Polycyclic Aromatic Hydrocarbons, Anal. Chem. 75 (2003) 5870.

[8] H. Zhao, S. Xia, P. Ma, Use of ionic liquids as "green" solvents for extractions – A review, J. Chem. Technol. Biotechnol. 80 (2005) 1089.

[9] C. Mehnert, R. Cook, N. Dispenzière, M. Afeworki, Supported Ionic Liquid Catalysis – A New Concept for Homogeneous Hydroformylation Catalysis, J. Am. Chem. Soc. 124 (2002) 12932.

[10] R. de Souza, J. Padilha, R. Gonçalves, J. Dupont, Room temperature dialkylimidazolium ionic liquid-based fuel cells, Electrochem. Comm. 5 (2003) 728.

[11] M. Guo, J. Fang, H. Xu, W. Li, X. Lu, C. Lan, K. Li, Synthesis and characterization of novel anion exchange membranes based on imidazolium-type ionic liquid for alkaline fuel cells, J. Membrane Science 362 (2010) 97.

[12] J. Wang, S. Hsu, Enhanced high-temperature polymer electrolyte membrane for fuel cells based on polybenzimidazole and ionic liquids, Electrochim. Acta 56 (2011) 2842.

[13] W. Lu, A. Fadeev, B. Qi, E. Smela, B. Mattes, J. Ding, G. Spinks, J. Mazurkiewicz, D. Zhou, G. Wallace, D. MacFarlane, S. Forsyth, M. Forsyth, Use of Ionic Liquids for π-Conjugated Polymer Electrochemical Devices, Science 297 (2002) 983.

[14] J. Stoimenovski, D. MacFarlane, K. Bica, R. D. Rogers, Crystalline vs. Ionic Liquid Salt Forms of Active Pharmaceutical Ingredients: A Position Paper, Pharm. Res. 27 (2010) 521.

[15] A. Lewandowski, A. Olejniczak, M. Galinski, I. Stepniak, Performance of carbon-carbon supercapacitors based on organic, aqueous and ionic liquid electrolytes, J. Power Sources 195 (2010) 5814.

[16] C. Arbizzani, M. Biso, D. Cericola, M. Lazzari, F. Soavi, M. Mastragostino, Safe, high-energy supercapacitors based on solvent-free ionic liquid electrolytes, J. Power Sources 185 (2008) 1575.

[17] A. Lewandowski, A. Swiderska, Electrochemical capacitors with polymer electrolytes based on ionic liquids, Solid State Ionics 161 (2003) 243.

[18] A. Balducci, U. Bardi, S. Caporali, M. Mastragostino, F. Soavi, Ionic liquids for hybrid supercapacitors, Electrochem. Comm. 6 (2004) 566.

[19] B. Xin, F. Wu, R. Chen, G. Cao, S. Chen, G. Wang, Y. Yang, Room temperature molten salts as electrolyte for carbon nanotube-based electric double layer capacitors, J. Power Sources 158 (2006) 773.

[20] A. Balducci, R. Dugas, P. L. Taberna, P. Simon, D. Plée, M. Mastragostino, S. Passerini, High temperature carbon-carbon supercapacitor using ionic liquid as electrolyte, J. Power Sources 165 (2007) 922.

[21] L. Timperman, H. Galiano, D. Lemordant, M. Anouti, Phosphonium-based protic ionic liquid as electrolyte for carbon-based supercapacitors, Electrochem. Comm. 13 (2011) 1112.

[22] W. Xu, C. Angell, Solvent-Free Electrolytes with Aqueous Solution-Like Conductivities, Science 302 (2003) 422.

[23] D. Rochefort, A. L. Pont, Pseudocapacitive behaviour of RuO_2 in a proton exchange ionic liquid, Electrochem. Comm. 8 (2006) 1539.

[24] R. Mysyk, E. Raymundo-Piñero, M. Anouti, D. Lemordant, F. Béguin, Pseudo-capacitance of nanoporous carbons in pyrrolidinium-based protic ionic liquids, Electrochem. Comm. 12 (2010) 414.

[25] W. A. Henderson, S. Passerini, Phase-behavior of ionic liquid-LiX mixtures: Pyrrolidinium cations and $TFSI^-$ anions, Chem. Mater. 16 (2004) 2881.

[26] E.G. Calvo, E.J. Juárez-Pérez, J.A. Menéndez, A. Arenillas, Fast microwave-assisted synthesis of tailored mesoporous carbon xerogels, J. Colloid Interface Sci. 357 (2011) 541.

[27] K. Babel, K. Jurewicz, KOH activated carbon fabrics as supercapacitor material, J. Phys. Chem. Solids 65 (2004) 275.

[28] V. Ruiz, R. Santamaria, M. Granda, C. Blanco, Long-term cycling of carbon-based supercapacitors in aqueous media, Electrochim. Acta 54 (2009) 4481.

[29] S. Baranton, D. Bélanger, In situ generation of diazonim cations in organic electrolyte for electrochemical modification of electrode surface, Electrochim. Acta 53 (2008) 6961.

[30] T. L. Greaves, D. F. Kennedy, A. Weerawardena, N. M. K. Tse, N. Kirby, C. J. Drummond, Nanostructured protic ionic liquids retain nanoscale features in aqueous solution while precursor Brønsted acids and bases exhibit different behaviour, J. Phys. Chem. B 115 (2011) 2055.

[31] K. Jurewicz, E. Frackowiak, F. Béguin, Towards the mechanism of electrochemical hydrogen storage in nanostructured carbon materials, Appl. Phys. A 78 (2004) 981.

[32] L. Demarconnay, E. Raymundo-Piñero, F. Béguin, Adjustment of electrodes potential window in an asymmetric carbon/MnO_2 supercapacitor, J. Power Sources 196 (2011) 580.

[33] E. Frackowiak, G. Lota, J. Pernak, Room-temperature phosphonium ionic liquids for supercapacitor application, Appl. Phys. Lett. 86 (2005) 164104.

[34] A. Krause, A. Balducci, High voltage electrochemical double layer capacitor containing mixtures of ionic liquids and organic carbonate as electrolytes, Electrochem. Comm. 13 (2011) 814.

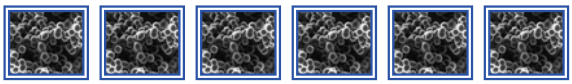

6. Conclusiones

Esta memoria, y los artículos presentados en ella, muestran los resultados derivados del estudio de la síntesis de xerogeles de carbono con propiedades porosas y químicas controladas y su posterior aplicación como material de electrodo en supercondensadores. A continuación se presentan las conclusiones más relevantes derivadas de dicho trabajo.

Síntesis de xerogeles de carbono asistida con microondas

- El calentamiento con microondas permite obtener xerogeles de carbono, cuyas propiedades se pueden diseñar en función de las condiciones de operación, a partir de un procedimiento más rápido y sencillo que los métodos de síntesis que emplean un calentamiento convencional.

- La variación del pH inicial utilizado en la síntesis inducida por microondas permite controlar las propiedades porosas de los xerogeles de carbono resultantes. El rango de porosidad afectado por el pH corresponde con la meso/macroporosidad, mientras que la microporosidad permanece prácticamente invariable. Por ello, se han podido sintetizar xerogeles de carbono micro-mesoporosos o micro-macroporosos mediante ligeras modificaciones en el pH de la mezcla resorcinol-formaldehído.

- Existen ciertas diferencias entre la porosidad de los xerogeles de carbono obtenidos mediante síntesis convencional y aquellos producidos con microondas. Bajo las mismas condiciones de operación, los dos tipos de xerogeles de carbono contienen un volumen de microporos similar, mientras que la meso/macroporosidad se ve ligeramente modificada, tanto en lo que respecta al tamaño como al volumen de poros. Así, a bajos valores de pH, la síntesis convencional produce xerogeles de carbono micro-macroporosos frente a los micro-mesoporosos obtenidos mediante la síntesis asistida con microondas, como consecuencia del colapso parcial que sufre la estructura porosa al someterse a dicha radiación.

- La tecnología microondas ha permitido sintetizar miliesferas de xerogel de carbono (tamaño entre 0.5-2.0 mm) mediante un método sencillo y sin la adición de ningún tipo de surfactante. La

porosidad y el tamaño de las miliesferas de xerogel de carbon se ha modificado gracias a la variación del pH de la disolución precursora.

Procesos de activación

❖ La activación de xerogeles orgánicos asistida con microondas (hidróxido de potasio como agente activante) ha permitido obtener xerogeles de carbono altamente microporosos (S_{BET} > 2000 m^2 g^{-1}), convirtiéndolos en materiales prometedores para la aplicación estudiada en el presente trabajo (almacenamiento de energía en supercondensadores).

❖ Se ha demostrado que los procesos de activación llevados a cabo en un horno microondas permiten preservar, dependiendo de las condiciones de activación, parte de la meso/macroporosidad creada durante la síntesis del xerogel orgánico. Las mejores condiciones de activación en horno microondas implican utilizar temperaturas próximas a 700 ºC y tiempos de activación inferiores a 30 minutos, ya que garantizan que la mesoporosidad originada durante las reacciones de polimerización entre los monómeros resorcinol/formaldehído no se haya destruido y, además, que se alcancen elevados volúmenes de microporos.

Almacenamiento de energía en supercondensadores

❖ El uso de supercondensadores asimétricos basados en MnO_2/xerogel de carbono ha permitido incrementar el voltaje de trabajo por encima de los valores asociados a supercondensadores simétricos basados en electrolitos acuosos, incremento que repercute en una mayor densidad de energía. En este sentido, el voltaje de trabajo de una celda electroquímica MnO_2/xerogel de carbono que utiliza una disolución de Na_2SO_4 como electrolito ha sido de aproximadamente 1.6 V.

❖ Se ha demostrado que la adición de nanotubos de carbono mejora las propiedades conductoras de los electrodos fabricados. Así un electrodo compuesto por un xerogel de carbono activado ha presentado un valor de conductividad eléctrica de 25 mS cm^{-1}, mientras que la adición de nanotubos de carbono (18 %, en masa) lleva asociada un valor de conductividad de 115 mS cm^{-1}.

❖ Se ha aplicado un modelo físico-químico que permite determinar parámetros estructurales y cinéticos de los supercondensadores. Así, se ha podido conocer la fracción del electrodo que participa activamente en la formación de la doble capa eléctrica o su conductividad efectiva, parámetros que ayudan a entender la respuesta electroquímica de diferentes materiales de electrodo. Los xerogeles de carbono evaluados han mostrado una matriz porosa electroquímicamente accesible superior a la de un carbón activo comercial, probablemente como consecuencia de su contenido en mesoporos.

❖ Todas las publicaciones recogidas en la presente memoria han puesto en evidencia la importancia de la distribución del tamaño de poros sobre la capacidad de almacenamiento de energía

de los materiales de electrodo. Los resultados revelan que xerogeles de carbono micro-mesoporosos (mesoporos de pequeño-mediano tamaño) llevan asociados valores de capacidad específica superiores a los obtenidos con diversos carbones activos comerciales formados, en su mayoría, por microporos.

❖ El pH del electrolito tiene gran influencia sobre la capacidad de almacenamiento de energía de los xerogeles de carbono. De esta manera, se ha alcanzado una capacidad específica próxima a 200 F g^{-1} utilizando una disolución de H_2SO_4 como electrolito frente a ~ 100 F g^{-1} cuando el electrolito empleado fue KOH. Este resultado se ha justificado por la mayor conductividad iónica del ácido sulfúrico y, probablemente, la mayor actividad de los grupos oxigenados del xerogel de carbono en dicho medio, actividad que incrementa la capacidad de almacenamiento de energía del dispositivo debido a una contribución pseudofaradaica.

❖ Los líquidos iónicos próticos (PILs) han demostrado ser electrolitos muy prometedores para la aplicación estudiada en esta Tesis Doctoral puesto que permiten incrementar el voltaje de trabajo de las celdas electroquímicas. En este tipo de electrolitos, tanto el pH del medio como su contenido en agua es fundamental puesto que determinan la capacidad específica y el voltaje de trabajo del supercondensador. Los resultados revelan que un incremento de 7 a 11 en el valor pH de un líquido iónico da lugar a una mayor cantidad de energía almacenada (121 F g^{-1} frente a 201 F g^{-1} para el líquido iónico $PyNO_3$). Con respecto a la cantidad de H_2O contenida en el líquido iónico, como era de esperar, el voltaje de trabajo de la celda se ha visto incrementado al disminuir el contenido en H_2O (2.5 V para un líquido iónico que presenta un contenido en H_2O de 200 ppm frente a 1.6-2.0 V cuando la presencia de agua en el líquido iónico es de alrededor de 5000 ppm).

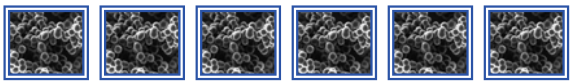

6. Conclusions

This work shows the results derived from the study of the synthesis of carbon xerogels with tailored porous and chemical properties and their subsequent application as electrode material in supercapacitors. The most important conclusions derived from this study are summarized below:

Microwave-induced synthesis of carbon xerogels

❖ Carbon xerogels with tailored properties according to the operating conditions can be synthesized by means of microwave heating, which is a more rapid and simple synthesis method than those based on conventional heating.

❖ By modifying the initial pH used in the microwave-induced synthesis it is possible to control the porous texture of the resulting carbon xerogels. The porosity range affected by the modification of the pH corresponds to meso/macroporosity, whereas the microporosity remains virtually unchanged. Thus, micro-mesoporous or micro-macroporous carbon xerogels can be synthesized by slightly varying the pH of the resorcinol-formaldehyde mixture.

❖ There are some distinctive features between porosity of conventionally synthesized carbon xerogels and those produced through microwave radiation. Under the same operating conditions, the two types of carbon xerogels display a similar micropore volume, whereas the meso/macroporosity is slightly different, as regards both the size and volume of pores. At low pH values, conventional synthesis leads to micro-macroporous carbon xerogels, whereas microwave heating gives rise to micro-mesoporous samples, as a result of the partial collapse of the porous structure.

❖ Carbon xerogel millispheres (0.5-2.0 mm) can be synthesized using a simple method based on microwave radiation without the addition of any surfactant. The porosity and size of the carbon xerogel millispheres has been modified by varying the pH of the precursor solution.

Activation processes

❖ The activation of organic xerogels by means of microwave radiation (potassium hydroxide as activating agent) yielded highly microporous carbon xerogels (S_{BET} > 2000 m^2 g^{-1}), which makes them very promising materials for the application studied in this work (energy storage in supercapacitors).

❖ It has been shown that the activation processes in a microwave furnace allow the meso/macroporosity created during the synthesis of organic xerogels to be partially preserved, depending on the activation conditions. The best activation conditions with microwave heating involve temperatures of around 700 ºC and activation times below 30 minutes to ensure that the mesoporosity originated during the polymerization reactions between the resorcinol/formaldehyde monomers is not destroyed and that a high micropore volume is achieved.

Energy storage in supercapacitors

❖ The use of asymmetric supercapacitors based on MnO_2/carbon xerogel allows the cell voltage to be increased above the typical values associated with symmetric supercapacitors composed of aqueous electrolytes, resulting in a greater energy density. For example, the cell voltage of a MnO_2/carbon xerogel system with a Na_2SO_4 solution as electrolyte was approximately 1.6 V.

❖ It has also been shown that the addition of carbon nanotubes improves the conductive properties of electrodes. Thus, an electrode composed of an activated carbon xerogel displayed an electrical conductivity value of 25 mS cm^{-1}, while the addition of carbon nanotubes (18 wt. %) yielded a conductivity value of 115 mS cm^{-1}.

❖ A physicochemical model was applied to determine the structural and kinetic parameters of the supercapacitors assembled. Thus, it was possible to determine the fraction of electrode surface involved in the formation of the double layer or the effective conductivity, parameters that may contribute to an understanding of the electrochemical response of different electrode materials. The carbon xerogels synthesized in this work showed an electrochemically accessible porous matrix higher than that of a commercial activated carbon, probably as a consequence of their mesopore content.

❖ All the publications reported in this work have highlighted the relevance of pore size distribution on the energy storage capacitance of electrode materials. The results reveal that micro-mesoporous carbon xerogels (small and medium size mesopores) are associated with higher specific capacitance values than those achieved with activated carbons, formed mostly by micropores.

❖ The pH of the electrolyte has a significant influence on the energy storage capacitance of carbon xerogels. A specific capacitance value of 200 F g^{-1} was achieved using a H_2SO_4 solution as electrolyte compared to ~ 100 F g^{-1} when the electrolyte used was a solution of potassium hydroxide.

This result is due to the higher ionic conductivity of sulphuric acid and, probably, the greater activity of the oxygenated groups of carbon xerogels in this medium, which increases their energy storage capacitance due to pseudofaradaic contributions.

❖ Protic Ionic Liquids (PILs) have proved to be very promising electrolytes for the application studied in this Thesis since it is possible to increase the potential window of electrochemical devices. In this type of electrolyte, both the pH of the medium and the water content are critical since they determine the specific capacitance and cell voltage. The results reveal that an increase from 7 to 11 in the pH value of a protic ionic liquid improves the specific capacitance (121 F g^{-1} compared to 201 F g^{-1} for an electrolyte based on $PyNO_3$). As expected, a decrease in the amount of water in the ionic liquid led to an increase in the operating voltage (2.5 V for an ionic liquid with a water content of 200 ppm versus 1.6-2.0 when the water content is around 5000 ppm).

7. Referencias Bibliográficas

Abdallah, T.; Lemordant, D.; Claude-Montigny, B. "Are room temperatura ionic liquids able to improve the safety of supercapacitors organic electrolytes without degrading the performances?". *J. Power Sources* 201 (2012) 353-359.

Al-Muhtaseb, S.A.; Ritter, J.A. "Preparation and Properties of Resorcinol-Formaldehyde Organic and Carbon Gels". *Adv. Mater.* 15 (2003) 101-114.

Alonso, A.; Ruiz, V.; Blanco, C.; Santamaría, R.; Granda, M.; Menéndez, R.; de Jaer, S.G.E. "Activated carbon produced from Sasol-Lurgi gasifier pitch and its application as electrodes in supercapacitors". *Carbon* 44 (2006) 441-446.

An, H.; Wang, Y.; Wang, X.; Zheng, L.; Wang, X.; Yi, L.; Bai, L.; Zhang, X. "Polypyrrole/carbon aerogel composite materials for supercpacitor". *J. Power Sources* 195 (2010) 6964-6969.

Anouti, M.; Couadou, E.; Timperman, L.; Galiano H. "Protic ionic liquid as electrolyte for high-densities electrochemical double layer capacitors with activated carbon electrode material". *Electrochim. Acta* 64 (2012) 110-117.

Arbizzany, C.; Biso, M.; Cericola, D.; Lazzari, M.; Soavi, F.; Mastragostino, M. "Safe, high-energy supercapacitors based on solvent-free ionic liquid electrolytes". *J. Power Sources* 185 (2008) 1575-1579.

Arenillas, A.; Menéndez, J.A.; Zubizarreta, L.; Calvo, E.G. "*Procedimiento de obtención de xerogeles orgánicos de porosidad controlada*". Patente Española, nº publicación 2 354 782 (2009).

Balducci, A.; Bardi, U.; Caporali, S.; Mastragostino, M.; Soavi, F. "Ionic liquids for hybrid supercapacitors". *Electrochem. Commun.* 6 (2004) 566-570.

Baños, R.; Manzano-Agugliaro, F.; Montoya, F.G.; Gil, C.; Alcayde, A.; Gómez, J. "Optimization methods applied to renewable and sustainable energy: A review". *Renewable Sustainable Energy Rev.* 15 (2011) 1753-1766.

Batanero, P.S.; Pingaron, J.M. "Química electroanalítica: Fundamentos y Aplicaciones". *Editorial Síntesis* Vol. 1 (2003) pp. 282-296.

Bleda-Martínez, M.J.; Maciá-Agulló, J.A.; Lozano-Castelló, D.; Morallón, E.; Cazorla-Amorós, D.; Linares-Solano, A. "Role of surface chemistry on electric double layer capacitance of carbon materials". *Carbon* 43 (2005) 2677-2684.

Bordjiba, T.; Mohamedi, M.; Dao, L.H. "Charge storage mechanism of binderless nanocomposite electrodes formed by dispersion of CNTs and carbon aerogels". *J. Electrochem. Society* 155 (2008) 115-124.

Burke, A. "Ultracapacitors: why, how and where is the technology". *J. Power Sources* 91 (2000) 37-50.

Calvo, E.G.; Ania, C.O., Zubizarreta, L.; Menéndez, J.A.; Arenillas, A. "Exploring new routes in the synthesis of carbon xerogels for their application in electric double-layer capacitors". *Energy Fuels* 24 (2010) 3334-3339.

Centeno, T.A.; Stoeckli, T. On the specific double-layer capacitance of activated carbons, in relation to their structural and chemical properties. *J. Power Sources* 154 (2009) 314-320.

Chae, J.-H.; Chen, G.Z. "1.9 V aqueous carbon-carbon supercapacitors with unequal electrode capacitances". *Electrochim. Acta* 86 (2012) 248-254.

Chmiola, J.; Yushin, G.; Gogotsi, Y.; Portet, C.; Simon, P.; Taberna, P.-L. "Anomalous Increase in Carbon Capacitance at Pore Sizes Less Than 1 Nanometer". *Science* 313 (2006) 1760-1763.

Contreras, M.S.; Páez, C.A.; Zubizarreta, L.; Léonard, A.; Bracher, S.; Olivera-Fuentes, C.G.; Arenillas, A.; Pirard, J.-P.; Job, N. "A comparison of physical activation of carbon xerogels with carbon dioxide with chemical activation using hydroxides". *Carbon* 48 (2010) 3157-3168.

Conway, B.E. "Electrochemical supercapacitors: scientific fundamentals and technological applications*". New York: Kluwer Academic/Plenum* (1999).

Demarconnay, L.; Raymundo-Piñero, E.; Béguin, F. "A symmetric carbon/carbon supercapacitor operating at 1.6 V by using a neutral aqueous solution". *Electrochem. Commun.* 12 (2010) 1275-1278.

Du, J.; Shao, G.; Qin, X.; Wang, G. "High surface area MnO_2 electrodeposited under supergravity field for supercapacitors and its electrochemical properties". *Mater. Lett.* 84 (2012) 13-15.

Dubinin, M.M. "Investigation of the porous structure of solids by adsorption methods. The application of various methods in studies of the structure of intermediate and macropores of activated carbon". *Zhurnal Fizicheskoi. Khimii* 34 (1960) 2019-2029.

Edwards, P.P.; Kuznetsov, V.L.; David, W.I.F.; Brandon, N.P. "Hydrogen and fuel cells: Towards a sustainable energy future". *Energy Policy* 36 (2008) 4356-4362.

Escribano, S.; Berthon, S.; Ginoux, J.L.; Achard, P. "Characterization of carbon aerogels". *Eurocarbon 98 Strasbourg* (1998) 841-842.

Evans, S.; Hamilton, W.S. "The mechanism of demineralization at carbon electrodes". *J. Electrochem. Soc.* 113 (1966) 1314-1319.

Fairén-Jiménez, D.; Carrasco-Marín, F.; Moreno-Castilla, C. "Porosity and surface area of monolithic carbon aerogels prepared using alkaline carbonates and organic acids as polimerization catalysts". *Carbon* 44 (2006) 2301-2307.

Fan, L.Z.; Maier, J. "High-performance polypyrrole electrode materials for redox supercapacitors". *Electrochem. Commun.* 8 (2006) 937-940.

Fernández, J.A.; Tennison, S.; Kozynchenko, O.; Rubiera, F.; Stoeckli, F.; Centeno, T.A. "Effect of mesoporosity on specific capacitance of carbons". *Carbon* 47 (2009) 1598-1604.

Figueiredo, J.L.; Pereira, M.F.R.; Freitas, M.M.A.; Órfao, J.J.M. "Modification of the surface chemistry of activated carbons". *Carbon* 37 (1999) 1379-1389.

Frackowiak, E. "Carbon materials for supercapacitor application". *Phys. Chem. Chem. Phys.* 39 (2007) 1774-1785.

Galinski, M; Lewandowski, A.; Stepniak, I. "Ionic liquids as electrolytes". *Electrochim. Acta* 51 (2006) 5567-5580.

Gallegos-Suárez, E.; Pérez-Cadenas, A.F.; Maldonado-Hódar, F.J.; Carrasco-Marín, F. "On the micro- and mesoporosity of carbon aerogels and xerogels. The role of the drying conditions during the synthesis processes". *Chem. Eng. J.* 181 (2012) 851-855.

García, B.B.; Candelaria, S.L.; Liu, D.; Sepheri, S.; Cruz, J.A.; Cao, G. "High performance high-purity sol-gel derived carbon supercapacitors from renewable sources". *Renewable Energy* 36 (2011) 1788-1794.

Guo, P.; Gu, Y.; Lei, Z.; Cui, Y.; Zhao, X.S. "Preparation of sucrose-based microporous carbons and their application as electrode materials for supercapacitors". *Microporous Mesoporous Mater.* 156 (2012) 176-180.

Gutmann, G. "Applications – Transportation; Electric Vehicle: Batteries". *Encyclopedia of Electrochem. Power Sources* (2009) 219-235.

Halama, A.; Szubzda, B.; Pasciak, G. "Carbon aerogels as electrode material for electrical double layer supercapacitors – Synthesis and properties". *Electrochim. Acta* 55 (2010) 7501-7505.

Hall, P.J.; Bain, E.J. "Energy-storage technologies and electricity generation". *Energy Policy* 36 (2008) 4352-4355.

Hydar, S.; Moreno-Castilla, C.; Ferro-García M.A.; Carrasco-Marín, F.; Rivera-Utrilla, J.; Perrard A.; Joly, J.P. "Regularities in temperature-programmed desorption spectra of CO_2 and CO from activated carbons". *Carbon* 38 (2000) 1297-1308.

Hong, M.S.; Lee, S.H.; Kim, S.W. "Use of KCl Aqueous Electrolyte for 2 V Manganese Oxide/Activated Carbon Hybrid Capacitor". *Electrochem. Solid-State Lett.* 5 (2002) 227-230.

Horikawa, T.; Hayashi, J.; Muroyama, K. "Controllability of pore characteristics of resorcinol-formaldehyde carbon aerogel". *Carbon* 42 (2004) 1625-1633.

Hsieh, C.-T.; Teng, T. "Influence of oxygen treatment on electric double-layer capacitance of activated carbon fabrics". *Carbon* 40 (2002) 667-674.

Hulicova-Jurcakova, D.; Seredych, M.; Lu, G.Q.; Kodiweera, N.K.A.C.; Stallworth, P.E.; Greenbaum, S.; Bandosz, T.J. "Effect of surface phosphorus functionalities of activated carbons containing oxygen and nitrogen on electrochemical capacitance". *Carbon* 47 (2009) 1576-1584.

Inagaki, M.; Konno, H.; Tanaike, O. "Carbon materials for electrochemical applications". *J. Power Sources* 195 (2010) 7880-7903.

International Energy Agency. Key World Energy Statistics 2012. www.iea.org

Ioannidou, O.; Zabaniotou, A. "Agricultural residues as precursors for activated carbon production – a review". *Renewable Sustainable Energy Rev.* 11 (2007), 1966-2005.

IUPAC "IUPAC Recommendations". *Pure Appl. Chem.* 57 (1985) 603-619.

IUPAC "Definitions, terminology and symbols in colloidal and surface chemistry". *Pure Appl. Chem.* 31 (1972), 579-638.

Jiang, J.; Kucernak, A. "Electrochemical supercapacitor material based on manganese oxide: preparation and characterization". *Electrochem. Acta* 47 (2002) 2381-2386.

Job, N.; Panariello, F.; Crine, M.; Pirard, J.-P.; Leonard, A. "Rheological determination of the sol-gel transition during the aqueous synthesis of resorcinol-formaldehyde resins. *Colloids Surf. A* 293 (2007), 224-228.

Job, N.; Pirard, R.; Marien, J.; Pirard, J.-P. "Porous carbon xerogels with texture tailored by pH control during sol-gel process". *Carbon* 42 (2004) 619-628.

Juárez-Pérez, E.J.; Calvo, E.G.; Arenillas, A.; Menéndez, J.A. "Precise determination of the point of sol-gel transition in carbon gels synthesis using a microwave heating method". *Carbon* 48 (2010) 3305-3308.

Jurewicz, K.; Delpeux, S.; Bertagna, V.; Béguin, F.; Frackowiak, E. "Supercapacitors from nanotube/polypyrrole composites". *Chem. Phys. Lett.* 347 (2001) 36-40.

Kaldellis, J.K.; Zafirakis, D. "Optimun energy storage techniques for the improvement of renewable energy sources-based electricity generation economic efficiency". *Energy* 32 (2007) 2295-2305.

Khomenko, V.; Raymundo-Piñero, E.; Béguin, F. "Optimisation of an asymmetric manganese oxide/activated carbon capacitor working at 2 V in aqueous medium". *J. Power Sources* 153 (2006) 183-190.

Khomenko, V.; Raymundo-Piñero, E.; Béguin, F. "A new type of high energy asymmetric capacitor with nanoporous carbon electrodes in aqueous electrolyte". *J. Power Sources* 195 (2010) 4234-4241.

Kim, I.-H.; Kim, K.-B. "Electrochemical Characterization of Hydrous Ruthenium Oxide Thin-Film Electrodes for Electrochemical Capacitor Applications". *J. Electrochem. Soc.* 153 (2006) 383-389.

Kötz, R.; Carlen, M. "Principles and applications of electrochemical capacitors". *Electrochim. Acta* 45 (2000) 2483-2498.

Kumar, D.; Hashmi, S.A. "Ionic liquid based sodium ion conducting gel polymer electrolytes". *Solid State Ionics* 181 (2010) 416-423.

Kurzweil, R.; Brandt, K. "Secondary batteries – Lithium rechargeable systems – Overview". *Encyclopedia of Electrochemical Power Sources* (2009) 1-26.

Laforgue, A.; Simon, P.; Sarrazin, C.; Fauvarque, J.-F. "Polythiophene-based supercapacitors". *J. Power Sources* 80 (1999) 142-148.

Largeot, C.; Portet, C.; Chmiola, J.; Taberna, P.L.; Gogotsi, Y.; Simon, P. "Relation between the ion size and pore size for an electric double-layer capacitor". *J. Am. Chem. Soc.* 130 (2008) 2730-2731.

Lewandowski, A.; Olejniczak, A.; Galinski, M.; Stepniak, I. "Performance of carbon-carbon supercapacitors based on organic, aqueous and ionic liquid electrolytes". *J. Power Sources* 195 (2010) 5814-5819.

Li, B.; Xie, H. "Synthesis of graphene oxide/polypyrrole nanowire composites for supercapacitors". *Mater. Lett.* 78 (2012) 106-109.

Li, M.; Li, W.; Liu, S. "Hydrothermal synthesis, characterization and KOH activation of carbon spheres from glucose". *Carbohydr. Res.* 346 (2011A) 99-104.

Li, X.; Wei, B. "Supercapacitors based on nanostructured carbon". *Nano Energy* 2 (2013) 15-173.

Li, Y.; Li, K.; Sun, G. "A facile synthesis method for millimeter polyacrylonitrile-based activated carbon spheres with radiate tunnel-like macropores". *Mater. Lett.* 65 (2011B) 1022-1024.

Lin, C.; Ritter, J.A. "Carbonization and activation of sol-gel derived carbon xerogels". *Carbon* 38 (2000) 849-861.

Lin, C.; Ritter, J.A.; Popov, B.N. "Characterization of Sol-Gel-Derived Cobalt Oxide Xerogels as Electrochemical Capacitors". *J. Electrochem. Soc.* 145 (1998) 4097-4103.

Liu, X.; Pickup, P.G. "Ru oxide supercapacitors with high loadings and high power and energy densities". *J. Power Sources* 176 (2008) 410-416.

Lokhande, C.D.; Dubal, D.P.; Joo, O.-S. "Metal oxide thin film based supercapacitors – review". *Curr. Appl. Phys.* 11 (2011) 255-270.

Lota, G.; Centeno, T.A.; Frackowiak, E.; Stoeckli, F. "Improvement of the structural and chemical properties of a commercial activated carbon for its application in electrochemical capacitors". *Electrochim. Acta* 53 (2008) 2210-2216.

Lozano-Castelló, D.; Cazorla-Amorós, D.; Linares-Solano, A.; Shiraishi, S. "Influence of pore structure and surface chemistry on electric double layer capacitance in non-aqueous electrolyte". *Carbon* 41 (2003) 1765-1775.

Macdonald, J.R.; Kenan, W.R. "Impedance Spectroscopy: Emphasizing Solid Materials and Systems". Edit by J.R. Macdonald, IBN 0-471-83122-0, United States.

Maciá-Agulló, J.A.; Moore, B.C.; Cazorla-Amorós, D.; Linares-Solano, A. "Activation of coal tar pitch carbon fibres: Physical activation vs. chemical activation". *Carbon* 42 (2004) 1367-1370.

Mahata, N.; Pereira, M.F.R.; Suárez-García, F.; Martínez-Alonso, A.; Tascón, J.M.D.; Figueiredo, J.L. "Tuning of texture and surface chemistry of carbon xerogels". *J. Colloid Interface Sci.* 324 (2008) 150-155.

Mi, H.; Zhang, X.; Yang, S.; Ye, X.; Luo, J. "Polyaniline nanofibers as the electrode material for supercapacitors" *Mater. Chem. Physics* 112 (2008) 127-131.

Morales-Torres, S.; Maldonado-Hódar, F.J.; Pérez-Cadenas, A.F.; Carrasco-Marín, F. "Structural characterization of carbon xerogels: From film to monolith". *Microporous Mesoporous Mater.* 153 (2012).

Moreno-Castilla, C.; Maldonado-Hódar, F.J. "Carbon aerogels for catalysis applications: An overview". *Carbon* 43 (2005) 455-465.

Mysyk, R.; Raymundo-Piñero, E.; Anouti, M.; Lemordant, D.; Béguin, F. "Pseudo-capacitance of nanoporous carbons in pyrrolidinium-based protic ionic liquids". *Electrochem. Commun.* 12 (2010) 414-417.

Mysyk, R.; Raymundo-Piñero, E.: Béguin, F. "Saturation of subnanometer pores in an electric double-layer capacitor". *Electrochem. Commun*. 11 (2009) 554-556.

Nishino, A. "Capacitors: operating principles, current market and technical trends". *J. Power Sources* 60 (1996) 137-147.

Nomoto, S.; Nakata, H.; Yoshioka, K.; Yacida, A.; Moneda, A. "Advanced capacitors and their application". *J. Power Sources* 97 (2001) 807-811.

Obreja, V.V.N. "On the performance of supercapacitors with electrodes based on carbon nanotubes and carbon activated material – A review". *Physica E* 40 (2008) 2596-2605.

Okada, K.; Yamamoto, N.; Kameshima, Y.; Yasumori, A. "Porous properties of activated carbons from waste newspaper prepared by chemical and physical activation". *J. Colloid Interface Sci.* 262 (2003), 179-193.

Olivares-Marín, M.; Fernández, J.A.; Lázaro, M.J.; Fernández-González, C.; Macías-García, A.; Gómez-Serrano, V.; Stoeckli, F.; Centeno, T.A. "Cherry stones as precursor of activated carbons for supercapacitors". *Mater. Chem. Phys.* 114 (2009) 323-327.

Pandolfo, A.G.; Hollenkamp, A.F. "Carbon properties and their role in supercapacitors". *J. Power Sources* 157 (2006) 11-27.

Panić, V.V.; Dekanski, A.B.; Stevanović, R.M. "Sol-gel processed thin-layer ruthenium oxide/carbon black supercapacitors: A revelation of the energy storage issues". *J. Power Sources* 195 (2010) 3969-3976.

Pekala, R.W. "Organic aerogels for the polycondensation of resorcinol and formaldehyde". *J. Mater. Sci.* 24 (1989) 3221-3227.

Peng, C.; Zhang, S.; Jewell, D.; Chen, G.Z. "Carbon nanotube and conducting polymer composites for supercapacitors". *Prog. Nat. Sci.* 18 (2008) 777-788.

Pico, F.; Morales, E.; Fernández, J.A.; Centeno, T.A.; Ibañez, J.; Rojas, R.M.; Amarillas, J.M.; Rojo, J.M. "Ruthenium oxide/carbon composites with microporous or mesoporous carbon as support and prepared by two procedures. A comparative study as supercapacitor electrodes". *Electrochim. Acta* 54 (2009) 2239-2245.

Qu, D.; Shi, H. "Studies of activated carbons used in double-layer capacitors". *J. Power Sources* 74 (1998) 99-107.

Quin, C.; Lu, X.; Yin, G.; Jin, Z.; Tan, Q.; Bai, X. "Study of activated nitrogen-enriched carbon and nitrogen-enriched carbon/carbon aerogel composite as cathode materials for supercapacitors". *Mater. Chem. Phys.* 15 (2011), 453-458.

Radovic, L.R.; Moreno, C.C.; Rivera, U.J. "Carbon Materials as Adsorbents in Aqueous Solutions". *In Chemistry and Physics Carbon. A Serie of Advances*. 1ª Edición 293-297, Marcel Dekker, New York (2000).

Ramya, R.; Sivasubramanian, R.; Sangaranarayanan, M.V. "Conducting polymers-based electrochemical supercapacitors: Progress and prospects". *Electrochim. Acta* http://dx.doi.org/10.1016/j.electacta.2012.09.116.

Rasines, G.; Lavela, P.; Macías, C.; Haro, M.; Ania, C.O.; Tirado, J.L. "Electrochemical response of carbon aerogel electrodes in saline water". *J. Electroanal. Chem.* 671 (2012) 92-98.

Raymundo-Piñero, E.; Khomenko, V.; Frackowiak, E.; Béguin, F. "Performance of manganese oxide/CNTs composites as electrode materials for electrochemical capacitors". *J. Electrochem. Soc.* 152 (2005) 229-235.

Roberts, A.J.; Slade, R.C.T. "Effect of specific surface area on capacitance in asymmetric carbon/α-MnO_2 supercapacitors". *Electrochim. Acta* 55 (2010) 7460-7469.

Rodríguez-Reinoso, F.; Molina-Sabio, M. "Activated carbons from lignocellulosic materials by chemical and/or physical activation: An overview". *Carbon* 30 (1992) 1111-1118.

Ruiz, V.; Roldán, S.; Villar, I.; Blanco, C.; Santamaría, R. "Voltage Dependence of Carbon – Based Supercapacitors for Pseudocapacitance Quantification". *Electrochim. Acta* http://dx.doi.org/10.1016/j.electacta.2013.02.056.

Saliger, R.; Fischer, U.; Herta, C.; Fricke, J. "High surface area carbon aerogels for supercapacitors". *J. Non-Cryst. Solids* 225 (1998) 81-85.

Salinas-Torres, D.; Sieben, J.M; Lozano-Castelló, D.; Cazorla-Amorós, D.; Morallón, E. "Aymmetric hybrid capacitors based on activated carbon and activated carbon fibre-PANI electrodes" *Electrochim. Acta* 89 (2013) 326-333.

Salitra, G.; Soffer, A.; Eliad, L.; Cohen, Y.; Aurbach, D. "Carbon electrodes for double-layer capacitors". *J. Electrochem. Society* 147 (2000) 2486-2493.

Sattler, G. "Fuel cells going on-board". *J. Power Sources* 86 (2000) 61-67.

Schmit, C.; Pröbstle, H.; Fricke, J. "Carbon cloth-reinforced and activated aerogel films for supercapacitors". *J. Non-Cryst. Solids* 285 (2001) 277-282.

Serp, Ph.; Feurer, R.; Kalck, Ph.; Kihn, Y.; Faria, J.L.; Figueiredo, J.L. "A chemical vapour deposition process for the production of carbon nanospheres". *Carbon* 39 (2001) 621-626.

Sepehri, S.; García, P.B.; Zhang, Q.; Cao, G. "Enhanced electrochemical and structural properties of carbon cryogels by surface chemistry alteration with boron and nitrogen". *Carbon* 47 (2009) 1436-1443.

Serfaty, S.; Griesmar, P.; Gindre, M.; Gouedard, G.; Figuiere, P. "An acoustic technique for investigating the sol-gel transition". *J. Mater. Chem.* 8 (1998) 2229-2231.

ShoyebMohamad, F.S.; Lim, J.Y.; Joo, O.-S. "Electrochemical supercapacitors of electrodeposited PANI/H-RuO_2 hybrid nanostructure". *Curr. Appl. Phys.* 13 (2013) 758-761.

Sivakkumar, S.R.; Kim, W.J.; Choi, J.-A.; MacFarlane, D.R.; Forysth, M.; Kim, D.-W. "Electrochemical performance of polyaniline nanofibres and polyaniline/multi-walled carbon nanotube composite as an electrode material for aqueous redox supercapacitors". *J. Power Sources* 171 (2007) 1062-1068.

Staiti, P.; Lufrano, F. "A study of the electrochemical behaviour of electrodes in operating solid-state supercapacitors". *Electrochim. Acta* 53 (2007) 710-719.

Staiti, P.; Lufrano, F. "Study and optimisation of manganese oxide-based electrodes for electrochemical supercapacitors". *J. Power Sources* 187 (2009) 284-289.

Sun, G.; Li, K.; Wang, J.; He, H.; Wang, J.; Li, Y.; Liu, Y.; Gu, J. "A novel approach for fabrication of hollow carbon spheres with large size and high specific surface area". *Microporous Mesoporous Mater.* 139 (2011) 207-210.

Taberna, P.-L.; Chevallier, G.; Simon, P.; Plée, D.; Aubert, T. "Activated carbon-carbon nanotube composite porous film for supercapacitor applications". *Mater. Res. Bull.* 41 (2006) 478-484.

Tarascón, J.M.; Armand, M. "Issues and challenges facing rechargeable lithium batteries". *Nature* 414 (2001) 359-367.

Tashima, D.; Taniguchi, M.; Fujikawa, D.; Kijima, T.; Otsubo, M. "Performance of electric double layer capacitors using nanocarbons produced from nanoparticles of resorcinol-formaldehyde polymers". *Mater. Chem. Phys.* 115 (2009) 69-73.

Washburn, E.W. "The Dynamics of Capillary Flor". *Phys. Rev.* 17 (1921) 273-283.

Wei, D.; Wakeham, S.J.; Ng, T.W.; Thwaites, M.J.; Brown, H.; Beecher, P. "Transparent, flexible and solid-state supercapacitors based on room temperature ionic liquid gel". *Electrochem. Commun.* 11 (2009) 2285-2287.

Winter, M.; Brod, R.J. "What are batteries, fuel cells and supercapacitors". *Chem. Rev.* 104 (2003) 4245-4269.

Wu, F.-C.; Tseng, R.-L.; Hu, C.-C.; Wang, C.-C. "Physical and electrochemical characterization of activated carbons prepared from firwoods for supercapacitors". *J. Power Sources* 138 (2004) 351-359.

Wu, H.; Wang, X.; Jiang, L.; Wu, C.; Zhao, Q.; Liu, X.; Hu, B.; Yi, L. "The effects of electrolyte on the supercapacitive performance of activated calcium carbide-derived carbon". *J. Power Sources* 226 (2013) 202-209.

Wu, M.; Gao, J.; Zhang, S.; Chen, A. "Comparative studies of nickel oxide films on different substrates for electrochemical supercapacitors". *J. Power Sources* 159 (2006) 365-369.

Wu, N.L.; Wang, S.Y.; Han, C.Y.; Wu, D.S.; Shiue, L.R. "Electrochemical capacitor of magnetite in aqueous electrolytes". *J. Power Sources* 113 (2003) 173-178.

Xu, B.; Hou, S.; Duan, H.; Cao, G.; Chu, M.; Yang, Y. "Ultramicroporos carbon as electrode material for supercapacitor". *J. Power Sources* 228 (2013) 193-197.

Xu, B.; Wu, F.; Chen, R.; Cao, G.; Chen, S.; Wang, G.; Yang, Y. "Room temperature molten salts as electrolyte for carbon nanotube-based electric double layer capacitors". *J. Power Sources* 158 (2006) 773-778.

Xu, B.; Wu, F.; Chen, S.; Zhang, C.; Cao, G.; Yang, Y. "Activated carbon fiber cloths as electrodes for high performance electric double layer capacitors". *Electrochim. Acta* 52 (2007) 4595-4598.

Xu, X.; Zhu, J.; Faria, J.L.; Li, J.; Figueiredo, J.L. "Tuning the textural and surface properties of carbon xerogels to be used as supports for gold catalysts". *Cent. Eur. J. Chem*. 10 (2012) 1867-1874.

Yamada, Y.; Sasaki, T.; Tatsuda, N.; Weingarth, D.; Yano, K.; Kötz, R. "A novel model electrode for investigating ion transport inside pores in an electrical double-layer capacitor: Monodispered microporous starburst carbonspheres". *Electrochim. Acta* 81 (2012) 138-148.

Yang, X.; He, Y.-S.; Jiang, G.; Liao, X.-Z.; Ma, Z.-F. "High voltage supercapacitors using hydrated grapheme film in a neutral aqueous electrolyte". *Electrochem. Commun.* 13 (2011) 1166-1169.

Ye, K.-H.; Liu, Z.-Q.; Xu, C.-W.; Li, N.; Chen, Y.-B.; Su, Y.-Z. "MnO_2/reduced graphene oxide composite as high-performance electrode for flexible supercapacitors". *Inorg. Chem. Commun.*. 30 (2013) 1-4.

Young, D.M.; Crowell, A.D. *Physical Adsorption of Gases*. Butterworths, London (1962).

Yu, H.; Wu, J.; Fan, L.; Lin, Y.; Xu, K.; Tang, Z.; Cheng, C.; Tang, S.; Lin, J.; Huang, M.; Lan, Z. "A novel redox-mediated gel polymer electrolyte for high-performance supercapacitor". *J. Power Sources* 198 (2012) 402-407.

Zapata-Benabithe, Z.; Carrasco-Marín, F.; Moreno-Castilla, C. "Preparation, surface characteristics, and electrochemical double layer capacitance of KOH-activated carbon aerogels and their O- and N-doped derivatives". *J. Power Sources* 219 (2012) 80-88.

Zapata-Benabithe, Z.; de Vicente, J.; Carrasco-Marín, F.; Moreno-Castilla, C. "Synthesis, surface characteristics, and electrochemical capacitance of Cu-doped carbon xerogel microspheres". *Carbon* 55 (2013) 260-268.

Zhang, D.; Zhang, X.; Chen, Y.; Yu, P.; Wang, C.; Ma, Y. "Enhanced capacitance and rate capability of graphene/polypyrrole composite as electrode material for supercapacitors". *J. Power Sources 196* (2011) 5990-5996.

Zhang, J.; Kong, L.-B.; Wang, B.; Luo, Y.-C.; Kang, L. "In-situ electrochemical polymerization of multi-walled carbon nanotube/polyaniline composite films for electrochemical supercapacitors". *Synth. Met.* 159 (2009) 260-266.

Zheivot, V.I.; Molchanov, V.V.; Zaikovskii, V.I.; Krivoruchko, V.N.; Zaitseva, N.A.; Shchuchkin, M.N. "Carbon xerogels: Nano- and adsorption textures, chemical nature of the surface and gas chromatography properties". *Microporous Mesoporous Mater.* 130 (2010) 7-13.

Zheng, J.P.; Cygan, P.J.; Jow, T.R. "Hydrous ruthenium oxide as an electrode material for electrochemical capacitors". *J. Electrochem. Soc.* 142 (1995) 2699-2703.

Zhu, X.; Dai, H.; Hu, J.; Ding, L.; Jiang, L. "Reduced graphene oxide-nicked oxide composite as high performance electrode materials for supercapacitors". *J. Power Sources* 203 (2012) 243-249.

Zhu, Y.; Hu, H.; Li, W.; Zhang, X. "Resorcinol-formaldehyde based porous carbon as an electrode material for supercapacitors". *Carbon* 45 (2007) 160-165.

Zubizarreta, L.; Arenillas, A.; Domínguez, A.; Menéndez, J.A.; Pis, J.J. "Development of microporous carbon xerogels by controlling synthesis conditions". *J. Non-Cryst. Solids* 354 (2008A) 817-825.

Zubizarreta, L.; Arenillas, A.; Pirard, J.P.; Pis, J.J.; Job, N. "Tailoring the textural properties of activated carbon xerogels by chemical activation with KOH". *Microporous Mesoporous Mater.* 115 (2008B), 480-490.

Anexo

Además de las publicaciones científicas recogidas en la presente memoria, la labor de investigación desempeñada durante estos años en el Instituto Nacional del Carbón (INCAR-CSIC) ha dado lugar a la publicación de los siguientes artículos:

- Calvo, E.G.; Arenillas, A.; Menéndez, J.A.; Zubizarreta, L. "Propiedades, ventajas e inconvenientes de los materiales utilizados en supercondensadores". *Afinidad* 66 (2009) 380-387.

- Menéndez, J.A.; Arenillas, A.; Fidalgo, B.; Fernández, Y.; Zubizarreta, L.; Calvo, E.G.; Bermúdez, J.M. "Microwave heating processes involving carbon materials". *Fuel Proces. Technol.* 91 (2010) 1-8.

- Calvo, E.G.; Ania, C.O.; Zubizarreta, L.; Menéndez, J.A.; Arenillas, A. "Exploring new routes in the synthesis of carbon xerogels for their application in electric double-layer capacitors". *Energy Fuels* 24 (2010) 3334-3339.

- Juárez-Pérez, E.-J.; Calvo, E.G.; Arenillas, A.; Menéndez, J.A. "Precise determination of the point of sol-gel transition in carbon gels synthesis using a microwave heating method". *Carbon* 48 (2010) 3305-3308.

- Moreno, A.H.; Arenillas, A.; Calvo, E.G.; Bermúdez, J.M.; Menéndez, J.A. "Carbonisation of resorcinol-formaldehyde organic xerogels: Effect of temperature, particle size and heating rate on the porosity of carbon xerogels. *J. Anal. Appl. Pyrolysis* 100 (2013) 111-116.

- Moreno, A.H.; Arenillas, A.; Calvo, E.G.; Rey-Raap, N.; Bermúdez, J.M.; Menéndez, J.A. "Xerogeles de carbono competitivos y a medida de la aplicación". *Avances en Ciencia e Ingeniería* (aceptada).